Title
Primary cilia mediate vertebrate Hedgehog signaling through the regulation of Smoothened and Gli2

Author
Santos, Nicole

Publication Date
2012

Peer reviewed|Thesis/dissertation

Primary cilia mediate vertebrate Hedgehog signaling through the regulation of Smoothened and Gli2

by

Nicole M. Santos

DISSERTATION

Submitted in partial satisfaction of the requirements for the degree of

DOCTOR OF PHILOSOPHY

in

Biomedical Sciences

Acknowledgments

My nephew Nathan once asked me, “Is it fun being a scientist?” Trying to make it easy for a nine-year old to understand, I told him it was a lot like his soccer games. Sometimes you win, sometimes you lose, and while it can be frustrating, along the way you become a better player…

Without a doubt, graduate school has been difficult. The myopia I have acquired over the past few years has been difficult. The countless failed experiments, the inconsistent data, the dead-end projects… they’ve been difficult. But, in the end, I look back and realize how graduate school has made me a better player, not just in science, but also in life. Resiliency has been a hard-earned virtue, and learning how to come out with confidence has been one of the greatest things I will ever learn.

I would have never made it to the other side without many key people who have mentored me, laughed with me, cried with me, and always reminded me of the truly important things in life.

Scientifically, I would like to thank Jeremy Reiter, the “crazy smart” professor I watched twirl his baseball cap around in Tissue and Organ Biology. Many things about Jeremy impress me – his breadth of knowledge, his cool nerdiness, his uncompromising work ethic, and most of all, his passion for science. J, thank you for the many pep talks and mentoring me to be a better scientist. Your willingness to take scientific risks to ask interesting questions is a quality I will always admire.

I also thank current and past members of the Reiter lab. Kevin Corbit was instrumental in training me in the lab and before Wiki, he was my Kevinpedia. He showed me my first primary cilium, and was always there to help me troubleshoot experiments and giggle immaturely. To Veena, Julie and Monika, by giving me weekends off, you've kept me (relatively) sane.

I have also received great support from my thesis committee members, Matthias Hebrok and Mark von Zastrow. They have been very generous with their time and advice. Upon rotating with Matthias my first quarter as a graduate student, I immediately knew that behind that somewhat intimidating German exterior, he was a great mentor.

To my classmates, Nikki, April, Angela and Shuyi, commiserating with you over drinks and good food has been a lifeline throughout this journey. Veena and Victoria, we met in lab and have since become great friends. Thank you for the endless support, advice, and listening to me complain about everything and anything. Margaritas at Chevy's will always be our go to. To Joyce, Cindy, Huong, even though you have no idea what I do, you are a constant source of support and friendship. Our TGG nights have kept things in perspective. To AWS, thank you for the weekly reminder of the bigger picture. The opportunity to be apart of the family has been life-changing.

To my family: Peggy, Gary and Garrett, thank you for being so welcoming and genuinely supportive, I can't wait to make it official. Michelle, as my sister and best friend, I don't know what I would do without you. JR, Tony and Kathy, I know you can't choose family, but I got really lucky being your sister. Nathan, Jacob and Kaitlin, your laughter and curiosity have been a true joy in my life.

To Alex, we first started dating six months into graduate school. You have been there through it all, and somehow, you still want to spend your life with me. You are more than my best friend… you're my travel buddy, my running coach, my dive and dance partner. Most of all, you're my favorite person to just do nothing with. I look forward to the many adventures ahead.

To Mom and Dad.

Thank you for teaching me and showing me true work ethic, unconditional love and compassion. To the moon and back.

Primary cilia mediate vertebrate Hedgehog signaling through the regulation of Smoothened and Gli2

Nicole M. Santos

Graduate Advisor: Jeremy F. Reiter M.D., Ph.D.

During development, the Hedgehog (Hh) signaling pathway controls growth, cell fate decisions and morphogenesis. Hh signaling has long been an intense area of research, as defects in this pathway are associated with a number of congenital defects and cancers. Within the past few years, studies have illuminated that vertebrate Hh signaling requires primary cilia, microtubule-based organelles that project from the surface of most cells. To elucidate how cilia regulate Hh signaling, we chose to focus on the two central activators of the pathway, the seven transmembrane protein, Smoothened, and its downstream effector, Gli2.

Vertebrate Smo (vSmo) translocation to the primary cilium is a necessary and regulated step in the Hh pathway. Cilia, however, are dispensable in Drosophila Hh signaling and dSmo requires other mechanisms for activation. To explore how Smo activation and the requirement for the primary cilium have evolutionarily diverged, we examined vSmo phosphorylation and generated a panel of dSmo-vSmo chimeric proteins. We demonstrate that vSmo may be phosphorylated by CKIδ/ε, proteins which localize to the base of the primary cilium. Although phosphorylation by Grk2 and interaction with βarrestin2 have been implicated in vSmo ciliary localization and activation, we show that neither are necessary. Through our chimeric analyses, we observe that the cytoplasmic tail, which contains a previously described ciliary localization motif, is necessary, but not sufficient, for ciliary translocation.

Gli2 is the primary transcriptional activator of the Hh pathway and has been shown to be enriched at the primary cilium, particularly upon pathway activation. However, the molecular mechanisms that regulate this translocation remain largely unexplored. To investigate Gli2 subcellular dynamics, we used recombinant gene technology to specifically modify the Gli2 locus in mouse embryonic stem cells. We generated a knock-in mouse model expressing Gli2-GFP and find that this allele functions as a hypomorph in vivo. We demonstrate how specific domains and post-translational modifications regulate Gli2 nuclear enrichment, binding partners and function. We identify a central region of Gli2 that is required, but not sufficient for Gli2 ciliary localization. Together, these studies provide insight into how Gli2 may be functioning at the subcellular level, particularly at the primary cilium.

Table of Contents

Page

Appendix I: Building it up and taking it down: the regulation of vertebrate ciliogenesis

List of Figures

Figures **Page**

Chapter I

Introduction

Developmental biology is the study of how a complex multi-cellular organism develops from a single cell. Developmental processes are orchestrated by a handful of signaling pathways whose collective output tells a cell when and where it needs to grow, survive, die, replicate, move or differentiate. Through this diverse array of cellular changes, signaling pathways give complex form and function to all organisms and are the genetic forces that establish body plan, organize tissues, and place anatomical organs. In a post-embryonic organism, these pathways remain crucial for maintaining normal tissue homeostasis. Misregulation can spur disease, such as congenital anomalies, cancer and degenerative diseases. Thus, understanding how these pathways function at a cellular level can illuminate the basis for both development and disease.

Used in a variety of contexts within the developing embryo, the key developmental signaling pathways include the bone morphogenetic protein (BMP), Wnt, receptor tyrosine kinase, Notch and Hedgehog (Hh) pathways. In vertebrates, early defects in the Hh pathway can cause holoprosencephaly, cleft lip and palate, polydactyly and cyclopia [1-3]. Post-embryonic hyper-activation of the pathway disrupts normal homeostasis of adult tissues and can cause disease. Indeed, mutations in Hh pathway components have been linked to the initiation and maintenance of many cancers, including basal cell carcinomas, medulloblastomas, colon and pancreatic cancer [4-6].

The core components of the Hedgehog pathway

The *Hh* gene was first discovered in a genetic screen for mutations that affect early embryonic development of the fruit fly, *Drosophila melanogaster* [7]. Compared to wild

type larvae, *Hh* mutants exhibited a shortened body shape and a lawn pattern of denticles, resulting in an appearance reminiscent of its spiny mammalian namesake. Further research identified *Hh* as a segment polarity gene important for defining the anterior-posterior axis of the segmented body plan [8-10]. The downstream components of the fly Hh signaling cascade were further elucidated by genetic analyses, with subsequent characterization of vertebrate orthologues [11]. Although absent from the genome of the nematode *Caenorhabditis elegans*, the core Hh component genes are conserved from flies to vertebrates [12, 13].

Fundamental components of the Hh pathway include a twelve pass transmembrane receptor Patched (Ptc), a seven transmembrane protein Smoothened (Smo), and effector proteins, Cubitus interruptus (Ci) in flies and the Gli transcription factors in vertebrates. In the absence of Hh signaling, Ptc functions to inhibit Smo, leading to the nuclear translocation of Ci/Gli transcriptional repressors. Upon Hh ligand binding to Ptc, inhibition of Smo is relieved, and Ci/Gli activator forms accumulate in the nucleus to turn on target genes (**Figure 1a**). Below, each core Hh signaling component is briefly described, in addition to how each has evolutionarily diverged between Drosophila and vertebrates.

Hh: Hh proteins are auto-cleaved to yield two fragments, with the N-terminal fragment possessing all its signaling activity. This fragment is palmitoylated and covalently coupled to cholesterol. These lipid modifications are crucial for Hh's secretion and its ability to act as a morphogen [14, 15]. Orthologues of Hh vary between vertebrate species and play either overlapping or distinct roles [16, 17]. For instance, in the mouse, Hh ligands include Sonic, Indian and Desert Hedgehog. *Shh* and *Ihh* play essential roles in embryonic development, while *Dhh* regulates spermatogenesis [3, 18, 19]. In

the zebrafish *Danio rerio*, at least three Hh proteins, Sonic, Echidna and Tiggywinkle, play a role in embryonic patterning [20-23].

Ptc: Also discovered as a segment polarity gene in Drosophila, Ptc is the receptor for the Hh ligand [24-26]. Ptc encodes a twelve-pass transmembrane protein that is structurally related to the resistance nodulation division (RND) family of proteins [27, 28]. Ptc contains a sterol-sensing domain, similar to Niemann-Pick C type1 (NPC1). Because RND proteins are proton-driven transmembrane transporters and NPC1 plays a role in intracellular cholesterol trafficking [28, 29], it has been suggested that Ptc's role in repressing Smo involves lipid trafficking [30]. In support of this, Ptc's SSD is necessary to repress Smo [31], Smo and Ptc do not appear to directly interact [32] and Hh pathway activity is altered with a variety of oxysterols [28]. Loss of *PTC* is sufficient to over-activate the Hh pathway and cause disease, such as rhabdomyosarcoma and Gorlin's syndrome, an autosomal dominant genetic disorder characterized by susceptibility to basal cell carcinoma and medulloblastoma [4]. In mice and zebrafish, there are two Ptc genes (*Ptc1* and *Ptc2*), whereas Drosophila possesses only a single gene [33, 34]. Ptc1 appears to be the major Hh receptor, as Ptc2 mutants exhibit a mild phenotype [35].

Smo: Smo is required for all Hh signal transduction and activating missense mutations have been linked to sporadic basal cell carcinomas [36-39]. While other Hh genes have been duplicated through evolution, a single *Smo* gene is conserved in flies and vertebrates. As a seven transmembrane protein, Smo displays homology to G-protein coupled receptors (GPCRs) and several studies have suggested that Smo may function through GTP-binding regulatory proteins [40-42]. Smo is not known to bind any ligands and does not bind Ptc [32], but several pharmacological agents that alter Hh signaling bind directly to Smo [43, 44]. dSmo and vSmo possess highly divergent C-terminal tails

[45, 46], which contribute in part to their evolutionary distinct mechanisms of activation, discussed further in Chapter 2.

Ci/Gli: The function of the downstream transcriptional factor Cubitus interruptus (Ci) in Drosophila has been distributed among the Gli proteins (Gli1, Gli2, Gli3) in mouse (**Figure 1b**) [46, 47]. Gli proteins are so named for their isolation from a human glioma tumor and have subsequently been shown to be upregulated in many other types of cancer [48, 49]. Moreover, deleterious mutations in *Gli3* have been linked to a number of congenital diseases that affect craniofacial and limb development, while *Gli2* mutations have been identified in patients with holoprosencephaly and pituitary abnormalities [47]. These transcription factors contain conserved C2H2-type zinc fingers that bind target DNA at the consensus sequence 5'-GACCACCCA-3' [50]. In the absence of Hh ligand in Drosophila, Ci, a 155kDa protein, is proteolytically cleaved into an N-terminal fragment, Ci-75. This truncated form acts as a transcriptional repressor that turns off target genes [51]. Upon Hh activation of dSmo, Ci processing is inhibited and full length Ci, Ci-155, functions as a transcriptional activator. Ultimately, Hh mediates its affects by altering the levels of repressor versus activator forms. In vertebrates, Gli2 and Gli3 are most like Ci, in that they possess both dual activator and repressor capabilities, although Gli2 functions mainly as a transcriptional activator, while Gli3 is readily cleaved into a repressor form. Gli1 is a transcriptional target of Gli2 and acts as a feedback enhancer of the pathway [47, 52]. The Gli proteins will be discussed in depth in Chapters 3 and 4.

In addition to the core components, Hh, Ptc, Smo and Ci/Gli, there are a vast number of other proteins that play auxiliary roles in the signaling cascade, some of which will be discussed below. For instance, these include proteins that aid in Hh ligand secretion,

kinases that phosphorylate dSmo and Ci/Gli, and protein interactors that mediate Ci/Gli processing and stability. Through evolution, the role of some of these accessory proteins have been modified or lost, while others have emerged as novel players in the Hh cascade [45, 46].

Hedgehog signaling is required for vertebrate development

Hh signals govern fundamental cellular processes, like cell fate specification and proliferation. In vertebrates, Hh ligand can act as a switch for adjacent cells, or as a morphogen to regulate cells further away. In the vertebrate neural tube, for instance, Hh acts as a long-range morphogen to establish neuronal cell types along the dorsal-ventral axis [53-56]. Ultimately, cell fates are determined by the concentration and duration of Hh ligand they are exposed to. The notochord serves as the Hh source, establishing a gradient of signal that specifies the floorplate and ventral neuronal sub-types through the functions of GliA (**Figure 2a**). Mutants with a total loss of Hh signaling, for instance by the loss of *Smo*, lack all ventral neural cell types [57]. Reciprocally, mutants with a gain of Hh signaling, like *Ptc1* mutants, possess an expansion of ventral neural cell types [33]. In this context, Hh signals mediate cell specification through a gradient of GliA levels.

In some tissues, however, restraint of the Hh pathway drives cell fate decisions and subsequent tissue pattering. Gli3 and its repressor form (Gli3R) are important in the developing limb bud, for instance. Shh is expressed in the posterior limb mesenchyme in the zone of polarizing activity (ZPA), and establishes a gradient of high anterior GliR levels and low posterior GliR levels to specify digit number and identity (**Figure 2b**) [58, 59]. Mice lacking Hh signaling lose digits 2-5, while mice with an excess of Hh signaling

exhibit polydactyly and loss of digit specification [60] [61]. Thus, in this context, GliR is required for proper tissue patterning through a gradient of GliR levels.

Primary cilia mediate Hedgehog signaling

In 2003, Huangfu and Anderson published a seminal article that first connected vertebrate Hh signaling with a mysterious cellular organelle, the primary cilium (**Figure 3a**) [62]. They identified etylnitrosourea-induced mutations that caused both an open neural tube and preaxial polydactyly, reminiscent of both a gain and a loss of Hh signaling, respectively. Surprisingly, they mapped these mutations to intraflagellar transport genes, which encode the machinery that build and maintain primary cilia [63-66]. *Drosophila* Hh signaling does not rely on this microtubule-based projection, pointing to one intriguing point of evolutionary divergence between fly and vertebrate Hh signaling (**Figure 4 and 5b**) [67].

Primary cilia are ancient organelles that characterize both simple single-celled organisms and complex multi-cellular organisms. Primary cilia extend from the surface of most vertebrate cells and were once thought to be vestigial organelles. However, within the past decade, it has become clear that primary cilia play important roles in receiving and interpreting information [63, 66]. Cilia establish proper left-right patterning, regulate intracellular calcium levels, and act as signaling centers for a variety of pathways, including Hh, platelet-derived growth factor (PDGF), Wnt and PCP [68-74]. Given the diverse cellular functions of primary cilia during both development and adult tissue homeostasis, it is not surprising that a variety of diseases are attributed to ciliary dysfunction [75]. The term “ciliopathies” has been coined to describe a vast number of human disorders whose underlying cause is abnormal and malfunctioning primary cilia [76]. Defects in ciliary motility can lead to altered left–right axis patterning and primary

cilia dyskinesia (PCD), while defects in immotile primary cilia function are frequently associated with kidney cysts, retinal degeneration, polydactyly, obesity, and/or neural tube defects. The pleiotropic nature of these human diseases highlights the importance of understanding how these organelles are built and maintained (**Appendix 1)** [77].

Dynamic intracellular remodeling events initiate the formation of the primary cilium. In quiescent cells, the mother centriole migrates and docks to the plasma membrane and becomes the basal body, a microtubule-organizing center [78]. Nine doublet microtubules of the ciliary axoneme extend from the nine triplet microtubules of the basal body. Because protein synthesis does not occur within the cilium, elongation of the axoneme at the distal tip relies on intraflagellar transport (IFT). This bidirectional transit system carries cargo within the cilium, and was first described in *Chlamydomonas reinhardtii*, a single green algae [65]. Together with IFT A and B complexes, cargo is transported from ciliary base to tip in the anterograde direction by the kinesin-2 motor and in the retrograde direction by a cytoplasmic dynein motor (**Figure 3b**).

Disruption of either the IFT motors themselves, IFT complex A/B composition, or certain basal body proteins can lead to impaired cilia assembly [65, 78]. As mentioned, mice harboring some of these ciliary mutations exhibit morphological and patterning phenotypes that echo altered Hh signaling [62, 79]. Epistasis analyses further demonstrate that IFT proteins and cilia act downstream of Ptc and Smo, but upstream of the Gli transcription factors. More specifically, intact cilia are required for the production of GliA and GliR, and since the effect of Hh is determined by the levels of GliA versus GliR, some tissues exhibit a loss of Hh signaling, while others exhibit a gain of Hh signaling upon compromised ciliary function. For instance, loss of Kif3a, a component of the KIF3 kinesin motor complex, or Ift88, a component of the IFT B complex leads to a

dorsalization of the neural tube, as well as polydactyly, reminiscent of a loss and gain of Hh signaling, respectively (**Figure 2, 4c**) [62, 79].

Supporting genetic evidence that cilia are required for proper Hh signal transduction, several studies have elucidated that many of the pathway's core components localize to the primary cilium. Ciliary localization of Ptc and Smo is ligand-dependent [80, 81], whereas Gli1, Gli2 and Gli3 appear to shuttle dynamically in and out [82-85]. Specifically, in the absence of Hh ligand, Ptc localizes to the cilium. Upon Hh binding to Ptc, vertebrate Smo translocates to the cilium and the Gli proteins subsequently accumulate at the ciliary tip (**Figure 4**). When Smo cannot reach the cilium, either through pharmacological means or mutation of a conserved hydrophobic domain [80], Hh signaling is abrogated. Thus, movement of vertebrate Smo to the primary cilium is a critical and regulated step in the pathway [84]. The mechanisms of how information is transmitted from Smo to Gli at the primary cilium, however, remain enigmatic.

In addition to IFT and primary cilia, another protein, Suppressor of fused (Sufu), has emerged as an important regulator of the vertebrate Hh pathway. In Drosophila, dSufu's main role is to antagonize the function a serine/threonine kinase Fused, which is essential to activate high level signaling. However, its role in Drosophila is dispensable, as *Sufu* null flies are viable and fertile [86]. In zebrafish, however, *Sufu* knockdown by morpholino exhibits a slight gain of function phenotype in muscle patterning, suggesting that Sufu's role may have diverged in function [87, 88]. Indeed, *Sufu* null mice die at mid-gestation and exhibit a strong gain of function Hh phenotype, including a severely ventralized neural tube [88, 89]. Humans heterozygous for *Sufu* are more predisposed to medulloblastoma, prostate cancer and basal cell carcinomas [90, 91]. Thus, Sufu is

essential for restricting Hh signaling in the developing vertebrate embryo and maintaining adult tissue homeostasis.

As a critical negative regulator of the vertebrate Hh pathway, Sufu interacts with the Ci/Gli proteins and is believed to regulate Gli shuttling between the cytoplasm and nucleus [92-97]. However, recent evidence has suggested that Sufu may play a role in Gli regulation specifically at the primary cilium. While the Gli proteins can localize to the cilium in the absence of Sufu, Sufu cannot localize to the cilium in the absence of the Gli proteins [82, 83, 98]. Gli2/3 accumulate at the ciliary tip in response to pathway stimulation and this subsequently leads to the dissociation of Sufu from Gli. Thus, it is possible that the primary cilium is the specialized subcellular site of Hh-mediated dissociation of Gli from Sufu. In support of this hypothesis, Sufu-Gli dissociation does not occur in cells lacking Kif3a, an intraflagellar protein required for ciliogenesis [99]. Although pharmacological inhibition of protein kinase A (PKA) has been shown to disrupt ciliary localization of Gli-Sufu complexes, PKA deficient mice exhibit an increase in Gli2 ciliary accumulation [98, 100, 101]. Thus, the specific mechanisms by which the Gli proteins and Sufu localize to the cilium remain enigmatic.

In an effort to further understand how the primary cilium mediates vertebrate Hh signaling, I have examined the mechanisms of Smo and Gli2 activation at the primary cilium. Since Smo is the central activator of the Hh pathway and Gli2 is the primary downstream transcriptional activator that turns on Hh target genes, it is critical to understand how these proteins are regulated subcellularly. Chapter 2 will focus on Smo, where I investigate its potential for phosphorylation and interaction with arrestin proteins. I also describe chimera analyses between Drosophila and vertebrate Smo that provide insight into the evolutionary divergence for the primary cilium. In Chapters 3 and 4, I

describe genetic manipulation of the *Gli2* locus in mouse embryonic stem cells using the Floxin technology. Using this knock-in strategy, I examine mutant alleles of *Gli2* and concomitant changes in ciliary dynamics and function to shed light on how this organelle mediates Gli2 function. I also illustrate how the Floxin system can be used to study Gli2 dynamics in vivo by generation of a Gli2-GFP mouse model. Lastly, given that the Gli2 is a nucleo-cytoplasmic protein, I consider parallels between ciliary trafficking and trafficking across the nuclear pore complex.

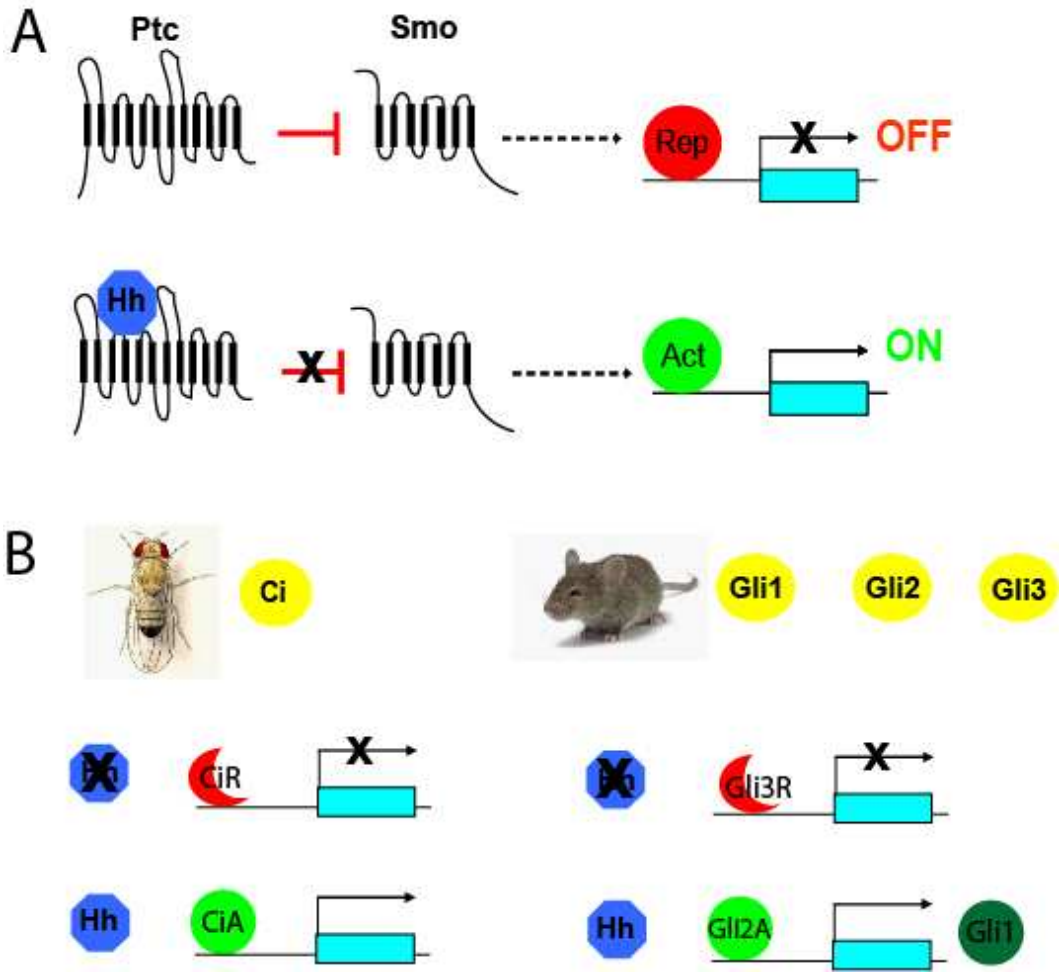

Figure 1. The core components of the Hedgehog pathway.
(A) The core components of the Hh pathway. Fundamental components of the Hh pathway include a twelve pass transmembrane receptor Patched (Ptc), a seven transmembrane protein Smoothened (Smo), and effector proteins, Ci in Drosophila and the Gli proteins in vertebrates. In the absence of Hh signaling, Ptc functions to repress Smo, leading to the nuclear translocation of transcriptional repressors. Upon Hh ligand binding to Ptc, inhibition on Smo is relieved, and Ci/Gli activator forms accumulate in the nucleus to turn on target genes. **(B) The function of Ci has been distributed among the Gli proteins.** In Drosophila, the downstream effector of the Hh pathway is Ci. In the absence of Hh, Ci phosphorylation leads to partial proteolysis which generates a repressor form, Ci-75 or CiR. In the presence of ligand, phosphorylation of Ci is prohibited and Ci remains in its full length form. Ci-155, or CiA, activates Hh target genes. In vertebrates, the role of Ci has been distributed among the Gli proteins. Gli3 can be proteolytically processed into Gli3 repressor (GliR) and thus function like CiR. Full length Gli2 is the primary activator of the pathway and is most like full length Ci. Gli1 is a transcriptional target of Gli2 and is a feedback enhancer of the pathway.

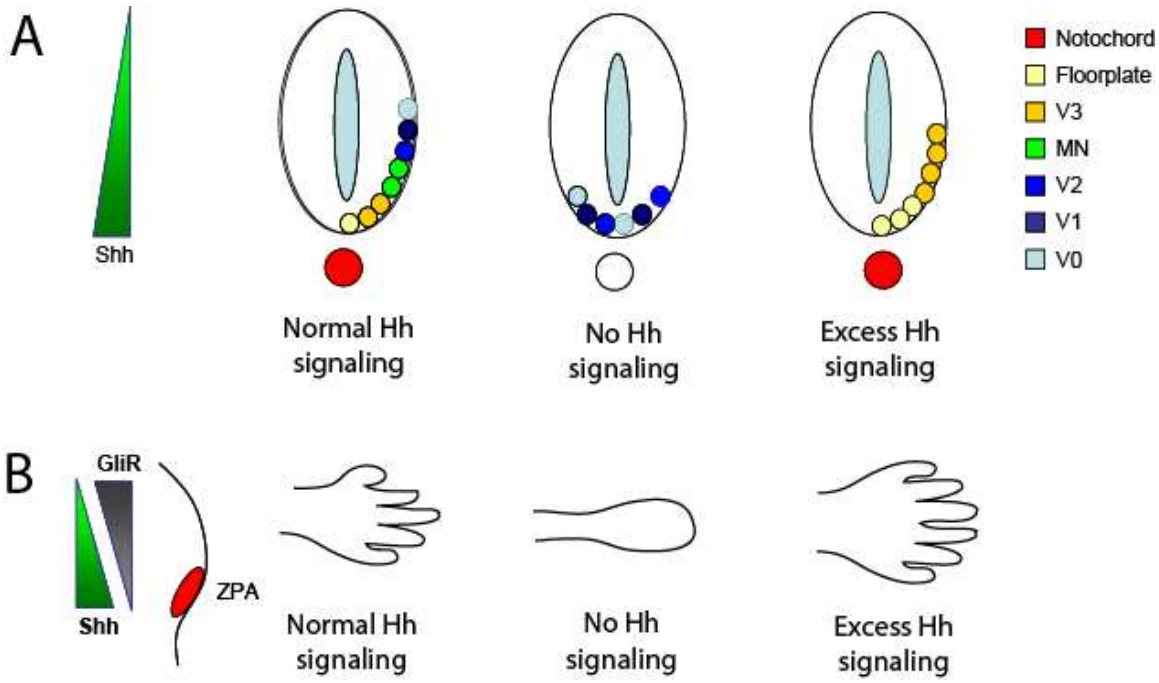

Figure 2. Hedgehog signaling is required for proper patterning and development.
(A) Hh signaling in the vertebrate neural tube. In a wild type neural tube, Hh ligand is produced in the notochord, leading to the highest levels of Hh signaling in the floor plate and a gradient of Hh morphogen emanating from the ventral side. This leads to the specification of neuronal subtypes along the dorsal-ventral axis. Loss or diminished Hh signaling results in either an absence of neuronal specification, or dorsalization of neural tube. Conversely, excess Hh signaling leads to ventralization of the neural tube.
(B) Hh signaling in the vertebrate limb bud. The zone of polarizing activity (ZPA) in the posterior limb bud mesenchyme is the source of Shh ligand. It results in a gradient of high anterior GliR levels and low posterior GliR levels. The concentration and duration of Hh exposure determines digit number and identity. Mice lacking Hh signaling lose digit specification and patterning, while mice with an excess of Hh signaling exhibit polydactyly.

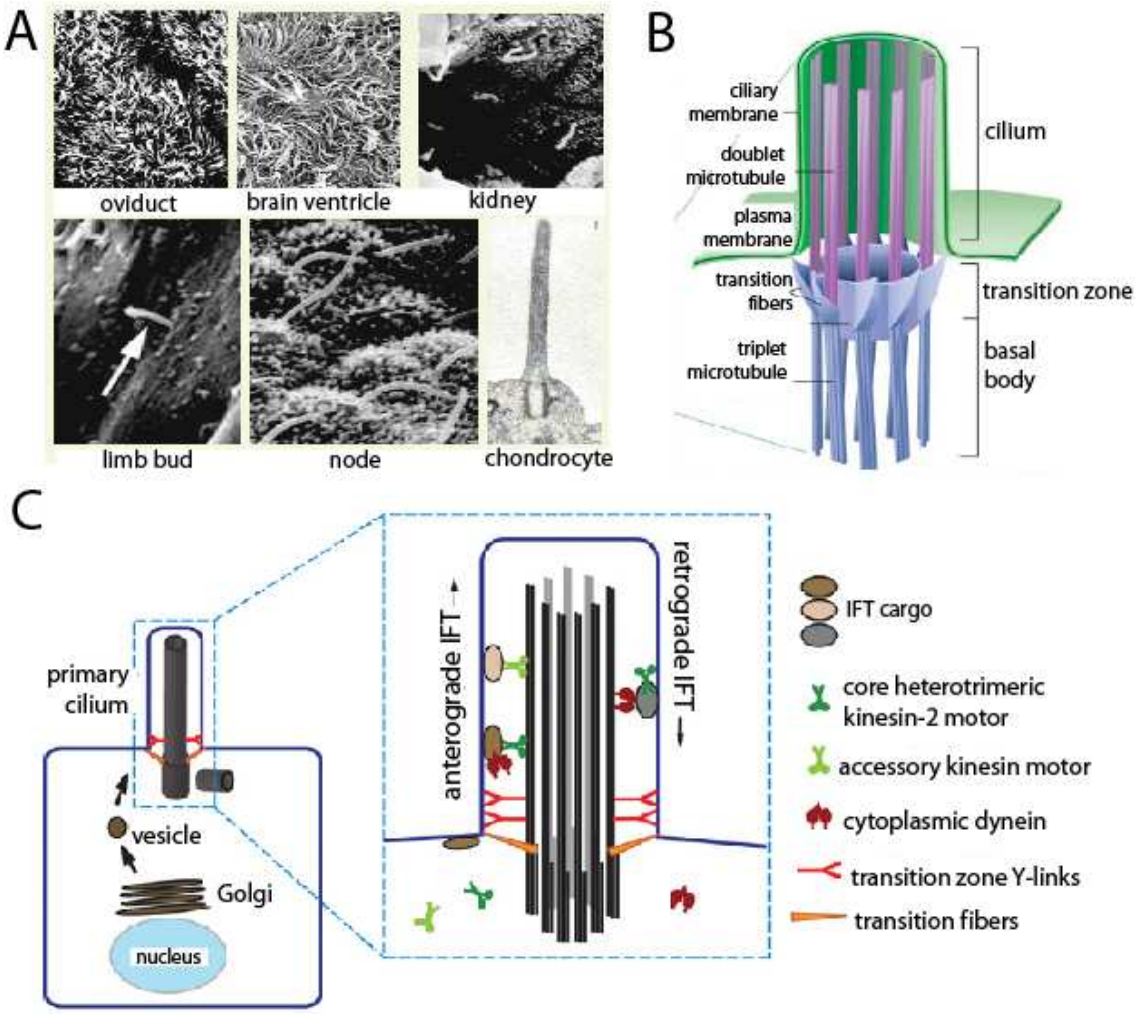

Figure 3. Primary cilia are ubiquitous organelles that rely on intraflagellar transport.

(A) Primary cilia are found on the surface of a variety of vertebrate cells (adapted from [64]). **(B) The primary cilium extends from the basal body** (adapted from [66]). The ciliary axoneme consists of nine doublet microtubules that extend from the triplet microtubules of the basal body, which is derived from the mother centriole. The transition zone is marked by the presence of transition fibers and Y-links (schematized in Figure 3c). **(C) The primary cilium relies on intraflagellar transport** (adapted from [102]). The bi-directional movement of IFT particles and ciliary cargo is driven by kinesin and dynein motors. Kinesin motors facilitate anterograde movement from base to tip, while cytoplasmic dynein drives retrograde movement from tip to base.

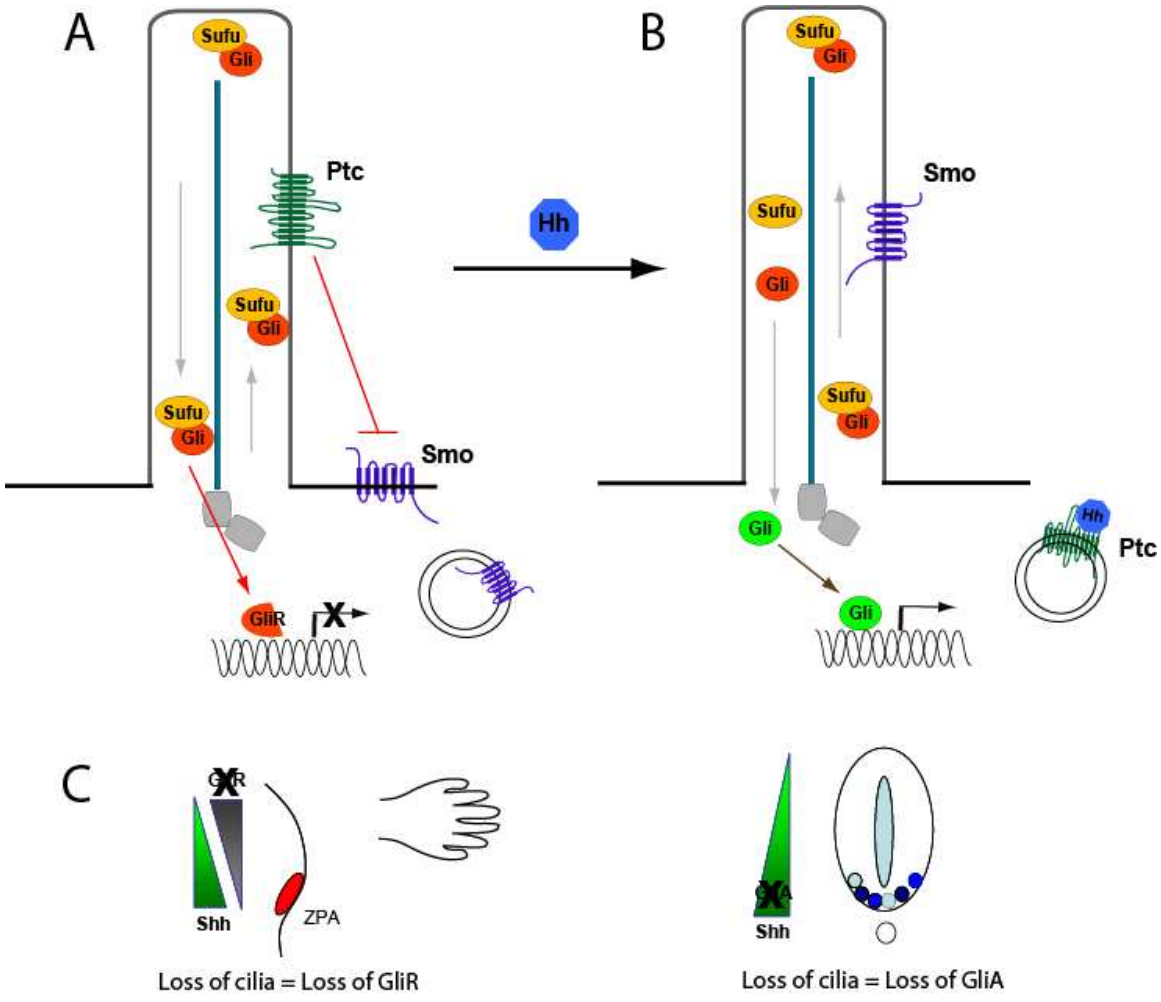

Figure 4. Vertebrate Hh signaling requires the primary cilium.
(A) Primary cilia mediate the formation of GliR in the absence of Hh signaling. In the absence of Hh ligand, Ptc localizes to the primary cilium and inhibits Smo, which is excluded from the cilium. Sufu and Gli complexes dynamically shuttle in and out of the cilium. In response to no pathway activation, Gli is proteolytically processed into a repressor form, or actively degraded (not shown, See Chapter 4). GliR enters the nucleus to repress target genes. **(B) Smo translocates to the primary cilium in response to Hh ligand and leads to Gli activation.** Upon Hh ligand binding to Ptc, Smo inhibition is relieved and can enter the cilium. Active Smo transmits information to the Sufu and Gli complexes, which accumulate at the cilium in response to Hh signal. Through an unknown mechanism, postulated to be the dissociation of Sufu from Gli, Gli is activated and can turn on target genes. **(C) Loss of cilia results in the loss of both GliA and GliR.** Tissues that require GliR for proper patterning, like the limb bud, resemble a gain of Hh phenotype. Tissues that require GliA for proper patterning, like the neural tube, resemble a loss of Hh phenotype.

Chapter II

Mechanisms of Smoothened ciliary localization and activation

Abstract

During development, the Hedgehog (Hh) signaling pathway controls growth, cell fate decisions and morphogenesis. The seven transmembrane protein Smoothened (Smo) is the central activator of the pathway and in vertebrates, translocates to the primary cilium upon Hh stimulation. However, these microtubule structures are dispensable in Drosophila Hh signaling and other activation steps are required for Smo (dSmo) function, like extensive phosphorylation and cell surface accumulation. The basis for this evolutionary divergence and the mechanisms that dictate changes in vertebrate Smo (vSmo) ciliary translocation are unclear. Here, we demonstrate that vSmo may be phosphorylated by casein kinase I (CKI) and CKI isoforms delta and epsilon (CKIδ/ε) localize to the base of the primary cilium. Moreover, although phosphorylation by GPCR kinase 2 (Grk2) and interaction with βarrestin2 has been implicated in vSmo ciliary localization and activation, we show that neither are necessary for the propagation of Hh signals. To explore how vSmo and its requirement for the primary cilium have evolutionarily diverged, we built a panel of dSmo-vSmo chimeric proteins. We observe that the cytoplasmic tail which contains a previously described ciliary localization motif is necessary, but not sufficient for ciliary translocation.

Introduction

Smoothened (Smo) is the central activator of the Hh pathway. While other Hh proteins are duplicated through evolution, a single *Smo* gene is conserved. *Smo* was first identified in Drosophila (dSmo) as a segment polarity gene that when mutated, phenocopied the *Hh* mutant [7, 36, 103]. Similarly, *Smo* mouse mutants (mSmo or vSmo) resemble *Shh Ihh* mutants, presenting with defects in embryo turning, a linear heart tube, an open gut and cyclopia [38]. These shared phenotypes suggest that Smo is absolutely essential for the transduction of Hh signals in both Drosophila and vertebrates. Importantly, oncogenic mutations in *SMO* have been identified in sporadic basal cell carcinomas, thus understanding how Smoothened is activated in response to Hh signals is a question of clinical relevance [37].

Smo contains seven transmembrane domains and belongs to the serpentine receptor family of G-protein coupled receptors (GPCRs). Structurally, Drosophila Smo and vertebrate Smo are very similar **(Figure 5a)**. Several studies have examined the role of G-proteins in Hh signaling, but findings are inconsistent [42]. Smo is structurally most similar to the Frizzled (Fz) receptors of the Wnt pathway [103, 104]. As seen in Fz proteins, the N-terminal extracellular domain (ECD) of Smo contains a cysteine-rich domain that is conserved from cnidarians to humans [11]. Unlike the Fz proteins, however, Smo has not been shown to bind any extracellular ligands. Deletion of this cysteine-rich domain (CRD) in Drosophila renders dSmo non-functional, while deletion of the CRD in zebrafish is detrimental to high level Hh signaling [105, 106]. The central region of the Smo protein is comprised of seven transmembrane (TM) domains. Smo contains three extracellular loops (EC) and three intracellular loops (IC). Cysteines within EC1 and EC2 appear to be important for dSmo conformation and subsequent function, presumably through disulphide bonds [106, 107]. Within IC3, a missense

mutation of R474C has been shown to inactivate dSmo [106]. Downstream of the 7TM, the intracellular cytoplasmic tails of dSmo and vSmo are highly dissimilar from the Fz's and each other (discussed below). This region is required for all intracellular responses to Hh in both Drosophila and vertebrates [45, 104, 108].

In Drosophila, Hh ligand induces opposite changes in the turnover and subcellular localization of Ptc and dSmo (**Figure 5b**) [109, 110]. Hh binding to Ptc leads to its internalization from the cell surface and the simultaneous cell surface accumulation of dSmo. Once in its active form, dSmo is extensively phosphorylated at several serine/threonine residues [111-113]. Specifically, protein kinase A (PKA) phosphorylates the carboxy tail of dSmo at serines 667, 687 and 740, priming it for further phosphorylation by casein kinase 1α (CKIα). Treatment with PKA and CKI inhibitors in vitro and analysis of un-phosphorylatable and phospho-mimetic forms of dSmo in vivo demonstrated that these kinases are essential for Hh pathway activation [114]. Phosphorylation of dSmo is believed to induce a conformational change that promotes exposure of its cytoplasmic tail by antagonizing an arginine-rich autoinhibitory domain [115]. This conformational change promotes dSmo cell surface accumulation and interaction with kinesin-related protein Cos2 and serine/threonine kinase Fused. In the absence of Hh ligand, Fused, Sufu and Cos2 form a complex with Ci to promote its cleavage into CiR [116]. In response to Hh ligand, Cos2 and Fused preferentially bind dSmo, sequestering the complex away from Ci and hence, prevents its processing [117]. Together, dSmo cell surface accumulation and phosphorylation are required for its activation and the prevention of Ci processing.

In vertebrates, changes in Smo subcellular compartmentalization also appear to be necessary for Hh signal transduction (**Figure 4**). However, unlike dSmo, vSmo does not

contain conserved PKA sites in the cytoplasmic tail, nor does it appear to bind the Cos2 or Fused vertebrate homologs, Kif7 and Stk36, respectively (**Figure 5a**) [45, 118]. Rather, vSmo moves to the primary cilium specifically in response to Hh signals and possesses a conserved hydrophobic motif that determines the ciliary localization of other seven transmembrane proteins in both worms and mammals [80, 105]. This WR motif is located just C-terminal to the 7TM of vSmo, and its mutation blocks Smo ciliary localization, as well as Hh pathway activation in vitro (**Figure 5c, 11c**). This allele, termed CLDSmo for Ciliary Localization Defective Smo, does not rescue in vivo function upon injection in *Smo* mutant zebrafish (*Smu-/-*). Therefore, Hh pathway activation requires Smo translocation to the cilium. Notably, this ciliary targeting sequence is conserved in dSmo, which do not utilize the primary cilium in Hh signaling [67].

Trafficking of vSmo to the cilium may involve the transport of an intracellular pool via IFT, or through lateral transport from the plasma membrane to the ciliary membrane [119, 120]. Importantly, Smo ciliary localization is necessary, but not sufficient for Smo activation [121]. Smo M2, an oncogenic allele of Smo, constitutively localizes to the primary cilium independent of Hh stimulation and over-activates the pathway. However, it was observed that over-expressed wild type Smo-GFP can reach the cilium comparably to SmoM2-GFP without equivalent pathway activation, hinting at the requirement for another step in Smo activation [121]. Furthermore, an antagonist of the Hh pathway, cyclopamine appears to promote ciliary Smo accumulation, despite inactivation of the pathway [120, 121]. Thus, a second mechanism is necessary to activate Smo once in the cilium.

GPCR kinases (GRKs) have also been implicated in Hh signaling, both in Drosophila and vertebrates. GRKs are known to phosphorylate activated GPCRs and promote the

recruitment of cytosolic arrestins to the receptor for clathrin-mediated endocytosis [122, 123]. In Drosophila, Grk2 was recently identified as a positive regulator of dSmo that affected function, but not accumulation to the plasma membrane [124, 125]. A subsequent study, however, suggests that Grk2 is crucial for normal cAMP regulation and affects dSmo through indirect effects on PKA activity [126]. There is only one non-visual arrestin in Drosophila which is encoded by *kurtz*. While there is no Hh phenotype upon *kurtz* deletion, over-expression of kurtz leads to dSmo internalization and degradation [127], suggesting that Grk2 and kurtz function in the turnover of dSmo. Similarly, in mammalian cell culture experiments, over-expression studies using tagged versions of vSmo and βarrestin2 suggest that Hh induces vSmo phosphorylation by Grk2, βarrestin2 recruitment to the cell membrane and subsequent Smo internalization [128-130]. Additionally, *βarrestin2* morphant zebrafish exhibit partial cyclopia and abnormal somite and pectoral fin development, reminiscent of abrogated Hh signaling [130, 131]. Intriguingly, siRNA-mediated knockdown of *βarrestin1/2* disrupted the localization of Smo to primary cilia and abrogated Hh signaling and βarrestin2 localizes to the primary cilium in quiescent cells [128, 132, 133]. Together, these data suggest that Grk2 and arrestins may regulate Smo function in vertebrates by modulating turnover and/or ciliary trafficking.

It is unclear how vSmo localization to the primary cilium is determined and how it is activated once there. As the central transducer of the Hh pathway, elucidating the mechanisms by which this occurs is fundamental to understanding how Hh activity is properly regulated. Not only will this provide a cell biological understanding of how this fundamental pathway is regulated in a developing organism, but it will also shed light as to how it may be de-regulated in Hh-mediated disease. Since phosphorylation of dSmo is a critical step in Hh signal transduction in Drosophila, it is possible that vSmo

phosphorylation could be the secondary activation step that occurs at the primary cilium. Although the carboxy tails of dSmo and vSmo are highly divergent and dSmo's PKA phosphorylation sites are not conserved [45, 46], this does not eliminate phosphorylation as a potential post-translational modification of vSmo by PKA or other kinases. Indeed, several CKI and Grk2 phosphorylation consensus sites (pS/T-X-X-S/T and S/T within acidic environments, respectively) are located in the third intracellular loop and cytoplasmic tail of vSmo (**Figure 8a, Figure 10c**). These sites are conserved among chordates and are not present in dSmo. To examine the role of CKI and Grk2 in vertebrate Hh signaling, I investigated vSmo's potential for phosphorylation by CKI, as well as the role of Grk2 and βarrestin2 in ciliary localization of vSmo.

Additionally, in an attempt to shed light on the evolutionary divergence of the primary cilium role in Hh signaling, I generated a panel of dSmo-mSmo chimeric proteins. Drosophila mutants lacking dSas4, a centriolar protein, exhibit a loss of centrioles and centrosomes during embryonic development, but progress through larval stages. However, these mutants die soon after pupation, perhaps due to lack of cilia on sensory neurons [67]. These mutants do not exhibit Hh defects, suggesting that primary cilia do not play a role in Hh signaling during Drosophila development. Thus, the divergent role of the primary cilium in Hh signaling offers a unique and tractable approach to dissecting the mechanisms of the pathway, particularly at the level of Smo.

Results

vSmo phosphorylation by CKI and Grk2

The CKI family of serine-threonine protein kinases has been shown to play a role in Wnt, Hh and circadian rhythm [134]. These kinases are defined by homology within their catalytic kinase domain and possess a consensus site of S/Tp-X-X-S/T, where the first

S/T is primed by another kinase. Drosophila has eight CKI isoforms, while vertebrates have seven. CKIα, CKIδ and CKIε have been implicated in *Drosophila* Hh signaling, as negative (CKIα) and positive (CKIδ/ε) regulators of Ci and dSmo [111, 114, 135]. CKIα has recently been implicated in vSmo phosphorylation and ciliary localization [124]. CKIδ and CKIε are 98% identical within their catalytic domain and 53% identical in their long C-terminal extensions.

We found that endogenous CKIε localizes to the basal body from which the primary cilium extends (**Figure 6a**). CKIα and CKIδ, however, were not observed at or near the cilium, although this may reflect limitations of available antibodies. GFP-tagged versions of both CKIδ and CKIε (a gift from L. Ptacek), however, accumulated at the base of the primary cilium in transiently transfected NIH 3T3 cells (**Figure 6a**). These data are consistent with previous reports that CK1δ co-localizes with the centrosomal marker γ-tubulin, and myc-tagged CK1δ or CK1ε also co-localizes with pericentrin [136].

Pharmacological inhibitors of CKI have been previously described to be ATP-competitive inhibitors of CKI isoforms [137, 138]. D4476 (Calbiochem) is thought to inhibit CKIδ by more than 90%, while having little effect on other kinases. Similarly, IC261 (Calbiochem) is reported to be a potent and selective inhibitor of CKIδ and CK1ε, and at much higher concentrations, CKIα. Notably, D4476 was found to be a more effective inhibitor of CKI as compared to IC261 [138]. To assess if inhibition of CKIδ/ε affected the Hh pathway, we utilized Shh-Light2 cells, which are NIH-3T3 cells stably expressing a Gli-luciferase reporter and control plasmid pRLTK (ATCC). Treatment with D4476 for 18 hours abrogated Hh pathway activation more robustly than cyclopamine, a known Hh antagonist, while IC261 exhibited less of an effect, particularly upon Hh treatment (**Figure 6b**) [43]. D4476 had the same effect in NIH-3T3 cells assayed for *Gli1* transcript

levels by qRTPCR following Hh stimulation (**Figure 6c**). In both experiments, neither drug exhibited any adverse effects on ciliation (data not shown). To examine possible off-target effects by D4476, we assessed if siRNA-mediated knockdown of CKIα, CKIδ and CKIε would phenocopy CKI pharmacological inhibition. Indeed, we observed that Hh responsiveness was diminished in the presence of *CKI* siRNA in Shh-Light2 cells (**Figure 6d**), despite inefficient knockdown as determined by Western blot. Knockdown of all isoforms (CKIα/δ/ε) appeared to diminish Hh signaling, although scramble controls did not, suggesting that these three CKI proteins may positively regulate the pathway.

The simultaneous exposure of cells to both recombinant Hh and CKI inhibitors prevented activation of the Hh pathway, suggesting that CKI might act downstream of Hh ligand binding to Ptc. Thus, to determine if CKI acts at the level of Smo, we evaluated if D4476 caused defects in over-expressed vSmo ciliary localization. Notably, detection of endogenous Smo proved to be difficult due to the lack of effective antibodies. Both wild type and an oncogenic allele of vSmo (SmoM2) reached the cilium in the presence of D4476 and Hh ligand (**Figure 7a**). However, this finding could be due to non-relevant levels of exogenous Smo as compared to endogenous levels of CKI. Consequently, we determined if CKI could directly phosphorylate mouse Smo in vitro. First, we performed in vitro kinase assays using recombinant CKIδ kinase (NEB) and Smo-myc that was immunoprecipitated from transiently transfected cells (**Figure 7b**). This experiment yielded suggestive results in that two bands were detected in the experimental lane (*myc IP + CKIδ, lane 4), which correspond to two Smo-myc forms that represent different glycosylation states, as one is endoH-sensitive (red arrow) and the other is endoH-resistant (black arrow) [43]. However, because control lanes (lanes 3 and 5) exhibited weak ghost bands of the same size, we sought another in vitro kinase method for detecting Smo phosphorylation.

Since the majority of the putative CKI phosphorylation motifs (S/Tp-X-X-S/T) are located in the cytoplasmic tail of Smo, we used purified mSmo cytoplasmic tail as a substrate and commercially available recombinant CKIδ and Grk5 kinase (NEB). These in vitro kinase assays indicated that recombinant CKIδ robustly phosphorylates mSmo cytoplasmic tail, but Grk5 does not (**Figure 7c**). Furthermore, when CKIε is immunoprecipitated from cell lysate and exposed to recombinant Smo C-tail in the presence of increasing levels of D4476, phosphorylation of the substrate is prevented (**Figure 7d**). IC261 did not replicate these results, but perhaps this is due to differences in drug efficiencies.

Three putative CKI phosphorylation consensus sites (pS/T-X-X-S/T) and one divergent CKI site are located in the third intracellular loop and cytoplasmic tail of vSmo (**Figure 8a**). Sites found in the cytoplasmic tail (denoted as 2,3 and 4) are conserved in dSmo, whereas IC3 site (denoted as 1) is only found in chordates. To examine if loss or gain of phosphorylation at these particular sites affects vSmo localization and function, we generated phospho-dead and phospho-mimetic alleles using site-directed mutagenesis. Serine and threonines were mutated to alanine and aspartic acid residues, respectively, and denoted as 1A and 1D, for instance. These myc-tagged constructs were transiently transfected into NIH 3T3 cells and assessed for ciliary localization and function in the presence and absence of Hh stimulation (**Figure 8b**). We hypothesized that phospho-dead alleles would fail to reach the cilium and lack Hh responsiveness, while phospho-mimetic alleles would constitutively localize to cilia and hyper-activate the pathway. We observed that all phospho-dead alleles reached the cilium in response to ligand, behaving similarly to wild type Smo. Functionally, these alleles appeared to respond to Hh, although not as robustly as wild type Smo (**Figure 8a, c**). These data correlate with

the findings of a previous alanine scan which examined residues S620, T545A and S594 [45]. Phospho-mimetic alleles 1D and 2D did not localize to cilia in the absence of Hh ligand, while alleles 3D and 4D did. Over-expressed wild type Smo, however, has been observed at the cilium without Hh pathway stimulation likely due to exogenous levels of Smo protein. Accordingly, by Western blot of total lysate, protein levels of 3D and 4D are significantly higher than 1D and 2D (**Figure 8d**). 1D, 3D and 4D all translocated to the cilium when stimulated with Hh (**Figure 8c**). Smo mutant 2D, which did not localize to the cilium in response to ligand, was functionally dead. These data reiterate the fact that vSmo ciliary localization is necessary for Hh signaling. By Western analysis, most mutants displayed the two forms of protein that reportedly represent different glycosylation states (**Figure 8d**) [43]. Alleles 2A/2D obviously lacked the endoH-resistant band (black arrow), but the former effectively reaches the cilium and activates signaling. This suggests that a small amount of protein can exit the ER despite lack of detection of a maturely glycosylated form by Western blot. Notably, oncogenic SmoM2 which localizes constitutively to the cilium, is detected only as the non-glycosylated form [43]. Since 1A/D are expressed at lower levels, detection of the glycosylated form is difficult. 3A/D and 4A/D possess both the endoH sensitive and endoH resistant bands, as observed in wild type Smo-myc. Taken together, these data suggest that at least individually, the mutation of these putative CKI sites in vSmo are not necessary for ciliary localization, but can adversely affect Hh signal transduction.

To investigate the role of Grk2 and arrestins in vertebrate Hh signaling, we obtained wild type, *βarrestin1*-/-, *βarrestin2*-/- and *βarrestin1/2*-/- MEF lines (a gift from R. Lefkowitz) [139]. In wild type MEFs, endogenous βarrestin2 localized to the primary cilium as reported [132] (**Figure 9a**). We found that the same is true in *Smo*-/- mutant MEFs (a gift from J. Taipale), suggesting that localization of βarrestin2 occurs independent of

Smo. Upon stimulation with recombinant Hh ligand, Smo ciliary localization and an increase in *Gli1* transcript levels were intact in cells lacking the βarrestin proteins (**Figure 9b,d**). Thus, βarrestin1/2 are not necessary for Smo translocation to the cilium and downstream pathway activation.

Grk2 has been shown to phosphorylate serine/threonine residues within acidic environments [112], and putative regions exist in the cytoplasmic tail of vSmo. These residues are conserved among chordates (**Figure 9c**). To assess if Grk2 was necessary for vSmo translocation to the primary cilium, we obtained *Grk2* wild type and mutant cell lines (a gift from N. Freedman) [140]. As seen in *βarrestin1/2* mutants, Smo ciliary localization remained intact, as did Hh pathway activation by Gli-luciferase reporter assay (**Figure 9c,d**). Grk2 inhibition by a pharmacological agent [141] (Calbiochem) altered Hh readout by Gli-luciferase reporter assay, although not as robustly as cyclopamine or CKI inhibition (**Figure 6b**). Neither Grk2 nor Grk5 appeared to localize to the primary cilium, and recombinant Grk5 did not phosphorylate mSmo's cytoplasmic tail (**Figure 7c**). Together, these data suggest that neither βarrestin1/2 nor Grk2 are absolutely required for vSmo ciliary localization and its downstream signal transduction.

To determine if Smo phosphorylation occurs globally in vitro, we labeled cells in culture with the radiolabel ^{33}P. First, we determined if phosphorylation occurred in the presence or absence of cilia, using *Kif3a* wild type and knockout cells. Kif3a is a component of intraflagellar transport, and cells lacking this protein are unciliated (**Figure 28d**). These embryonic fibroblasts were originally isolated from e10.5 littermates and immortalized by T-antigen [68]. Cells were transfected with Smo-myc and treated with media containing ^{33}P with or without recombinant Hh. Following immunoprecipitation by myc antibody,

SDS-PAGE and autoradiography, we did not observe robust ^{33}P labeling of Smo-myc (**Figure 10a**). Efficient immunoprecipitation of Smo-myc was detected by Western blot, and only non-specific bands were detected by autoradiography. When we repeated the experiment using Dvl3-HA, a known phosphorylated substrate of the Wnt pathway, ^{33}P labeled endogenous Dvl3 and HA-tagged Dvl3 with and without Wnt stimulation. Smo-myc, however, remained unlabeled by ^{33}P in the absence and presence of Hh stimulation (**Figure 10b**). Together, these data indicate that phosphorylation of mSmo may not be a post-translational modification that occurs robustly, at least by this in vitro assay.

Evolutionary divergence between dSmo and vSmo: a chimeric analysis

In both Drosophila and vertebrates, changes in subcellular compartmentalization are necessary for the function and activation of Smo. In flies, dSmo translocation to the cell membrane is an important step that coordinates downstream pathway activation, while in vertebrates, translocation to the primary cilium is necessary for all signal transduction (**Figure 5b**).

To explore the divergent mechanisms of Smo activation and the major evolutionary shift to the primary cilium between species, we explored if dSmo can reach the primary cilium in mammalian cells. dSmo-myc failed to localize to the cilium in *Smo*-/- MEFs upon Hh ligand stimulation, and consequently failed to activate the pathway by Gli-luciferase readout **(Figure 11a,d)**. This finding underscores distinct mechanisms for Smo activation in Drosophila versus vertebrates. Notably, we sometimes observed dSmo accumulation at the base of the cilium, independent of Hh stimulation **(Figure 11a)**. Using an N-terminal antibody to dSmo (a gift from T. Kornberg), dSmo was detected at

the cell surface of mammalian cells in response to recombinant Hh, similarly to mSmo when an N-terminal HA-tag was introduced **(Figure 11b,c)**.

Thus, taking advantage of these differences in subcellular localization, we sought to examine which domains of vSmo mediate ciliary localization. Given that vSmo's ciliary localization motif WR is located just N-terminal to the 7TM, we were particularly interested if mSmo's cytoplasmic tail was sufficient to promote ciliary localization, or if other domains were necessary. To this end, we built a panel of dSmo-mSmo chimeric proteins. In addition to determining these chimeras' abilities to reach the cilium, we also examined if they could exit the ER as assessed by examining co-localization with the ER protein calnexin. Cell surface localization was determined by staining with ECD-specific antibodies prior to cell permeabilization. We obtained a dSmo antibody which recognized the extracellular domain of dSmo's N-terminus, and Smo-myc was dually tagged on the N-terminus by HA and the C-terminus by myc. We further correlated subcellular localization of Smo chimeras with functional readout by Gli-luciferase in *Smo*-/- MEFs (**Figure 11c,d**).

As summarized in **Figure 11d**, many of the chimeric proteins appeared to possess folding defects, as they were retained in the ER and did not reach the cell surface. The hydrophobic nature of Smo's seven transmembrane domains could render these chimeric proteins vulnerable to aggregation and folding defects, and ER-retained chimeras were considered to not yield any informative results. Notably, only the region spanning the first intracellular loop (IC) to the first extracellular (EC) loop was interchangeable between species. Chimera mSmo dSmo IC1-EC1 mSmo behaved like wild type Smo, in that it was able to reach the cilium and cell surface in response to Hh stimulation (**Figure 11b**). Confirming that ciliary localization is required for downstream

Hh signaling, this chimeric protein was functional, as assessed by Gli-luciferase reported (**Figure 11c**). Correlating with evidence that a domain within the cytoplasmic tail is required for vSmo ciliary localization, we observed that substituting mSmo's cytoplasmic tail with that of dSmo created a chimera that could effectively reach the cell surface, but not the primary cilium (mSmo dSmo-CTD). Conversely, a chimera that possesses the region spanning mouse IC3 and CTD (dSmo-ECD-TM5 mSmo) reached the cell surface effectively, but not the cilium. Together, these data suggest that the cytoplasmic tail of mSmo is necessary, but not sufficient, for ciliary localization.

Discussion

CKI and GRKs in vSmo phosphorylation

First, it should be noted that following my investigation of Grk2 and βarrestins in Smo ciliary trafficking, two groups published additional data that βarrestin1/2 and Grk2 may mediate vSmo ciliary localization. First, CKIα and Grk2 have been shown to phosphorylate vSmo at multiple phosphorylation sites in the carboxy-terminal tail [128]. They postulate that Hh-induced phosphorylation promotes the binding of βarrestin2 to Smo, and this promotes Smo anterograde trafficking into the cilium. Their data recapitulates my findings that recombinant CKIδ can phosphorylate Smo's cytoplasmic tail in vitro, but they also used a phospho-specific Smo antibody to demonstrate that phosphorylation kinetics increase upon Hh stimulation and ciliary localization. In addition to phosphorylating vSmo, CKIα was shown to localize to cilia and its knockdown blocked Hh pathway activation in C3H10T1/2 cells [128, 142]. Aside from in vitro kinase assays using recombinant CKIδ, the functions of both CKIδ/ε remain unexplored in the literature. Additionally, it has been proposed that Growth Arrest Specific 8 (Gas8), a microtubule associated subunit of the Dynein Regulatory Complex (DRC) cooperates with Grk2 to regulate Smo ciliary localization [143]. Gas8, Grk2 and βarrestin2 morphant

zebrafish exhibit unorganized somite patterning, although this phenotype is very mild compared to *Smo* mutant somites (*Smo*^{S294}) [143].

PKA and CKI have been shown to phosphorylate dSmo's cytoplasmic tail. These kinases recognize consensus sites, RRXS and pSXXS, respectively. Vertebrate Smo lacks putative PKA phosphorylation sites, but possesses one CKI consensus site in the third intracellular loop and three others in the cytoplasmic tail. The three CKI sites in the cytoplasmic tail are conserved in dSmo, while the IC3 site is not. Preliminary data that CKI inhibitors abrogated Hh signaling prompted us to further examine CKI phosphorylation of vSmo. siRNA-mediated knockdown of *CKIα*, *CKIδ* and *CKIε* appeared to phenocopy these results, suggesting that off-target effects were not attributable to this observation [142]. Since CKI inhibitor D4476 preferentially targets CKIδ/ε, recombinant CKIδ phosphorylated Smo substrate, and we observed both CKIδ/ε isoforms at the base of the primary cilium, we believed these isoforms were the kinases responsible for Smo activation [136]. Typically, CKIδ and CKIε have been described as having similar or redundant activities, since they are 87% and 97% identical in their N-terminal and kinase domains, respectively. However, the seven CKI mammalian isoforms share 53-98% identity in their kinase domain and recognize the same consensus site. Thus, it is possible that CKIα and CKIδ/ε may compensate one another [134].

Our data suggests that vSmo can be phosphorylated by recombinant CKIδ, but global phosphorylation does not occur when cells are labeled with ^{33}P in vitro. These discrepant data could be due to experimental artifact and/or experimental limitations. First, in vitro kinase assays can lead to phosphorylation events that are irrelevant to in vivo biology. However, another group has observed phosphorylation of vSmo's

cytoplasmic tail using recombinant CKIδ, validating our data [128]. Second, the majority of our assays involved over-expressed Smo due to the lack of effective endogenous or phospho-specific antibodies. By exogenously expressing Smo, non-relevant levels of protein may have overwhelmed endogenous kinase levels. Thus, phosphorylation may not have been robustly detected. Perhaps co-expression of CKIδ/ε would have mitigated this. However, in contradiction to this, we were able to detect ^{33}P labeling of over-expressed Dvl3-HA. Dvl3 and vSmo are similar in size (90-100kDa) and epitope tag-mediated immunoprecipitation of Dvl3 and Smo appeared to be comparable. Perhaps the inability to detect pSmo-myc could have been due to differences in the exposure times of Wnt and Hh ligand.

Our analyses of Smo phospoho-mutants indicate that single mutations of putative CKI sites do not robustly affect ciliary localization. Graded levels of phosphorylation may dictate subcellular localization and function, so perhaps mutating these residues in tandem is necessary to observe a phenotype. Indeed, Chen et al found that only upon tandem mutation of putative CKIα and Grk2 sites could localization and functional defects be observed [128]. Moreover, it is possible that other phosphorylation sites exist that were not assayed in this study, perhaps since they are vertebrate-specific or non-consensus motifs.

Nevertheless, we found that the phospho-mimetic allele of 2D (T542, T545) abrogated ciliary localization and subsequent activation. The 2D consensus site is located just C-terminal to the oncogenic SmoM2 mutation found in the 7TM (W535L) and just a few amino acids before the ciliary localization domain WR. Although the phospho-dead version of this consensus site did not alter localization or function, perhaps introducing an acidic residue is sufficient to affect conformation and the unknown mechanism that

facilitates Smo ciliary localization. Thus, this mutation builds on existing data that the junction between vSmo's 7TM and the cytoplasmic tail is important for Smo function. It is also possible that this mutant merely fails to exit the ER, since Western analysis demonstrates a lack of the endoH-resistant, presumably post-ER form of the protein. However, this is arguable since its phospho-dead counterpart lacks this band but can still translocate to the cilium. Moreover, SmoM2 has been previously shown to only exhibit the endoH-sensitive form and is constitutively at the primary cilium [45]. Phospho-mimetic mutants 3D (S594, T597) and 4D (S620) constitutively localized to the cilium in the absence of Hh stimulation, but this could be due to high levels of protein. They did not possess an increase in function compared to wild type Smo, further suggesting that a secondary activation step is required after Smo ciliary localization.

We also found that genetic loss of *Grk2* does not preclude vSmo ciliary localization. A recent study proposed that phosphorylation of vSmo by CKIα and Grk2 promotes ciliary accumulation [128]. This difference in data can be attributed to compensation by other Grk isoforms in *Grk2*-/- MEFs, or even other kinases. Indeed, there are seven mammalian Grks, with four (Grk 2,3,5,6) isoforms expressed ubiquitously and the remaining expressed in specific organs (Grk1 and 7 in photoreceptors and Grk4 in the testes, kidney and cerebellum) [144]. Amino acid sequence similarity ranges from 53-93%, thus it is feasible that the loss of Grk2 can be compensated by other Grks.

In argument with this, however, Grk1 and Grk2 are the most divergent among the six mammalian Grk's and *Grk2* -/- mice are embryonic lethal due to cardiac defects. These in vivo data suggests that Grk2's function is not compensated by the other Grk's. So, perhaps another non-Grk kinase can contribute to phosphorylation at these sites. Alternatively, these Grk2 phosphorylation events may represent secondary post-

translational modifications that are not absolutely, or at least initially, required for Smo ciliary localization and function.

We also demonstrated that loss of βarrestin1/2 does not affect vSmo ciliary localization and function. Our data analysis conflicts with a previous report that the βarrestin proteins are required for Smo ciliary translocation [132]. This previous study used siRNA-mediated knockdown of the βarrestin proteins, so perhaps off-target effects contributed to the observed phenotype. Compensation by other arrestin proteins in *βarrestin1/2* double knockout cells is unlikely, since there are four arrestin proteins, with arrestin 1 and 4 being expressed by the photoreceptor rods and cone cells, respectively [145]. Arrestins 2 and 3, known as βarrestin1 and βarrestin2, share 80% similarity and are ubiquitously expressed. Notably, *βarrestin1* and *βarrestin2* mutant mice have been generated, with neither exhibiting overt Hh defects [146, 147]. Both are viable, with *βarrestin1*-/- mice exhibiting a larger cardiac ejection and *βarrestin*2-/- mice demonstrating no tolerance to morphine. Double *βarrestin*1/2 mutants are embryonic lethal, but their phenotype remains poorly characterized. Moreover, as Grk2 has been shown to phosphorylate dSmo, it is worth noting that genetic deletion of the only non-visual βarrestin in Drosophila, kurtz, does not result in a Hh phenotype [127]. Taken together, it is difficult to reconcile these data with published data.

Chimeric analysis of dSmo and mSmo

We observed that dSmo did not localize to the primary cilium in mammalian cells, and consequently did not activate the pathway. This finding has also been observed by Chen et al [83]. Our observation that dSmo could reach the cell surface and could sometimes accumulate at the base of the primary cilium was intriguing, as it demonstrated that the machinery that drives dSmo's cell surface accumulation is present

in vertebrate cells. However, while the unknown mechanism that traffics vSmo to the basal body also recognizes dSmo, the steps required for Smo ciliary entry does not occur. Thus, we anticipated that an analysis of dSmo-mSmo chimeras could shed light on how the two proteins and their connection to the primary cilium have diverged evolutionarily.

Many of our chimeric proteins failed to exit the ER, although we attempted to mitigate this by joining the Drosophila and mouse Smo proteins at domain junction points. ER retention was unsurprising given the hydrophobic nature of Smo's seven transmembrane domains which, if misfolded, could render these chimeric proteins vulnerable to aggregation. We did not include these ER-retained chimeras in our interpretation of data. We found that only one chimera mSmo dSmo IC1-EC1 mSmo behaved like wild type Smo, in that it was able to reach the cilium and cell surface in response to Hh stimulation. This indicates that the region spanning IC1 to EC1 is interchangeable between species. In support of this, dSmo and vSmo possess conserved cysteines in EC1 and EC2 that are necessary for proper conformation and function, and many GPCRs possess cysteines in their EC loops that stabilize receptor conformation [107, 148].

Since both dSmo and vSmo's cytoplasmic tails possess important residues, domains and interaction sites (including a motif required for vSmo ciliary localization [80]), we were particularly interested in how swapping these intracellular domains would affect both cell surface localization and ciliary localization. A membrane tethered dSmo cytoplasmic tail is sufficient to activate low level signaling in Drosophila, presumably by sequestering Cos2 away from Ci [104, 108]. In contrast, a membrane tethered mSmo cytoplasmic tail does not induce the Hh pathway by Gli-luciferase [45]. We observed

that interchanging mSmo's cytoplasmic tail with that of dSmo's created a chimera that effectively reached the cell surface, but not the primary cilium (mSmo dSmo-CTD). This protein was unable to activate the Gli-luciferase reporter, highlighting that ciliary localization is required for Smo function. Varjosalo et al, however, showed that a mSmo with the majority of its cytoplasmic tail replaced with that of dSmo C-terminal was able to induce Gli-luciferase readout, although not as robustly as wild type mSmo [45]. Discrepancies in these data could be attributed to the fact that Varjosalo did not use dSmo's entire cytoplasmic tail. Rather, they only replaced "most of the mSmo C-terminal region with the dSmo C-terminal sequences." Thus, it would be interesting to dissect the non-overlapping sequences of these chimeras to determine the crucial cytoplasmic tail regions necessary for mSmo's function. Conversely, however, a chimera that possesses the region spanning mouse IC3 and CTD (dSmo-ECD-TM5 mSmo) reached the cell surface effectively, but not the primary cilium. These data indicate that this intracellular region is not sufficient to reach the cilium alone, and that other regions within mSmo are required for translocation. For instance, data in zebrafish demonstrate that deletion of the cysteine rich domain within the ECD does not alter ciliary localization, but does abrogate signaling [105]. A mutation within this region, however, does affect zebrafish Smo localization. Thus, perhaps vSmo requires at least two distinct regions for optimal ciliary localization and function.

Supplementary data

Smo dimerization

In addition to vSmo phosphorylation, we also examined dimerization as a potential mechanism of ciliary localization. Smo displays sequence and structural similarity to GPCR proteins. Several GPCRs and their downstream signal transduction have been demonstrated to rely on homo- or heterodimerization. For instance, dimerization of

$GABA_b$ receptor isoforms is necessary for cell surface accumulation and downstream signal transduction, and dimerization of Frizzled3 correlates with activation of the Wnt pathway in Xenopus embryos [149, 150]. Moreover, the prototypical GPCR, rhodopsin, functions at a specialized primary cilium of retinal rod cells, and atomic force microscopy revealed that native rhodopsin forms rows of dimers, as well as higher order complexes, within the expanded ciliary tip [151]. How dimerization correlates with function remains unclear, but this structural arrangement may be pertinent to GPCR activation at the primary cilium [152]. More recently, dimerization has been implicated in dSmo activation. Arginine-rich clusters in dSmo's cytoplasmic tail are believed to maintain intramolecular electrostatic interactions that keep dSmo in an inactive conformation [115]. Hh-induced phosphorylation at multiple serine/threonine residues in dSmo's cytoplasmic tail antagonizes this interaction and allows dSmo to undergo a conformational switch. This leads to dimerization of dSmo cytoplasmic tails at the cell surface, which is necessary for downstream signal transduction. While vSmo contains arginine-rich clusters within its cytoplasmic tail, this study found that forced clustering of the tails alone was insufficient to activate the pathway. However, it is possible that other domains, such as the extracellular domain or intracellular loops, mediate homotypic interactions.

Preliminary evidence suggested that wild type Smo may self-associate specifically in response to Shh stimulation in NIH3T3 cells. When wild type Smo-myc and Smo-HA were co-expressed, immunoprecipitation of myc specifically pulled down Smo-HA only in the presence of Hh stimulation. Notably, CLDSmo-HA failed to associate with WT Smo-myc, suggesting that homotypic interaction may occur specifically at the primary cilium (**Figure 12a**, unpublished data K. Corbit). To examine if dimerization is sufficient for Smo ciliary localization, we utilized a rapamycin-based system that conditionally

dimerizes two proteins of interest [153]. Briefly, rapamycin is a macrolide antibiotic that simultaneously binds to FK506 binding protein (FKBP) and the 89 amino acid domain of mammalian target of rapamycin (mTOR), known as the FKBP-rapamycin binding domain (FRB). Rapamycin can therefore dimerize two proteins that are fused to FKBP and the FRB domain (**Figure 12b**). As expected, wild type Smo-FKBP and Smo-FRB both localize to the cilium in response to Hh stimulation, while CLDSmo-FRB did not (**Figure 12d**). To determine if rapamycin induces interaction between Smo-FKBP and Smo-FRB, we co-transfected Smo-FKBP and Smo-FRB into NIH 3T3 cells and performed reciprocal IP's for HA and Myc. While untreated and Hh stimulated IP's appeared to pull down co-transfected proteins perhaps non-specifically due to the hydrophobic nature of over-expressed Smo, rapamycin treatment specifically induced interaction with post-ER Smo (**Figure 12c**). Interaction appeared most robust after 2 and 8 hour time points, but less so after thirty minutes and 12 hours. However, by immunofluorescence, 2 hour exposure of rapamycin did not induce wild type Smo-FKBP or Smo-FRB translocation to the cilium independent of Hh stimulation. Moreover, rapamycin did not induce ciliary localization of CLDSmo-FRB in the presence of Hh stimulation and WT Smo-FKBP, suggesting that forced dimerization with a wild type allele is not sufficient to rescue ciliary defectiveness (**Figure 12d**).

These data do not eliminate the possibility that vSmo proteins form homotypic interactions. As an artificial system that relies on pharmacological treatment, this experimental approach may not be ideal. FRET between two differentially-tagged Smo molecules may offer a more quantitative approach that can distinguish between cytoplasmic, cell surface and ciliary dimerization.

Generation of CKIδ-/- CKIε-/- mice

No vertebrate genetic analyses have assessed the combinatorial function of CKIδ/ε in vivo. To determine if CKI plays a role in Hh signaling in mice, we obtained *CKIδ* and *CKIε* heterozygous mice (a gift from L. Ptacek). In both mammals and Drosophila, CKI isoforms have been shown to function in circadian rhythm, as they regulate the circadian phosphorylation of the period protein PER [134]. In mice, mutations in *CKIδ* have been associated with familial advanced sleep phase syndrome and CKI has been associated with pathological accumulation of tau in several neurodegenerative diseases [154, 155]. *CKIδ* -/- mice are perinatal lethal due to unknown causes (Conde 2008, Weaver Lab, thesis). *CKIε* -/- mice are viable and fertile, and despite a lengthened circadian period, display no overt deleterious phenotype [156]. Furthermore, CKIδ/ε have been shown to propagate Wnt signals. *CKIε* mRNA injection induced body axis duplication in *Xenopu*s embryos, while injection of a kinase dead version caused defects in convergent extension during gastrulation [157]. Over-expression of dbt (Drosophila CKIδ/ε) leads to Wnt hyper-activation [158].

We first generated trans-het mice, *CKIδ*+/- *CKIε*+/-, which were born at expected Mendelian ratios. By crossing trans-hets, we hoped to assess the phenotypes of the following genotypes: *CKIδ*+/- *CKIε*-/-, *CKIδ*-/- *CKIε*+/-, CKIδ-/- *CKIε*-/-. At birth, no mutant animals with these genotypes were discovered. We found stillborn *CKIδ*-/- animals, which echoed previous reports that these knockout mice are perinatal lethal. At e8.5-9, we found embryos with *CKIδ*-/-, *CKIε*-/- and *CKIδ*+/- *CKIε*-/- genotypes, with all mutants resembling control littermates, with no obvious developmental defects. No *CKIδ*-/- *CKIε*-/- double knockout mice were obtained, perhaps due to early convergent extension defects. Given the low percentages of genotypes of interest, this study did not yield any conclusive results.

Materials and Methods

Constructs and cloning

Wild type Smo-myc and CLDSmo-myc are described previously [80]. pGE Smo-myc was used to generate all modified mouse Smo plasmids, and BluScript-dSmo was a gift from T. Kornberg. The latter was cloned into pCMV Tag1 to generate pCMV dSmo-myc. To generate dSmo-mSmo chimeras, all relevant sequences were amplified by high fidelity PCR and sub-cloned using TOPA vector (Invitrogen). All amplified products were sequence verified.

Transfections

NIH 3T3 cells were grown in DMEM H21 supplemented with 10% calf serum and pen/strep. For DNA transfections, cells were transfected with JetPrime per manufacturer's instructions. 24 hours post-transfection, cells were starved for an additional 18 hours in Optimem containing 1% FBS and pen/strep. Commercial *CKI* siRNA transfections were performed using siRNA and transfection reagent (Santa Cruz Biotechnology) according to the manufacturer's instructions.

Pharmacological reagents

The following reagents were used for both immunofluorescence and functional assays: D4476 (Calbiochem, 10μM); Recombinant Hh (R&D Biosystems, 1μM) or Hh-conditioned media; cyclopamine (EMD Biosciences, 10μM); Rapamycin (Sigma, 50nM); IC261 (Calbiochem, 10μM); Grk2 inhibitor (Calbiochem, 10μM). 1 hour Hh stimulation was used for immunofluorescence assays, while 18 hour treatments were used for activity assays.

Gli-luciferase assay

For drug treatment assays, Shh-Light2 cells were obtained from ATCC, and plated in triplicate in 24-well plates. These NIH 3T3 cells stably express Gli-luciferase report (eight tandem Gli binding sites driving luciferase) and a control plasmid, pRLTK. At confluence, cells were starved in Optimem supplemented with 1% FBS and pen/strep for 18hrs with or without pharmacological inhibitors/Hh for 18 hours. Cells were assayed by Dual Luciferase Reporter Kit (Promega), as described previously [80].

For Smo transfections, *Smo*-/- MEFs (a gift from J. Taipale) were transfected with JetPrime per manufacturer's instructions in DMEM H21 supplemented with 10% FBS and pen/strep. DNA was comprised of 50% construct of interest, 40% Gli-luc and 10% pRLTK. 24 hours post-transfection, cells were starved in Optimem for and additional 18 hours with or without Hh stimulation. Cells were assayed by Dual Luciferase Reporter Kit (Promega), as described previously [80].

Immunofluorescence

Cells were fixed for 7 minutes in 4% PFA, washed in PBS and incubated in PBS with 0.1% Triton X-100 (PBST) for 20 minutes. Cells were then blocked in 2% BSA in PBS for 1 hour at 4C, and then incubated overnight with primary antibody at 4C. The next day, cells were washed in PBS, incubated in Alexafluor (Invitrogen) secondary antibody for 1hr at room temperature and mounted with either Vectashield Hardset with DAPI. Images were acquired on a Nikon C1 confocal.

For cell surface localization studies, the same antibodies and incubation times were used, but N-terminal antibodies were introduced prior to detergent permeabilization. Following the addition of secondary antibody to the N-terminal antibodies, cells were

washed with PBS, then permeabilized with 0.1% Triton X-100 in PBS. A second round of immunofluorescence was performed to detect intracellular proteins.

Antibodies used for immunofluorescence include: c-myc (Santa Cruz, 1:1000); myc (Covance, 1:1000); HA (Roche, 1:500); acetylated tubulin (Sigma,1:1000); glutamylated tubulin (Chemicon, 1:500); Calnexin (a gift from M. von Zastrow, 1:500); CKIε (Santa Cruz H-60, C-20, R-19, 1:200); CKIδ (Santa Cruz C-18, R-19, 1:200); CKIα (Santa Cruz C-19, 1:200); Grk2 (Abcam 1:500); Grk5 (Santa Cruz, 1:200); βarrestin (a gift from R. Lefkowitz, 1:200); dSmo Antibody (a gift from T. Kornberg, 1:50).

Western blots

Cells were lysed with buffer containing 50mM Tris-HCl (pH 7.4), 0.5% NP-40, 0.25% NaDoc, 150mM NaCl and fresh protease (Calbiochem) and Halt phosphatase (Pierce) inhibitors. Lysates were cleared at 13.2k rpm for 10 minutes and protein concentration was quantified by Bradford assay. Antibodies for western include: c-myc (Santa Cruz, 1:1000); HA (Roche, 1:500); Grk2 (Abcam 1:500); actin (Sigma, 1:5000); secondary antibodies (Jackson Immuno) 1:10000

Quantitative PCR

RNA was extracted using Rneasy Plus (Qiagen). cDNA synthesis was performed using First Strand cDNA Synthesis Kit (Fermentas). Transcript levels were measured in quadruplicate using a 7300 Real-time PCR machine (Applied Biosystems) and normalized to relative βactin transcript. Primer sequences are: βactinF 5'-CACAGCTTCTTTGCAGCTCCTT-3' and βactinR 5'-CGTCATCCATGGCGAACTG-3'; Gli1-F 5'GGTGCTGCCTATAGCCAGTGTCCTC-3' and Gli1-R 5'-GTGCCAATCCGG TGGAGTCAGACCC-3'.

In vitro kinase assays using recombinant kinase and immunoprecipitated Smo

Wild type *Kif3a* cells were transfected with Smo-myc and lysed 48 hours post-transfection in buffer containing 50mM Tris-HCl (pH 7.4), 0.5% NP-40, 0.25% NaDoc, 150mM NaCl and fresh protease (Calbiochem) and Halt phosphatase (Pierce) inhibitors. Lysates were cleared at 13.2k rpm for 10 minutes and protein concentration was quantified by Bradford assay. 500µg of total cell lysate was immunoprecipitated with 2µg rabbit myc (Sigma, A7470) overnight, and captured with rProtein G-agarose beads (Invitrogen). Washed beads were subjected to the following 50µl reaction for 45 minutes at 30C with frequent vortexing: 10ul 5x kinase buffer, 5uM cold ATP, 5uC hot ATP, 1500 units of CKIδ (NEB). Reactions were stopped with 6x loading buffer, run out on 7% SDS-PAGE and assessed by autoradiography.

In vitro kinase assays using recombinant kinase and substrate

A total volume of 25µl was used. 15µl of cold reaction buffer (5µl of 5x kinase buffer and 10µl water) was added to 10µl of hot reaction buffer (5µM cold ATP, 500ng substrate, 5µC hot ATP, water to 10µl) containing either 7.5ng of Grk5 (Upstate) or 1500 units of CKIδ (NEB). Reactions were incubated at 30C for 30 minutes and stopped with 6x loading buffer, run out on 7% SDS-PAGE and assessed by autoradiography. Inhibitors or DMSO vehicle were added directly to in vitro kinase reactions: D4476 and IC261 (10µM, 50µM, 100µM).

^{33}P cell labeling

Cells were transfected with Smo-myc or Dvl3-HA in 10cm dishes with JetPrime according to the manufacturer's instructions. 24 hours post-transfection, cells were washed once in PBS and starved overnight with Optimem supplemented with 1% FBS

and pen/strep. 18 hours later, cells were washed in HBSS (Gibco) and treated with low phosphate/low serum media (DMEM without glutamine, phosphate supplemented with 2% FBS, pen/strep, HEPES) containing ^{33}P (0.1mCi/ml) and either recombinant Hh (1μM) or vehicle control (DMSO) for 1 hour. Cells were washed in TBS, lysed as described above, and pre-cleared with rProtein G-agarose beads (Invitrogen) for 30 minutes at 4C. Immunoprecipitation was performed overnight with 2μg of mouse 9E10 antibody (Santa Cruz) or 2μg of rat HA (Roche), followed by antibody capture with rProtein G-agarose beads. Pelleted beads were washed three times in lysis buffer and resuspended in 20μl of 3x sample buffer. Samples were run on a 7% SDS-PAGE gel and detected by autoradiography. Control lysate was run in parallel for Western blot detection of myc.

Acknowledgements

We thank L. Ptacek for CKI constructs and *CKI* mice, N. Freedman for *Grk2* cell lines, R. Lefkowitz for βarrestin2 antibody and *βarrestin1/2* cell lines, J. Taipale for *Smo*-/- MEFs and T. Kornberg for dSmo cDNA and sequencing primers.

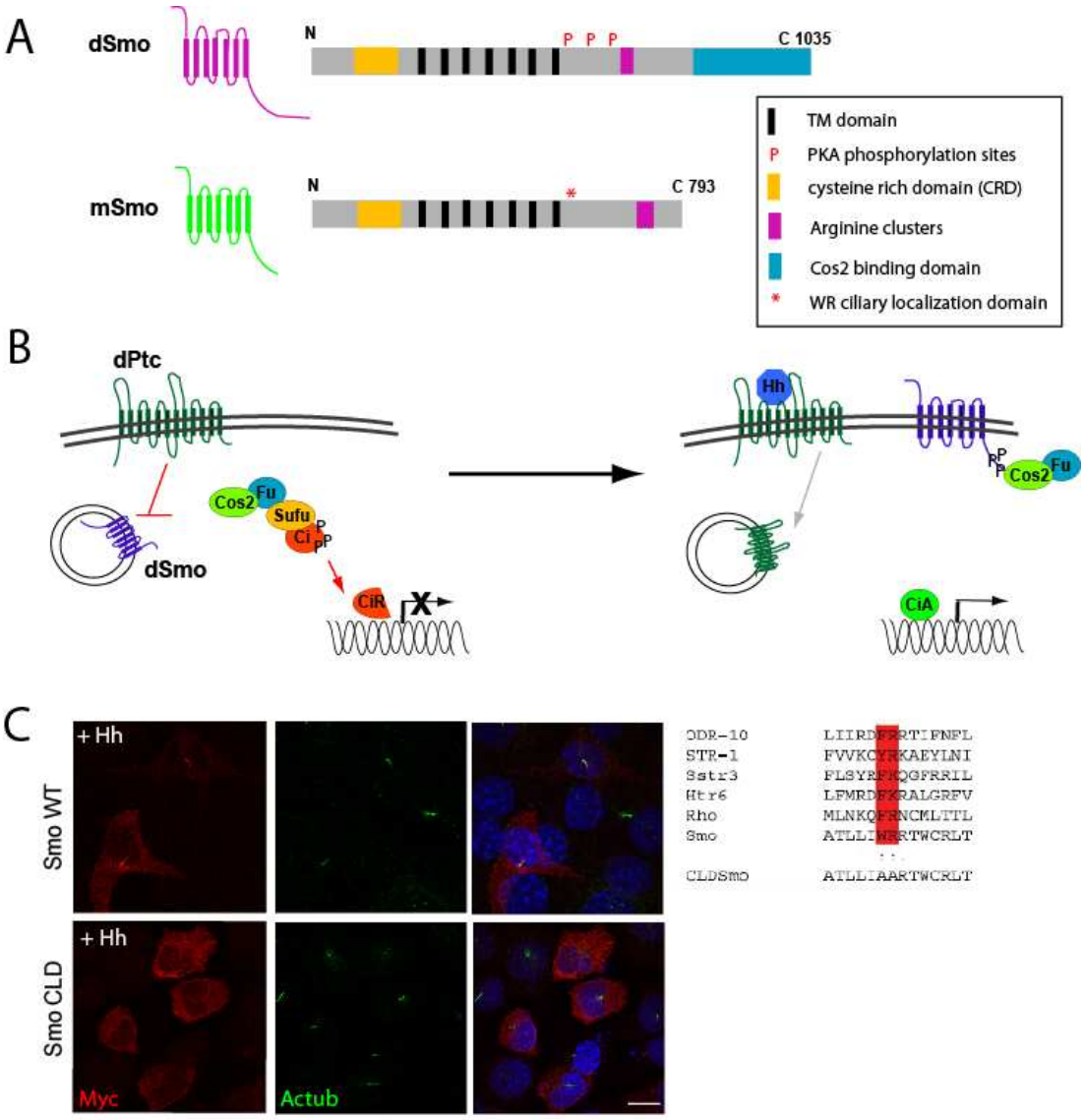

Figure 5. Drosophila and vertebrate Smo possess different mechanisms of activation.

(A) Structural similarities and differences between Drosophila Smo and vertebrate Smo. Smo is structurally characterized by an N-terminal extracellular domain (ECD), seven transmembrane (TM) domains and a C-terminal cytoplasmic tail. The ECD contains a conserved cysteine-rich domain, while the cytoplasmic tails are highly divergent between dSmo and vSmo. Several dSmo post-translational modifications and protein interactions are mediated by this region. Ciliary localization of vSmo required a small hydrophobic motif that is just C-terminal to the 7TM. **(B) Drosophila Hh signaling requires opposite changes in the turnover and subcellular localization of Ptc and dSmo.** In the absence of Hh ligand, Ptc localizes to the cell surface while Smo remains in intracellular vesicles. Fused, Sufu and Cos2 form a complex with Ci to promote its phosphorylation by PKA, CKI and GSK3. Phosphorylation marks Ci for partial proteolysis into the repressor form, CiR. In the presence of Hh ligand, Ptc is internalized and dSmo accumulates at the cell surface. Phosphorylation of dSmo is believed to induce a conformational change that promotes dSmo interaction with Cos2 and Fused. Ci is then freed of the processing machinery, and full length CiA can activate target genes. **(C) Hh-dependent translocation to cilia is essential for vSmo activity.** In the presence of Hh ligand (1μM, 1hr), vSmo (myc, red) robustly localizes to the primary cilium (actub, green) in NIH 3T3 cells (DAPI, blue). Scale bar ~10μm. This subcellular translocation depends upon a conserved hydrophobic and basic residue sequence homologous to a domain previously shown to be required for the ciliary localization of seven-transmembrane proteins in worms (adapted from [80]).

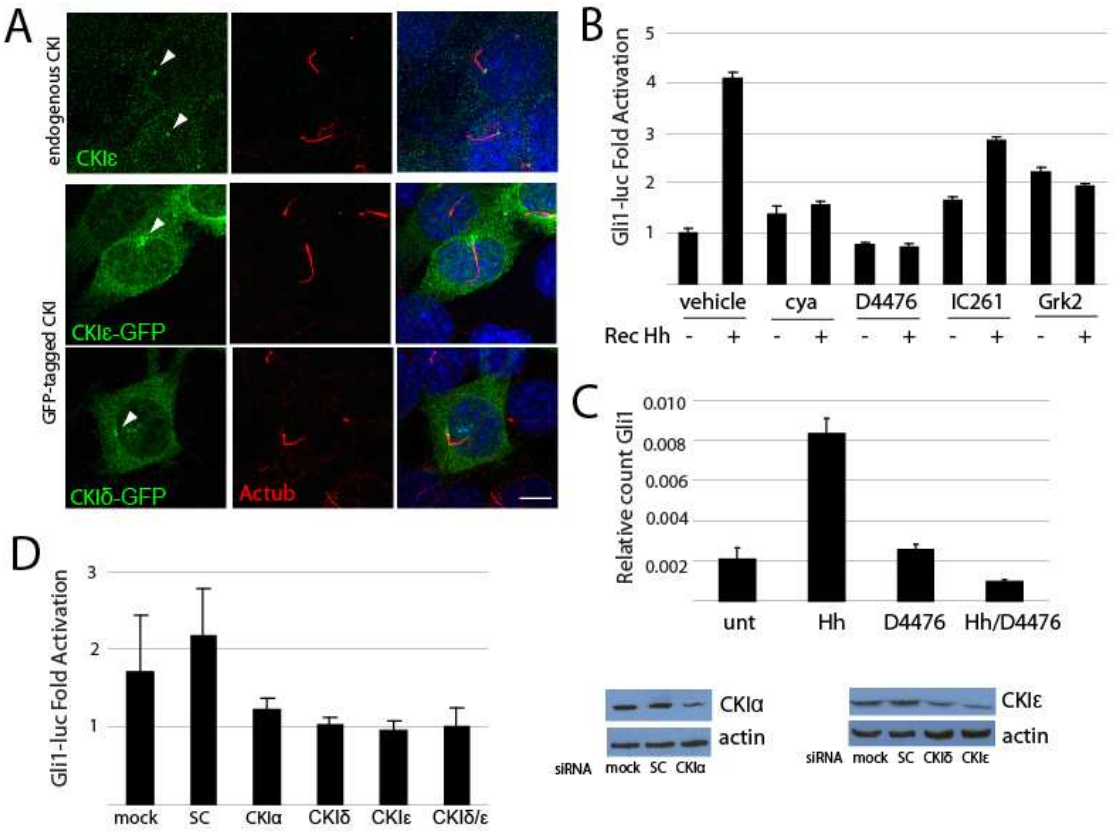

Figure 6. CKIδ/ε localize to the basal body and CKI inhibition abrogates Hh signaling.

(A) CKIδ and CKIε localize to the basal body. Endogenous CKIε (green) was detected at the basal body from which the primary cilium (actub, red) extends (top panel). GFP-tagged versions of both CKIδ and CKIε (green) also accumulate at the base of the primary cilium (actub, red) in transiently transfected NIH 3T3 cells (bottom two panels). White arrows indicate basal body accumulation. Scale bar ~5μm. **(B) Pharmacological inhibition of CKI leads to Hh pathway abrogation.** Shh-Light2 cells, which are NIH 3T3 cells stably expressing a Gli-luciferase reporter and control plasmid pRLTK, were treated for 18 hours with Hh (1μM), cyclopamine, D4476 (10μM), IC261 (1μM) and a Grk2 inhibitor (10μM). While D4476 and cyclopamine negatively affected luciferase readout, IC261 and Grk2 inhibitor exhibited a less drastic effect. **(C) D4476 abrogates *Gli1* transcript levels by qRTPCR.** *Gli1* transcript levels (normalized to actin) by qRTPCR were assessed in NIH 3T3 cells following Hh stimulation and D4476 treatment. **(D) siRNA knockdown of CKIδ/ε decreases Hh-mediated pathway activation.** Hh responsiveness was assayed in the presence of CKIδ and CKIε siRNA in Shh-Light2 cells. Knockdown was inefficient, as determined by Western blot.

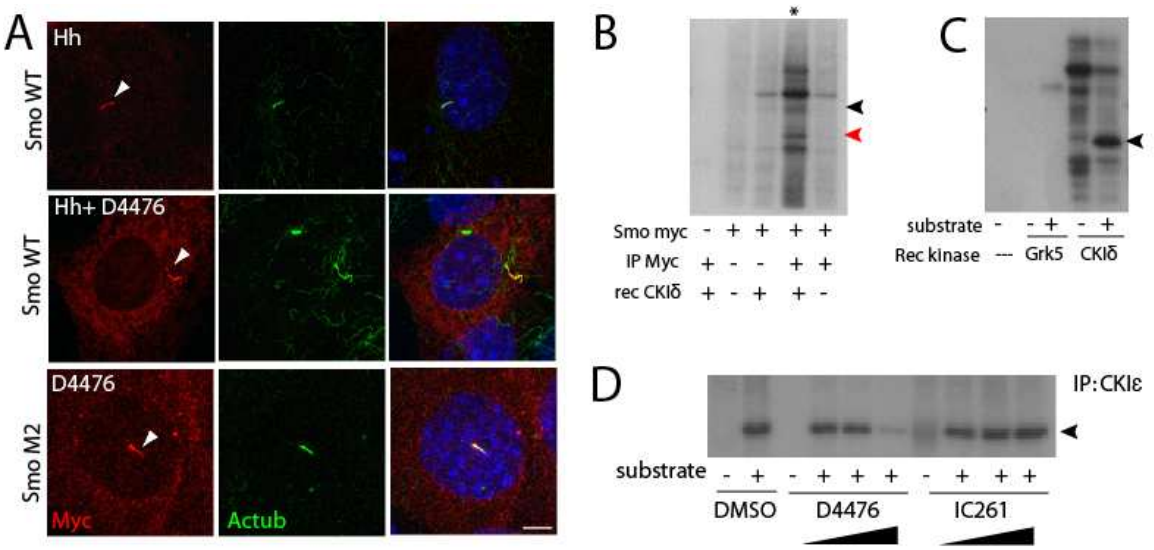

Figure 7. CKIδ/ε can phosphorylate Smo *in vitro*.
(A) Over-expressed Smo ciliary localization is not perturbed by D4476. Wild type and oncogenic vSmo, Smo WT and SmoM2 (myc, red), were transiently expressed in NIH 3T3 cells and treated with Hh ligand and CKI inhibitor D4476 (10μM). Both Smo WT and Smo M2 reached the primary cilium (actub, green), as indicated by white arrows. Scale bar ~5μm. **(B) Recombinant CKIδ may phosphorylate Smo-myc.** Smo-myc was immunoprecipitated from transiently transfected NIH 3T3 cells and subjected to an in vitro kinase assay using recombinant CKIδ kinase (NEB). Two bands were detected in the experimental lane (*myc IP + CKIδ) and may correspond to two Smo-myc forms that represent Smo's glycosylation states. EndoH-sensitive (red arrow), EndoH-resistant (black arrow). Faint bands of the same size are observed in control lanes 3 and 5. **(C) Recombinant CKIδ, but not Grk5, phosphorylates Smo C-tail.** Purified mSmo cytoplasmic tail was used as a substrate with recombinant CKIδ and Grk5 kinase (NEB). Whereas CKIδ robustly phosphorylates mSmo cytoplasmic tail (black arrow), Grk5 does not. **(D) High concentration of D4476 diminishes CKI-mediated phosphorylation of Smo's C-tail.** Immunoprecipitated CKIε can phosphorylate purified Smo's cytoplasmic tail (black arrow). In the presence of increasing levels of D4476 but not IC261, phosphorylation of the substrate is prevented. D4476 and IC261 were used at 10μM, 50μM and 100μM.

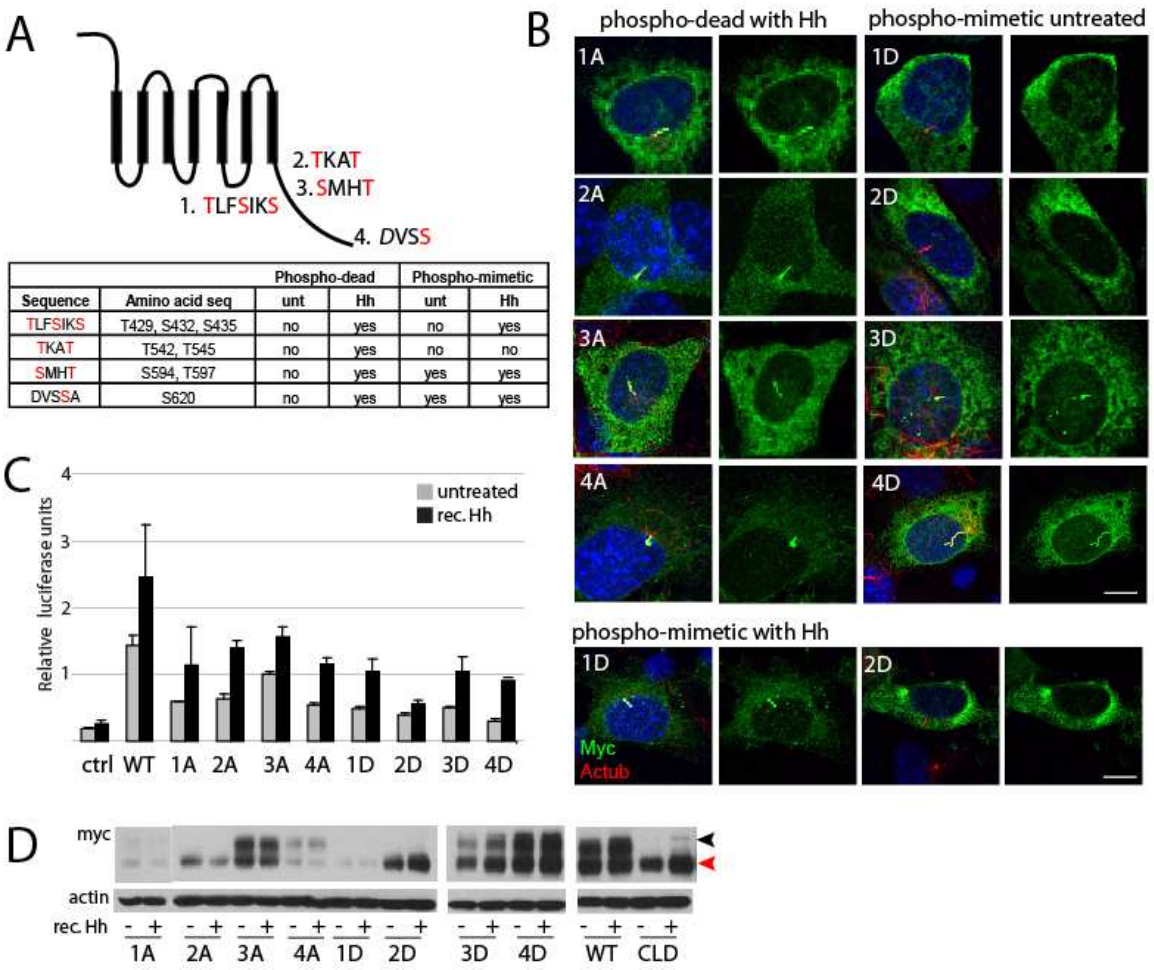

		Phospho-dead		Phospho-mimetic	
Sequence	Amino acid seq	unt	Hh	unt	Hh
TLFSIKS	T429, S432, S435	no	yes	no	yes
TKAT	T542, T545	no	yes	no	no
SMHT	S594, T597	no	yes	yes	yes
DVSSA	S620	no	yes	yes	yes

Figure 8. Mutation of putative CKI sites affects Smo function, but not localization.
(A) vSmo contains four putative CKI sites. vSmo contains CKI phosphorylation consensus sites, described as pS/T-X-X-S/T. One of these sites (4) possesses an aspartic acid in place of the first phospho-residue. The table specifies amino acid sequences and locations, and summarizes ciliary localization of phospho-mutants in the presence and absence of Hh stimulation. **(B) Ciliary localization varies among phospho-mutant Smo alleles.** Smo constructs (myc, green) were transiently transfected in NIH 3T3 cells and assessed for ciliary localization by immunofluorescence. All phospho-dead alleles reached the cilium (actub, red) in response to ligand, behaving similarly to wild type Smo. Phospho-mimetic alleles 3D and 4D were found to localize to the cilium in the absence of Hh signaling, while 1D and 2D were not. Upon Hh stimulation, the former reached the cilium, while the latter did not. Scale bar ~5μm. **(C) Phospho-mimetic Smo alleles 2D and 4D display altered function.** Myc-tagged Smo constructs were transfected in Smo-/- MEFs and assayed for activity potential by Gli-luciferase reporter. All mutants activated the pathway, except phospho-mimetic mutant 2D. **(D) Phospho-mutants are expressed at varying levels, and some may be retained in the ER.** NIH 3T3 cells were transiently transfected and myc expression was assessed by Western blot of total lysate. Actin was used as a loading control. Some mutants do not readily exhibit the endoH resistant, post-ER form (black arrow). All mutants exhibited expression of the endoH-sensitive form (red arrow).

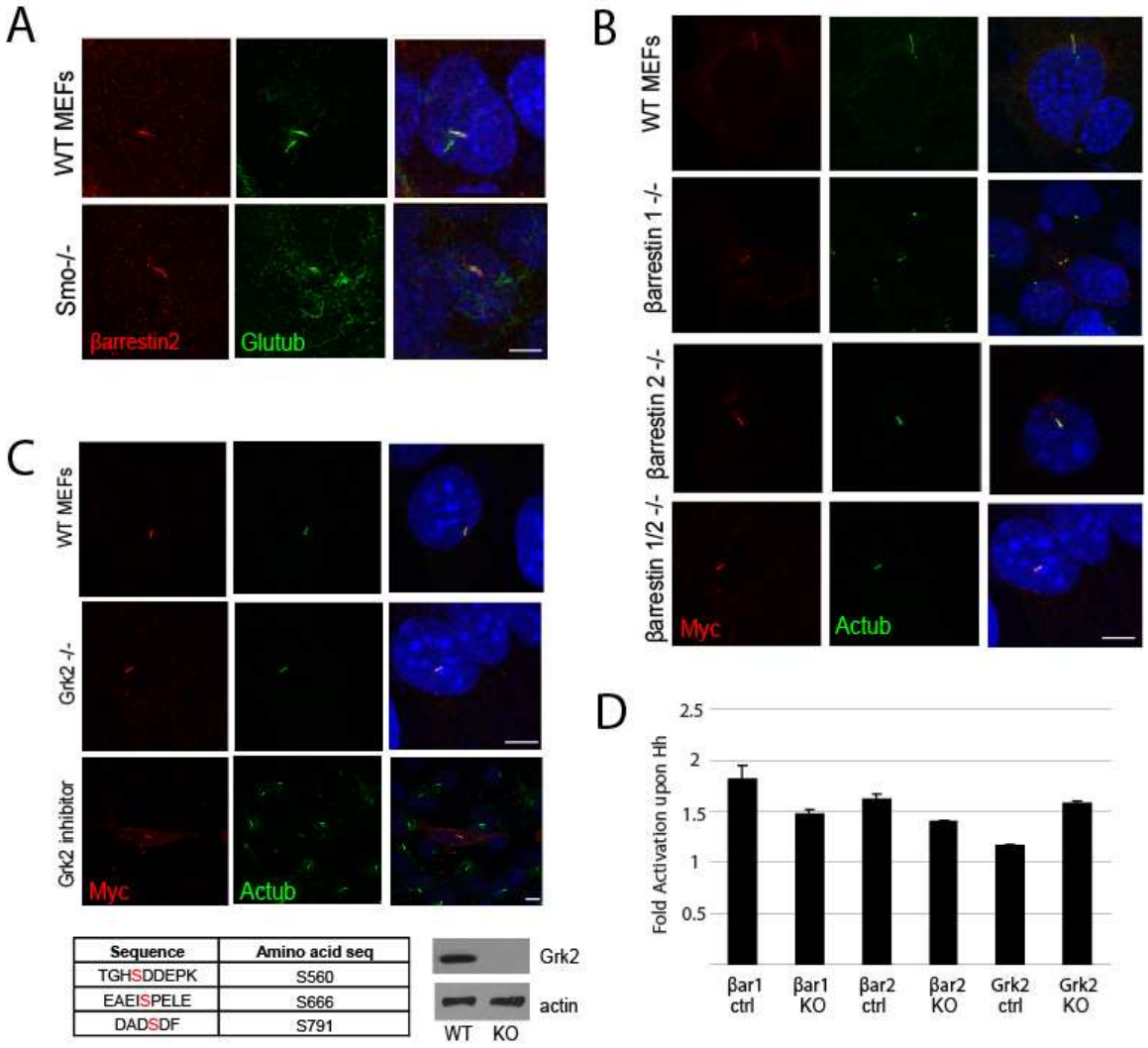

Figure 9. βarrestin1/2 and Grk2 are dispensable for Smo localization and function.
(A) *β*arrestin2 localizes to cilia independent of the Hh pathway. Wild type and *Smo*-/- MEFs were probed for endogenous βarrestin2 (red) and primary cilia (glutamylated tubulin or glutub, green). **(B) Smo ciliary localization is intact in mutant *β*arrestin cell lines.** Myc-tagged wild type Smo (red) transfected into *βarrestin1*-/-, *βarrestin2*-/- and *βarrestin1/2*-/- MEF lines. Ciliary localization was assessed by co-localization with actub (green). **(C) Smo ciliary localization is intact in Grk2-/- cell lines and upon treatment with a Grk2 inhibitor.** Wild type Smo possesses putative Grk2 phosphorylation sites, described as S/T embedded in acidic environments. Smo-myc (red) was transfected in Grk2-/- MEFs, which were confirmed by Western blot for Grk2 protein. Smo ciliary localization was also assessed upon treatment with a Grk2 pharmacological inhibitor (10μM). All scale bars ~5μm. **(D) Hh signaling is functionally intact in mutant *β*arrestin and Grk2 MEFs.** *βarrestin1*-/-, *βarrestin2*-/-, *βarrestin1/2*-/- and *Grk2*-/- MEF lines were assessed for *Gli1* levels by qRTPCR following 18 hour stimulation with Hh ligand. *Gli1* transcript levels were normalized to actin.

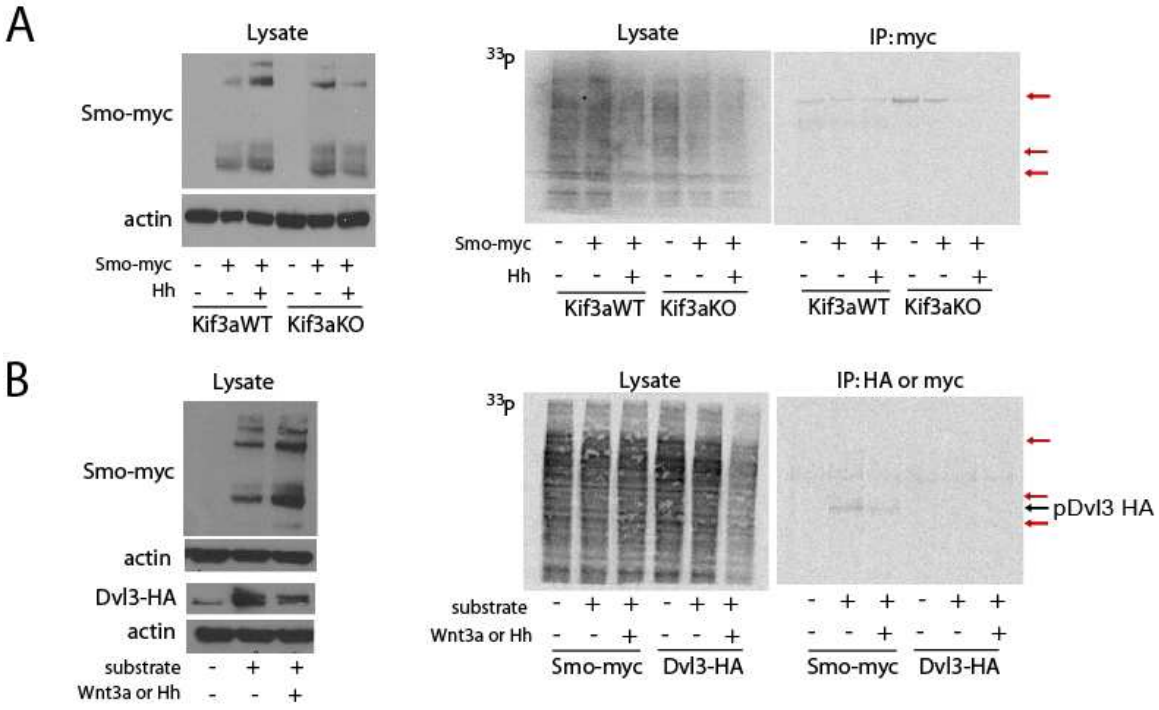

Figure 10. Smo is not phosphorylated by ^{33}P in vitro.
(A) ^{33}P of Smo-myc in ciliated and non-ciliated cells. Cells were transfected with Smo-myc and exposed in culture to ^{33}P (0.1mCi/ml) and Hh ligand (1μM) for one hour. After labeling, cells were lysed and expression was confirmed by Western blot for myc. Following immunoprecipitation by myc and SDS-PAGE on a 7% gel, we assessed phosphorylation of Smo-myc by autoradiography. Phosphorylated Smo-myc was not detected, where red arrows indicate endoH-sensitive, endoH-resistant Smo forms and aggregates of expected ^{33}P-labeled Smo. **(B) ^{33}P labeled Dvl3-HA, but not Smo-myc.** Dvl3-HA, a known phosphorylated substrate of the Wnt pathway, was used as a positive control for ^{33}P labeling, as above. ^{33}P labeled endogenous Dvl3 and HA-tagged Dvl3 with and without Wnt stimulation (black arrow). Smo-myc (red arrows), however, remained unlabeled by ^{33}P in the absence and presence of Hh stimulation.

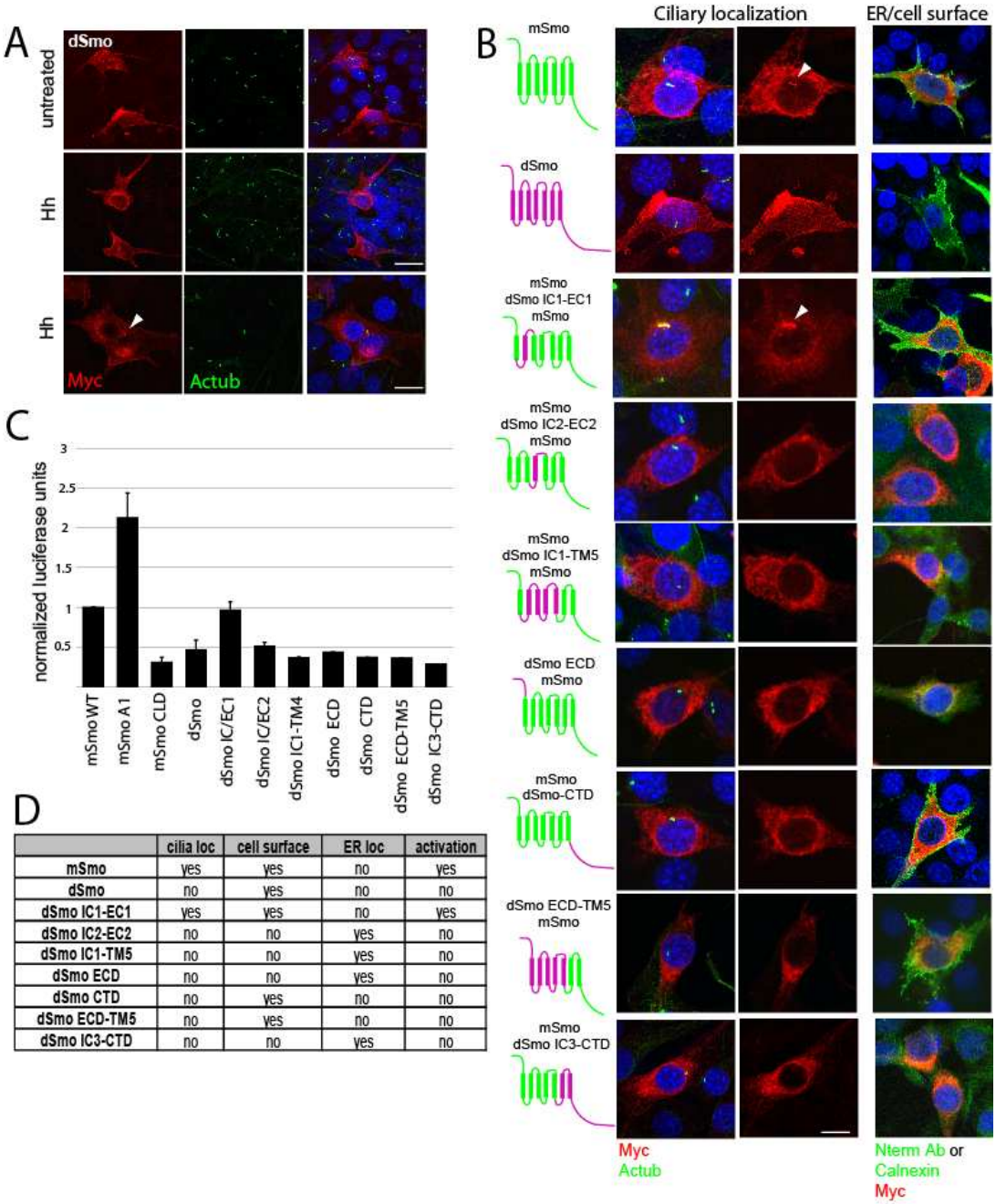

	cilia loc	cell surface	ER loc	activation
mSmo	yes	yes	no	yes
dSmo	no	yes	no	no
dSmo IC1-EC1	yes	yes	no	yes
dSmo IC2-EC2	no	no	yes	no
dSmo IC1-TM5	no	no	yes	no
dSmo ECD	no	no	yes	no
dSmo CTD	no	yes	no	no
dSmo ECD-TM5	no	yes	no	no
dSmo IC3-CTD	no	no	yes	no

Figure 11. Localization and functional analyses of dSmo-mSmo chimeras
(A) dSmo does not reach the cilium. dSmo-myc (red) was transiently transfected in *Smo*-/- MEFs and assessed for ciliary localization (actub, green) in the absence and presence of Hh ligand. Scale bar ~20μm. dSmo accumulation near the base of the cilium also occurred (white arrow), independent of Hh stimulation. Scale bar ~10μM. **(B) Localization analysis of dSmo mSmo chimeras.** We built a panel of dSmo-mSmo chimeric proteins (myc, red) and determined localization by immunofluorescence. We determined each chimera's ability to reach the cilium (actub, green), exit the ER by co-localization with the ER protein calnexin (green). The ability to reach the cell surface was accomplished by staining with an antibody against the extracellular N-terminus (green) prior to cell permeabilization. For dSmo, we obtained an antibody which recognized the ECD of dSmo's N-terminus, and mSmo was dually tagged on the N-terminus by HA and the C-terminus by myc. Scale bar ~5μm. **(C) dSmo and chimeras are not functional in mammalian cells.** Wild type and chimeric proteins were transfected in *Smo*-/- MEFs and assessed for activation potential by Gli-luciferase readout. Activation was observed with the only chimera that could reach the primary cilium, dSmo IC/EC1 (white arrow). **(D) Summary of chimera analysis.**

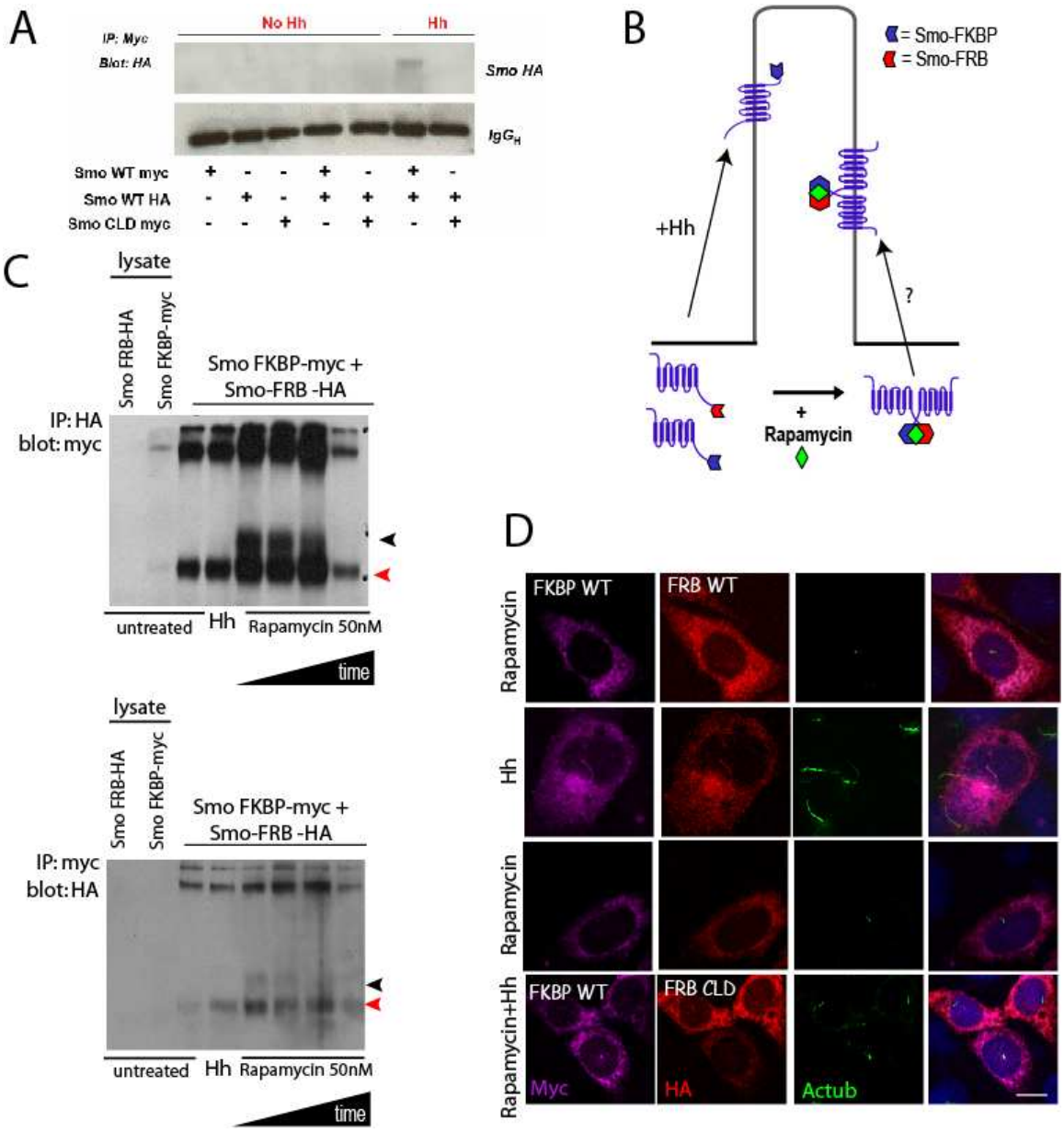

Figure 12. Rapamycin-induced dimerization of vSmo

(A) Wild type Smo may self-associate specifically in response to Shh stimulation. When WT Smo-myc and Smo-HA were co-expressed, immunoprecipitation of myc specifically pulled down Smo-HA only in the presence of Hh stimulation. CLDSmo-HA failed to associate with WT Smo-myc, suggesting that homotypic interaction may occur specifically at the primary cilium (unpublished data K. Corbit). **(B) Hypothesis that rapamycin-induced dimerization can promote Smo ciliary localization.** Rapamycin simultaneously binds FKBP and FRB, and can therefore dimerize two proteins that are fused to FKBP and the FRB domain. We hypothesized that Smo dimerization would be sufficient to induce Smo ciliary localization in the absence of Hh stimulation. **(C) Rapamycin induces an interaction between Smo-FKBP and Smo-FRB.** Smo-FKBP and Smo-FRB were co-transfected into NIH 3T3 cells and subjected to reciprocal IP's for HA and Myc. While untreated and Hh stimulated IP's appeared to pull down co-transfected proteins perhaps non-specifically due to the hydrophobic nature of over-expressed Smo, rapamycin treatment (30min, 2,8,12 hours) specifically induced interaction with post-ER Smo (black arrow). **(D) Rapamycin does not induce Smo ciliary localization in the absence of Hh stimulation.** NIH 3T3 cells were transfected with wild type Smo-FKBP (myc, purple) or Smo-FRB (HA, red). Ciliary localization (actub, green) upon Hh stimulation and rapamycin treatment (50nM, 2 hours) was assessed by immunofluorescence. Scale bar ~5μm.

Chapter III.

The Floxin system: a useful tool to examine Gli2 subcellular dynamics

Abstract

Gli2 is the primary transcriptional activator of the Hh pathway and has been shown to be enriched at the primary cilium, particularly upon pathway activation. Our lab has previously introduced the Floxin system which efficiently targets and modifies gene trapped loci in mouse embryonic stem cells (mESCs). Here, we demonstrate Floxin of the *Gli2* locus with a GFP-tagged allele. Floxin Gli2-GFP behaves similarly to the wild type allele, in that ciliary dynamics and relevant protein interactions are maintained. To assess germline competency, we generated a mouse model using these genetically modified mESCs. We show, that this allele acts as a hypomorph in vivo and some developmental defects associated with abnormal Hh signaling are penetrant. Nevertheless, this system provides a useful tool to examine Gli2 dynamics and function in vitro and in vivo.

Introduction

The analysis of gene function can be achieved by gene knock-out and knock-in strategies, both of which rely on the manipulation of mouse embryonic stem cells. Knock-out approaches are primarily used to examine loss of function consequences and have traditionally been accomplished by transgene insertion, homologous recombination, or gene trapping. Knock-in studies, on the other hand, enable more precise manipulation of a particular gene, and can be designed to maintain transcriptional control by the endogenous locus and its cis-acting elements. In addition to gene disruption, knock-in approaches can be used to investigate expression patterns by reporter fusion or epitope tagging, functional divergence by insertion of a related gene, or modeling of human disease by introduction of specific mutations [159].

Our lab has previously introduced the flanked *lox* site insertion, or Floxin, system, a recombinase-mediated cassette exchange knock-in technology [160]. Floxin is compatible with gene trap cell lines derived from pGTLxf and pGTLxr vectors, and over 24,000 Floxin-compatible cell lines have been generated by BayGenomics and Sanger Institute to date [161]. This technology targets and modifies gene trap loci using the shuttle vector pFloxin and Cre-recombinase, and enables directional and irreversible insertion of defined cDNA sequences. We have previously demonstrated how the Floxin method can be used to biochemically isolate tagged proteins, model human genetic mutations and elucidate protein function and subcellular localization [162]. The gene trap and Floxin method is briefly summarized below (**Figure 13**):

a) Gene trap: A pGTLxF or pGTLxR gene trap is introduced into an intron of a given autosomal gene of interest (GOI) in mESCs. This results in a GOI-βgeo fusion

protein from the gene trapped allele, and subsequent expression of β-galactosidase (βgal) and neomycin resistance.

b) Reversion: To revert the gene trap, transient expression of Cre excises the exogenous splice acceptor that is flanked by lox sites. This leaves a single lox71 site, and rescues normal splicing and expression of the GOI.

c) To modify the gene trap locus post-reversion, our lab created pFloxin shuttle vectors that contain a lox66 site. Cre causes recombination between the pFloxin lox66 site and the genomic lox71 site, leading to directional insertion of the shuttle vector. Irreversible integration is achieved because recombination of the lox66 and lox71 sites produces one inactive lox site and one loxP site. The shuttle vector also contains the βactin promoter that upon proper Floxin, drives expression of βgeo. This allows modified clones to be screened by βgal and neomycin resistance.

d) Since vector sequence may affect normal gene expression, the gene trap and pFloxin shuttle vectors also contain FRT sites that flank the βactin promoter and βgeo cassette. Transient expression of a Flp construct allows βactin-βgeo excision and removal of this genomic scar.

In summary, the Floxin methodology allows efficient genetic manipulation of a GOI at its endogenous locus and has several advantages over traditional knock-in and knock-out approaches. Rather than relying on methods like homologous recombination and transgenes, this approach facilitates the robust integration of defined sequences, such as post-translational modifications, relevant disease mutations and tagged proteins. Moreover, cells can be electroporated, screened and analyzed in a matter of weeks, highlighting the ease of the system.

The role of Gli2 in mESCs and mouse development

Hh signaling plays a minimal role in maintaining ESC pluripotency and proliferation, but becomes critical during the differentiation toward the neuronal lineage [163-165]. Primary cilia and Hh signaling components have been previously described in both mouse and human ESCs, and in hESCs, Gli2 localizes in a punctuate pattern along the ciliary axoneme and at the tip, but is absent from the nucleus [163]. Highlighting the necessity of primary cilia for Hh signal transduction, loss of primary cilia due to the deletion of the ciliogenic protein OFD1 also leads to defects in the differentiation of mESCs into the neuronal lineage [165].

The Gli proteins are absolutely essential for vertebrate development. They are expressed in tissues derived from ectoderm and mesoderm [166]. While Gli2 and Gli3 are expressed broadly during gastrulation and neurulation, Gli1 is expressed near Shh-expressing cells [167]. Mouse mutants lacking the Gli proteins have different phenotypes. *Gli3* mutant mice (*Gli3*$^{xt/xt}$) possess many developmental abnormalities, including dorsal brain defects and limb polydactyly, but have a relatively normal spinal cord [168-170]. Since these phenotypes are reminiscent of Shh gain of function, Gli3 appears to be essential in repressing the Hh pathway. *Gli2* mutant mice (*Gli2*$^{zfd/zfd}$) possess a variety of developmental defects and die at birth. On a gross morphological level, they are smaller in size, exhibit microcephaly, edema and a flattened head [171]. They also exhibit loss of floor plate, abnormal notochord regression, loss of lobe formation in the right lung, skeletal defects like cleft palate, a shortened sternum and the absence of intervertebral discs, and an imperforate anus [171-175]. These defects are similar, yet milder, than those observed in *Shh* mutants, suggesting that Gli2 is required for Hh pathway activation.

In contrast to *Gli2* and *Gli3* mutants, *Gli1* mutant mice that lack the exons encoding the zinc fingers (*Gli1*$^{zfd/zfd}$) are viable and appear normal [176], suggesting that Gli1 is dispensable for Hh signaling and that perhaps the role of Gli1 can be compensated for by Gli2 or Gli3. Intriguingly, in the heterozygous state of *Gli2* (*Gli1*$^{zfd/zfd}$ *Gli2*$^{zfd/+}$), these mutants die at birth and all have defects in floorplate development, notochord regression and lung lobe formation, reminiscent of *Gli2* mutants. A small percentage (4%) that survive to weaning age are smaller, possess smaller lungs, undescended testes and a distended gut, a phenotype more mild than that of *Gli2* mutant mice. These observations suggest that Gli1 and Gli2 have different extents of overlapping function in different tissues types. In support of this hypothesis, *Gli1* knock-in to the *Gli2* locus can rescue the loss of Gli2 in embryonic development [177].

Results

Generation of Floxin Gli2-GFP mESCs

Endogenous Gli2 is robustly expressed in wild type E14 mESCs, and both Gli2 and Sufu are readily detectable as distinct foci at ciliary tips (**Figure 14a**). Immunoprecipitation with Sufu effectively pulls down Gli2, indicating that this interaction which has been observed in over-expression studies and in various cell types, is maintained in mESCs [96, 97, 99, 100]. Despite proper localization of Hh components, however, undifferentiated mESCs do not robustly upregulate transcriptional target *Gli1* in response to the Hh agonist SAG **(Figure 14b).** This is not surprising as mESCs are not well ciliated and Gli2 can reach the cilium independent of Hh pathway activation, as observed in *Smo*$^{-/-}$ MEFs (**Figure 19a,b**) [100]. Upon differentiation of mESCs by removal of LIF for 6-8 days, both ciliation and Hh responsiveness dramatically increase. Smo translocates to the cilium in a Shh-dependent manner and increased levels of *Gli1* transcript are robustly detected (**Figure 14b**). Taken together, we demonstrate that wild

type mESCs exhibit ciliary localization of Hh pathway components, and are only Hh responsive upon differentiation.

Given that Gli2 can localize to cilia in mESCs and these cells can be differentiated into Hh responsive cells, we sought to explore Gli2 subcellular dynamics using a Floxin-compatible gene trap mESC line from BayGenomics, *Gli2*$^{gt/+}$. We chose gene trap line XG045 since insertion of pGT1Lxf is located within the first intron after the ATG start codon of mouse *Gli2*. The first forty-six codons of the *Gli2* gene are upstream of the gene trap and the remainder of the *Gli2* gene is fused to a βgeo cassette. Since the majority of the protein is not translated, including the elements necessary to bind target DNA, it is unlikely that the gene trapped allele produces a functional protein. This cell line is termed *Gli2*$^{gt/+}$ genotype, where the gene trapped allele produces Gli2-βgeo and the other wild type allele remains intact.

Reversion of *Gli2*$^{gt/+}$ was efficient with 74% of the *Gli2*$^{Rev/+}$ clones exhibiting loss of both βgal activity and neomycin resistance. To insert the remaining *Gli2* coding sequence into the revertant line, we cloned exons 2-14 into the pFloxin shuttle vector in frame with a C-terminal GFP tag. Floxin-mediated insertion of the wild type *Gli2* coding sequence was 100% efficient by βgal activity and neomycin resistance. Six independent clones were further confirmed by genotyping and GFP immunofluorescence, and two *Gli2*$^{GFP/+}$ clones were chosen for all future experiments. Notably, FRT sites in the gene trap and Floxin shuttle vector enable Flp-mediated excision of the βactin promoter and βgal/Neo cassette (**Figure 13**).

First, to verify that Gli2-GFP protein was expressed at similar levels to the endogenous allele, we blotted total cell lysate with a Gli2 antibody (a gift from J. Eggenshwiler) [178].

The GFP shift in size of approximately 26 kDa readily differentiated between the endogenous and tagged allele. We also immunoprecipitated both *Gli2*$^{Rev/+}$ and *Gli2*$^{GFP/+}$ cell lines with both GFP-Trap agarose and Sufu antibody. Immunoprecipitation by GFP pulled down only the GFP-tagged Gli2 protein, while immunoprecipitation with Sufu showed robust interaction with both wild type Gli2 and the slower migrating Gli2-GFP (**Figure 15a**). Since immunoprecipitation by GFP does not pull down both wild type and the tagged version of Gli2, homodimerization between Gli2 proteins does not appear to occur, at least in this context. Gli2 message appears to be comparable in *Gli2*$^{GFP/+}$, *Gli2*$^{Rev/+}$ and *Gli2*$^{+/+}$ cell lines. Together, these data suggest that protein expression from both alleles is comparable, and Gli2-GFP can maintain relevant protein-protein interactions.

Second, to determine if Gli2-GFP behaves similarly to endogenous Gli2 subcellularly, we assessed its localization by immunofluorescence. We detected distinct foci of GFP at ciliary tips, as defined by co-staining with the basal body marker ninein. As expected, Gli2-GFP also co-localized with endogenous Gli2 and Sufu **(Figure 15b)**. Furthermore, while nuclear localization of GFP was not readily detectable, treatment of differentiated cells with 20nM Leptomycin B, an inhibitor of nuclear export, increased GFP signal in the nucleus, as reported for Ci upon Hh activation [179]. Nuclear-cytoplasmic fractionation of *Gli2*$^{GFP/+}$ mESCs also revealed that Gli2-GFP exists in the both subcellular compartments **(Figure 15c).**

Several reports have demonstrated that ciliary accumulation of endogenous Gli2 relies on Hh pathway activation. Wen and colleagues, for instance, showed an increase in Gli2 accumulation after one hour of Hh stimulation in mouse embryonic fibroblasts [85]. In order to correlate localization with Hh responsiveness, we grew mESCs cells in a

monolayer without LIF for 8 days. Gli2-GFP retained similar kinetics in spontaneously differentiated cells, as quantification of both overall GFP ciliary localization and GFP foci intensity were significantly increased upon incubation with a Hh agonist, SAG (**Figure 15d**). Functionally, because a wild type allele is intact in *Gli2*$^{gt/+}$ and *Gli2*$^{GFP/+}$ cells, Hh responsiveness remained intact as determined by *Gli1* and *Ptc* transcript (**Figure 15e**). This is expected, as *Gli2* is haplosufficient, with *Gli2*$^{+/-}$ mice being viable and fertile.

Generation of a Floxin Gli2-GFP mouse model

We have demonstrated that Gli2-GFP behaves similarly to the wild type allele in vitro. To assess pluripotency of these genetically modified mESCs, we examined levels of Nanog, a known regulator of pluripotency (**Figure 30a**). Moreover, *Gli2*$^{GFP/+}$ cells possess alkaline phosphotase expression and normal embryonic stem cell colony formation and morphology [160]. To test germline competency of these cells, we attempted to generate Floxin Gli2-GFP mice from two independent *Gli2*$^{GFP/+}$ mESCs clones. Notably, these Floxin cells retained the βgeo cassette, as Flp-mediated removal of this cassette would be accomplished in vivo by breeding with βactin-FlpO mice.

Following blastocyst injection by the Gladstone Institute Transgenics Core, chimeric males were crossed with wild type Bl6 females. Chimeras generated with *Gli2*$^{GFP/+}$ Clone 5 and 12 both exhibited germline transmission. Thus, two independent clones of Floxin Gli2-GFP possessed germline competency.

Gli2$^{GFP/+}$ mice are viable and fertile. Various tissues from adult heterozygote *Gli2*$^{GFP/+}$ and control mice were analyzed for the presence of *Gli2, GFP* and *Gli1* transcript by quantitative PCR (**Figure 16a**). Brain and lung expressed the highest levels, and Gli2-GFP protein was detected from lysate upon immunoprecipitation by GFP or Sufu. Upon

Sufu and GFP immunoprecipitation from total lung lysate, Gli2-GFP was discerned to interact with Sufu. Moreover, protein expression of wild type Gli2 was comparable to Gli2-GFP, as observed in cell culture experiments, and cells derived from lungs also expressed GFP at ciliary tips (**Figure 16b**).

To assess if the Floxin Gli2-GFP allele maintained ciliary kinetics, mouse embryonic fibroblast (MEFs) were derived from *Gli2*$^{GFP/+}$ and control embryos at e11.5. Hh responsiveness was assessed by transcript levels of Hh target *Gli1*, while Gli2-GFP ciliary localization was assessed by immunofluorescence of GFP. Levels of Gli2 transcript were comparable across genotypes and both Gli2 and Gli2-GFP increased at the ciliary tips in a Hh responsive manner (**Figure 16c**).

To determine if Gli2-GFP could fully rescue the function of wild type Gli2 in vivo, we crossed *Gli2*$^{GFP/+}$ mice with *Gli2*$^{zf/+}$ mice. *Gli2*$^{zf/+}$, now referred to as *Gli2* $^{+/-}$, were originally generated by homologous recombination and previously described by Mo and colleagues [171]. These mutants possess a deletion in the exons encoding zinc fingers 3-5, which are essential for DNA binding. Analyses of *Gli2*$^{GFP/-}$MEFs were performed, as above, to assess ciliary dynamics and Hh responsiveness (**Figure 16c-d**). These MEFs recapitulated what we observed in *Gli2*$^{GFP/+}$ MEFs, in that they were also Hh-responsive by Gli2-GFP ciliary accumulation and *Gli1* levels.

Assessment of progeny from an intercross between *Gli2*$^{+/-}$ and *Gli2*$^{GFP/+}$ mice at birth indicated that they were present at the expected Mendelian ratio of roughly 25% (**Figure 17a**). *Gli2*$^{GFP/-}$ embryos did not phenocopy the gross morphology of *Gli2*$^{-/-}$ embryos, which are smaller in size and possess flattened heads and subcutaneous edema [171]. Analysis of P0 embryos indicated that lung and skeletal defects normally seen in Gli2

mutants were not observed in *Gli2*$^{GFP/+}$ mice (**Figure 17b**). However, *Gli2*$^{GFP/-}$ mice were subviable with age, as most died between P1-P7, with a minority surviving past one week (**Figure 17c**). These mice were runted a few days after birth, and eventually died. The minority of *Gli2*$^{GFP/-}$ mice that survived past 5 weeks exhibited imperforate anus and recto-urethral fistula, previously described in *Gli2*$^{-/-}$ embryos and *Gli1*$^{ZF/ZF}$ *Gli2*$^{+/-}$ mice (**Figure 17d**) [175, 176, 180]. Female animals possessed a shorter distance between their vaginal opening and rectum, and often exhibited recto-urethral fistula. Thus, we believe that *Gli2*^{GFP} is a hypomorph allele and can rescue Gli2 function in some, but not in all tissues.

Importantly, the presence of the vector sequence could potentially be affecting normal gene expression, thus leading to adverse effects. To remedy this, we crossed βactin FlpO mice with *Gli2*$^{GFP/+}$ mice to achieve Flp-mediated removal of the βactin promoter and the βgeo cassette in vivo. Absence of LacZ and neomycin were assessed by qPCR, and these mice were crossed with Gli2$^{+/-}$ mice to determine functional rescue. Indeed, a higher percentage of *Gli2*$^{GFP\Delta\beta geo/-}$ mice reach weaning age as compared to their βgeo-positive counterparts (**Figure 17e**). A small percentage die soon after birth, and the majority that survive past weaning age still exhibit urorectal abnormalities (**Figure 17d**). Thus, removal of the βgeo cassette is not sufficient to rescue the full wild type function of Gli2.

Generation of *Gli2*$^{GFP/GFP}$ mice with the βgeo cassette in vivo has also been assessed, albeit by quantitative methods rather than qualitative PCR. The original gene trap is located within an intron of over 100kb and its precise location remains unmapped. Because the Floxin method is an insertional modification rather than a replacement strategy and the remainder of the endogenous *Gli2* exons and introns after the gene trap

remain intact, we were unable to assess loss of the wild type allele. Thus, to assay homozygousity of these animals in the presence of the βgeo cassette, we used quantitative PCR to assess LacZ and neomycin levels as compared to autosomal control genes, Dec2 and Il2. *Gli2*$^{GFP/GFP}$ embryos are present at Mendelian ratios at embryonic day e9.5, but exhibit sub-Mendelian ratios at birth and at weaning age. Some *Gli2*$^{GFP/GFP}$ mice appeared to be viable and were crossed to each other to validate the genotyping method, and to assess fertility. Progeny were homozygous for LacZ and Neo, as their parents, but appeared runted compared to heterozygous and wild type litters (**Figure 17f**). Consistent with this, a previous study showed that reduced Hh signaling results in smaller body size in mice [181]. To date, three litters of 6-7 pups were born to *Gli2*$^{GFP/GFP}$ and*Gli2*$^{GFP/GFP}$ crosses, with 17/20 pups surviving past P7. *Gli2*$^{GFP/GFP}$ crosses in the absence of the βgeo cassette remains to be performed, as genotyping methods will need to be further optimized.

Discussion

Advantages and limitations of the Floxin system

Here, we demonstrate how a specialized knock-in strategy, the Floxin system, can be a useful resource to analyze protein dynamics and function. Locus specificity and the ability to insert defined sequences minimizes artifact and allows one to track their protein of interest with either endogenous antibodies or one of many epitope tags. These features make the Floxin technology amenable to gene mutation or reporter knock-in studies, protein purification and other biochemical assays, live imaging and other forms of subcellular localization analyses, and a wide range of functional studies.

Gli2, in particular, serves as a great example of how the Floxin method is advantageous over heterologous expression experiments. Due to a lack of good commercial Gli2

antibodies in the field, many experiments use Gli2-GFP over-expression in transiently transfected cells. This over-expressed protein localizes to the cilium, the cytoplasm and the nucleus, independent of Hh pathway activation (**Figure 19c**). This suggests that over-expressed Gli2 may bypass normal regulatory mechanisms, and that these experiments may be prone to artifact or may mask subtle subcellular changes. For instance, assessing Hh-mediated Gli2 ciliary accumulation would be difficult in this context. The Floxin system poses a more relevant experimental situation and has the added benefit of epitope tagging.

We show that Floxin mESC possess the potential for germline transmission, and believe that the Floxin technology, even in the heterozygous case, can be useful in a wide range of applications, including investigation of subcellular dynamics, modeling of human diseases and protein purification from specific tissues. This study validates how this strategy can be used for tissue-specific analyses in vivo, and one can imagine many avenues of Gli2 research the Floxin system can facilitate. For instance, Gli2-GFP dynamics, mass spectrometry and ChIP-Seq can be examined in the context of cancer upon introduction of oncogenic Smoothened or inactivation of Ptc or Sufu.

While the Floxin system holds great potential, it is not without limitations. First, this technology is only compatible with a subset of approximately 4,500 genes that are pGTIxF and pGTLxR gene trapped, and within this population, some may not be useful due to gene trap location. As in our case, gene trap location may be difficult to assess, depending on the size of the intronic region it is located. Second, unless one is examining a hemizygous, haploinsufficient or dominant negative gene, the intact wild type allele may restrict functional analyses. Indeed, in this study, the wild type Gli2 allele masked any readout of loss of function, and over-expression assays were more

indicative of functional insight. Targeting the remaining wild type allele for knock out or RNAi-mediated knockdown are also options we continue to explore. Third, dependence on the manipulation of mESCs may or may not be useful, depending on the gene of interest. We were fortunate in that mESCs can be differentiated into Hh responsive cells, but if one were to investigate a gene important in definitive endoderm, for instance, robust protocols for this endpoint may not yet be optimized. Fourth, although our gene of interest successfully achieved germline transmission, there will undoubtedly be locus and gene-dependent variations.

Gli2 ciliary dynamics are conserved in mESCs

Gli2 has been shown to localize to the primary cilium in a number of cell lines, including primary and immortalized lines and human ESCs [82-85, 163]. Localization occurs independent of Hh pathway activation, whereas Gli2 ciliary accumulation requires pathway activation [84, 85]. Indeed, localization of Gli2 remains intact in fibroblasts lacking Smoothened, the central activator of the pathway and in Hh unresponsive IMCD3 cells derived from inner medullary collecting duct kidney cells (**Figure 19a**). Here, we demonstrate that the same is true for Gli2 in mouse ESCs. Gli2, both the endogenous protein and a GFP-tagged version, can localize to cilia in mESCs despite being Hh unresponsive in the undifferentiated state. This is not too surprising because mESCs proliferate with very short gap phases, and thus do not linger in G1 or G0, stages that promote ciliation [77, 182]. Upon spontaneous differentiation, ciliation drastically increases and this heterogeneous population of cells can robustly respond to Hh or Hh agonist, SAG. This observation is consistent with the fact that primary cilia are required for Hh signaling.

Modification of the Gli2 locus by the Floxin method appears to not alter pluripotency, as these Floxin cells retain pluripotency markers Oct4 and Nanog and are germline-competent (**Figure 30a**) [160]. Anecdotally, however, as passage number of Floxin Gli2-GFP cells increased, more cilia were observed. Moreover, SAG treatment of mESCs grown continuously in LIF results a modest increase in Gli2 ciliary accumulation (**Figure 19b**). Perhaps this is due to a subtle loss of stem cell character and increased differentiation, and/or basal levels of Hh signaling that are present in mESCs.

Gli2-GFP functions as a hypomorphic protein in vivo

We have demonstrated that Floxin technology can be used to generate a mouse model expressing Gli2-GFP from the endogenous *Gli2* locus. In assessing if Gli2-GFP can rescue the *Gli2* null phenotype, we determined that this tagged protein acts as a hypomorphic allele despite intact subcellular ciliary dynamics. Importantly, the presence of the wild type allele prevents assessment of a true loss of function phenotype conferred by Gli2-GFP in vitro. Because the mouse exhibits Gli2-specific phenotypes, it is unlikely that sub-viability is due to a misregulation or disruption of genes other than *Gli2* that are altered by the gene trap and subsequent Floxin.

The fact that Gli2-GFP is not a total loss of function allele is apparent at birth, as $Gli2^{GFP/-}$ mice do not phenocopy $Gli2^{-/-}$ mice in gross morphology. However, since the majority of these mice die within the first week of life, it is clear that Gli2-GFP does not possess the same functions and capabilities of endogenous Gli2. While skeletal and lung defects appear to be rescued in these mice, hindgut development remains abnormal. In some cases, this proves not fatal, and some adult $Gli2^{GFP/-}$ mice possessing urorectal fistula are viable past six months of age. The presence of the GFP tag or the Gli2 exons and introns that are retained downstream of the gene trap may contribute to this phenotype.

Given that imperforate anus is a relatively common congenital human disease with an incidence of 1 in 5000 [180], perhaps this mouse could be useful to investigate this congenital malformation. Moreover, this mouse model could be useful in the context of other relevant post-embryonic diseases where Hh signaling is compromised. Together, these data suggest that Gli2 and the levels of Hh signaling it activates are different from tissue type to tissue type. While skeletal and lung formation may require a lower threshold of Gli activator activity, hindgut develop appears to possess a higher threshold. Our *Gli2*$^{GFP/GFP}$ and *Gli2*$^{GFP/-}$ phenotypes are consistent with that observed in *Gli2*$^{+/-}$ *Gli1*$^{-/-}$ mice, where it is postulated that Gli2 gene dosage is critical for appropriate Hh readout [177].

In summary, by modifying the *Gli2* locus by Floxin technology, this study demonstrates that this knock-in strategy can be used to generate specific and defined alleles, as well as an in vivo model. This is a useful genetic tool that holds much potential for the generation of relevant disease models.

Supplementary data

Generation of Floxin Gli2-Flag/His and mass spectrometry

Importantly, we first created a Floxin Gli2 allele with a smaller C-terminal tag, consisting of 3xFlag and 6xHis. By Western blot, Gli2-FlagHis with and without the βgeo cassette (Flox, FlpO, respectively) was detected at similar levels to endogenous Gli2 in wild type and Revertant cell lines (**Figure 18a**). Gli2-FlagHis also robustly interacted with Sufu and was detected by immunofluorescence as ciliary foci in both undifferentiated and differentiated cells (**Figure 18b**). Given intact expression levels and subcellular localization, we attempted to find novel Gli2 interacting proteins by mass spectrometry using tandem Flag-His purification, as well as Flag purification alone. N. Krogan's

laboratory performed three rounds of MS/MS comparing Revertant and Gli2-Flag-His cells by both in-gel and gel-free analysis. While Gli2 coverage was not extracted, we recovered peptide hits for Sufu by both methods (**Figure 18c**). Our minimal data set prompted us to utilize GFP for an alterative purification method. Additionally, generation of a Floxin mouse model with a smaller epitope tag, may prove useful in terms of minimizing potential deleterious side effects in vivo and additional downstream components.

We attempted to perform mass spectrometry from Floxin Gli2-GFP mESCs, as well as from lung lysate from *Gli2*$^{GFP/+}$ mice. We followed a previously described protocol for the purification of GFP-tagged proteins [183]. Peptides for neither Gli2 nor Sufu were recovered, although several other interesting and previously implicated cilia-related proteins were. Potential for mass spectrometry of Gli2 will be further discussed in Chapter 5.

Materials and Methods

Cell lines and cell culture

Gli2$^{gt/+}$ (XG045) E14 ESC lines were obtained from BayGenomics. Cells were cultured on 0.1% gelatin in Knockout DMEM (Invitrogen) supplemented with 10% FBS, glutamine, pyruvate, non-essential amino acids, β-mercaptoethanol and leukemia inhibitory factor (LIF). Floxin cell lines were selected with and grown in 150μg/ml G418. Spontaneously differentiated cells in a monolayer or embryoid bodies were grown in the absence of LIF for 8 days. SAG (Enzo), a Hedgehog pathway agonist, was added to fresh differentiation media at 1μM in DMSO for 18 hours. Leptomycin B (Sigma L2913), an inhibitor of nuclear export, was used at a concentration of 20nM for 90 minutes.

CDNA constructs and cloning

Gli2 cDNA was a gift from H. Sasaki, and exons 2-14 were amplified with appropriate restriction enzymes and cloned into pFloxin, in frame with the C-terminal GFP tag. High Fidelity polymerase (Roche) was used for amplification, while QuikChange II XL site directed mutagenesis kit (Stratagene) was used correct point mutations. All products were sequenced before electroporation.

Electroporation, selection and screening

Electroporation for Reversion, Floxin and FlpO were performed as previously described by Singla et al [160]. Preliminary clones were assessed by genomic PCR and β-galactosidase activity using the Galacto-Light Plus System (Applied Biosystems).

Immunofluorescence and Microscopy

Cells were plated on coverslips coated with poly D-lysine and 1% Matrigel. Cells were fixed for 7 minutes in 4% PFA, washed in PBS and incubated in PBS with 0.1% Triton X-100 (PBST) for 20 minutes. Cells were then blocked in 2% BSA in PBS for 1 hour at 4C, and then incubated overnight with primary antibody at 4C. The next day, cells were washed in PBS, incubated in Alexafluor (Invitrogen) secondary antibody for 1hr at room temperature and mounted with either Vectashield Hardset with DAPI or Prolong Gold with DAPI. Images were acquired on one of the following: a Zeiss Axio Observer D1, a Nikon C1 confocal, a Leica TCS SP5 or a Leica TCS SPE. Image J or Fiji (NIH) were used for quantification of integration densities, as described below and previously [85].

Integrated Density Quantification

Images were acquired by confocal microscopy using identical settings within experiments, and experiments were repeated three times. Image J was used to

measure an 8x8 circular region of interest encompassing Gli2-GFP (ROI_{GFP}). An identical ROI was taken in an adjacent region to account for background (ROI_{BACK}). Integrated density readings, or pixel intensities, were measured as ROI_{GFP} - ROI_{BACK} and binned into four equal data clusters. Bin 1 (+) represents ID readings with the lowest pixel intensity, while Bin 4 (++++) represents ID readings with the highest pixel intensity.

Western blots

Cells were lysed with buffer containing 50mM Tris-HCl (pH 7.4), 0.5% NP-40, 0.25% NaDoc, 150mM NaCl and fresh protease (Calbiochem) and Halt phosphatase (Pierce) inhibitors. Lysates were cleared at 13.2k rpm for 10 minutes and protein concentration was quantified by Bradford assay. NE-PER Nuclear Cytoplasmic Reagent (Pierce) was used for cell fractionation assays.

Antibodies

Antibodies used for immunofluorescence include: GFP (Aves Lab GFP-1020, 1:1000); Acetylated tubulin (Sigma T6793 1:1000); Ninein (gift from J. Sillibourne, 1:20000); Sufu (Santa Cruz, 1:1000); Flag M2 (Sigma, 1:1000). Alexafluor secondaries (Invitrogen) were used at 1:1000. Antibodies used for immunoprecipitation include: Sufu (Santa Cruz) 2µg; GFP-Trap Resin (Allele); Flag M2 agarose (Sigma). Antibodies used for Western detection include: GFP (as above); Sufu (as above); alpha-tubulin (Sigma 1:5000); secondary antibodies (Jackson Immuno) 1:10000.

Quantitative RT- PCR

RNA was extracted from mESCs or spontaneously differentiated cells using Rneasy Plus (Qiagen). cDNA synthesis was performed using First Strand cDNA Synthesis Kit (Fermentas). Transcript levels were measured in quadruplicate using a 7300 Real-time

PCR machine (Applied Biosystems) and normalized to relative βactin transcript. Primer sequences are: βactinF 5'-CACAGCTTCTTTGCAGCTCCTT-3' and βactinR 5'-CGTCATCCATGGCGAACTG-3'; Gli2 F 5'-GCTGCACCAAGAGGTACACA-3' and Gli2R 5'-GGACATGC ACATCATTACGC-3'; Gli1-F 5'GGTGCTGCCTATAGCCAGTGTCCTC-3' and Gll1-R 5'-GTGCCAATCCGGTGGAGTCAGACCC-3'; and PtcF 5'-CTCTGGA GCAGATTTCCA AGG-3' and PtcR 5'-TGCCGCAGTTCTTTTGAATG-3'; gfpF 5'-CGACCACTACCAGCAGAACA-3' and gfpR 5'-GAACTCCAGCAGGACCATGT-3'.

Blastocyst Injection

Two independent clones of Floxin Gli2-GFP mESCs were karyotyped and tested for mycoplasma (MycoAlert) and alkaline phosphotase activity (StemTag) prior to blastocyst injection. On the day of injection, a single cell suspension of 10^6 cells/ml was collected in 25mM HEPES buffered DMEM containing 10% FBS. mESCs were injected by the Gladstone Institute Transgenic Core.

Mouse breeding and cell culture

Floxin Gli2-GFP chimeric mice were crossed with wild type B6 females (Jax) to establish germline transmission, as well as backcrossing three generations to the Bl6 background. Mice were crossed with βactin-FlpO mice (Jax) to excise the βactin-βgeo cassette. Fibroblasts were generated from both e11.5 embryos and adult tail tips. RNA and protein were isolated from adult organs that were first perfused with phosphate buffered saline to minimize contaminants.

Genotyping

Gli2+/- mice were genotyped as previously described [171]. Gli2-GFP mice were genotyped using a common forward primer within Gli2, and an intronic and GFP specific

primer to detect Gli2 WT and Gli2-GFP, respectively. Gli2 commonF 5'-TGTTTTCTGGTGCACTGAGC-3'; Gli2-WTR 5'-TAGGCCAAACAGCAGA GAGG-3'; Gli2-GFPR 5'GAACTTCAGGGTCAGCTTGC-3'. Quantitative methods were used to quantify levels of genomic LacZ, neomycin and Gli2, as compared to control autosomal genes, Dec2 and Il2. LaczF 5'-CCGATATTATTTGCCCGATGT-3'; LaczR 5'-CTGTAAACGGGGATACTGACG-3'; Neo76F 5'-CCTGATGCTCTTCGTCCAGAT -3'; Neo76R 5'-ATTCGACCACCAAGCGAAAC-3'

Skeletal analysis

Skeletal preps were stained with alizarin red and alcian blue using previously describe techniques [171].

Purification for Mass spectrometry

Twenty 15cm plates of Revertant and Floxin Gli2-FlagHis mESCs were grown to confluence and lysed in 10mL buffer containing 50mM Tris-HCl (pH 7.4), 0.5% NP-40, 0.25% NaDoc, 150mM NaCl and fresh protease (Calbiochem) and Halt phosphatase (Pierce) inhibitors. Lysates were nutated at 4C for 45 minutes, and subsequently spun down at 13.2k rpm for 10 minutes. For tandem purification, 5mg of Dynal His beads (Invitrogen) were added to samples and incubated at 4C for 1 hour. Beads were collected by magnet, and washed 3x with lysis buffer. Supernatants were then incubated with 200µl of Flag M2 beads (Invitrogen) at 4C for 1 hour. Beads were washed by centrifugation 3x with lysis buffer, and eluted with either 3x sample buffer or 3x Flag peptide (Sigma). Lysate and output samples were assessed by Western blot for Flag and by Silver Stain (Pierce).

Floxin Gli2-GFP mESCs were grown to similar quantities and purification was performed using the protocol previously described [183].

Acknowledgements

We thank J. Eggenshwiler for Gli2 antibody, H. Sasaki for Gli2 cDNA, J. Taipale for Smo-/- MEFs, N. Krogan for mass spectrometry and E. Carlson for help with quantitative genotyping. We acknowledge UCSF Nikon Imaging Center for use of microscopes, and the Gladstone Institute Transgenic Core for blastocyst injection.

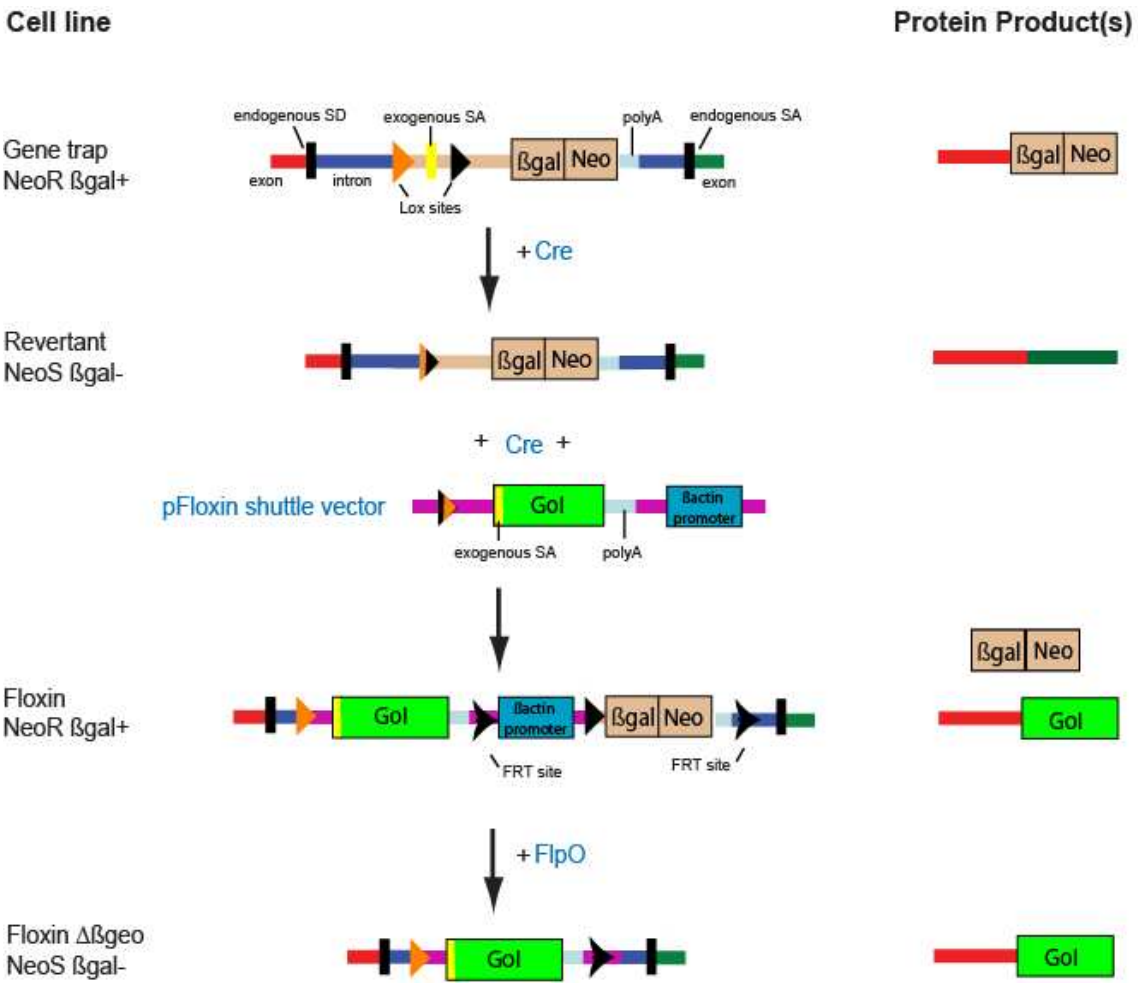

Figure 13. The Floxin strategy for reversion and modification of gene trap loci.
In the gene trap allele, pGTLxF or pGTLxR is introduced into an intron of a given autosomal gene of interest (GOI) in mESCs. This results in a GOI-βgeo fusion protein and subsequent expression of β-galactosidase and neomycin resistance. To revert the gene trap, transient expression of Cre excises the exogenous splice acceptor that is flanked by lox sites. This leaves a single lox71 site, and rescues normal splicing and expression of the GOI. To Floxin the reverted locus, Cre causes recombination between pFloxin shuttle vector's lox66 site and the genomic lox71 site. The β-actin promoter in the shuttle vector drives expression of βgeo upon proper Floxin. The gene trap and pFloxin shuttle vectors also contain FRT sites that flank the βactin promoter and βgeo cassette. Transient expression of a Flp construct allows βactin-βgeo excision. Adapted from [160].

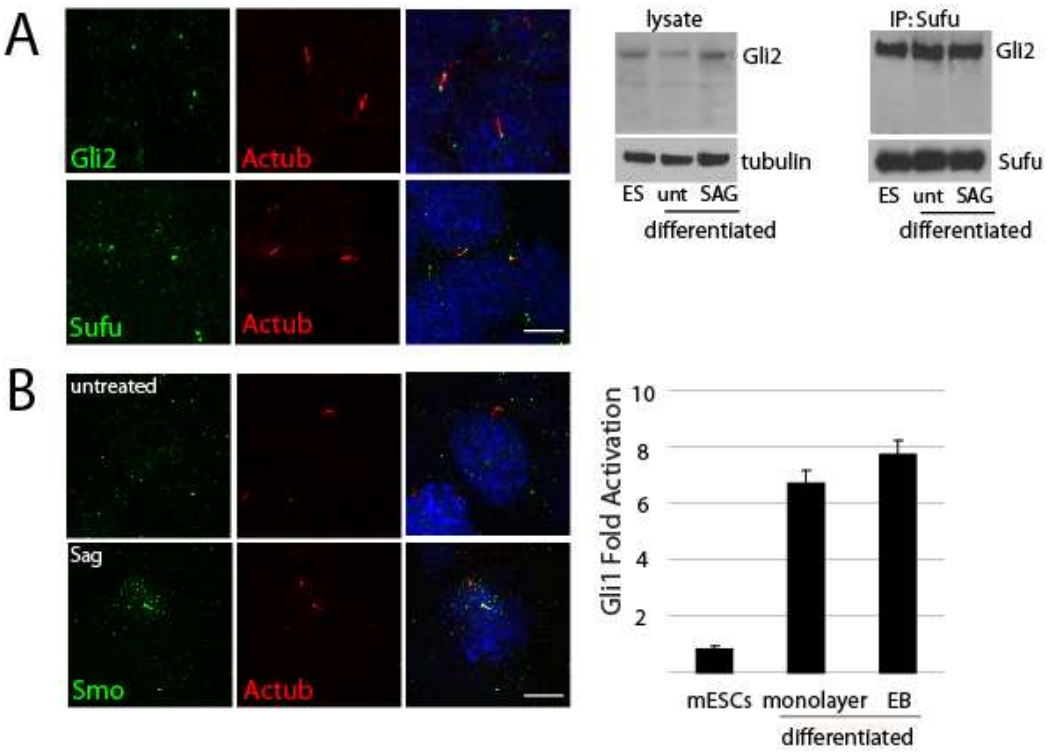

Figure 14. Hh components are expressed in wild type mESCs.
(A) Sufu and Gli2 localize to cilia in wild type ES cells. Wild type E14 mESCs were probed for primary cilia (actub, red), Gli2 and Sufu (green) by immunofluorescence. Western analysis for Gli2 and Sufu and immunoprecipitation with Sufu was performed on lysate from wild type mESCs and spontaneously differentiated mESCs generated by the removal of LIF. Scale bar ~5μm. **(B) Smo translocates to the cilium in differentiated mESCs which are Hh-responsive.** Undifferentiated mESCs and differentiated mESCs were assessed for *Gli1* levels following 18 hour treatment with Hh agonist SAG (1μM). Data was normalized to actin. Differentiated cells following the removal of LIF for 8 days were stained for endogenous Smo (green) and cilia (actub, red), in the presence and absence of Sag. Scale bar ~5μm.

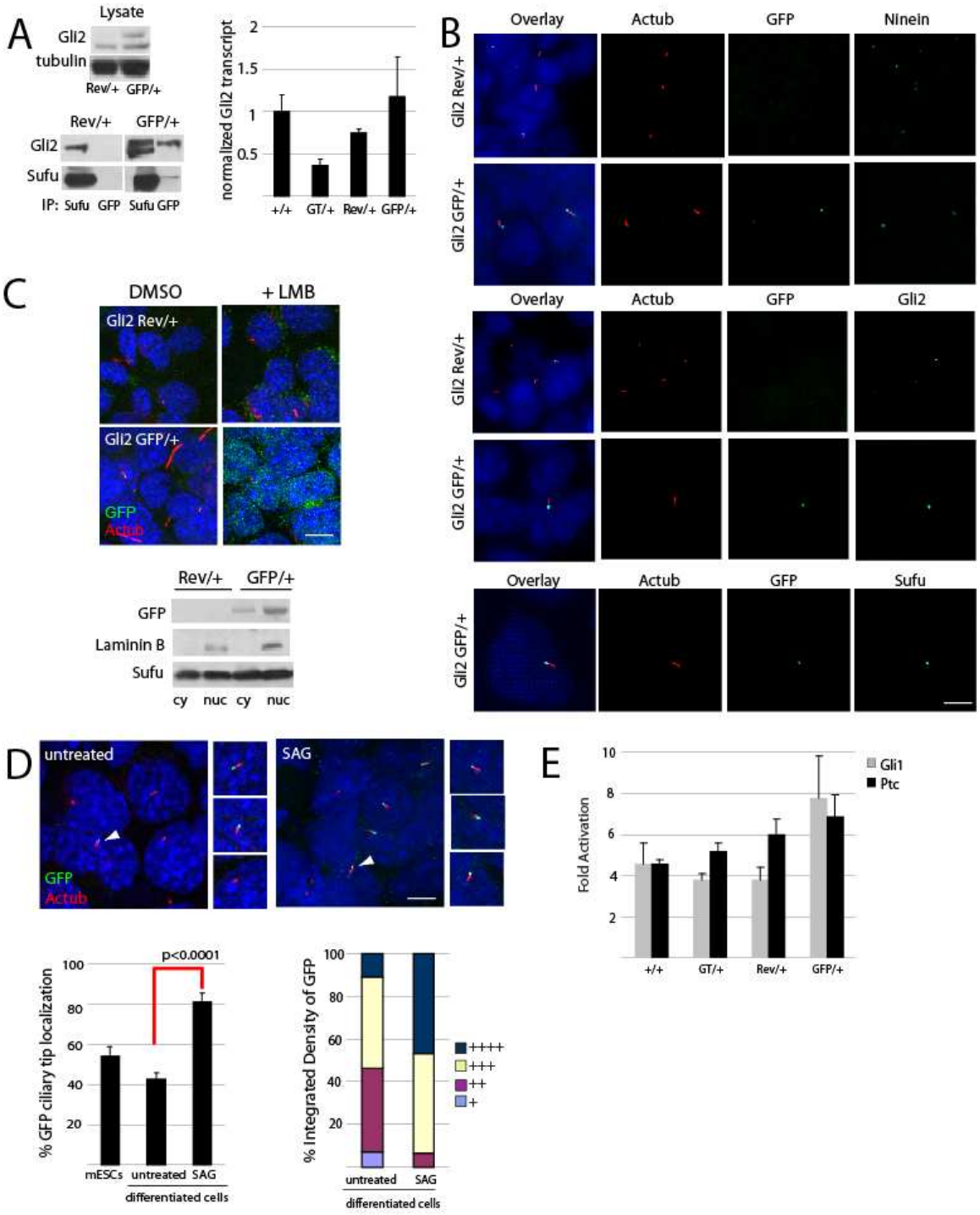

Figure 15. Floxin Gli2-GFP behaves comparably to wild type Gli2.

(A) Endogenous and Floxin Gli2-GFP are expressed at comparable levels. Total cell lysate was blotted with a Gli2 antibody. The GFP shift in size of approximately 26 kDa can differentiate between endogenous Gli2 and Gli2-GFP. Cell lysate was immunoprecipitated with GFP and Sufu and probed for Gli2. *Gli2* message was assessed by qRTPCR and normalized to actin. **(B) Gli2-GFP localizes to the primary cilium with Gli2 and Sufu.** Floxin Gli2-GFP mESCs were stained for GFP (green), cilia (actub, red) and ninein, a marker of the basal body (cyan). For co-localization, these cells were stained for endogenous Gli2 and Sufu (cyan). Scale bar ~5μm. **(C) Gli2-GFP can translocate to the nucleus.** The presence of Gli2 in the nucleus was assessed in differentiated mESCs cells treated with or without 20nM

Leptomycin B, an inhibitor of nuclear export. A nuclear-cytoplasmic lysis method was used to detect Gli2 in these subcellular fractions by Western blot. Nuclear (nuc), cytoplasmic (cy). Scale bar ~10μm. **(D) Gli2-GFP ciliary localization increases upon Hh stimulation.** Floxin Gli2-GFP mESCs cells were grown in a monolayer without LIF for 8 days and assessed for GFP (green) localization to the primary cilium (actub, red). Scale bar ~5μm. GFP localization was counted in the absence and presence of SAG (1μM, 1 hour), a Hh agonist. Integrated density readings of Gli2-GFP foci were obtained by Image J analysis. **(E) Floxin Gli2-GFP cells activate the Hh pathway normally.** Wild type, Gene trap, Revertant and Floxin mESCs were spontaneously differentiated in the absence of LIF for 8 days and treated overnight with 1uM Sag. *Gli1* and *Ptc* transcript levels were assessed by qRTPCR and normalized to actin. Data is presented as fold activation of SAG treatment compared to unstimulated cells.

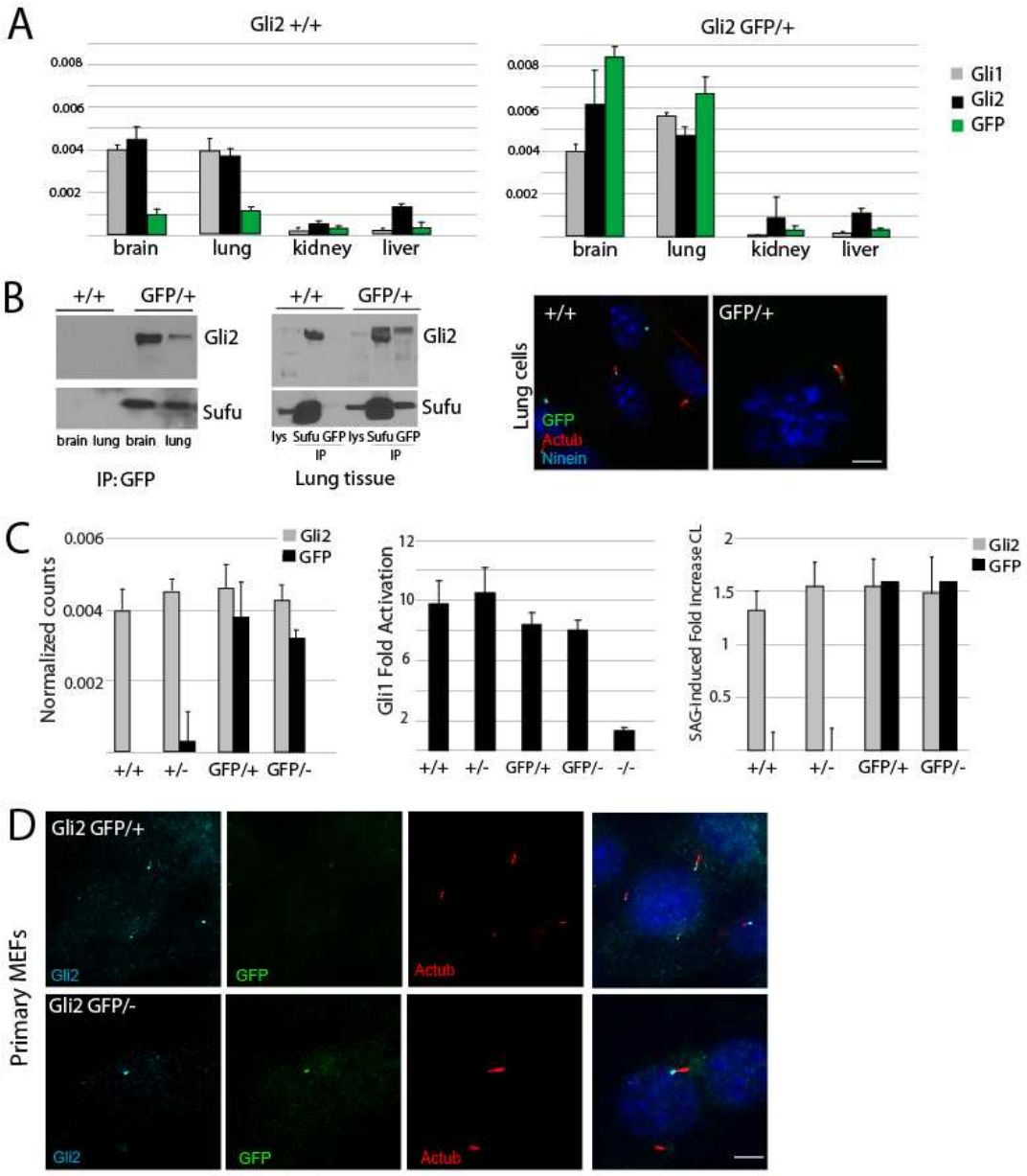

Figure 16. Floxin Gli2$^{GFP/+}$ mice are viable and express ciliary Gli2-GFP

(A) Gli2-GFP can be detected in various tissues. RNA was extracted from various tissues from adult heterozygote *Gli2*$^{GFP/+}$ and control mice. qRTPCR was used to quantify levels of Gli2, GFP and Gli1 transcript, normalized to actin. **(B) Gli2-GFP can be detected in brain and lung tissue.** Brain and lung lysate were probed and immunoprecipitated with GFP or Sufu. Cells were derived from *Gli2*$^{GFP/+}$ adult lungs and assessed for Gli2-GFP by staining with GFP (green), cilia (actub, red) and basal body marker ninein (cyan). Scale bar ~5µm. **(C) *Gli2*$^{GFP/+}$ MEFS maintain ciliary dynamics and Hh responsiveness.** MEFs were obtained from *Gli2*$^{GFP/+}$, *Gli2*$^{GFP/-}$ and control embryos at e11.5. MEFs were assessed by qRTPCR for transcript levels of Gli2, GFP and Gli1 and normalized to actin. Gli1 data is presented as fold activation of Sag-treated cells over unstimulated cells. *Gli2-/-* cells were used as a control. Ciliary localization (CL) data is presented as the fold increase of ciliary Gli2 or Gli2-GFP upon SAG treatment, as assessed by immunofluorescence. **(D) Gli2-GFP can be detected at the primary cilium.** Primary MEFs were stained with GFP (green), Gli2 (cyan) and cilia (actub, red). Scale bar ~5µm.

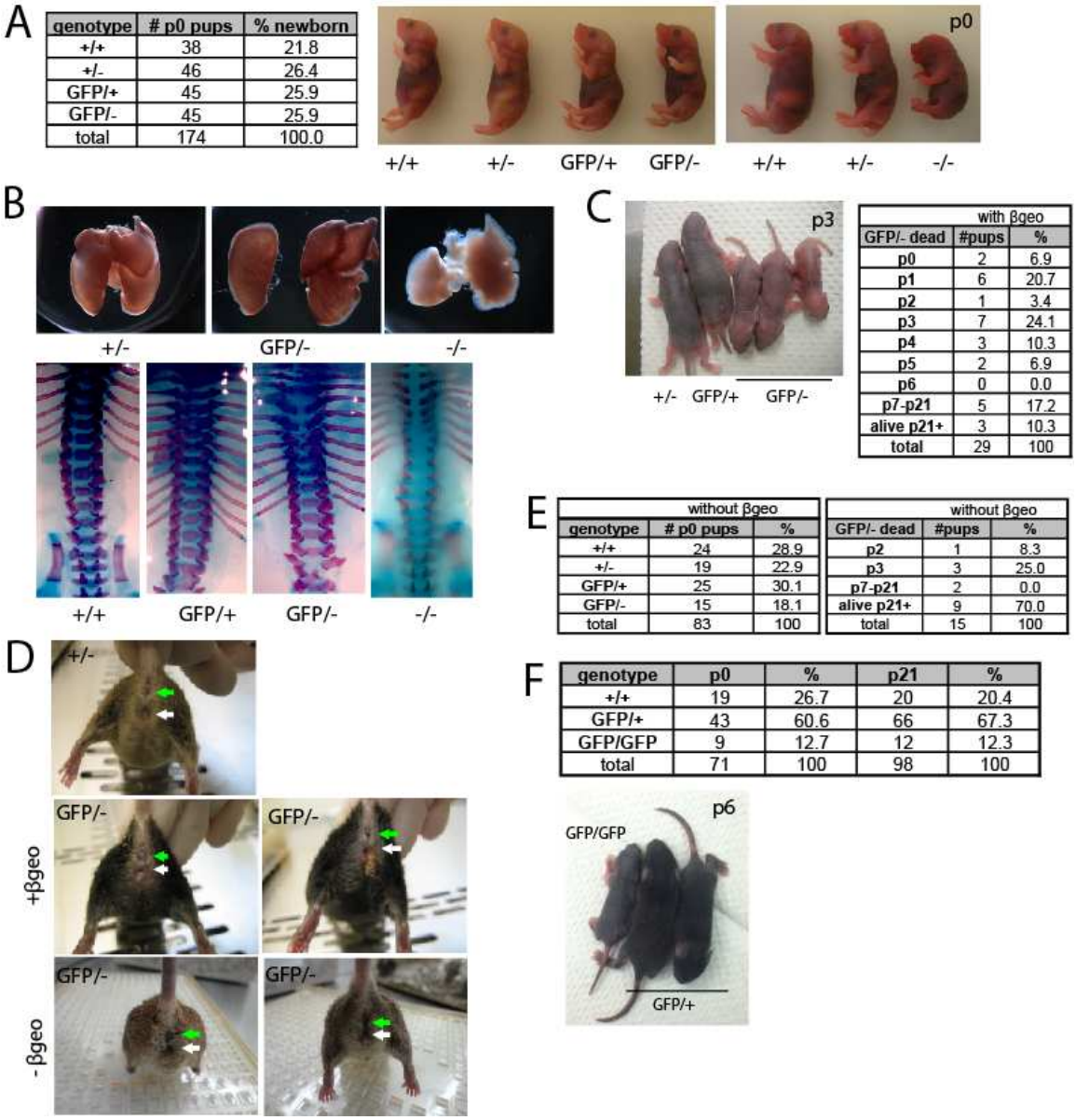

genotype	# p0 pups	% newborn
+/+	38	21.8
+/-	46	26.4
GFP/+	45	25.9
GFP/-	45	25.9
total	174	100.0

	with βgeo	
GFP/- dead	#pups	%
p0	2	6.9
p1	6	20.7
p2	1	3.4
p3	7	24.1
p4	3	10.3
p5	2	6.9
p6	0	0.0
p7-p21	5	17.2
alive p21+	3	10.3
total	29	100

	without βgeo	
genotype	# p0 pups	%
+/+	24	28.9
+/-	19	22.9
GFP/+	25	30.1
GFP/-	15	18.1
total	83	100

	without βgeo	
GFP/- dead	#pups	%
p2	1	8.3
p3	3	25.0
p7-p21	2	0.0
alive p21+	9	70.0
total	15	100

genotype	p0	%	p21	%
+/+	19	26.7	20	20.4
GFP/+	43	60.6	66	67.3
GFP/GFP	9	12.7	12	12.3
total	71	100	98	100

Figure 17. Gli2-GFP acts as a hypomorph in vivo: Gli2$^{GFP/-}$ mice are sub-viable
(A) *Gli2*$^{GFP/-}$ mice are born at Mendelian ratios. Assessment of *Gli2*$^{+/-}$ x *Gli2*$^{GFP/+}$ progeny at birth indicated that they were present at the expected Mendelian ratio of roughly 25%. Gross morphology of control and experimental P0 embryos. **(B) Gli2$^{GFP/-}$ do not exhibit lung or skeletal malformations.** Lungs were dissected from experimental and control P0 embryos. The right lung of *Gli2*$^{-/-}$ animals lack proper lobe formation, while *Gli2*$^{GFP/-}$ possessed a fully formed right lung. Skeletal analysis of P0 embryos show that the intervertebral discs that are absent in *Gli2*$^{-/-}$ animals are intact in *Gli2*$^{GFP/-}$ mice. **(C) *Gli2*$^{GFP/-}$ mice were sub-viable with age.** Some *Gli2*$^{GFP/-}$ mice appear runted by day 3. Summary of survival rates in mice with the βgeo cassette. **(D) *Gli2*$^{GFP/-}$ mice exhibit urorectal defects.** *Gli2*$^{GFP/-}$ mice that survived past 5 weeks exhibited imperforate anus and recto-urethral fistula. This phenotype was particularly obvious in females, as they possessed a shorter distance between their vaginal opening (white arrow) and rectum (green arrow). This phenotype was observed upon FlpO of the βgeo cassette. **(E) Flpout of the βgeo cassette improves *Gli2*$^{GFP/-}$ viability.** Summary of birth and survival rates in mice lacking the βgeo cassette. **(F) *Gli2*$^{GFP/GFP}$ mice sub-viable.** Summary of birth and survival rates in homozygous mice with the βgeo cassette. *Gli2*$^{GFP/GFP}$ mice appear runted compared to heterozygous controls.

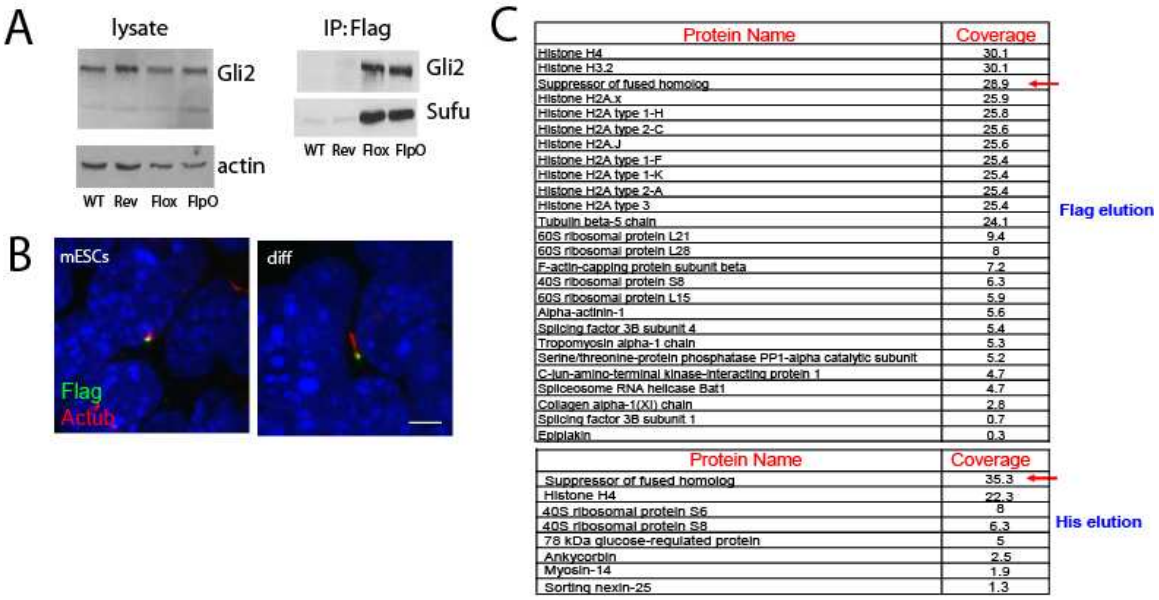

Figure 18. Analysis and protein purification from Floxin Gli2^{FlagHis} mESCs

(A) Gli2-FlagHis behaves similarly to endogenous Gli2. Lysate from control and Floxin Gli2-FlagHis with and without the βgeo cassette (Flox, FlpO, respectively) were probed for Gli2 levels by Western blot. Flag immunoprecipitation was performed to assess Gli2-Sufu interaction. **(B) Gli2-FlagHis localizes to the cilium.** Undifferentiated and differentiated Gli2-FlagHis cells were stained by immunofluorescence for Flag (green) and cilia (actub, red). Scale bar ~5μm. **(C) Mass spectrometry data failed to detect Gli2, but detected Sufu, a known Gli2 interactor.** A data set from one experiment is shown. While Sufu peptides were covered, Gli2 failed to be detected. All other proteins were not consistent between the first purification step by Flag and the second purification step by His. Two other data sets were comparable in that Sufu was covered, but Gli2 was not.

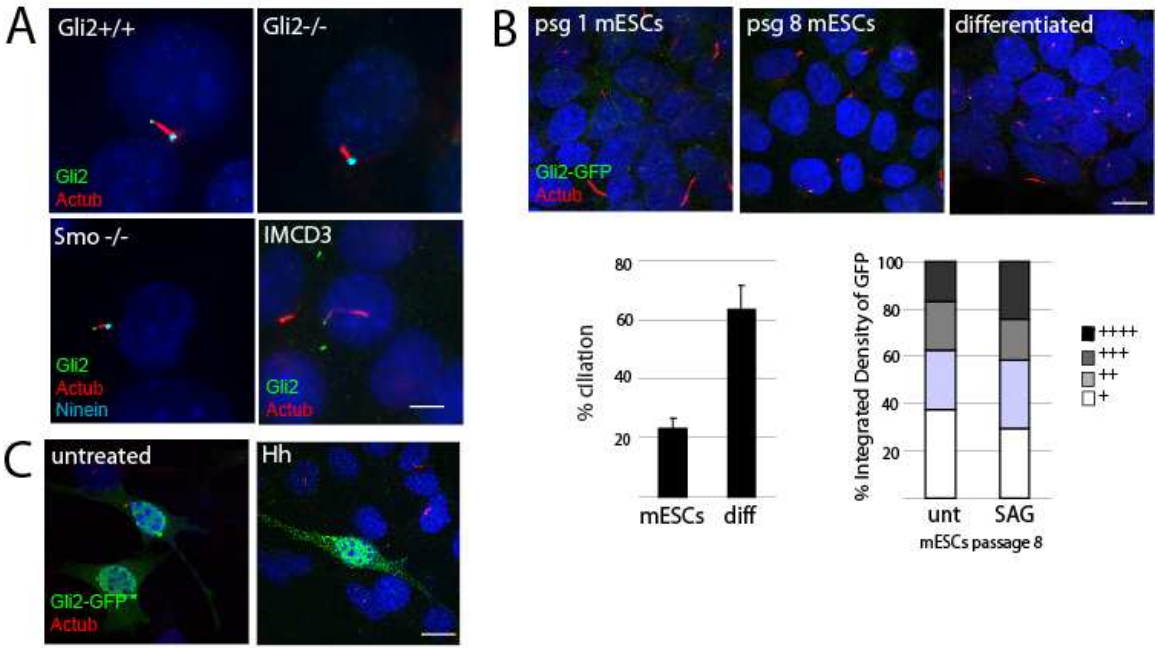

Figure 19. Supplemental figures

(A) Gli2 can reach the cilium in Hh unresponsive cell lines. Gli2 wild type and knockout MEFs were obtained from e11.5 embryos. *Smo*-/- MEFs lack the central activator of the pathway, while IMCD3 cells are derived from kidney collecting ducts. Cell lines were stained for a C-terminal Gli2 antibody (green) and cilia (actub, red). Scale bar ~5μm. **(B) mESCs are well-ciliated upon differentiation and in later passage mESCs.** Ciliation was assessed in Floxin Gli2-GFP cells at different passage numbers and upon differentiation. Quantification was determined by ciliary staining (actub, red) over total Dapi. mESCs at passage 8 were treated with SAG (1μM) and the integrated density readings of GFP foci was analyzed by Image J. Scale bar ~10μm. **(C) Over-expressed Gli2-GFP localizes to the cytoplasm and nucleus, independent of Hh stimulation.** NIH 3T3 cells were transfected with Gli2-GFP and stained with GFP (green) and cilia (actub, red). Over-expressed Gli2-GFP localizes to the cytoplasm and nucleus independent of Hh stimulation. Scale bar ~10μm.

Chapter IV.

Discrete domains mediate Gli2 localization and function

Abstract

Vertebrate Hedgehog (Hh) signaling requires primary cilia. The effectors of the pathway, the Gli transcription factors, accumulate at ciliary tips in response to Hh ligand. However, the molecular mechanisms that regulate this translocation remain unexplored. In this study, we utilize a knock-in approach called the Floxin system to examine how various domains regulate Gli2 subcellular localization and subsequent function. We show that only full length Gli2 is able to reach the cilium, and identify regions and post-translational modifications of Gli2 that influence its nuclear enrichment, stability and function. We shed light on the parallels between nuclear trafficking and ciliary trafficking and address this as a potential mechanism for Gli2 ciliary import and export. Lastly, we identify a central region of Gli2 that is required, but not sufficient for Gli2 ciliary localization. Together, these studies provide significant insight into how Gli2 may be functioning at the subcellular level.

Introduction

Initially identified as a putative oncogene amplified in glioblastomas, the glioma-associated oncogene family members (Gli1, Gli2, Gli3) are the transcription factors of the Hedgehog (Hh) pathway. Although the Gli proteins are highly related, they possess different biochemical properties and play distinct roles in development. Gli2 and Gli3 are absolutely required for vertebrate development, while Gli1 is dispensable as it acts to enhance the expression of Hh target genes after their initial activation [176, 177]. *Gli1* and *Gli2* mRNA are detected close to Hh sources, while *Gli3* mRNA is not [184], suggesting that Gli3 functions differently than Gli2 in vivo. Moreover, in addition to cancer, the Gli proteins have been implicated in a variety of congenital malformations, such as cephalopolysyndactyly and Pallister-Hall syndrome (reviewed in Chapter 3 and [47]).

Given their clinical relevance, extensive studies have focused on the idea that sequence similarities and differences among the Gli proteins can illuminate how they are differentially regulated. Moreover, conservation between Ci, the Drosophila homolog, and the Gli family has also provided some insight into Gli biology (**Figure 20a**). Most obviously, Ci/Gli proteins share homology in five tandem C2-H2 zinc fingers (ZFs) that bind the same target DNA sequence 5'-GACCACCCA-3' [50, 185]. The crystal structure of the Gli ZFs has been solved and the last three ZFs bind DNA most extensively [186]. The first two ZFs retain 58% homology across phyla, suggesting a potential conserved function. $Ci^{\Delta ZF1\text{-}2}$ exhibits a gain of function phenotype due to defects in Ci proteolysis [187]. In Gli2, loss of the first two ZFs and the entire sequence N-terminal to it, leads to a functionally inactive allele by Gli-luciferase reporter [188].

Gli2/3 possess both activator and repressor domains

The bipotential function of Gli2 is due to the presence of both activator and repressor domains at the C-terminus and N-terminus, respectively. C-terminal deletions of Gli2 abrogate Hh signaling demonstrating that this region is necessary for Gli2 and its ability to activate target genes. Sasaki et al described two discrete C-terminal regions that are sufficient to induce transcription [188]. Gli2 proteins lacking either of these domains can function in vitro as repressor, as they deactivate full length Gli1 and Gli2 upon co-expression. They postulate that two mechanisms of transactivation are involved, based on evidence observed in Ci and Gli1. First, the histone acetyltransferase dCBP binds to the C-terminus of Ci and functions as a co-activator. Accordingly, loss of dCBP disrupts Hh signaling [189, 190]. The Drosophila CBP-binding motif in Ci is well-conserved in Gli2 and Gli3, but not Gli1 [52]. Second, the TATA box-binding protein-associated factor$TAF_{II}31$, a component of the basic transcriptional machinery, has been suggested to directly interact with Gli1. This motif found in the C-terminal tail of Gli1 is also conserved in Gli2 [191]. Thus, it is possible that both interaction with CBP/p300 and $TAF_{II}31$ are both necessary for Gli2 function.

Conversely, N-terminal deletions of Gli2 have been shown to over-activate Hh signaling both in vitro and in vivo. Specifically, loss of the first 280 amino acids of Gli2 dramatically increased Gli-luciferase activation and can ventralize the neural tube of transgenic mouse embryos [188]. Deletion of this repressor region in Ci activated ectopic *ptc* expression in Drosophila embryos, while deletion in Gli3 converted the repressor into an activator [188, 192]. Given the hyperactive phenotype associated with Gli2Δ1-280, this allele has been used in several mouse models examining Hh-mediated tumorigenesis in the skin and pancreas, for instance [193-195]. How this domain restrains Gli2 function remains unclear, but a sub-domain within this region has been

shown to be important for Gli1 degradation. Specifically, loss of a fifty amino acid stretch in Gli1 leads to protein stabilization and accelerated BCC formation in transgenic animals, and has thus been characterized as a degron [196]. In Ci, deletion of an overlapping domain, termed the N-terminal regulatory domain (NRD), causes no overt developmental phenotype, but this mutant Ci protein is sequestered in the nucleus, rather than the cytoplasm [187]. However, this mutant extends its deletion to the Sufu binding motif, described below. These regions are 57% homologous among human, mouse and Drosophila protein and contain many conserved serine residues. Together, these data suggests that the N-terminus of Ci/Gli is important for Gli2 function, stability and localization.

PKA phosphorylation of Ci and Gli2/3 mediate processing and degradation

Ci and the Gli proteins retain a cluster of phosphorylation sites downstream of the ZFs [197, 198]. Ci is phosphorylated by protein kinase A (PKA), casein kinase I (CKI) and gylcogen synthase kinase 3 (GSK3). Phosphorylation marks Ci for partial degradation by the proteasome by recruiting the E3 ubiquitin ligase SCF Slimb/βTRCP, and generates an N-terminal repressor protein in the absence of Hh (**Figure 5b**) [135, 199-203]. In the unphosphorylated state, full length Ci functions as a transcriptional activator. Thus, these phosphorylation sites modulate Ci's bipotential function. As noted previously, the function of Ci has been distributed in vertebrates among the Gli proteins (**Figure 1b**). Despite retaining three conserved PKA phosphorylation sites, Gli1 is not proteolytically processed and functions only as a strong activator [52, 188, 204]. Most similar to Ci, Gli3 is phosphorylated by PKA, CKI and GSK3β in the absence of Hh signaling. Upon phosphorylation, Gli3 is targeted for limited proteolysis by the proteasome to generate Gli3R [59, 205, 206]. Several βTRCP binding sites related to the $DSGX_{2-4}S$ motif are interspersed among these phosphorylation sites, and

ubiquitination of Gli3 occurs by SCF Slimb/βTRCP [205]. Thus, Gli3 functions most similarly to the repressor form of Ci. However, full-length Gli3 has been shown to act as a weak activator in vivo [55, 172, 177, 207].

Sharing 44% identity with Gli3, Gli2 also possesses these conserved phosphorylation sites. However, phosphorylation marks Gli2 for complete degradation by the proteasome, rather than limited proteolysis [208, 209]. A small amount of Gli2R is formed, but can only be detected upon enrichment by Gli immunoprecipitation. Like Gli3, βTRCP binding sites are found within Gli2, and mutation of these sites causes stabilization of Gli2 protein in vitro [210]. Moreover, homozygous mice lacking the first four Gli2 PKA phosphorylation sites, *Gli2*$^{P1-4}$, die in utero due to over-stabilized Gli2 protein and subsequent over-activation of the Hh pathway [211]. Consistent with this, mice lacking active PKA die at midgestation and exhibit a completely ventralized neural tube, reminiscent of *Ptc1* and *Sufu* knockout mice [101, 212].

Contributing to the difference between Gli2 and Gli3 proteolysis is the presence of a processing determinant domain (PDD) that stretches approximately 200 amino acids between the zinc finger binding domain and PKA phosphorylation cluster [209]. It is postulated that the sequences of Gli3's PDD and Gli2's PDD leads to partial versus total proteasome-mediated degradation, respectively [208, 209, 211]. Substituting Gli2's PDD with that of Gli3 (*Gli2*^{3PDD}) leads to increased Gli2 repressor formation both in vitro and in vivo [213]. Ultimately, however, while *Gli2*^{3PDD} mice exhibit lower body weight, they are viable and fertile, with no obvious Hh defects. This study adds to mounting evidence that Gli2 likely does not act as a repressor in vivo. Since knock-in of *Gli1* into the endogenous *Gli2* locus rescues the *Gli2* null phenotype, it appears Gli2 only acts as an activator [177]. Conflicting with this, G*li2 Gli3* double mutants show an exacerbated

phenotype in somite development, suggesting that Gli2 may have weak repressor activity, albeit only in the absence of Gli3 [214, 215].

It should also be noted that in addition to SCF Slimb/βTRCP-mediated proteolytic processing and degradation, Ci/Gli proteins have been shown to be targeted for the ubiquitination machinery via other mechanisms. In Drosophila, full length Ci degradation in the nucleus is induced by binding to Hib/Roadkill , which recruits the Cul3-based E3 ubiquitin ligase [216, 217]. Hib's mammalian homology SPOP (speckle-type PDZ protein) has been shown to interact with Gli2/3, but not Gli1 or Gli3R, and promotes their processing and degradation [83, 85, 216]. Additionally, Gli1 is targeted by another E3 ubiquitin ligase, Itch [218].

Interestingly, PKA has been shown to localize to the base of the primary cilium [101, 219]. Mutation of PKA sites 1-4 in Gli2, and the subsequent phosphorylation sites of CKI and GSK3, to either phospho-mimetic or phospho-dead alleles, however, does not alter its ciliary localization [98]. However, while inhibition of PKA by forskolin (FSK) has been shown to diminish the ciliary localization of Gli-Sufu complexes, *PKA* null cells display an increase in Gli2 accumulation at ciliary tips [85, 98, 100, 101]. Reconciling these discrepant data, the authors of the latter study also show that FSK treatment of PKA null cells also leads to a decrease in Gli2 ciliary translocation, suggesting that the effects of FSK are independent of PKA itself. In any case, it appears PKA may modulate Gli2 stability upon entry to or exit from the primary cilium. Likewise, cilia may promote Gli3 PKA phosphorylation and processing in a similar manner work. Many groups have demonstrated that mouse mutants lacking functional cilia possess impaired Gli3 processing and subsequent polydactyly [62, 79, 82, 220-222]. However, it is unclear if Gli3 processing occurs before or after transport into the cilium.

Subcellular distribution of the Gli proteins to the cytoplasm, nucleus and primary cilium

While Drosophila mutants lacking Sufu are viable and only exhibit subtle patterning defects, Sufu is critical for negatively regulating the Hh pathway in vertebrates [86, 88, 89]. Although the reason for Sufu's evolved dispensability remains unclear, Sufu appears to anchor Ci/Gli in the cytoplasm in the absence of Hh stimulation in both Drosophila and vertebrates [92, 223-225]. Mutational analyses identified a SYGH motif in the N-terminus of Gli/Ci proteins that is required for Sufu binding, while additional studies have demonstrated that Sufu can bind Gli1 through interaction sites at both the N and C-termini [94, 96, 97]. Ci lacking this SYGH motif exhibits nuclear accumulation, while deletion in Gli1 leads to a similar phenotype [96, 187]. Thus, cytoplasmic and nuclear localization are regulated by the interaction of Gli with Sufu. Additionally, Sufu may stabilize Gli2/3 by inhibiting the SPOP Cul3-based E3 ubiquitin ligase, as *Sufu*-/- cells display decreased levels of Gli protein [83, 85, 226].

Another subcellular compartment occupied by the Gli proteins is the microtubule-based organelle, the primary cilium [82]. Sufu is not required for Gli translocation to the primary cilium. Rather, Sufu localizes to the cilium in a Gli-dependent manner [83, 98, 100]. Zeng et al. dissected the domains that are necessary for Gli ciliary localization by over-expression of mutagenized N-terminally tagged GFP-Gli2 alleles [98]. They indicated that a central region of Gli1-3 is required, but not sufficient, for ciliary localization. This region spans the end of the ZFs to downstream of the PKA phosphorylation cluster. Moreover, Gli2 missing the first half of the protein also showed diminished ciliary localization, suggesting that an N-terminal region plays an important, but not essential role in ciliary trafficking. Ci fails to reach the cilium in mammalian cells as well, suggesting that just like Smo, there are mechanisms for Ci activation in Drosophila that are distinct from those of the Gli proteins in vertebrates.

How the Gli proteins translocate to the primary cilium is unclear. One hypothesis is that Kif7, a mammalian homolog of Cos2, is involved. In Drosophila, Ci has been shown to complex with Sufu, serine-threonine kinase Fused (Fu) and a kinesin-like protein Costal2 (Cos2) (**Figure 5b**) [116]. While the role of Fu in Hh signaling has diverged through evolution, a vertebrate homolog of Cos2, Kif7, is required for normal Hh signaling [227-229]. Cos2 plays a dual role in Drosophila Hh signaling, in that interaction with Ci in the absence of signaling promotes Ci repressor formation, while interaction with dSmo in the presence of Hh signaling promotes Ci activation. Cos2 can bind microtubules, but its motor function has been disrupted [45, 230]. Thus, Cos2 acts both as a negative and positive regulator of the Hh pathway in Drosophila. In vertebrates, Kif7 interacts with the Gli proteins and *Kif7-/-* mice exhibit compromised Gli3R formation, suggesting that the negative regulatory role has been conserved from flies [118, 231]. Since Kif7 retains motor domains and has been observed at the base and tip of the cilium, it has been postulated that it acts as a motor that carries the Gli proteins away from and into the ciliary compartment [63, 229]. Since Kif7-/- cells exhibit an upregulation Gli2/3 and Sufu ciliary accumulation, rather than a loss of localization, Kif7 could traffic Gli2/3 away from the cilium in the absence of Hh stimulation [232]. Upon Hh stimulation, it is postulated that Kif7 somehow promotes the dissociation of Gli-Sufu complexes within the cilium [232]. Importantly, human mutations in *Kif7* have been linked to the ciliopathy Joubert Syndrome, further suggesting that this kinesin plays a role in microtubule and ciliary dynamics [233].

Ciliary trafficking parallels with nuclear trafficking

Recent evidence has illuminated a possible parallel between nuclear trafficking and ciliary trafficking, although the Gli proteins have not been studied in this regard. Briefly, macromolecules that are generally bigger than 40kDa in mass or 5nm in diameter pass

bi-directionally across the nuclear envelope by way of structures called nuclear pore complexes (NPC). Cargoes are selected based on the presence of a transport signal that mediate their binding to shuttle proteins. Importins bind to cargoes containing nuclear localization signals (NLS) and transport them from the cytoplasm into the nucleus. A few NLS sequences have been described, with the classical NLS being a cluster of positively charged residues (e.q. KKKRK) ([234, 235]. Conversely, proteins called exportins bind to cargoes containing nuclear export signals (NES) and carry them from the nucleus into the cytoplasm. The most characterized NES is a hydrophobic leucine-rich domain that is recognized by Exportin1/Crm1. The binding and release of cargo relies on the small GTPase Ran. The nucleus contains high levels of Ran-GTP that facilitates the binding of exportins to NES-containing cargo. Once in the cytoplasm, high Ran-GDP levels leads to cargo release. Reciprocally, dissociation of import complexes from their cargo is mediated from high Ran-GTP in the nucleus.

Recent work has found that endogenous βimportin2 localizes to the primary cilium and centrosomes of epithelial cells [236, 237]. Furthermore, Ran-GTP was detected at the primary cilium, suggesting that the Ran gradient present in the nucleus may be present in the ciliary compartment, as well. Kif17, an IFT ciliary motor, contains two NLS's, and when one of these sequences is mutated, ciliary localization of Kif17 and its interaction with βimportin2 is prevented [236]. Similarly, retinitis pigmentosa 2 (RP2) possesses an M9 NLS sequence that upon mutation, leads to defects in ciliary localization, as well as interaction with βimportin2 [237]. Additionally, several nucleoporins have been shown to localize to the base of the primary cilium, and the entry of cytoplasmic molecules into the cilium appears to be regulated by a size-dependent diffusion barrier [238]. Together, these data begin to suggest that the mechanisms that drive the import of proteins into the nucleus may also be used to traffic proteins into the cilium.

Sufu and Ci/Gli retain classical leucine-rich nuclear export signals. Sufu exists in both the nuclear and cytoplasmic fractions and functions in regulating the nuclear-cytoplasmic shuttling of the Gli proteins [96, 225, 239]. Ci/Gli proteins appear to be mostly cytoplasmic and enter the nucleus upon the presence of Hh ligand [55]. However, deletion of putative NES signals within Sufu, Gli1 and Gli2, as well as treatment with Leptomycin B, an inhibitor of Crm1-dependent nuclear export, show varied results, depending on cell type and expression levels [90, 96, 179, 225, 239]. Gli1 possesses two nuclear localization signals (NLS) that are conserved in Ci and Gli2/3 [225]. Thus, the nuclear and cytoplasmic distribution of the Gli proteins may be mediated by a combination of mechanisms, including Sufu tethering in the cytoplasm or active nuclear import and export. Whether or not NLS and NES mediate Gli ciliary import and export remains to be explored.

Other putative Gli2 post-translational modifications

In addition to phosphorylation by PKA and CKI, the Gli proteins are thought to undergo other post-translational modifications (PTMs). First, phosphoinositide 3-kinase-dependent activation of Akt has also been implicated in Hh signaling at the level of Gli2 [240]. The PI3-kinase/Akt pathway has been previously shown to act synergistically with Hh signaling in tumor initiation [241, 242]. Gli2 possesses a putative Akt phosphorylation site (RXRXXS) that can also be found in Ci, Gli1 and Gli3. Mutation of this domain does not prevent dominant negative dnAKT-mediated repression of the Hh pathway, however [243]. Second, histone deacetylase I (HDAC1) has been shown to interact with and positively modulate Gli1 activation. Deacetylation of a conserved lysine in Gli1 (K518) promotes transcriptional activation, suggesting that this PTM may be important for regulating Gli function [244]. Gli1 K518 is conserved in Gli2, but not Gli3.

Lastly, sumoylation is another PTM that has been postulated to act on the Gli proteins [245]. Small ubiquitin-related modifier (SUMO) proteins conjugate to lysine residues of targets at consensus sites ψKXE and can promote a variety of cellular responses, including protein degradation, changes in subcellular localization and transcriptional activation or inhibition [246]. Sumoylation of the Gli proteins has been proposed to promote Gli activation of target genes, and this PTM is blocked by PKA activity [245]. Over-expression of the Sumo-E3 ligase Pias1 enhances Gli activity in vitro and was able to induce ectopic Nkx2.2 in the floorplate of chick embryos, and Pias1 has been identified as a potential interactor with Sufu [239]. These sumoylation sites are conserved in Gli1, Gli2 and Gli3, but not Ci.

Taken together, these studies have demonstrated that Gli2 is a complex transcription factor that holds the potential to both activate and repress target genes. It undergoes various post-translational modifications, and is differentially regulated in various subcellular compartments, including the nucleus, cytoplasm and the primary cilium. These Gli domains have been dissected by over-expression and deletion assays, comparative sequence analysis, domain swapping and mouse models (summarized in **Figure 20b**). However, many of these studies may be prone to artifact due to over-expression, and few have examined how these domains affect subcellular localization to the primary cilium. Therefore, we used the Floxin approach (discussed in Chapter 3) to dissect some of the domains and post-translational modifications that have been previously shown to influence Gli2 dynamics. Compared to previous approaches, the Floxin approach has the combined advantages of endogenous control to minimize non-relevant levels of Gli2, the potential to bypass limitations using endogenous antibodies, and the ability to generate a number of mutations and alleles in a time and cost-efficient

manner. Thus, this study has enabled us to analyze Gli2 subcellular localization, protein dynamics and function in a more-relevant context.

Data and Results

To explore specific domains and how they affect Gli2 subcellular localization, we created a panel of Floxin Gli2-GFP mutant cell lines using site directed mutagenesis of the wild type pShuttle vector. All sequences were confirmed prior to electroporation and clones were screened by neomycin resistance, βgal activity and genotyping, as described previously [160]. Two clones from each mutant Floxin line were assessed for GFP localization. Of note, the first 46 codons of Gli2 are upstream of the gene trap and are therefore present in all Floxin lines derived from gene trap XGO45. A summary of Floxin alleles, their localization and function are presented in **Figure 29**.

Activator and repressor domains influence Gli2 nuclear accumulation

The bipotential function of Gli2 is mediated by N-terminal and C-terminal repressor and activation domains, respectively. A previous study showed that deletion of the repressor region causes hyperactivity, while loss of the activator region renders Gli2 non-functional when expressed alone, and a repressor when co-transfected with full length Gli2 and Gli1 [188]. To determine if these repressor and activator domains play a role in regulating Gli2 subcellular localization, we created Floxin mutants Gli2ΔRep and Gli2ΔAct.

We found that while Gli2ΔRep and Gli2ΔAct retained ciliary localization, both were robustly enriched in the nucleus (**Figure 21a**). The overall percentage of GFP-positive cilia was comparable to the wild type allele, but the pixel intensities of GFP foci were decreased for both Gli2ΔRep and Gli2ΔAct (**Figure 21b**). This is likely due to

mislocalization of Gli2 rather than diminished protein levels, as the latter appeared similar to wild type Gli2 by Western blot (**Figure 21e**). Thus, these domains may influence efficient Gli2 ciliary localization, but are not independently required for it. However, the nuclear accumulation of Gli2ΔRep and Gli2ΔAct suggests that these domains may play a role in cytoplasmic tethering.

The nuclear accumulation of both Gli2ΔRep and Gli2ΔAct correlates with the functional phenotypes previously described. As reported, when Gli2ΔRep and Gli2ΔAct are over-expressed in *Smo*-/- MEFs, they function as a gain and loss of function allele, respectively (**Figure 21c**). Since these mutants maintain intact ciliary localization, this suggests that the mechanisms that lead to their altered function are downstream of cilia. It is unclear, however, if their functional phenotypes are solely attributed to their nuclear enrichment, or if secondary events mediate activation and repression of target genes.

Notably, when we assessed differentiated Floxin cells for Hh responsiveness by both *Ptc* and *Gli1* mRNA, we observed that Gli2ΔAct exhibited a dominant negative phenotype, in that it was able to abrogate pathway activation even in the presence of the remaining wild type allele (**Figure 21d**). This observation echoes over-expression data, but in a more relevant context, as Gli2ΔAct is expressed at similar levels to wild type Gli2 from the endogenous Gli2 locus (**Figure 21e**). The fact that Floxin Gli2ΔRep did not hyperactivate the Hh pathway provides evidence that this truncated protein may not be biologically relevant. Although this allele has been used as an oncogenic allele of Gli2, the mechanisms of its hyperactivation remain unclear. Together, given that these domains dictate transcriptional output, their accumulation in the nucleus correlates with a functional phenotype that is independent of ciliary localization.

Fundamental to the ability of Gli2 to act as both a transcriptional activator and repressor are the five tandem C2-H2 zinc fingers (ZF). ZFs mediate transcription factor binding to DNA and are structural motifs that can help stabilize protein folding. Surprisingly, deletion of this region does not abrogate ciliary localization (**Figure 21a**). Functional assays by over-expression shows that the ZF are required for transcriptional activity, but upon differentiation and SAG treatment, Floxin Gli2ΔZF cells are capable of Hh pathway activation, as assessed by *Gli1* and *Ptc* levels (**Figure 21c,d**). Intact Hh responsive is presumably due to the function of the wild type *Gli2* allele. These data indicate that the ZF domain is dispensable for ciliary localization.

Processed forms of Gli2 cannot reach the primary cilium

Previous reports have indicated that Gil2 is subject to full degradation by the proteasome upon phosphorylation by PKA [208, 209, 211]. Unlike Ci and Gli3, Gli2 is not efficiently proteolytically processed into a repressor form. However, there are conflicting data in the literature regarding whether a processed form of Gli2 functions as a repressor [173, 174, 176, 211, 215]. Thus, we generated mutants lacking domains that we hypothesized to affect PKA phosphorylation, and subsequent Gli2 protein stability and processing.

We generated and assessed the function of a mutant Gli2 lacking the PKA cluster, Gli2ΔPC. Deletion of this domain does not change Gli2's ability to translocate to the cilium, nor does it markedly increase Gli2 protein levels (**Figure 21a,e**). The former data are consistent with intact ciliary localization of phospho-dead and phospho-mimetic mutants of PKA1-4, while the latter conflicts with the mild stabilization phenotype seen in embryonic lysate from *Gli2*$^{P1-4}$ mutant mice [98, 211]. While discrepant data may be attributed to differences in vitro versus in vivo, our data support prior evidence that phosphorylation of these PKA sites does not directly facilitate Gli2 ciliary localization.

Gli1 has been shown to possess a N-terminal degron/N-terminal regulatory domain (NRD) that when mutated, stabilizes Gli1 and accelerates its oncogenic potential [196]. Gli2 possesses a homologous NRD domain. We deleted this highly conserved, serine-rich region and found that while transcript and protein levels appeared relatively normal compared to wild type Gli2, Gli2ΔNRD displayed increased activity when over-expressed (**Figure 21c**). This could be due to the fact that this region lies within Gli2's repressor domain, and hints that this specific stretch of amino acids plays a significant role in modulating Gli2 function. Moreover, as observed in Gli2ΔRep, Gli2ΔNRD localized to the cilium properly, but the intensity of these foci were considerably diminished compared to wild type. We observed enriched nuclear localization of Gli2ΔNRD, a possible reason for non-efficient ciliary localization (**Figure 22b**). Together, these data suggest that the NRD region within Gli2 possesses repressive elements, and is subjected to normal degradation.

Due to difficulties with the synthesis of a Floxin mutant allele lacking the processing determinant domain (PDD), we generated a myc-tagged over-expression construct, pCMV Gli2ΔPDD. By over-expression, this allele effectively reached the cilium and retained functional activity (**Figure21a,d**), suggesting that the region between the ZF domain and the PKA sites is dispensable for both Gli2 function and ciliary localization.

Full length Gli2 is readily detected, while a fragment of approximately 78kDa can be detected only upon immunoprecipitation [208, 209]. Gli2-78 is postulated to be the putative Gli2 repressor. To assess the function and localization of Glli2-78, we used the Floxin system to generate an allele that corresponds to this N-terminal protein fragment [226]. We also generated Gli2-110, the C-terminal remainder of Gli2 after proteolytic

processing. We assessed subcellular localization, function and protein levels of these truncated Gli2 alleles.

Neither Gli2-78 nor Gli2-110 localized to the primary cilium, although the former appeared to accumulate in the nucleus similarly to Gli2ΔAct (**Figure 21a**). The inability of these truncated forms to localize to cilia suggests that only full-length Gli2 can reach the cilium, and that both termini of Gli2 are required for this localization. Moreover, these data also imply that Gli2 processing likely occurs downstream of ciliary localization. Both Gli2-78 and Gli2-110 were unable to activate the Hh pathway by over-expression, but like Gli2ΔAct, Gli2-78 functioned as a dominant negative in differentiated Floxin cells (**Figure21c,d**). This data highlights the repressive potential of Gli2-78 in vitro.

When protein levels were assessed, Gli2-110 was de-stabilized compared to both wild type and Gli2-78 (**Figure 21e**). Long exposure of this GFP blot also detected a similar band of ~110kDa in wild type Gli2 lysate, although this band is not consistently or readily observed in wild type lysate or upon GFP immunoprecipitation. Since transcript levels in Gli2-110 cells were unaffected (**Figure 30a**), the C-terminal half of the protein is unstable. Indeed, this region contains the phosphorylation sites and βTRCP-binding motifs necessary for the recruitment of the Gli2 degradation machinery. Together, these data suggest that Gli2-78 can function as a repressor in vivo, and the by-product of this processing, Gli2-110, is actively degraded as it is non-functional.

Loss of Sufu binding affects Gli2 stability and subcellular localization

Sufu has been postulated to tether the Gli proteins to the cytoplasm through a N-terminal motif SYGH [96, 225]. Recent evidence has shown that Sufu also localizes to the

primary cilium in a Gli-dependent manner, and that active Smo translocation to the cilium is necessary for dissociation of Sufu from Gli [83, 98, 100]. Presumably, this is a necessary activation step in Gli function as Sufu is a strong negative regulator of the Hh pathway. To understand how interaction with Sufu modulates Gli2 function and subcellular localization, we created Floxin Gli2ΔSufuBS which lacks this SYGH motif.

Gli2ΔSufuBS exhibited intact ciliary localization and increased nuclear localization, as observed by both immunofluorescence and nuclear-cytoplasmic fractionation (**Figure 22a,b, 23e**). Protein levels were diminished, which is consistent with evidence that genetic loss of Sufu destabilizes Gli2 (**Figure 21e, 23e**) [83]. This decrease in overall Gli2ΔSufuBS levels, as well as the increase in nuclear Gli2ΔSufuBS, could be why GFP ciliary foci were less intense than wild type foci (**Figure 22a**). These data demonstrate that Sufu binding to the SYGH motif mediates Gli2 nuclear localization, but not ciliary localization. Indeed, as previously reported, we also found that Gli2 effectively reached the cilium in *Sufu*-/- MEFs (**Figure 22d**) [83].

Immunoprecipitation experiments suggest that dual sites may mediate Gli2-Sufu interaction. While Sufu interaction is significantly decreased upon deletion of the SYGH motif alone, a significant amount of Sufu can still be detected upon GFP immunoprecipitation of Gli2ΔSufuBS (**Figure 22b**) [96]. Indeed, previous reports demonstrate that a C-terminal domain within Gli1 also mediates Sufu binding [96, 97]. In support of this, our C-terminal Floxin deletions also exhibit robust nuclear accumulation (**Figure 21**).

Despite increased degradation and nuclear enrichment, a slight, but not significant, increase in both *Gli1* and *Ptc* mRNA levels and Gli-luciferase activity was observed in

differentiated Gli2ΔSufuBS Floxin cells and when over-expressed Smo-/- MEFs. This suggests that functionally, loss of Sufu interaction through this SYGH motif is not sufficient to hyperactivate Gli2 like the loss of the N-terminal repressor domain (**Figure 22c**). Thus, we conclude that gain of function is not conferred to Gli2 by mere dissociation from Sufu or aberrant nuclear accumulation, and that other regulatory actions maintain Gli2 function. Rather, the primary role of Sufu is to promote Gli2 cytoplasmic retention and/or inhibit its nuclear translocation. Altered subcellular localization upon diminished Sufu-Gli2 interaction could be the cause of increased Gli2 degradation.

Sumoylation may repress Gli2 function

Since it has been postulated the Sufu-Gli interaction is a major control point in the Hh pathway, we assayed if post-translational modifications could regulate this. Prior to work done by Cox et al, we recognized that Gli2 contains four consensus sites for sumoylation (**Figure 23a**) [245]. These sites flank the zinc finger domain and are conserved in Gli3, but not Gli1 or Ci. While Sumo proteins are similar to ubiquitin, sumoylation has been to shown to influence nucleo-cytosolic transport, transcriptional regulation and protein interaction [246].

We found that upon immunoprecipitation, Gli2-GFP could be sumoylated in vitro (**Figure 23b**). Single or tandem mutation of each of these four lysines to unsumoylatable arginines did not impact ciliary or nuclear localization or accumulation upon over-expression or Floxin mutation (**Figure 23c,d**). Surprisingly, however, our Gli-luciferase reporter assay indicates that a mutant in which sumoylation sites are rendered non-functional is hyperactive in a site-dependent manner (**Figure 23c**). When all four sumoylation sites are mutated, Gli2 can function similarly to the removal of the repressor

region, suggesting that sumoylation is a repressive mark that diminishes Gli2 function. Gli2ΔSumo is expressed similarly to wild type Gli2, suggesting that sumoylation does not target Gli2 for degradation. Gli2ΔSumo retains the ability to interact with Sufu, suggesting that this PTM does not abrogate Sufu-Gli interaction (**Figure 23d**). However, we failed to detect several Sumo pathway components at or near the primary cilium, including Sumo1,2,3, the proteases that mediate desumoylation Senp2,3,5 and an E3 sumo ligase, Pias□ (**Figure 23e**). We could not detect Gli2 interaction with any of the Sumo proteins by over-expression, either. Given that these components are highly expressed in the nucleus, it could be that desumoylation influences Gli2 transcriptional readout. The fact that Gli2ΔSumo does not aberrantly localize to the nucleus demonstrates that nuclear localization does not necessarily correlate with Gli2 function. Further work will discern if loss of sumoylation is a potential mechanism for Gli2 activation, at or downstream of the primary cilium.

In addition to sumoylation, we also assessed if phospho-dead and phospho-mimetic versions of the AKT site in Gli2 overtly affected ciliary localization or Sufu interaction. Both mutants, Gli2ΔSAktA and Gli2ΔSAktD, were detected in the cytoplasm, nucleus and the ciliary tip. Sufu interaction with these mutants was intact, unlike Gli2ΔSufuBS-FlagHis (**Figure 23f**). For Western analysis, these Akt mutants were generated in a different pFloxin vector that possesses a C-terminal FlagHis tag.

Nuclear pore-like trafficking may export Gli2 from cilia

In addition to Sufu mediating the subcellular localization of Gli2, we also examined if nuclear import and export signals dictate its nucleo-cytoplasmic and ciliary shuttling. Nuclear import can be mediated by a variety of nuclear localization signals (NLS), including single or bipartite lysine-rich motifs, glycine-rich domains and consensus

sequences like the M9 domain. On the other hand, Exportin1/Crm1 has been shown to interact with cargo via nuclear export signals (NES) that are rich in leucine residues [234, 235]. Given that recent studies have suggested that the mechanisms that mediate nucleo-cytoplasmic trafficking may also be used to regulate ciliary trafficking, we examined if loss of nuclear import and export signals regulates Gli2 ciliary entry [236, 237].

Two lysine-rich regions have been previously described in Gli1 as NLS's, but necessity and sufficiency for nuclear localization were not examined [225]. These regions span previously created Floxin mutant lines. The first lysine-rich motif spans the N-terminal regulatory domain (NRD), while the second is located at the end of the last zinc finger domain (**Figure 21**). The former reaches the cilium, but much less effectively than wild type Gli2, while the latter which disrupts a bipartite NLS, reaches the cilium robustly. We also identified one other lysine-rich domain, although it contains several leucine residues interspersed among these positively charged amino acids (**Figure 24a**).

We identified hydrophobic leucine-rich NES's within Gli2. We created Floxin lines deleting these regions singularly and since NES2 is characterized by both leucine and lysine rich residues and could potentially mediate both import and export, we created a tandem Floxin mutant lacking NES1, 3 and 4 only. We observed a slight increase in overall ciliary localization in most mutants (**Figure 24a**). Gli2ΔNES1 appeared to localize to the cilium effectively, but overall intensity of these foci was less than wild type, despite robust protein expression (**Figure 24b,c**). This domain lies within Gli2ΔNRD and Gli2ΔAct which also exhibited decreased ciliary intensities. The combinatorial mutant Gli2 ΔNES_{all} displays a decrease in low intensity GFP foci compared to single mutants and the wild type allele, suggesting that these NES's may cooperate to mediate

Gli2 ciliary export. However, we did not observe increased nuclear accumulation with these Floxin cell lines that presumably lack their nuclear export signals. Although endogenous Gli2 antibodies fail to detect nuclear Gli2 due to low expression levels, we have previously generated Floxin Gli2-GFP mutants that exhibit nuclear enrichment (**Figure 21, 30b**). Thus, it is possible that other signals mediate Gli2 export from the nucleus.

Recent work has found that endogenous βimportin2 localizes to the primary cilium and centrosomes of epithelial cells [236, 237]. Consistent with this, we found βimportin2 to localize to primary cilia in NIH 3T3 fibroblasts (**Figure 25a**). Since Exportin1/Crm1 has previously been reported to localize to centrosomes in order to facilitate the docking of centrosomal proteins, including pericentrin, we assessed if Crm1 localizes to the primary cilium as well [247]. Endogenous Crm1 was observed at the cilium in a minority of IMCD3 and NIH 3T3 cells. In NIH 3T3 cells, Crm1 localization varied from basal body staining, to punctae along the cilium, to the ciliary tip, while in IMCD3 cells, punctae staining was most prevalent (**Figure 25a**). This localization pattern is reminiscent of proteins being trafficked along the ciliary axoneme, including the Gli proteins. We observed Crm1 co-localization with Gli2 in a minority of 3T3 cells by immunofluorescence. In most cases, however, Crm1 appeared to stain the basal body while Gli2 was predominantly found at the ciliary tip (**Figure 25b**).

To see if Crm1 mediates ciliary Gli2 levels, we treated wild type primary MEFs with Leptomycin B and Ratjadone A, pharmacological inhibitors of Crm1. We found that upon LMB and RJA treatment, some cells displayed large foci of endogenous Gli2 at the ciliary tip. Upon quantification of both pixel intensity and area, we observed that inhibition of Crm1 led to an increase in the percentage of high intensity foci (**Figure 25c**).

We observed similar results with LMB-treated differentiated Floxin Gli2-GFP mESCs and NIH3T3 cells expressing GFP-Gli2 from a single integration site (**Figure 30c**). Notably, undifferentiated Floxin Gli2-GFP mESCs did not recapitulate this observation, but this could be due to cell type specificity and proliferative differences between mESCs and differentiated cells.

To determine the specificity of LMB and RJA for Crm1, as well as Crm1 localization to the primary cilium, we used siRNA to knockdown Crm1 in NIH 3T3 cells. Three different siRNA constructs were used to target Crm1 and assessed by immunofluorescence and western blot 72 hours after transfection. We observed decent knockdown, ranging from 40-60% based on Crm1 staining (**Figure 25d**). siRNA #2 exhibited the most efficient knockdown, but exhibited cell toxicity.

By immunofluorescence, Crm1 staining pattern along the cilium was still detected in cells exhibiting knockdown (**Figure 25e**). This suggests that either partial knockdown is inefficient to deplete ciliary Crm1 or that non-specificity of the Crm1 antibody detects false ciliary localization. Nevertheless, we assessed if endogenous Gli2 was enriched at the primary cilium upon knockdown. Comparing non-knockdown to knockdown cells, we did not detect a consistent and robust phenotype in Gli2 ciliary accumulation within and across three experiments (**Figure 25f**). Subtle changes in Gli2 ciliary localization were observed with siRNA#1, which displayed more efficient knockdown. siRNA#3, on the other hand, displayed weaker knockdown, and did not show a ciliary accumulation phenotype. Importantly, Gli2 ciliary localization in Crm1 siRNA transfected cells appeared diminished compared to scramble siRNA, suggesting that Crm1 knockdown could possess adverse side effects. The fact that siRNA#3 was less efficient in knockdown and retained higher intensity foci supports this.

Of note, we also assessed Gli2/3 interaction with Crm1. Using reciprocal immunoprecipitations for Floxin Gli2-GFP and endogenous Crm1 and Gli3, we did not observe any specific Gli-Crm1 interaction. MEFs treated with LMB, as well as Floxin ΔNES lines were also assayed. Known Gli interactor Sufu and known Crm1 interaction, nucleophosmin, were used as controls [248]. Thus, it is unlikely that Crm1 and Gli2 protein robustly interact, although this interaction could be highly transient. Taken together, this study starts to suggest that nuclear export may play a role in trafficking Gli2 out of the cilium. While Crm1 may not be the acting exportin, it is possible that LMB and RJA could target another exportin that directly affects Gli2 localization.

Identification of a domain necessary, but not sufficient for Gli2 ciliary localization

In our deletion analysis, we have found that much of Gli2 is dispensable for ciliary localization. However, two domains have not been covered, specifically the region between the Sufu binding site and the zinc fingers (aa271-416) and the region between the phosphorylation cluster and the C-terminal CBP activation domain. The former, when over-expressed, can be detected at the primary cilium (**Figure 30d**). We found that deletion of the latter, aa852-1183, however, was sufficient to cause a significant loss of Gli2 ciliary localization both by over-expression and Floxin (**Figure 26a**). Upon differentiation of Floxin cells, a very small percentage of Gli2Δ852-1183 reached the cilium and this was minimally enhanced upon SAG treatment. This defect in ciliary localization correlates with our finding that Gli2-78 cannot localize to the cilium, but Gli2ΔAct can (**Figure 21**).

To ensure normal protein expression, we assessed transcript levels of Gli2 and GFP, as well as protein expression by Western blot in mESCs and differentiated cells (**Figure 26b**). Given that both message and protein levels were comparable to wild type Gli2, we

concluded that Gli2Δ852-1183 was defective in ciliary localization. To determine if this analogous region is necessary for Gli3 ciliary localization, we deleted amino acids 912-1223 in hGli3-GFP. We found that while wild type Gli3 robustly reached the cilium, Gli3Δ912-1223 did not (**Figure 26c**).

Since this region appeared to be necessary for Gli2 and Gli3 ciliary localization, we tested if it was sufficient. First, when we over-expressed a myc-tagged allele of this Gli2 region of approximately 330 amino acids in NIH 3T3 cells, it failed to reach the cilium. This data corroborates with previous evidence that Gli2-110, which retains amino acids 676-1544, cannot localize to the cilium either (**Figure 21**). Second, we fused the C-terminal region of Gli2, amino acids 852-1544 to the N-terminal half of Ci, the Drosophila homologue of the Gli proteins that does not localize to the cilium (**Figure 26d**). This chimeric protein failed to reach the cilium, but did appear to form aggregates upon over-expression. Thus, we conclude that this domain is necessary, but not sufficient for ciliary localization.

Consistent with this, Floxin lines for the N-terminal and C-terminal truncated forms of Gli2, Gli2-78 and Gli2-110, did not localize to the primary cilium, hinting that tandem domains may be required for optimal localization (**Figure 21**). Moreover, N-terminal deletions of Gli2 appear to possess intact ciliary localization, although levels are diminished relative to wild type (**Figure 21-22**). Results from Zeng et al concur that a partially overlapping central domain is also necessary for ciliary localization (amino acids 570-967) and that Gli2 missing the first half of the protein also exhibited diminished ciliary localization, further suggesting that an N-terminal region plays an important, but not essential role in ciliary trafficking [98]. Differences in the exact amino acid sequence

between our study and Zeng et al could be attributed to differences in over-expression versus Floxin, as well as N-terminal versus C-terminal GFP tags.

Although this region of Gli2 is not a bonafide ciliary targeting domain, we sought to assess the consequences of compromised Gli2 ciliary localization. Functionally, Floxin cells only show a phenotype if the knock-in allele acts as a dominant negative. Gain of function and loss of function are more difficult to assess. Upon differentiation, Floxin Gli2Δ852-1183 does not act as an unequivocal dominant negative, like Gli2ΔAct or Gli2-78 (**Figure 21**). Rather, transcript levels of *Gli1* and *Ptc* in response to Hh stimulation appear diminished relative to controls. Upon over-expression, however, Gli2Δ852-1183 exhibits a loss of function phenotype, and upon co-expression with wild type Gli2, can act as a dominant negative (**Figure 27a**). This starts to suggest that the levels of Gli2Δ852-1183 are important for its functional output, and this allele can act as a dominant negative allele.

This loss of function phenotype and dominant negative potential has been previously shown in an overlapping region by Sasaki et al, where they postulated that the C-terminus of Gli2 can be divided into two activation domains, aa642-1183 and aa1183-1544 [188]. Gli2 mutants lacking aa642-1544 and aa1183-1544 both act as dominant negative alleles by over-expression. Our data indicates that aa852-1183 may specifically contribute to this phenotype. Since the Drosophila CBP-binding motif of Ci is conserved in Gli2 and Gli3 and lies within this region, we postulated that compromised CBP interaction is the cause of Gli2Δ852-1183 loss of function phenotype. We created and analyzed sub-deletion mutants, and found that only the mutants missing this CBP motif were functionally inactive by Gli-luciferase (**Figure 27b,c**). Deletion of this CBP motif specifically abrogates CBP interaction by co-immunoprecipitation, and this

interaction may occur in the nucleus as CBP localized exclusively to the nucleus and was not observed at the primary cilium (**Figure 27d**). Additionally, this CBP domain has previously been deleted in part, as it overlaps with a domain previously described as a Gli2 nuclear export signal (**Figure 24**) [225]. Unexpectedly, all sub-deletions generated within amino acids 852-1183 did not alter ciliary localization of Gli2, suggesting that multiple regions within this 330 amino acid stretch are required to mediate Gli2 ciliary localization (**Figure 27c**). Together, these data suggest that the functional phenotype we observe is not attributable to ciliary mislocalization, but rather compromised CBP interaction.

Previous studies have shown that Hh pathway activation stimulates the dissociation of Gli-Sufu complexes [99, 100]. Since Gli3 dissociation from Sufu does not occur in unciliated cells that lack Kif3a, it has been postulated that the cilium mediates this dissociation. For Gli2, Sufu immunoprecipitated a smaller amount of Gli2 upon Hh pathway stimulation [99]. To test if Gli2Δ852-1183 is chronically associated with Sufu due to its inability to reach the cilium, we performed reciprocal immunoprecipitations for GFP and Sufu in our mutant and wild type Floxin mESC cell lines. First, in non-differentiated Floxin mESCs, we observed that GFP immunoprecipitation of Gli2Δ852-1183 pulled down Sufu more robustly than Gli2 wild type. Reciprocally, immunoprecipitation by Sufu pulled down a visually more intense band for Gli2Δ852-1183, although Gli3 levels appeared equal. Protein levels appeared comparable between wild type and Gli2Δ852-1183 mESC lysate (**Figure 26a, 28b**), suggesting that Gli2Δ852-1183 does indeed associate with Sufu more robustly than wild type Gli2.

To test if SAG could induce wild type Gli2 and Gli2Δ852-1183 dissociation from Sufu, we spontaneously differentiated cells and performed reciprocal co-immunoprecipitations

following a one hour treatment with SAG. We found that upon pull-down with GFP, Sufu interaction was unperturbed, even in SAG-treated wild type Gli2-GFP cells. However, upon Sufu immunoprecipitation, Gli2Δ852-1183 was more robustly detected than wild type Gli2 (**Figure 28b**). The intensities of the SAG treated versus untreated bands did not appear diminished. Rather than chronic association with Sufu, however, this finding is likely due to stabilization of Gli2Δ852-1183 protein. Although increased protein levels in mESCs are not readily evident, upon differentiation Gli2Δ852-1183 is expressed higher compared to wild type Gli2 (**Figure 28b**). Thus, enhanced interaction between Gli2Δ852-1183 and Sufu cannot be determined as increased protein levels of Gli2Δ852-1183 preclude this.

Moreover, to determine if chronic Sufu interaction was the cause of Gli2Δ852-1183's inability to activate the Hh pathway, we deleted the Sufu binding domain in tandem with aa852-1183 and also transfected *Sufu* -/- MEFs with Gli2Δ852-1183 and the Gli-luciferase reporter. Deletion of the Sufu binding site and genetic loss of Sufu did not rescue the loss of function phenotype, implying that the negative function of Gli2Δ852-1183 acts downstream of Sufu (**Figure 28c**).

Transcript levels of Gli2 and GFP are comparable between wild type Gli2 and Gli2Δ852-1183, but the latter displays increased protein levels (**Figure 26b, 28a**). To ask if loss of Gli2 ciliary localization causes protein stabilization, we assessed endogenous Gli2 levels in unciliated cells. Our lab has previously generated cell lines lacking cilia, through the genetic deletion of *Ofd1, Kif3a* and *Ift88* [68, 162]. While Kif3a and Ift88 are IFT components, Ofd1 is a centriolar protein that causes defects in centriolar length and ciliogenesis. Gli2 protein stabilization has been observed in all cell lines lacking cilia and is most pronounced in *Kif3a*-/- MEFs (**Figure 28d** and [165]). Thus, loss of Gli2 ciliary

localization recapitulates total loss of cilia in that increased protein levels of Gli2Δ852-1183 are observed. Furthermore, loss of cilia has been shown to alter Gli3 processing and stability [62, 79]. We observed that Gli3Δ912-1223 is hyper-stabilized upon over-expression, but not robustly processed into its repressor form (**Figure 28d**). Thus, loss of Gli2 and Gli3 ciliary localization appear to possess similar phenotypes to loss of cilia, hinting that this organelle may mediate both Gli processing and degradation.

Discussion

In this study, we specifically and acutely modify the Gli2 locus, and evaluate how this important Hh transcriptional activator behaves at a subcellular level. Since Floxin Gli2-GFP appeared to behave very similarly to endogenous Gli2 in both mESCs and differentiated cells (Chapter 3), we constructed an extensive deletion panel of Gli2 domains using this methodology (**Figure 29**). We chose to first examine previously described domains and post-translational modifications of Gli2 that have been dissected by over-expression assays, comparative sequence analysis, domain swapping and mouse models. While these studies have been instrumental in dissecting the role of Gli2 in the transduction of the Hh signaling pathway, many did not specifically examine how this transcription factor functions at the subcellular level. This is due to limitations in available antibodies and the fact that it was fairly recently the primary cilium came into the Hh picture.

To assess how these domains may play a role Gli2 function and activation at the primary cilium, we used the Floxin approach. This methodology allowed us to query specific domains without the artifact introduced by over-expression and the limitations imposed by endogenous antibodies. Since over-expressed Gli2 can often localize to the nucleus, cytoplasm and cilium in unstimulated conditions (**Figure 19c**), our data is more relevant

as the Floxin method manipulates the endogenous locus. Moreover, the Floxin system afforded us the ability to generate a number of mutations in a time and cost-efficient manner. However, as discussed in Chapter 3, the Floxin method has its disadvantages. In this study particularly, the presence of the wild type allele made loss of function and gain of function alleles difficult to assess. We resorted to over-expression and Gli-luciferase reporter assays for functional assessment, and while this assay is the custom in the field, it can be prone to artifact.

Dominant negative activity of Gli2 upon loss of the C-terminus

Gli2 possesses bipotential function in that loss of the N-terminus leads to a hyperactive allele, while loss of the C-terminus leads to a functionally null allele. When the latter is over-expressed with Gli2 or Gli1, it acts as a dominant negative. We observed similar functional phenotypes in several mutants lacking the C-terminus, including Floxin Gli2-78, Gli2ΔAct and to some extent Gli2Δ852-1183. This data confirms previous reports that Gli2 has repressive and dominant negative potential. Since we have previously demonstrated that Floxin Gli2-GFP mESCs are germline competent, it would be interesting to determine if a mouse model expressing Gli2-78 or Gli2ΔAct would phenocopy Gli2-/- mice or if they would have other developmental anomalies that are associated with Gli3R function. Thus, this mouse model could more definitely determine what role, if any, Gli2R plays in development.

Nuclear enrichment of Gli2

Gli2 mutants lacking large regions of the N or C terminal regions exhibited an increase in nuclear localization. Gli2ΔRep, Gli2ΔNRD, Gli2ΔAct possess both gain of function and dominant negative phenotypes despite proper localization to cilia. These data suggest that the mechanisms that lead to their altered function are downstream of cilia, and likely

occur in the nucleus. Furthermore, these mutants, along with Gli2-78, suggest that Gli2 possesses important regions at both ends of the protein that modulate cytoplasmic tethering or nuclear retention. Since Sufu has been shown to tether the Gli proteins in the cytoplasm, it is possible that Sufu binds Gli2 at another site other than the SYGH motif previously described [96]. Indeed, we observed that while loss of this Sufu binding site at the N-terminus led to nuclear accumulation, Gli2ΔSufuBS appeared to still interact with Sufu in both Floxin Gli2-GFP and Floxin Gli2-FlagHis cells. Perhaps another Sufu binding site exists at the C-terminal half of the protein. Consistent with this hypothesis, Merchant et al observed that the amino terminus of Sufu binds to the carboxy end of Gli1 [97]. Determining if Gli2-110 interacts with Sufu will address this.

Post-translational regulation of Gli2

While PKA has been shown to modulate Gli2 degradation, it is unclear how PKA regulates Gli2 ciliary localization. Importantly, PKA has been shown to localize to the base of the primary cilium [101, 219]. Previous studies show that inhibition of PKA by forskolin diminishes Gli2 localization, and our data and that of Zeng et al demonstrate that the removal or mutation of the central PKA domain does not alter ciliary localization [98, 100]. In contradiction to FSK experiments, genetic loss of PKA leads to an increase in Gli2 ciliary localization. In our hands, however, Gli2ΔPC did not recapitulate this [101]. Perhaps manipulation of the two PKA sites downstream of PKA1-4 would render a clearer phenotype. Additionally, indirect effects of PKA phosphorylation remain a possibility, rather than direct phosphorylation of Gli2 itself. For instance, Sufu has been shown to be phosphorylated by PKA, and this phosphorylation stabilizes Sufu. Thus, loss of PKA could induce changes in Gli levels via Sufu degradation [249].

We also observed that another type of PTM, sumoylation, may modulate Gli2 function. While Cox et al proposed that Gli1/3 sumoylation promoted Hh signaling, our functional data suggests that de-sumoylation renders Gli2 hyper-active. Perhaps sumoylation maintains the balance of Gli function, depending on which sites, or which Gli proteins, are sumoylated. Moreover, Cox et al assessed the effects of sumoylation by over-expression of Pias1, rather than mutation of Gli itself. Since Pias1 acts as the Sumo E3 ligase, it is possible that indirect effects of Pias1 over-expression contribute to the phenotype they observed. Nonetheless, their data that both Gli1 and Gli3 can be sumoylated is consistent with our observation that Gli2 may undergo a similar PTM. Since we observed that many Sumo pathway components localize to the nucleus, we speculate that this is the subcellular site of sumo-modification, rather than the cilium. However, sumo-specific Gli2 antibodies would be the best way to assess this.

The possibility that Gli2 interacts with previously undescribed proteins is of outstanding interest, as well. While our mass spectrometry attempts of Gli2 from Floxin cells successfully pulled out Sufu, other potential protein interactors were not robustly and consistently isolated (**Figure 18**). This could be attributed to purification optimization, low expression, cell-type issues, or perhaps Gli2 simply does not interact with much else. To this end, we have attempted to detect interaction with Gli2, Gli3 and Smo, as well as interaction with ciliary motor and transport proteins, Kif3a and Ift88. None of these proteins appear to interact with Gli2 robustly. Optimizing protein purification from various *Gli2*$^{GFP/+}$ cell lines or mouse tissues for mass spectrometry analysis is of outstanding interest.

Parallels between ciliary and nuclear trafficking

Sufu and the Gli proteins are nucleo-cytoplasmic proteins, as they have been shown to localize to both cellular compartments. All possess putative nuclear localization sequences and export sequences. While NLS are varied, leucine-rich NES domains have been shown to bind Exportin1/Crm1. Deletion of conserved leucine-rich NES's within Gli2 yielded a mutant protein that was not aberrantly localized to the nucleus. Lack of nuclear enrichment suggests these NES's do not mediate Gli2 nuclear export, or that multiple mechanisms of cytoplasmic tethering or nuclear export are at play (i.e. Gli interaction with Sufu).

However, we observed ciliary enrichment upon deletion of these NES's in Gli2. The subtle differences compared to wild type Gli2 motivated us to examine Crm1 inhibition more directly. Pharmacological inhibitors of Crm1 consistently led to increased Gli2 ciliary and nuclear accumulation (**Figure 15c**), but partial knockdown of Crm1 by siRNA did not robustly phenocopy these results. Moreover, we were unable to detect a robust Gli2-Crm1 interaction, even by over-expression. Thus, perhaps LMB targets multiple exportin proteins that regulate Gli2 ciliary and nuclear export. Accordingly, not only have several components of the nuclear pore complex been shown to localize to the base of the cilium, proteomic analysis of IMCD3 cilia recovered hits for Importins 5 and 7, and Exportin 2 and 7 [238, 250]. Notably, off target effects of pharmacological inhibitors have previously been implicated in Gli2 studies, like PKA inhibition by forskolin [98, 100, 101]. Thus, while our evidence that Crm1 inhibitors leads to an increase in ciliary accumulation is convincing, further work will need to be done to assess if this mechanism truly regulates Gli2 ciliary localization.

Conversely, the role of nuclear import mechanisms still needs to be assessed for Gli2 entry into the cilium. While our study examined one lysine-rich domain that may be a NLS, others lysine-rich domains were not mutated in tandem. One putative NLS exists upstream of the gene trap insertion site, and cannot be manipulated using this Floxin method. Also, given the fact that NLS are more heterogeneous in nature, it may be difficult to identify a non-classical NLS. Moreover, it also remains to be investigated if the ciliary import and export of other proteins, including Gli1, Gli3 and Sufu, are regulated by similar mechanisms. Regarding Sufu, it is unclear if nuclear localization is mediated by Crm1. One study observed that Leptomycin B treatment had no effect on the subcellular distribution of endogenous Sufu, while others demonstrate that mutation of a putative NES and LMB treatment leads to Sufu nuclear enrichment [96, 239]. From a broader perspective, nonetheless, it will be interesting to determine if a "ciliary pore" acts as a gate for ciliary exclusivity, not just for Hh proteins.

Identification of a region that affects Gli2 degradation and ciliary localization

Similar to Gli2-110 which lacks the first 676 amino acids, Gli2Δ852-1183 did not localize to either the nucleus or the primary cilium. Gli2-110 was destabilized at the protein level, while Gli2Δ852-1183 exhibited the opposite phenotype in that it was stabilized compared to wild type. This suggests that perhaps important sites that mediate degradation may lie within amino acids 852-1183. Multiple E3 ubiquitin ligases play a role in Gli degradation, including SCF Slimb/βTRCP, SPOP and Itch [47]. Itch has recently been shown to recognize proline-rich or pSP motifs within Gli1, specifically within amino acids 755-1106 [218]. A portion of this region overlaps with Gli2 aa852-1183, a region that possesses several proline-rich and pSP motifs. Thus, it is possible that this domain possesses Itch-dependent degron sites. Alternatively, while βTRCP consensus sites have been mapped downstream of Gli2's PKA sites, SPOP has shown to interact with

portions of Gli2/3 carboxy terminus [226]. Specifically, aa961-1300 and aa1051-1328 mediate Gli2 and Gli3 interaction with SPOP, respectively. However, SPOP has been shown to promote degradation of full length Gli2, but not its truncated forms [226]. More work will discern if our ciliary defective mutant displays protein stabilization due to impaired degradation by one of the many several E3 ubiquitin ligases that act on the Gli proteins.

Unanswered questions

It remains to be determined if stabilization of the Gli proteins is a consequence of defective ciliary localization. We found that Gli2/3 protein levels are increased in unciliated cells and that ciliary defective Gli2/3 are also stabilized. Interestingly, upon over-expression of Gli2-78 and Gli2-110 in ciliated cells, the latter possessed similar staining patterns to SPOP (**Figure 30e**) [83]. In non-ciliated cells, the Gli2-110 SPOP-like aggregates were not observed. This data could suggest that cilia play a role in coordinating the degradation of Gli2, and that the amino acids retained in Gli2-110 (676-1544) are sufficient for this.

Importantly, several studies have shown that various non-Hh-responsive cell types exhibit Gli2 ciliary localization, including IMCD3 kidney cells, *Smo*-/- MEFs and undifferentiated human and mouse ESC. Thus, Gli2 ciliary localization can occur independently of pathway activation. To test if Gli2 activation can occur in the absence of cilia, we over-expressed full length Gli2 in MEFS lacking either Kif3a or Ift88. By Gli-luciferase reporter, Gli2 over-expression activated the pathway in the absence of cilia, suggesting that the regulation of Gli2 at the cilium can be circumvented (**Figure 30f**). We recognize that high levels of exogenously introduced Gli2 can overwhelm the

intrinsic Hh pathway, but nonetheless, these data suggest that the requirement for cilia can be bypassed and perhaps acts at the level of modulating Gli2 protein levels.

In summary, it has been postulated that the translocation of Smo to the primary cilium in response to Hh signals leads to the ciliary accumulation and subsequent dissociation of Sufu and Gli complexes. Active Smo prevents the cleavage of the Gli proteins and allows their import into the nucleus where they are converted to a functional activator. How the cilium translates information from Smo to the Gli-Sufu complexes and how Gli's are converted into labile activators are unknown. This study not only demonstrates the versatility of the Floxin method, it also demonstrates that multiple layers of regulation are critical for optimal Gli2 function. Subcellular localization to the cilium and the nucleus, post-translational modifications and binding partners all converge to ensure that Gli2 is properly regulated. Given Gli2's role in repressing and activating target genes throughout development and in tumorigenesis, this study provides important insight into Gli2 subcellular dynamics.

Materials and Methods

Cell lines and cell culture

Gli2$^{gt/+}$ (XG045) E14 ESC lines were obtained from BayGenomics. Cells were cultured on 0.1% gelatin in knockout DMEM (Invitrogen) supplemented with 10% FBS, glutamine, pyruvate, non-essential amino acids, β-mercaptoethanol and leukemia inhibitory factor (LIF). Floxin cell lines were selected with and grown in 150μg/ml G418. Spontaneously differentiated cells in a monolayer or embryoid bodies were grown in the absence of LIF for 8 days. *Smo*-/- MEFs (a gift from J. Taipale) and NIH 3T3 cells were cultured in DMEM H21 supplemented with 10% FBS and pen/strep.

SAG (Enzo), a Hedgehog pathway agonist, was added to fresh media at 1μM in DMSO for 18 hours for transcriptional assays, or 1 hour for localization assays. Leptomycin B (Sigma L2913), an inhibitor of nuclear export, was used at a concentration of 20nM for 90 minutes. Ratjadone A (Enzo), another inhibitor of nuclear export, was used at a concentration of 10ng/ml for 2 hours.

CDNA constructs and cloning

Gli2 cDNA was a gift from H. Sasaki, and exons 2-14 were amplified with appropriate restriction enzymes and cloned into pFloxin, in frame with the C-terminal GFP tag. QuikChange II XL-site directed mutagenesis kit (Stratagene) was used correct point mutations, and to introduce specific deletions within Gli2. Gli2 deletion primers were generated using QuikChange Primer Design (Agilent). All products were sequenced before electroporation.

Electroporation, selection and screening

Electroporation for Reversion, and Floxin were performed as previously described by Singla et al [160]. Preliminary clones were assessed by genomic PCR and β-galactosidase activity using the Galacto-Light Plus System (Applied Biosystems).

Gli luciferase reporter assays

Smo-/- MEFs (a gift from J. Taipale) were transfected with JetPrime per manufacturer's instructions. DNA was comprised of 50% construct of interest, 40% Gli-luc and 10% pRLTK. 24 hours post-transfection, cells were starved in Optimem for 18 hours and then assayed by Dual Luciferase Reporter Kit (Promega).

Quantitative PCR

RNA was extracted from mESCs or spontaneously differentiated cells using Rneasy Plus (Qiagen). cDNA synthesis was performed using First Strand cDNA Synthesis Kit (Fermentas). Transcript levels were measured in quadruplicate using a 7300 Real-time PCR machine (Applied Biosystems) and normalized to relative βactin transcript. Primer sequences are: βactinF 5'-CACAGCTTCTTTGCAGCTCCTT-3' and βactinR 5'-CGTCATCCATGGCGAACTG-3'; Gli2 F 5'-GCTGCACCAAGAGGTACACA-3' and Gli2R 5'-GGACATGC ACATCATTACGC-3'; Gli1-F 5'GGTGCTGCCTATAGCCAGTGTCCTC-3' and Gll1-R 5'-GTGCCAATCCGGTGGAGTCAGACCC-3'; and PtcF 5'-CTCTGGA GCAGATTTCCA AGG-3' and PtcR 5'-TGCCGCAGTTCTTTTGAATG-3'; gfpF 5'-CGACCACTACCAGCAGAACA-3' and gfpR 5'-GAACTCCAGCAGGACCATGT-3'.

Immunofluorescence and Microscopy

mESCs were plated on coverslips coated with poly D-lysine and 1% Matrigel and were not subjected to starve conditions. NIH 3T3 cells were transfected with JetPrime per manufacturer's instructions and starved 18 hours prior to fixation.

Cells were fixed for 7 minutes in 4% PFA, washed in PBS and incubated in PBS with 0.1% Trition X-100 (PBST) for 20 minutes. Cells were then blocked in 2% BSA in PBS for 1 hour at 4C, and then incubated overnight with primary antibody at 4C. The next day, cells were washed in PBS, incubated in Alexafluor (Invitrogen) secondary antibody for 1hr at room temperature and mounted with either Vectashield Hardset with DAPI or Prolong Gold with DAPI. Images were acquired on one of the following: a Zeiss Axio Observer D1, a Nikon C1 confocal, a Leica TCS SP5 or a Leica TCS SPE. Image J or

Fiji (NIH) were used for quantification of integration densities, as previously described [85].

Integrated Density Quantification

Images were acquired by confocal microscopy using identical settings within experiments, and experiments were repeated three times. Image J was used to measure an 8x8 circular region of interest encompassing Gli2-GFP (ROI_{GFP}). An identical ROI was taken in an adjacent region to account for background (ROI_{BACK}). Integrated density readings, or pixel intensities, were measured as ROI_{GFP} - ROI_{BACK} and binned into four equal data clusters. Bin 1 (+) represents ID readings with the lowest pixel intensity, while Bin 4 (++++) represents ID readings with the highest pixel intensity.

Western blots

Cells were lysed with buffer containing 50mM Tris-HCl (pH 7.4), 0.5% NP-40, 0.25% NaDoc, 150mM NaCl and fresh protease (Calbiochem) and Halt phosphatase (Pierce) inhibitors. Lysates were cleared at 13.2k rpm for 10 minutes and protein concentration was quantified by Bradford assay. NE-PER Nuclear Cytoplasmic Reagent (Pierce) was used for cell fractionation assays.

Antibodies

Antibodies used for immunofluorescence include: GFP (Aves Lab GFP-1020) 1:1000; Acetylated tubulin (Sigma T6793) 1:1000; Ninein (gift from J. Sillibourne) 1:20000; Crm1 (Santa Cruz, 1:200); βimportin2 (BD Biosciences, 1:200); Alexafluor secondaries (Invitrogen) were used at 1:1000. Antibodies used for immunoprecipitation include: Sufu (Santa Cruz) 2µg; GFP-Trap Resin (Allele); Flag M2 (Invitrogen). Antibodies used for Western detection include: GFP (as above) 1:1000; Sufu (as above) 1:2000; alpha-

tubulin (Sigma) 1:5000; Crm1 (Santa Cruz, 1:1000); CBP (Santa Cruz, 1:500); Gli2 (a gift from J. Eggenshwiler, 1:2000); Gli3 (a gift from Genentech 1:500); Secondary antibodies (Jackson Immuno) 1:10000.

In vitro sumoylation assays

IVS assays were carried out in 50ul reactions with immunoprecipitated Gli2-GFP, 0.12μM E1, 4μM Ubc9 and 10μM Sumo1 in a sumoylation buffer containing 50mM Tris-HCl (pH 8.0), 100mM NaCl, 10mM MgCl2, 2mM ATP and 2μM fresh dTT at 37C for 1.5 hours. Reactions were then resolved by 7.5% SDS PAGE and detected by Western blot. All Sumo enzymes were provided by H. Ingraham lab.

siRNA transfections

NIH3T3 and IMCD3 cells were plated at a density of 20000 cells per 24 well coverslip 24 hours before transfection. Crm1 siRNA (Invitrogen, 20nM) was transfected by RNAiMax per the manufacturer's instructions. After 36 hours, cells were starved in Optimem supplemented with 1% FBS for 36 additional hours to optimize ciliation. 72 hours post-transfection, cells were fixed and stained as described above.

Acknowledgements

We thank H. Sasaki for Gli2 cDNA, J. Taipale for Smo-/- MEFs, H. Ingraham for sumoylation reagents, S. Scales for Gli3 antibody, J. Eggenshwiler for Gli2 antibody and W. Dowdle for generation of pgLAP5-GFP-Gli2 NIH 3T3 cells. We acknowledge UCSF Nikon Imaging Center and CVRI Imaging Core for use of microscopes.

A

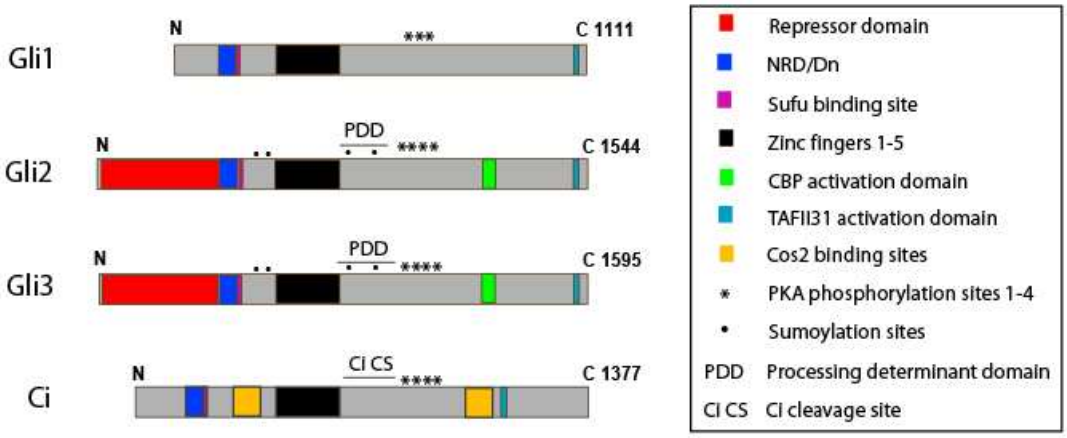

B

		Conserved in:			
Domain or PTM	**amino acids in mGli2**	**Gli3**	**Gli1**	**Ci**	**References**
Repressor region	1-280	yes	no	yes	Sasaki 1999
N-terminal regulatory domain	222-265	yes	yes	yes	Hunktzicker 2006
Sufu binding site	268-271	yes	yes	yes	Dunaeva 2003
Zinc fingers	417-569	yes	yes	yes	Pavletich 1993
Processing determinant domain	585-780	yes	no	yes	Pan 2007
PKA 1-4 cluster	786-855	yes	partial	yes	Pan 2006
Activation domain	642-1183; 1184-1544	yes	yes	yes	Sasaki 1999
Nuclear localization signal	561-578; 717-724	yes	yes	yes	Bamfield 2005
Nuclear export signal	887-895	yes	partial	partial	Bamfield 2005
Acetylation site	K740	no	yes	yes	Canettieri 2010
Akt phoshorylation site	S230	yes	yes	yes	Riobo 2006
Sumoylation	K375, K630, K716	yes	yes	no	Cox 2010

Figure 20. Summary of Ci/Gli domains and post-translational modifications
(A) The Gli proteins are highly conserved. The vertebrate Gli proteins are highly related to Ci in Drosophila. They possess different biochemical properties and play distinct roles in development. **(B) Summary of previously described domains and post-translation modification that act upon Gli2.** Many studies have been instrumental in identifying Gli2 domains that regulate its subcellular dynamics. Some of these sequences are conserved among the other Gli proteins and the Drosophila homolog, Ci.

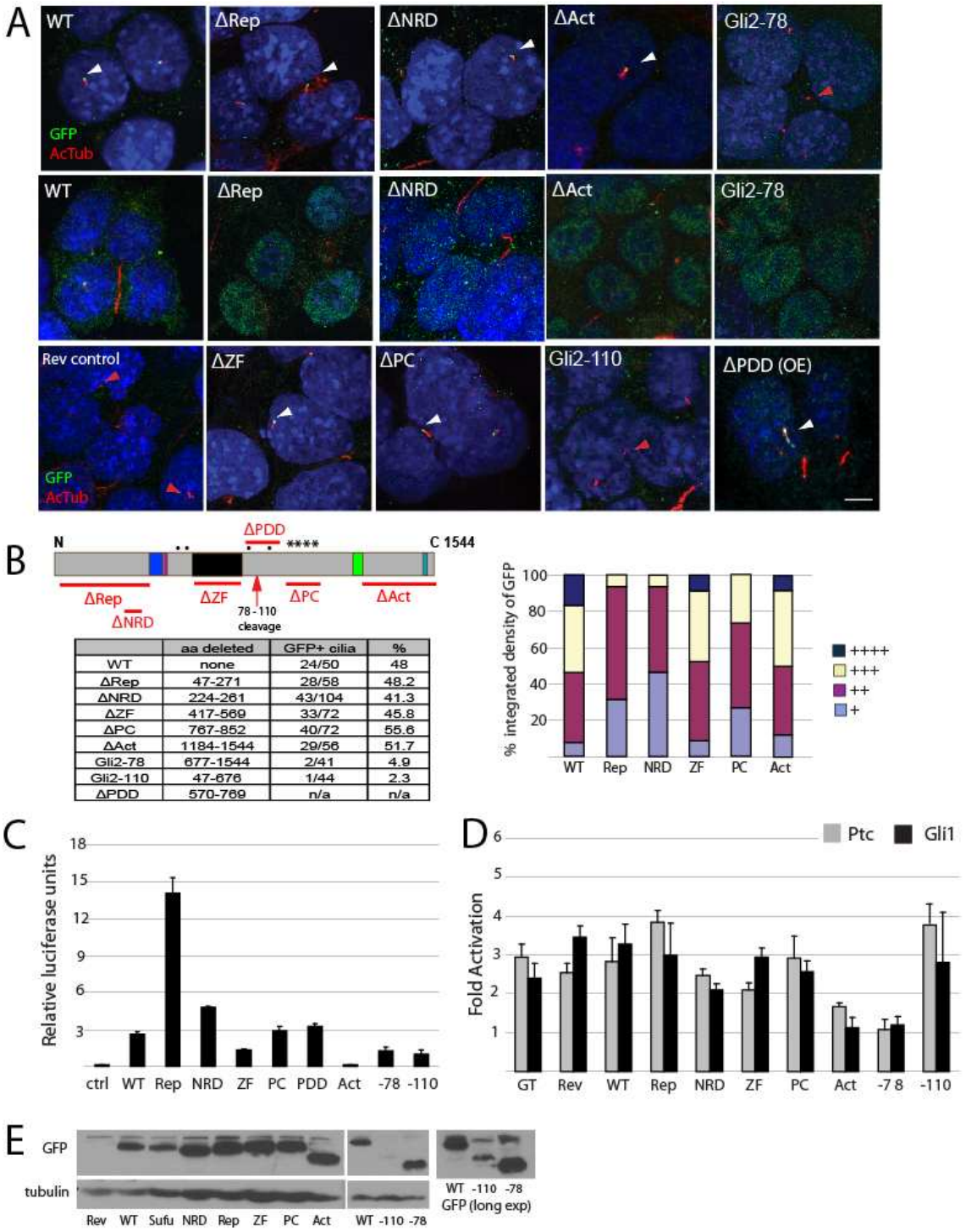

	aa deleted	GFP+ cilia	%
WT	none	24/50	48
ΔRep	47-271	28/58	48.2
ΔNRD	224-261	43/104	41.3
ΔZF	417-569	33/72	45.8
ΔPC	767-852	40/72	55.6
ΔAct	1184-1544	29/56	51.7
Gli2-78	677-1544	2/41	4.9
Gli2-110	47-676	1/44	2.3
ΔPDD	570-769	n/a	n/a

Figure 21. Floxin analysis of Gli2's bipotential function and processing

(A) Ciliary and nuclear localization of Floxin mutants. Floxin lines were assessed for ciliary (first row) and nuclear (second row) localization by immunofluorescence for GFP (green) and cilia (actub, red). Intact ciliary localization (white arrow), defective ciliary localization (red arrow). Scale bar ~5μm. **(B) Percentages and integrated density readings of Gli2-GFP+ ciliary tips.** Schematic of Gli2 and the domains deleted. Cells were assessed for GFP colocalization to cilia and overall ciliary localization was quantified. Intensity of GFP pixels was assessed by Image J integrated density analysis. + denotes low intensity GFP foci, while ++++ denotes high intensity GFP foci. **(C) Functional assessment of Gli2 mutant by over-expression**

Gli-luciferase assay. Wild type and mutant Gli2 constructs were transfected in *Smo*-/- MEFs and assessed for activation potential by Gli-luciferase readout. **(D) Functional assessment of Gli2 Floxin mutants.** Wild type and mutant Floxin mESCs were spontaneously differentiated in the absence of LIF for 12 days and treated overnight with 1μM Sag. *Gli1* and *Ptc* transcript levels were assessed by qRTPCR and normalized to actin. Data is presented as fold activation of SAG treated cells over untreated. **(E) Protein expression of Floxin Gli2 mutants.** Floxin protein from mutant alleles were detected by Western blot by GFP. Gli2-110 was not readily detectable, so a long exposure of this blot is provided.

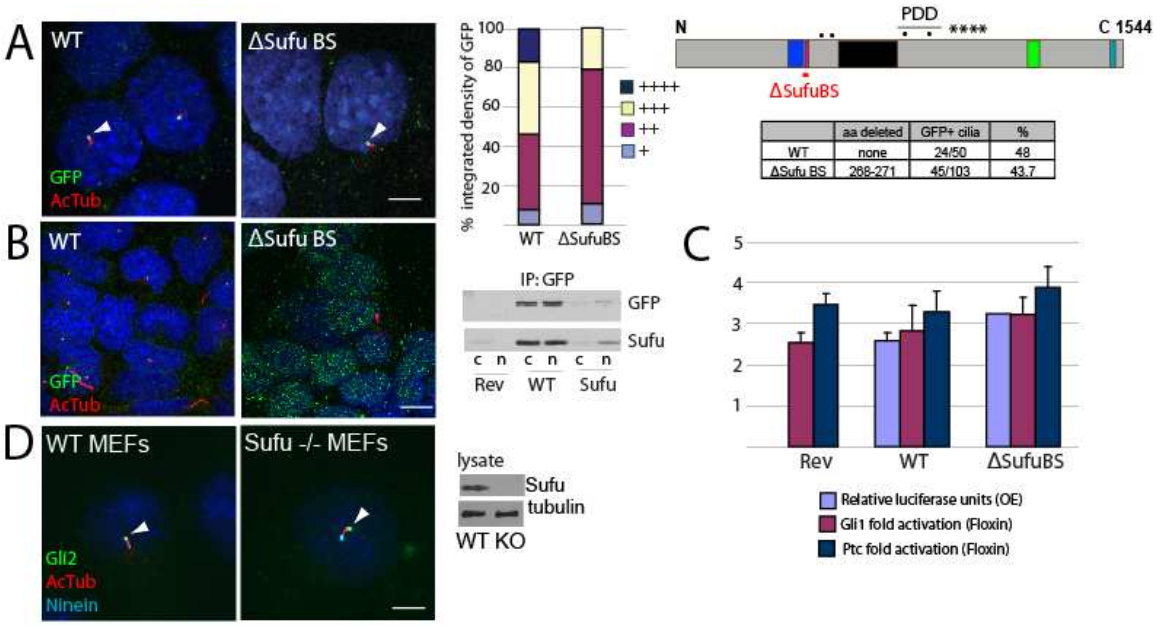

Figure 22. Loss of Sufu binding affects Gli2 stability and subcellular localization.
(A) Deletion of the Sufu binding domain does not affect ciliary localization. Gli2ΔSufuBS ciliary localization and foci intensity were quantified by immunofluorescence and Image J integrated density analysis (GFP, green and actub, red). Scale bar ~5μm. Schematic of SufuBS location within Gli2. **(B) Deletion of the Sufu binding domain affects nuclear accumulation.** Gli2ΔSufuBS is enriched in the nucleus, as evidence by immunofluorescence and Western blot for nuclear-cytoplasmic fractions. Sufu interaction is not totally abrogated in Gli2 ΔSufuBS mESCs, suggesting that dual sites may regulate Gli2 function. **(C) Deletion of the Sufu binding domain does not robustly affect Gli2 function.** Functional analysis was carried out by *Ptc* and *Gli1* transcript levels in differentiated wild type Gli2 and Gli2ΔSufuBS Floxin cells, as well as by over-expression in *Smo*-/- MEFs. Wild type and mutant Floxin mESCs were spontaneously differentiated in the absence of LIF for 8 days and treated overnight with 1μM SAG. Message levels were assessed by qRTPCR and normalized to actin. **(D) Genetic loss of Sufu does not affect Gli2 ciliary localization.** Primary MEFs were obtained from *Sufu* wild type and null e12.5 embryos. Lysate was probed for Sufu to validate absence of the protein. Gli2 (green), cilia (actub, red) and basal body (cyan) were stained by immunofluorescence. Scale bar ~5μm.

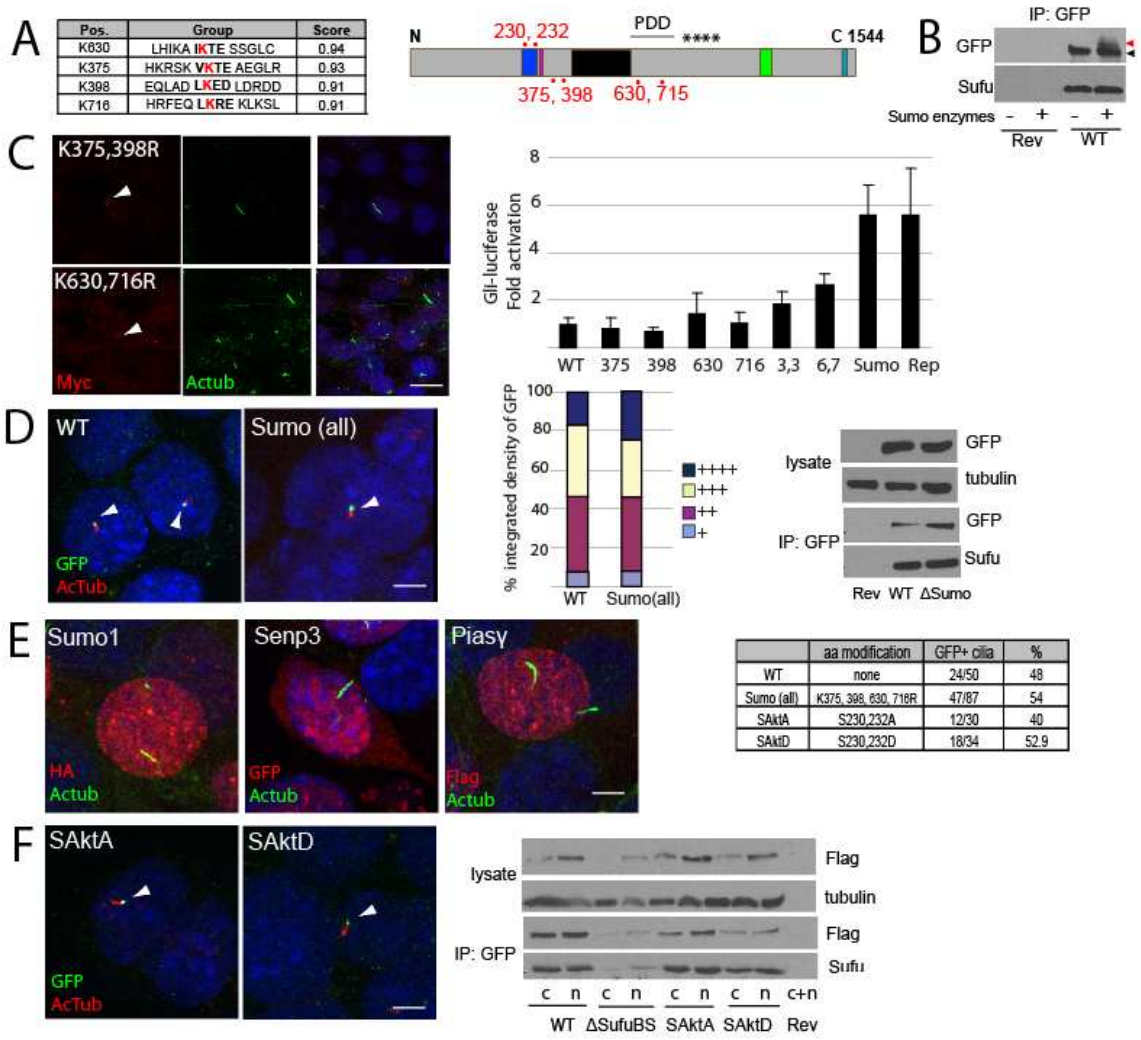

Figure 23. Sumoylation may repress Gli2 function.

(A) Gli2 contains four consensus sumoylation sites. Sumo-plot scores for four sumoylation sites that flank the zinc finger domain. **(B) Gli2-GFP can be sumoylated in vitro.** Immunoprecipitation of wild Gli2 from Floxin mESCs was subjected to an in vitro sumoylation assay. Gli2-GFP (black arrow) robustly interacts with Sufu and exhibits a slower migrating form (red arrow) when introduced to Sumo enzymes. **(C) Mutation of sumoylated lysines induces pathway hyperactivation.** Lysines within putative sumoylation sites were mutated to unsumoylatable arginines by site directed mutagenesis and assessed for localization by immunofluorescence in NIH 3T3 cells. Sumo mutants were transfected in *Smo*-/- MEFs to assess Gli-luciferase readout. Single mutations behave similarly to wild type Gli2, but upon increase number of mutations, becomes hyper-active. All mutants (red, myc) reached the cilium (actub, green) when transiently expressed in NIH 3T3 cells. (**D**) **Gli2ΔSumo reaches the cilium and interacts with Sufu.** As assessed by immunofluorescence and integrated density analysis, Floxin mutant containing all four sumoylation mutations in tandem reaches the cilium (actub, green) as effectively as wild type Gli2 (green, GFP). By Western blot and immunoprecipitation by GFP, Gli2ΔSumo is expressed at similar levels and interacts with Sufu. **(E) Sumo pathway components do not localize to primary cilia.** NIH 3T3 cells were transiently transfected with various tagged constructs of proteins (red) that are necessary for the sumoylation pathway. We did not observe ciliary localization (actub, green) of over-expressed Sumo1,2,3, Senp2,3,5 and a E3 sumo ligase, Pias□ (some data not shown). **(F) Disruption of Gli2's putative Akt site does not abrogate ciliary localization or Sufu interaction.** Phospho-dead and phospho-mimetic alleles of the AKT site retain intact ciliary localization and Sufu interaction, as evidenced by immunofluorescence and immunoprecipitation. Both mutants, Gli2SΔAktA and Gli2SΔAktD, were robustly detected in the cytoplasm and nucleus, where Sufu interaction is intact. All scale bars ~5μm.

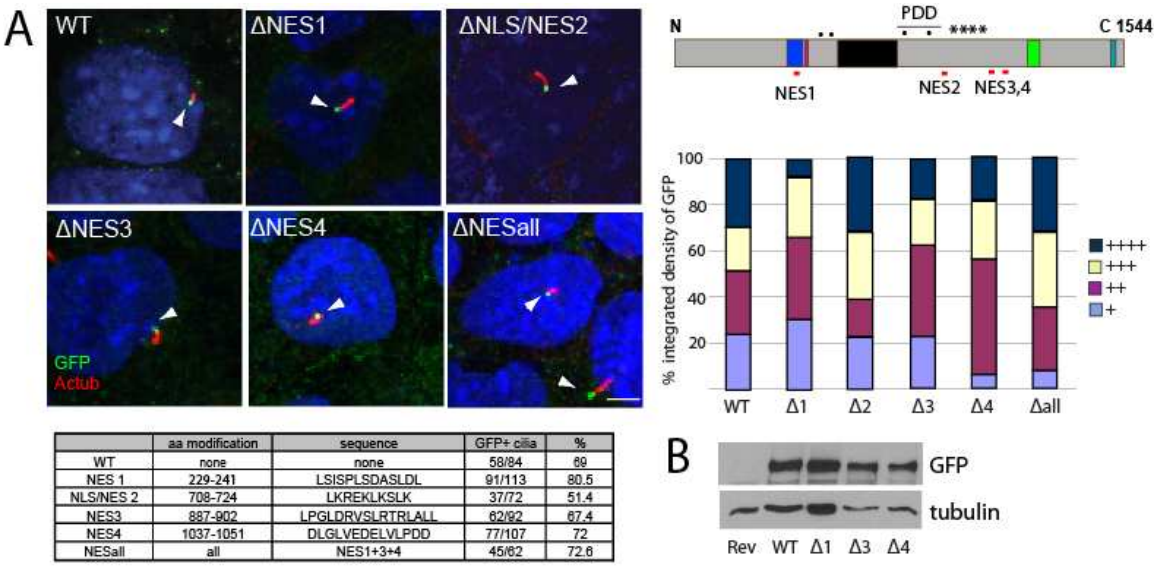

	aa modification	sequence	GFP+ cilia	%
WT	none	none	58/84	69
NES 1	229-241	LSISPLSDASLDL	91/113	80.5
NLS/NES 2	708-724	LKREKLKSLK	37/72	51.4
NES3	887-902	LPGLDRVSLRTRLALL	62/92	67.4
NES4	1037-1051	DLGLVEDELVLPDD	77/107	72
NESall	all	NES1+3+4	45/62	72.6

Figure 24. Loss of nuclear signals affects Gli2 ciliary localization.

(A) Deletion of putative nuclear trafficking signals in Gli2 leads to subtle changes in ciliary localization. We created Floxin mutants lacking classical NLS and NES sequences, as schematized. Ciliary localization was assessed by immunofluorescence (GFP, green; actub, red), while intensity of GFP foci was quantified by integrated density reading. All single and tandem mutants reached the cilium as effectively as wild type Gli2, with the exception of Gli2ΔNES2. Gli2ΔNES1 exhibited increased ciliary localization, although the intensity of these foci was diminished. Compared to wild type, Gli2ΔNES4 and Gli2ΔNESall exhibited fewer low intensity foci. Scale bar ~5μm. **(B) Gli2ΔNES mutants are expressed comparably to wild type Gli2.** Total lysate from Gli2ΔNES mutants were detected by GFP. Despite unequivalent loading of protein lysate, it appears that these single NES mutants are expressed comparably to wild type Gli2.

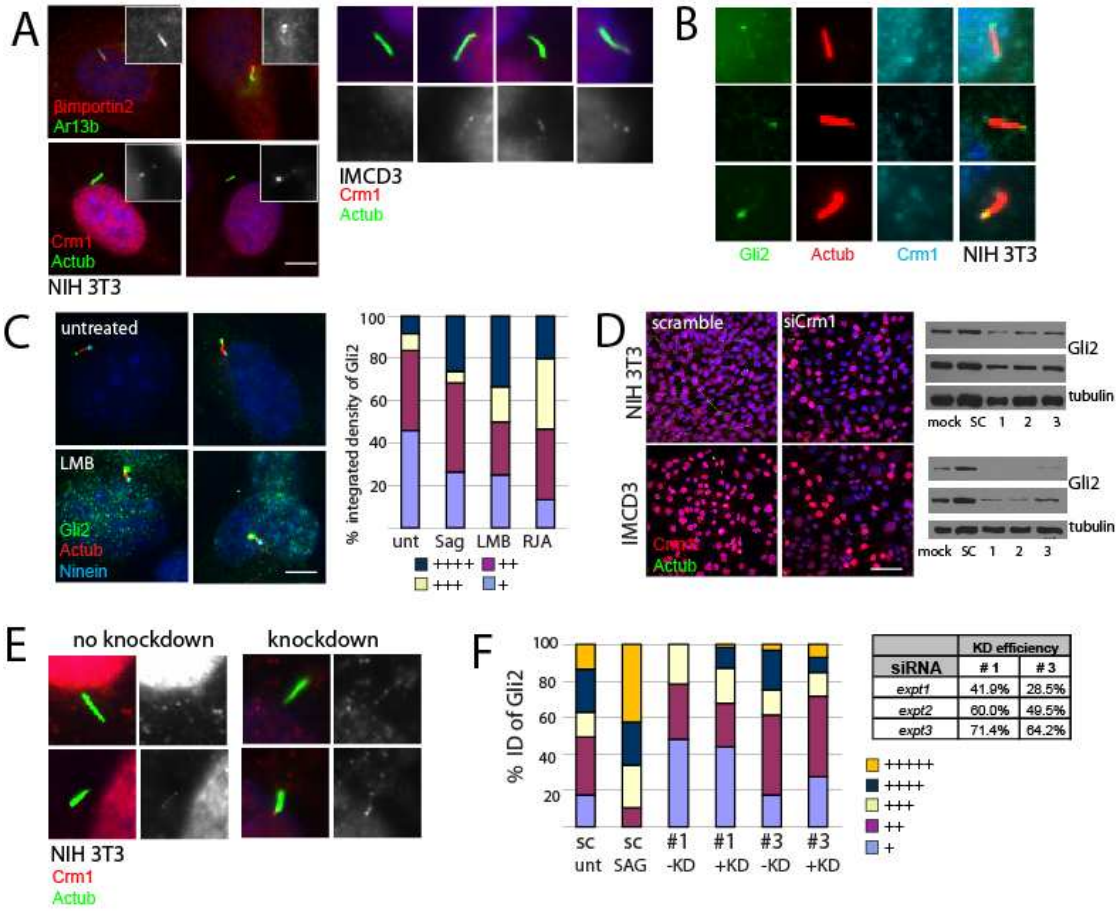

Figure 25. Exportins may play a role in Gli2 ciliary export.

(A) βimportin2 and Crm1 localize to the primary cilium. NIH 3T3 and IMCD3 cells were stained for cilia, βimportin2 and Crm1 (red) by immunofluorescence. Crm1 was detected at some cilia in both cell lines, and possessed varied staining patterns, including the basal body, ciliary tip, and punctuate along the ciliary axoneme. Scale bar ~5μm. **(B) Crm1 can co-localize with endogenous Gli2.** NIH 3T3 cells were stained for Gli2, Crm1 and cilia (green, red, cyan). Gli2 appeared as a distinct focus at the ciliary tip with a comet-like tail. Crm1 consistently stained the base of the cilium and could sometimes be seen at the ciliary tip, as well. **(C) Inhibition of Crm1 leads to increased Gli2 ciliary foci.** NIH 3T3 cells were starved for 24 hours in low serum, followed by treatment with Leptomycin B (20nM, 1.5 hours) and Ratjadone A (10ng/ml, 2 hours), pharmacological inhibitors of Crm1. SAG(1μM, 1 hour) was used as a positive control. Following immunofluorescence, we quantified the integrated density of foci by Image J using a method that incorporated size and background subtraction. LMB and RJA treatment increased the percentage of high pixel intensity foci, compared to untreated control cells. Scale bar ~5μm. **(D) Crm1 knockdown by siRNA.** Three different siRNA constructs were used to target Crm1 and assessed by immunofluorescence and western blot for Crm1 (only siRNA#1 shown). Cells exhibited significant loss of Crm1 nuclear staining (red), while the scramble control did not. Scale bar ~20μm. **(E) Crm1 localizes to the cilium in knockdown cells.** siRNA transfected cells were stained for Crm1 (red) and cilia (actub, green). Crm1 staining at the basal body and along the axoneme was detected in cells with and without knockdown, as assessed by the degree of nuclear immunofluorescence in the nucleus. **(F) Knockdown of Crm1 affects Gli2 ciliary localization.** Using siRNA #1 and #3, we compared non-knockdown to knockdown cells within each condition in three separate experiments. We averaged the binned data into five groups and compared knockdown efficiencies. Gli2 ciliary accumulation is observed with siRNA#1, but not siRNA#3. Gli2 ciliary localization appeared diminished compared to scramble siRNA, suggesting that Crm1 knockdown could possess adverse side effects.

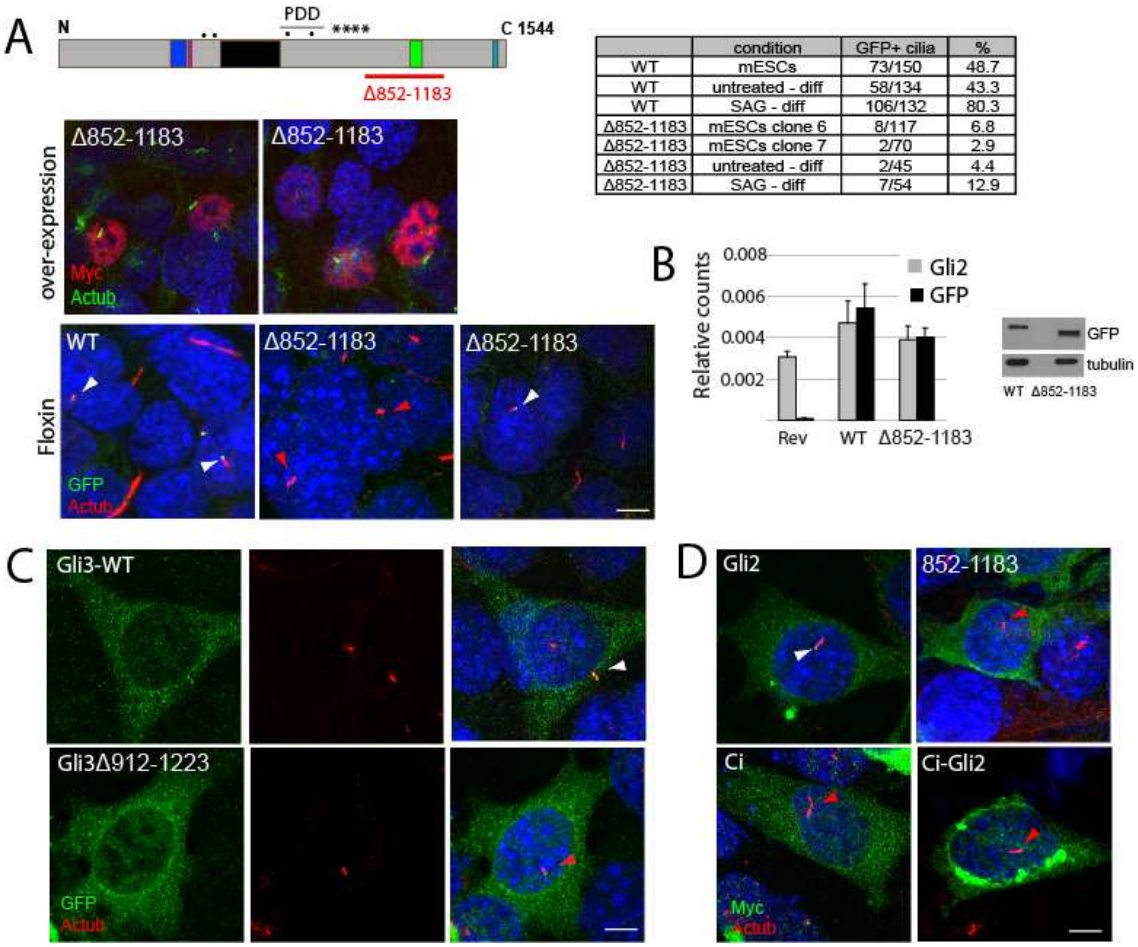

	condition	GFP+ cilia	%
WT	mESCs	73/150	48.7
WT	untreated - diff	58/134	43.3
WT	SAG - diff	106/132	80.3
Δ852-1183	mESCs clone 6	8/117	6.8
Δ852-1183	mESCs clone 7	2/70	2.9
Δ852-1183	untreated - diff	2/45	4.4
Δ852-1183	SAG - diff	7/54	12.9

Figure 26. Identification of a domain necessary, but not sufficient, for Gli2 ciliary localization.

(A) Amino acids 852-1183 are required for intact Gli2 ciliary localization. Floxin Gli2Δ852-1183 mESCs or cells transfected with Gli2Δ852-1183-myc (green) were assessed by immunofluorescence for ciliary localization (actub, red). Gli2Δ852-1183-myc was never assessed at the cilium. Floxin mESCs were spontaneously differentiated by the removal of LIF for 8 days, and ciliary localization was quantified in untreated and SAG-stimulated cells. **(B) Ciliary localization defects are not due to protein levels.** Transcript levels of both Gli2 and GFP in Gli2Δ852-1183 mESCs was assessed by qRTPCR, normalized to actin. Lysate was probed for GFP to detect protein expression levels. **(C) An analogous region is required for Gli3 ciliary localization.** NIH 3T3 cells were transiently transfected with wild type hGli3-GFP and hGli3Δ912-1223. While wild type Gli3 robustly reached the cilium upon over-expression (white arrow), Gli3Δ912-1223 did not (red arrow). **(D) Amino acids 852-1183 are not sufficient for ciliary localization.** A myc-tagged allele of this 330aa Gli2 region (red) was transfected in NIH 3T3 cells and assessed for ciliary localization. It failed to reach the cilium and was predominantly cytoplasmic. The C-terminal region of Gli2, amino acids 852-1544 was fused to the N-terminal half of Ci, the Drosophila homologue of the Gli proteins. Neither Ci nor Ci-Gli2 chimera (red) reached the cilium (actub, green), although the latter formed aggregates upon over-expression. All scale bars ~5μm.

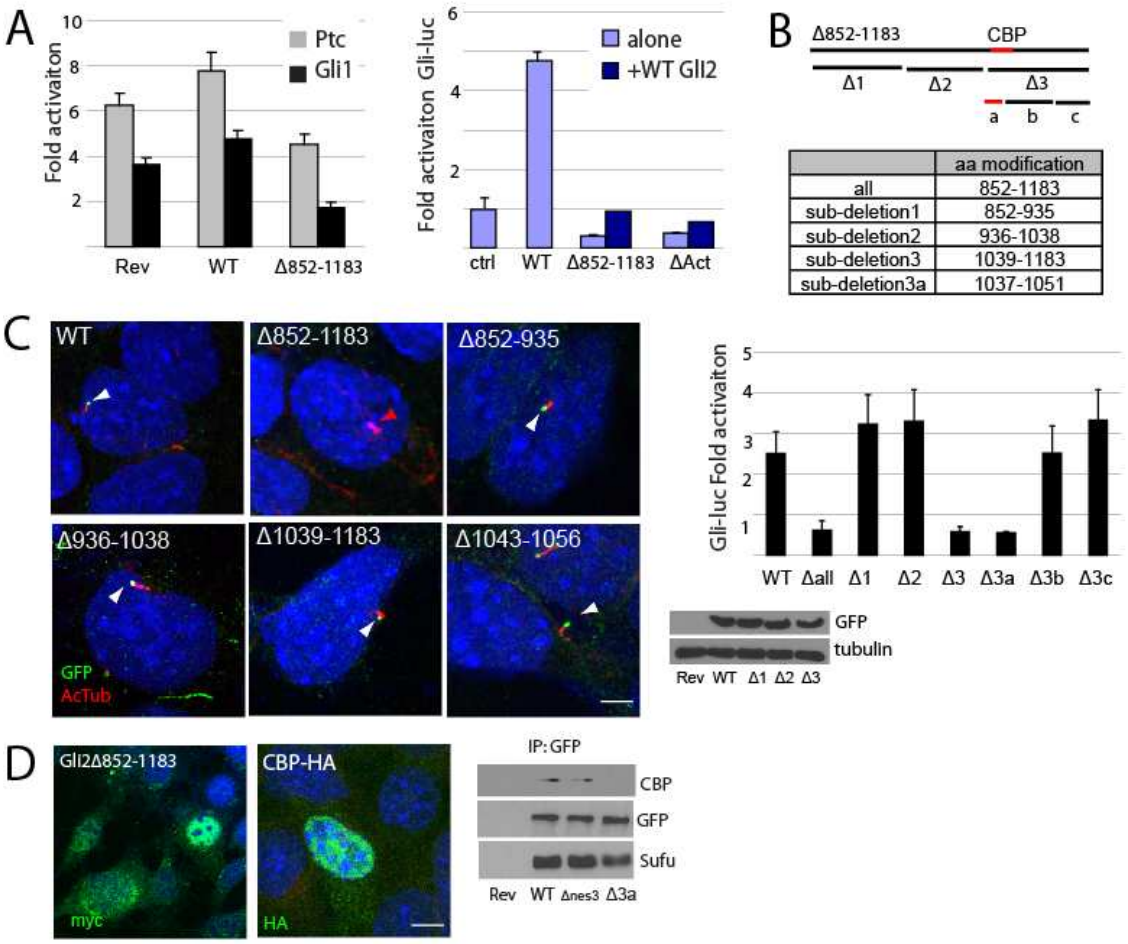

Figure 27. Gli2Δ852-1183 a loss of function allele.

(A) Gli2Δ852-1183 possesses loss of function and dominant negative phenotype. Gli2Δ852-1183 mESCs were assessed by qRTPCR for Hh responsiveness by *Gli1* and *Ptc* levels upon differentiation. Data is presented as fold activation of SAG treated cells compared to unstimulated cells. Wild type Gli2 and Gli2Δ852-1183 were transfected alone or in tandem in *Smo*-/- MEFs and assessed for activation potential by Gli-luciferase. **(B) Sub-deletion map of Gli2Δ852-1183.** Putative CBP binding motif is delineated in red. **(C) Sub-deletion mutants localize to primary cilia and are functionally inactive if the motif is missing.** Floxin lines were created for sub-deletions 1, 2, 3 and 3a. Ciliary localization was assessed by immunofluorescence for GFP (green) and cilia (actub, red). Sub-deletion over-expression constructs were transfected in *Smo*-/- MEFs and assessed for Gli-luciferase readout. Western analysis of mutant Floxin lines by GFP blot. **(D) Gli2Δ852-1183 and CBP localize to the nucleus.** Gli2 Δ852-1183 and CBP-HA were transfected in NIH 3T3 cells and assessed for localization by immunofluorescence. Floxin Gli2Δ3a/ΔNES4 and control lines were immunoprecipitated with GFP and probed for GFP, CBP and Sufu, as a positive control.

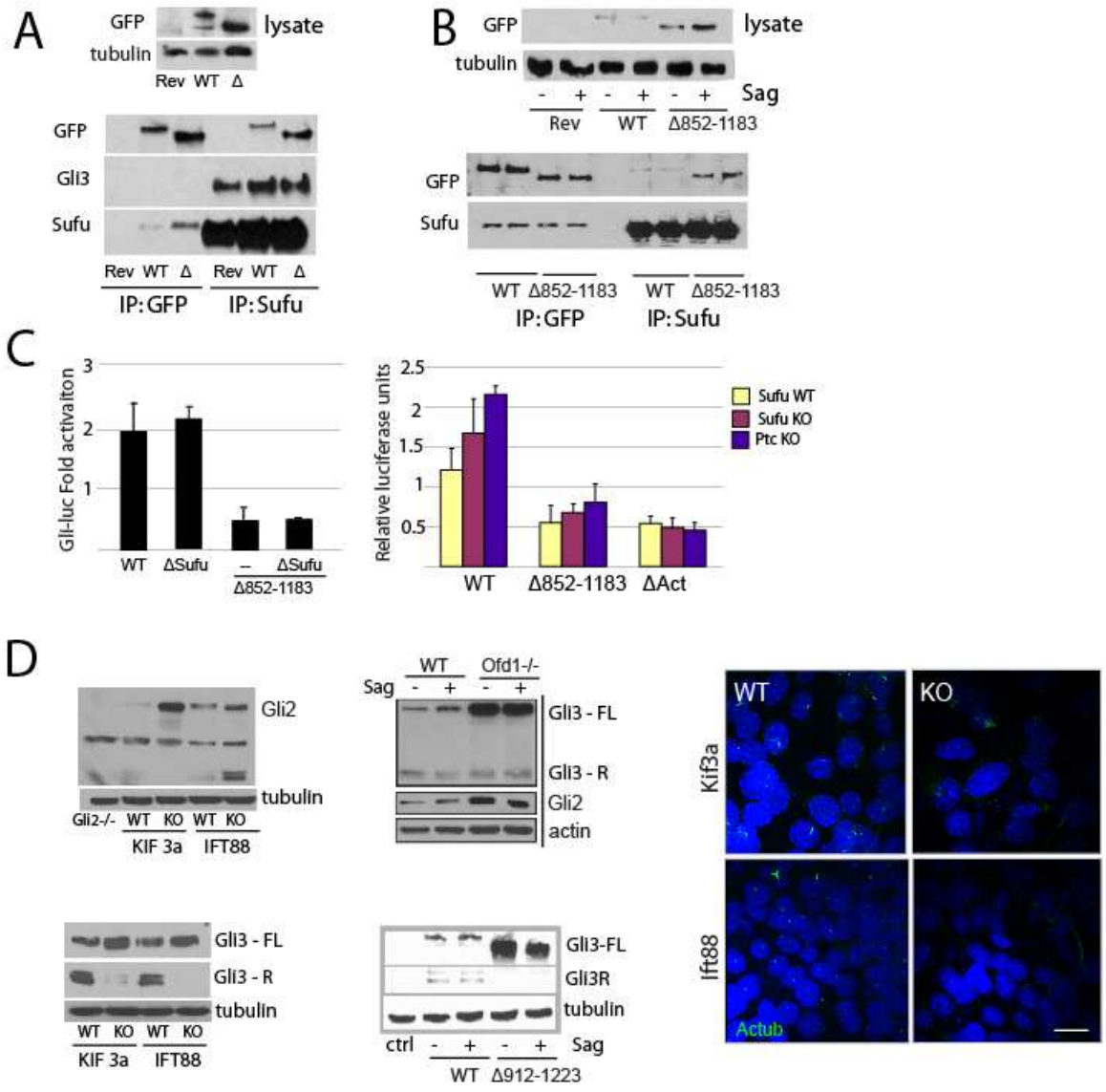

Figure 28. Gli2Δ852-1183 exhibits increased protein stabilization.
(A) and (B) Gli2Δ852-1183 protein is stabilized compared to wild type Gli2. Lysate from Gli2 Δ852-1183 (abbreviated Δ) cells were assessed by Western blot for GFP, and immunoprecipitated by GFP and Sufu. Gli3 was used as a positive control for Sufu pull-down. Differentiated cells were treated with SAG (1μM) for 1 hour prior to lysis. **(C) Disrupted Sufu binding does not rescue loss of function phenotype in Gli2Δ852-1183.** Deletion of the SYGH mutation was introduced into Gli2Δ852-1183 and in *Smo*-/- MEFs. Gli2Δ852-1183 was transfected in MEFs lacking *Ptc* or *Sufu*. Gli-luciferase readout was used to assess Hh responsiveness. **(D) Cells lacking cilia exhibit Gli protein stabilization.** Cells lacking *IFT88, Kif3a* and *Ofd1* were assessed for Gli2 and Gli3 protein levels by Western blot, and presence of cilia (actub, green) by immunofluorescence. Ofd1 data adapted from [165]. Gli3 lacking an analogous region to Gli2's 852-1183 exhibits an increase in full length Gli3 and a decrease in Gli3R formation.

Domain or PTM	aa in mGli2	Floxin allele deletion and name	Localization	Function
Repressor region	1-280	47-271; ΔRep	cil, nuc	GoF
N-terminal regulatory domain	222-265	224-261; ΔNRD	cil, nuc	GoF
Sufu binding site	268-271	268-271; ΔSufuBS	cil, nuc	+
Sufu to ZF	272-416	assessed by over-expression	cil	n/a
Zinc fingers	417-569	417-569; ΔZF	cil	LoF
Processing determinant domain	585-780	assesed by over-expression; ΔPDD	cil	n/a
PKA 1-4 cluster	786-855	767-852; ΔPC	cil	+
Activation domain (TAF)	642-1183; 1184-1544	1184-1544; ΔAct	cil, nuc	dom neg
Nuclear localization signal	561-578; 717-724	709-724; ΔNLS	cil	+
Nuclear export signal	887-895	229-241; 887-895; 1037-1051: ΔNES	cil	+
Akt phoshorylation site	S230	S230,232A/D; ΔAkt	cil	+
Sumoylation	K375, K630, K716	K375, 398,630,716R; ΔSumo	cil	GoF
Activation domain (CBP)	852-1183	Δ852-1183 and sub-deletions	none	dom neg/LoF
Gli2-78	1-675	47-675; Gli2-78	nucleus only	dom neg
Gli2-110	676-1544	676-1544; Gli2-110	none	LoF

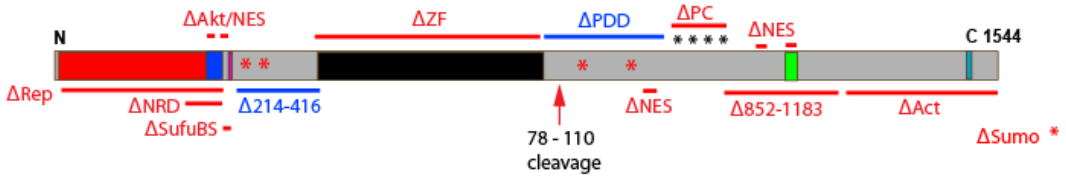

Figure 29 Summary of Gli2 deletion panel.
Table summary of all Gli2 deletion alleles created in this study. Ciliary localization (cil); nuclear localization (nuc); gain of function (GoF); loss of function (LoF); dominant negative (dom neg). Deletions in blue were only assessed by over-expression, deletions in red were assessed by Floxin and over-expression, if necessary.

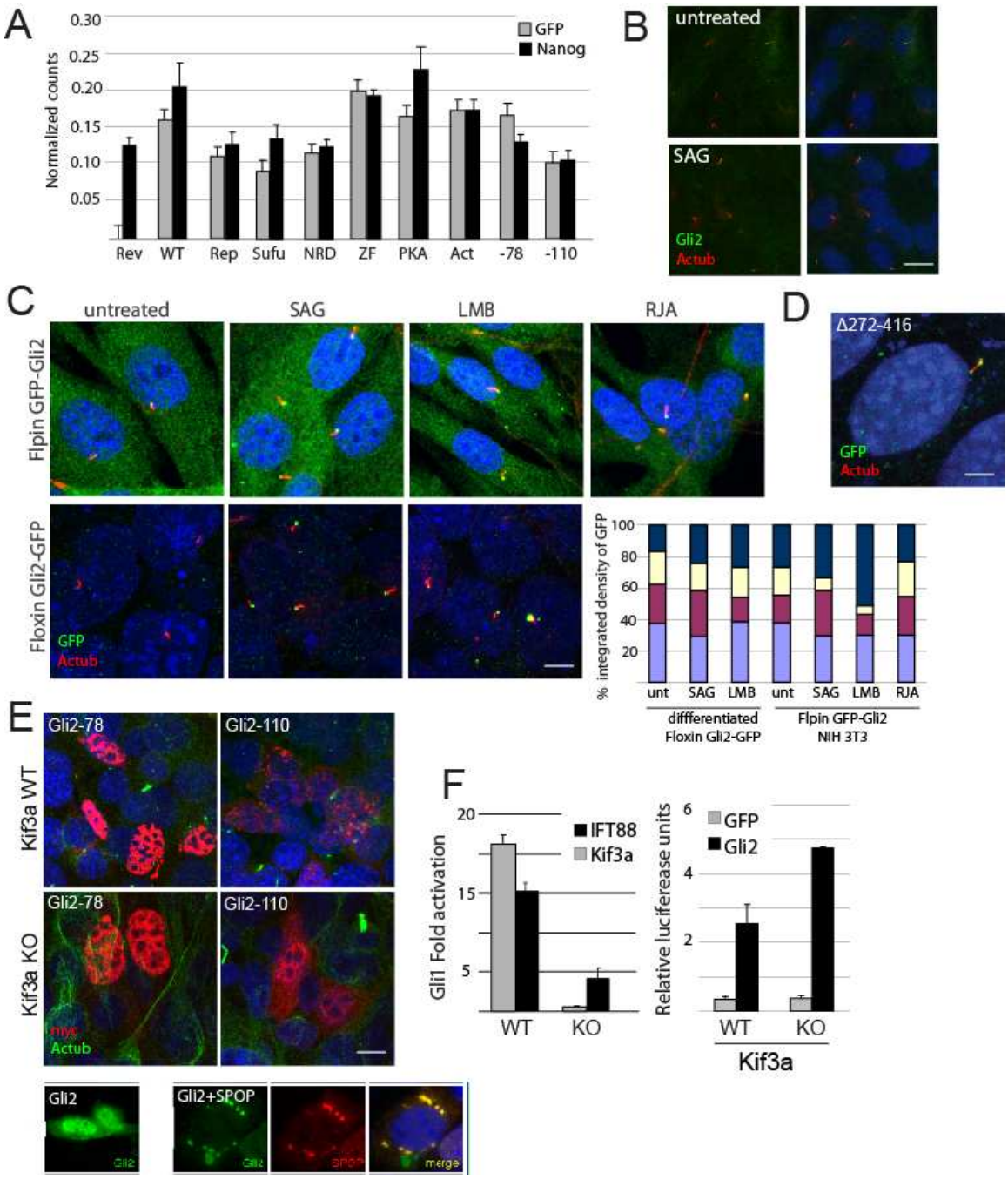

Figure 30. Supplementary figures

(A) Floxin mutant lines retain pluripotency and have comparable GFP transcript levels. Floxin control and mutant lines were assessed by qRTPCR for Nanog, a marker of pluripotency, and GFP. Data is normalized to actin. **(B) Nuclear Gli2 is not readily detectable in WT MEFs.** Primary wild type MEFs were stained with a C-terminal Gli2 antibody (green) and cilia (red) in the absence and presence of SAG (1μM, 1 hour). Scale bar ~10μm. **(C) Crm1 inhibition by LMB leads to ciliary accumulation across cell lines.** NIH 3T3 cells lines expressing GFP-Gli2 from a single integration site and differentiated Floxin Gli2-GFP cells were assessed by immunofluorescence following SAG treatment (1μm, 1hr) or LMB treatment (20nM, 90 minutes). Cells were stained for GFP (green) and cilia (red), and integrated density analysis was performed using Image J. Scale bar ~5μm. **(D) Gli2 Δ272-416 reaches the cilium.** Gli2 containing a deletion of the region spanning the Sufu binding site to the zinc fingers was transfected in NIH 3T3 cells and

assessed for ciliary localization by immunofluorescence of GFP (green) and cilia (actub, red). Scale bar ~5μm. **(E) Gli2-110 aggregates in SPOP-like clusters in ciliated cells.** Kif3a wild type and knockout cells were transfected with Gli2-78 and Gli2-100 and stained for myc (red) and cilia (actub, green). Gli2-110 exhibits different phenotypes in ciliated versus unciliated cells, with the former resembling SPOP aggregates in MEFs, adapted from [83]. Scale bar ~10μm. **(F) Over-expression of Gli2 bypasses the requirement for cilia.** Cells lacking *Kif3a* and *Ift88* were assessed for *Gli1* transcript levels following SAG treatment. Unciliated cells are not Hh responsiveness. *Kif3a* wild type and knockout cells were transfected with either GFP or wild type Gli2 and assessed for Gli-luciferase activity in the absence of SAG treatment.

Chapter V.

Conclusions and perspectives

Cilia were first discovered over a century ago, but this vestigial organelle came into the limelight when cilia mutants displayed Hh defects. Given Hh's clinical relevance in both congenital defects and cancers, the primary cilium became a focus, not just of academic labs trying to understand the how's and why's of this mysterious protrusion, but also of larger companies trying to discover cancer-fighting agents.

I chose to focus on the 7TM receptor Smoothened and its downstream effector, Gli2, since they are the two central activators of the Hh pathway. The studies presented in this dissertation raise more questions than they do answers, but highlight the complex nature of how this key developmental signaling pathway is regulated.

Why is the primary cilium a specialized subcellular site for Hh signaling?

1) One of the central questions addressed throughout this body of work is why vertebrate Hedgehog signaling is coupled to primary cilia. Many of the key players and components of the Hh pathway are conserved evolutionarily between Drosophila and vertebrates, so how did this mysterious organelle become indispensable in vertebrates? Furthermore, not all ciliated cells are Hh-responsive, and many non-Hh responsive cells possess ciliary Hh components.

2) Although this study has shed light on some of the potential mechanisms that regulate Gli2 function, it is still unclear how active Smo mediates Sufu dissociation from the Gli proteins. We have shown that abrogated Sufu interaction leads to Gli2 nuclear accumulation, but this change in subcellular localization is not sufficient to drastically

change pathway activation. Thus, it remains to be determined if other steps promote Gli2's maximal activation. Moreover, do these activation steps occur at the cilium or downstream of it?

3) Several degradation mechanisms converge on the Gli proteins. Since over-expression of Gli2 can circumvent the requirement for cilia, could cilia function primarily in modulating Gli2 protein levels? Could the cilium act as a reservoir that mediates Gli degradation and stability?

4) What other proteins do the Gli's interact with? Our mass spectrometry efforts from both Floxin cells and Floxin mice proved to yield no more than Sufu. Is it an issue with transient interactions, abundance or protocol shortcomings? NIH 3T3 expressing pgLAP5 GFP-Gli2 may be useful, as they are Hh-responsive and express higher levels of GFP-Gli2 from a single integration site.

5) Sufu and Gli proteins are enriched at the distal ciliary tip and are less often observed along the axoneme, or at the ciliary base. Is the ciliary tip a specialized site within the cilium, or is this accumulation just a byproduct of anterograde and retrograde IFT loading?

6) Upstream of the Gli proteins, what is the molecular basis for Ptc's ability to repress Smo? Does the cilium provide a defined space for a Ptc-trafficked molecule? This question has been of outstanding interest for some time since Ptc is similar to NPC1 and oxysterols can modulate the pathway exogenously.

7) In Drosophila, a kinesin-like protein Cos2 acts as a scaffold protein that complexes Ci with the degradation machinery. Since Kif7 is enriched at the basal body, is Kif7 the evolutionary linker that ties both Smo and the Gli's to the primary cilium?

Ciliary trafficking of proteins – why is it exclusive?

Misregulation of cilia assembly, maintenance and function obviously leads to a wide range of clinical manifestations, like situs inversus, retinal degeneration, obesity and kidney defects. Many proteins, not just those of the Hh pathway, localize to the primary cilium. Why ciliary proteins are there and how they gain access to this specialized compartment are unclear. In other words, how is the exclusivity of the ciliary compartment accomplished?

Trafficking of proteins into the cilium is multi-faceted and is likely cargo-specific and cell-type specific. Membrane proteins, like Smoothened, have been shown to enter the cilium both through lateral movement from the plasma membrane and intracellular vesicles. Other proteins possess ciliary targeting sequences are targeted from the Golgi via vesicle transport, while a ciliary gate analogous to the nuclear pore complex appears to regulate the targeting of Kif17 and RP2. Furthermore, our lab has also demonstrated how the transition zone, a region that is loosely defined as the region between the basal body and the axoneme regulates the localization of some, but not all ciliary proteins. Thus, it is increasingly apparent that the mechanisms that govern ciliary entry, and perhaps exit, are highly diverse and multi-layered. Whether or not these mechanisms of ciliary trafficking work in conjunction or independently also remains unanswered. In any case, however, elucidating these mechanisms will provide insight into the pathogenesis of many ciliopathies whose underlying defect is the mislocalization of ciliary proteins.

Can the cilium be a therapeutic target?

Since abnormal Hh signaling has been linked to the initiation and maintenance of many cancers, it will be interesting to see what role primary cilia play in the tumor environment. A few studies have demonstrated that the role of cilia in cancer depends on how the pathway is activated, for instance through oncogenic Smo or a constitutively activated Gli2. Thus, given that many tumors are heterogeneous in nature, can cilia become a target for therapeutics?

This possibility raises the question, however, of whether or not cilia are exclusively used for mediating the Hh pathway. IFT mutants only exhibit Hh defects, suggesting that cilia are dedicated to the Hh pathway at least in early development. However, developmental defects due to compromised signaling of other pathways may arise after IFT cilia mutants arrest. Indeed, cilia may restrain Wnt signaling, be involved in PDGFRα signaling and play roles in PCP signaling and tissue organization [63]. Thus, cilia may modulate other signaling pathways in specific tissues later in development or during adult tissue homeostasis. Dissecting how cilia are at the nexus of signaling pathways will undoubtedly be important in defining the potential for clinical therapeutics.

In summary, much remains to be elucidated in how primary cilia mediate Hh signaling. By addressing the fundamental questions of how components of the Hh pathway act at the subcellular level, we can better understand the mechanisms of development and disease.

REFERENCES

1. McMahon, A.P., P.W. Ingham, and C.J. Tabin, *Developmental roles and clinical significance of hedgehog signaling.* Curr Top Dev Biol, 2003. **53**: p. 1-114.
2. Villavicencio, E.H., D.O. Walterhouse, and P.M. Iannaccone, *The sonic hedgehog-patched-gli pathway in human development and disease.* Am J Hum Genet, 2000. **67**(5): p. 1047-54.
3. Chiang, C., et al., *Cyclopia and defective axial patterning in mice lacking Sonic hedgehog gene function.* Nature, 1996. **383**(6599): p. 407-13.
4. Barakat, M.T., E.W. Humke, and M.P. Scott, *Learning from Jekyll to control Hyde: Hedgehog signaling in development and cancer.* Trends Mol Med. **16**(8): p. 337-48.
5. Pasca di Magliano, M. and M. Hebrok, *Hedgehog signalling in cancer formation and maintenance.* Nat Rev Cancer, 2003. **3**(12): p. 903-11.
6. Reifenberger, J., et al., *Somatic mutations in the PTCH, SMOH, SUFUH and TP53 genes in sporadic basal cell carcinomas.* Br J Dermatol, 2005. **152**(1): p. 43-51.
7. Nusslein-Volhard, C. and E. Wieschaus, *Mutations affecting segment number and polarity in Drosophila.* Nature, 1980. **287**(5785): p. 795-801.
8. Forbes, A.J., et al., *Genetic analysis of hedgehog signalling in the Drosophila embryo.* Dev Suppl, 1993: p. 115-24.
9. Mohler, J., *Requirements for hedgehog, a segmental polarity gene, in patterning larval and adult cuticle of Drosophila.* Genetics, 1988. **120**(4): p. 1061-72.
10. Tabata, T., S. Eaton, and T.B. Kornberg, *The Drosophila hedgehog gene is expressed specifically in posterior compartment cells and is a target of engrailed regulation.* Genes Dev, 1992. **6**(12B): p. 2635-45.
11. Ingham, P.W., Y. Nakano, and C. Seger, *Mechanisms and functions of Hedgehog signalling across the metazoa.* Nat Rev Genet. **12**(6): p. 393-406.
12. Zugasti, O., J. Rajan, and P.E. Kuwabara, *The function and expansion of the Patched- and Hedgehog-related homologs in C. elegans.* Genome Res, 2005. **15**(10): p. 1402-10.
13. Burglin, T.R. and P.E. Kuwabara, *Homologs of the Hh signalling network in C. elegans.* WormBook, 2006: p. 1-14.
14. Lee, J.J., et al., *Autoproteolysis in hedgehog protein biogenesis.* Science, 1994. **266**(5190): p. 1528-37.
15. Beachy, P.A., et al., *Multiple roles of cholesterol in hedgehog protein biogenesis and signaling.* Cold Spring Harb Symp Quant Biol, 1997. **62**: p. 191-204.
16. Burglin, T.R., *Evolution of hedgehog and hedgehog-related genes, their origin from Hog proteins in ancestral eukaryotes and discovery of a novel Hint motif.* BMC Genomics, 2008. **9**: p. 127.
17. Hao, L., et al., *Comprehensive analysis of gene expression patterns of hedgehog-related genes.* BMC Genomics, 2006. **7**: p. 280.
18. Bitgood, M.J., L. Shen, and A.P. McMahon, *Sertoli cell signaling by Desert hedgehog regulates the male germline.* Curr Biol, 1996. **6**(3): p. 298-304.
19. St-Jacques, B., M. Hammerschmidt, and A.P. McMahon, *Indian hedgehog signaling regulates proliferation and differentiation of chondrocytes and is essential for bone formation.* Genes Dev, 1999. **13**(16): p. 2072-86.
20. Avaron, F., et al., *Characterization of two new zebrafish members of the hedgehog family: atypical expression of a zebrafish indian hedgehog gene in*

skeletal elements of both endochondral and dermal origins. Dev Dyn, 2006. **235**(2): p. 478-89.
21. Schauerte, H.E., et al., *Sonic hedgehog is not required for the induction of medial floor plate cells in the zebrafish.* Development, 1998. **125**(15): p. 2983-93.
22. Currie, P.D. and P.W. Ingham, *Induction of a specific muscle cell type by a hedgehog-like protein in zebrafish.* Nature, 1996. **382**(6590): p. 452-5.
23. Ekker, S.C., et al., *Patterning activities of vertebrate hedgehog proteins in the developing eye and brain.* Curr Biol, 1995. **5**(8): p. 944-55.
24. Marigo, V., et al., *Biochemical evidence that patched is the Hedgehog receptor.* Nature, 1996. **384**(6605): p. 176-9.
25. Zheng, X., et al., *Genetic and biochemical definition of the Hedgehog receptor.* Genes Dev. **24**(1): p. 57-71.
26. Stone, D.M., et al., *The tumour-suppressor gene patched encodes a candidate receptor for Sonic hedgehog.* Nature, 1996. **384**(6605): p. 129-34.
27. Ingham, P.W., A.M. Taylor, and Y. Nakano, *Role of the Drosophila patched gene in positional signalling.* Nature, 1991. **353**(6340): p. 184-7.
28. Eaton, S., *Multiple roles for lipids in the Hedgehog signalling pathway.* Nat Rev Mol Cell Biol, 2008. **9**(6): p. 437-45.
29. Ikonen, E. and M. Holtta-Vuori, *Cellular pathology of Niemann-Pick type C disease.* Semin Cell Dev Biol, 2004. **15**(4): p. 445-54.
30. Khaliullina, H., et al., *Patched regulates Smoothened trafficking using lipoprotein-derived lipids.* Development, 2009. **136**(24): p. 4111-21.
31. Martin, V., et al., *The sterol-sensing domain of Patched protein seems to control Smoothened activity through Patched vesicular trafficking.* Curr Biol, 2001. **11**(8): p. 601-7.
32. Taipale, J., et al., *Patched acts catalytically to suppress the activity of Smoothened.* Nature, 2002. **418**(6900): p. 892-7.
33. Goodrich, L.V., et al., *Altered neural cell fates and medulloblastoma in mouse patched mutants.* Science, 1997. **277**(5329): p. 1109-13.
34. Hooper, J.E. and M.P. Scott, *The Drosophila patched gene encodes a putative membrane protein required for segmental patterning.* Cell, 1989. **59**(4): p. 751-65.
35. Koudijs, M.J., et al., *The zebrafish mutants dre, uki, and lep encode negative regulators of the hedgehog signaling pathway.* PLoS Genet, 2005. **1**(2): p. e19.
36. van den Heuvel, M. and P.W. Ingham, *smoothened encodes a receptor-like serpentine protein required for hedgehog signalling.* Nature, 1996. **382**(6591): p. 547-51.
37. Xie, J., et al., *Activating Smoothened mutations in sporadic basal-cell carcinoma.* Nature, 1998. **391**(6662): p. 90-2.
38. Zhang, X.M., M. Ramalho-Santos, and A.P. McMahon, *Smoothened mutants reveal redundant roles for Shh and Ihh signaling including regulation of L/R asymmetry by the mouse node.* Cell, 2001. **105**(6): p. 781-92.
39. Varga, Z.M., et al., *Zebrafish smoothened functions in ventral neural tube specification and axon tract formation.* Development, 2001. **128**(18): p. 3497-509.
40. Ogden, S.K., et al., *G protein Galphai functions immediately downstream of Smoothened in Hedgehog signalling.* Nature, 2008. **456**(7224): p. 967-70.
41. Ayers, K.L. and P.P. Therond, *Evaluating Smoothened as a G-protein-coupled receptor for Hedgehog signalling.* Trends Cell Biol. **20**(5): p. 287-98.
42. Ruiz-Gomez, A., et al., *The cell biology of Smo signalling and its relationships with GPCRs.* Biochim Biophys Acta, 2007. **1768**(4): p. 901-12.

43. Chen, J.K., et al., *Inhibition of Hedgehog signaling by direct binding of cyclopamine to Smoothened.* Genes Dev, 2002. **16**(21): p. 2743-8.
44. Chen, J.K., et al., *Small molecule modulation of Smoothened activity.* Proc Natl Acad Sci U S A, 2002. **99**(22): p. 14071-6.
45. Varjosalo, M., S.P. Li, and J. Taipale, *Divergence of hedgehog signal transduction mechanism between Drosophila and mammals.* Dev Cell, 2006. **10**(2): p. 177-86.
46. Huangfu, D. and K.V. Anderson, *Signaling from Smo to Ci/Gli: conservation and divergence of Hedgehog pathways from Drosophila to vertebrates.* Development, 2006. **133**(1): p. 3-14.
47. Hui, C.C. and S. Angers, *Gli proteins in development and disease.* Annu Rev Cell Dev Biol. **27**: p. 513-37.
48. Kinzler, K.W., et al., *The GLI gene is a member of the Kruppel family of zinc finger proteins.* Nature, 1988. **332**(6162): p. 371-4.
49. Ruppert, J.M., et al., *The GLI-Kruppel family of human genes.* Mol Cell Biol, 1988. **8**(8): p. 3104-13.
50. Kinzler, K.W. and B. Vogelstein, *The GLI gene encodes a nuclear protein which binds specific sequences in the human genome.* Mol Cell Biol, 1990. **10**(2): p. 634-42.
51. Aza-Blanc, P., et al., *Proteolysis that is inhibited by hedgehog targets Cubitus interruptus protein to the nucleus and converts it to a repressor.* Cell, 1997. **89**(7): p. 1043-53.
52. Dai, P., et al., *Sonic Hedgehog-induced activation of the Gli1 promoter is mediated by GLI3.* J Biol Chem, 1999. **274**(12): p. 8143-52.
53. Lei, Q., et al., *Transduction of graded Hedgehog signaling by a combination of Gli2 and Gli3 activator functions in the developing spinal cord.* Development, 2004. **131**(15): p. 3593-604.
54. Jacob, J. and J. Briscoe, *Gli proteins and the control of spinal-cord patterning.* EMBO Rep, 2003. **4**(8): p. 761-5.
55. Lee, J., et al., *Gli1 is a target of Sonic hedgehog that induces ventral neural tube development.* Development, 1997. **124**(13): p. 2537-52.
56. Dessaud, E., A.P. McMahon, and J. Briscoe, *Pattern formation in the vertebrate neural tube: a sonic hedgehog morphogen-regulated transcriptional network.* Development, 2008. **135**(15): p. 2489-503.
57. Wijgerde, M., et al., *A direct requirement for Hedgehog signaling for normal specification of all ventral progenitor domains in the presumptive mammalian spinal cord.* Genes Dev, 2002. **16**(22): p. 2849-64.
58. Benazet, J.D. and R. Zeller, *Vertebrate limb development: moving from classical morphogen gradients to an integrated 4-dimensional patterning system.* Cold Spring Harb Perspect Biol, 2009. **1**(4): p. a001339.
59. Wang, B., J.F. Fallon, and P.A. Beachy, *Hedgehog-regulated processing of Gli3 produces an anterior/posterior repressor gradient in the developing vertebrate limb.* Cell, 2000. **100**(4): p. 423-34.
60. Litingtung, Y., et al., *Shh and Gli3 are dispensable for limb skeleton formation but regulate digit number and identity.* Nature, 2002. **418**(6901): p. 979-83.
61. te Welscher, P., et al., *Progression of vertebrate limb development through SHH-mediated counteraction of GLI3.* Science, 2002. **298**(5594): p. 827-30.
62. Huangfu, D., et al., *Hedgehog signalling in the mouse requires intraflagellar transport proteins.* Nature, 2003. **426**(6962): p. 83-7.
63. Goetz, S.C., P.J. Ocbina, and K.V. Anderson, *The primary cilium as a Hedgehog signal transduction machine.* Methods Cell Biol, 2009. **94**: p. 199-222.

64. Marshall, W.F. and S. Nonaka, *Cilia: tuning in to the cell's antenna.* Curr Biol, 2006. **16**(15): p. R604-14.
65. Rosenbaum, J., *Intraflagellar transport.* Curr Biol, 2002. **12**(4): p. R125.
66. Singla, V. and J.F. Reiter, *The primary cilium as the cell's antenna: signaling at a sensory organelle.* Science, 2006. **313**(5787): p. 629-33.
67. Basto, R., et al., *Flies without centrioles.* Cell, 2006. **125**(7): p. 1375-86.
68. Corbit, K.C., et al., *Kif3a constrains beta-catenin-dependent Wnt signalling through dual ciliary and non-ciliary mechanisms.* Nat Cell Biol, 2008. **10**(1): p. 70-6.
69. Eggenschwiler, J.T. and K.V. Anderson, *Cilia and developmental signaling.* Annu Rev Cell Dev Biol, 2007. **23**: p. 345-73.
70. Ross, A.J., et al., *Disruption of Bardet-Biedl syndrome ciliary proteins perturbs planar cell polarity in vertebrates.* Nat Genet, 2005. **37**(10): p. 1135-40.
71. Schneider, L., et al., *PDGFRalphaalpha signaling is regulated through the primary cilium in fibroblasts.* Curr Biol, 2005. **15**(20): p. 1861-6.
72. Hirokawa, N., et al., *Nodal flow and the generation of left-right asymmetry.* Cell, 2006. **125**(1): p. 33-45.
73. Yoder, B.K., *Role of primary cilia in the pathogenesis of polycystic kidney disease.* J Am Soc Nephrol, 2007. **18**(5): p. 1381-8.
74. Christensen, S.T., et al., *Primary cilia and coordination of receptor tyrosine kinase (RTK) signalling.* J Pathol. **226**(2): p. 172-84.
75. Bisgrove, B.W. and H.J. Yost, *The roles of cilia in developmental disorders and disease.* Development, 2006. **133**(21): p. 4131-43.
76. Hildebrandt, F., T. Benzing, and N. Katsanis, *Ciliopathies.* N Engl J Med. **364**(16): p. 1533-43.
77. Santos, N. and J.F. Reiter, *Building it up and taking it down: the regulation of vertebrate ciliogenesis.* Dev Dyn, 2008. **237**(8): p. 1972-81.
78. Pazour, G.J. and G.B. Witman, *The vertebrate primary cilium is a sensory organelle.* Curr Opin Cell Biol, 2003. **15**(1): p. 105-10.
79. Huangfu, D. and K.V. Anderson, *Cilia and Hedgehog responsiveness in the mouse.* Proc Natl Acad Sci U S A, 2005. **102**(32): p. 11325-30.
80. Corbit, K.C., et al., *Vertebrate Smoothened functions at the primary cilium.* Nature, 2005. **437**(7061): p. 1018-21.
81. Rohatgi, R. and M.P. Scott, *Patching the gaps in Hedgehog signalling.* Nat Cell Biol, 2007. **9**(9): p. 1005-9.
82. Haycraft, C.J., et al., *Gli2 and Gli3 localize to cilia and require the intraflagellar transport protein polaris for processing and function.* PLoS Genet, 2005. **1**(4): p. e53.
83. Chen, M.H., et al., *Cilium-independent regulation of Gli protein function by Sufu in Hedgehog signaling is evolutionarily conserved.* Genes Dev, 2009. **23**(16): p. 1910-28.
84. Kim, J., M. Kato, and P.A. Beachy, *Gli2 trafficking links Hedgehog-dependent activation of Smoothened in the primary cilium to transcriptional activation in the nucleus.* Proc Natl Acad Sci U S A, 2009. **106**(51): p. 21666-71.
85. Wen, X., et al., *Kinetics of hedgehog-dependent full-length Gli3 accumulation in primary cilia and subsequent degradation.* Mol Cell Biol. **30**(8): p. 1910-22.
86. Pham, A., et al., *The Suppressor of fused gene encodes a novel PEST protein involved in Drosophila segment polarity establishment.* Genetics, 1995. **140**(2): p. 587-98.

87. Wolff, C., S. Roy, and P.W. Ingham, *Multiple muscle cell identities induced by distinct levels and timing of hedgehog activity in the zebrafish embryo.* Curr Biol, 2003. **13**(14): p. 1169-81.
88. Cooper, A.F., et al., *Cardiac and CNS defects in a mouse with targeted disruption of suppressor of fused.* Development, 2005. **132**(19): p. 4407-17.
89. Svard, J., et al., *Genetic elimination of Suppressor of fused reveals an essential repressor function in the mammalian Hedgehog signaling pathway.* Dev Cell, 2006. **10**(2): p. 187-97.
90. Taylor, M.D., et al., *Mutations in SUFU predispose to medulloblastoma.* Nat Genet, 2002. **31**(3): p. 306-10.
91. Sheng, T., et al., *Activation of the hedgehog pathway in advanced prostate cancer.* Mol Cancer, 2004. **3**: p. 29.
92. Kogerman, P., et al., *Mammalian suppressor-of-fused modulates nuclear-cytoplasmic shuttling of Gli-1.* Nat Cell Biol, 1999. **1**(5): p. 312-9.
93. Pearse, R.V., 2nd, et al., *Vertebrate homologs of Drosophila suppressor of fused interact with the gli family of transcriptional regulators.* Dev Biol, 1999. **212**(2): p. 323-36.
94. Ding, Q., et al., *Mouse suppressor of fused is a negative regulator of sonic hedgehog signaling and alters the subcellular distribution of Gli1.* Curr Biol, 1999. **9**(19): p. 1119-22.
95. Stone, D.M., et al., *Characterization of the human suppressor of fused, a negative regulator of the zinc-finger transcription factor Gli.* J Cell Sci, 1999. **112 (Pt 23)**: p. 4437-48.
96. Dunaeva, M., et al., *Characterization of the physical interaction of Gli proteins with SUFU proteins.* J Biol Chem, 2003. **278**(7): p. 5116-22.
97. Merchant, M., et al., *Suppressor of fused regulates Gli activity through a dual binding mechanism.* Mol Cell Biol, 2004. **24**(19): p. 8627-41.
98. Zeng, H., J. Jia, and A. Liu, *Coordinated translocation of mammalian Gli proteins and suppressor of fused to the primary cilium.* PLoS One. **5**(12): p. e15900.
99. Humke, E.W., et al., *The output of Hedgehog signaling is controlled by the dynamic association between Suppressor of Fused and the Gli proteins.* Genes Dev. **24**(7): p. 670-82.
100. Tukachinsky, H., L.V. Lopez, and A. Salic, *A mechanism for vertebrate Hedgehog signaling: recruitment to cilia and dissociation of SuFu-Gli protein complexes.* J Cell Biol. **191**(2): p. 415-28.
101. Tuson, M., M. He, and K.V. Anderson, *Protein kinase A acts at the basal body of the primary cilium to prevent Gli2 activation and ventralization of the mouse neural tube.* Development. **138**(22): p. 4921-30.
102. Verhey, K.J., J. Dishinger, and H.L. Kee, *Kinesin motors and primary cilia.* Biochem Soc Trans. **39**(5): p. 1120-5.
103. Alcedo, J., et al., *The Drosophila smoothened gene encodes a seven-pass membrane protein, a putative receptor for the hedgehog signal.* Cell, 1996. **86**(2): p. 221-32.
104. Hooper, J.E., *Smoothened translates Hedgehog levels into distinct responses.* Development, 2003. **130**(17): p. 3951-63.
105. Aanstad, P., et al., *The extracellular domain of Smoothened regulates ciliary localization and is required for high-level Hh signaling.* Curr Biol, 2009. **19**(12): p. 1034-9.
106. Nakano, Y., et al., *Functional domains and sub-cellular distribution of the Hedgehog transducing protein Smoothened in Drosophila.* Mech Dev, 2004. **121**(6): p. 507-18.

107. Carroll, C.E., et al., *The extracellular loops of Smoothened play a regulatory role in control of Hedgehog pathway activation.* Development. **139**(3): p. 612-21.
108. Jia, J., C. Tong, and J. Jiang, *Smoothened transduces Hedgehog signal by physically interacting with Costal2/Fused complex through its C-terminal tail.* Genes Dev, 2003. **17**(21): p. 2709-20.
109. Denef, N., et al., *Hedgehog induces opposite changes in turnover and subcellular localization of patched and smoothened.* Cell, 2000. **102**(4): p. 521-31.
110. Zhu, A.J., et al., *Altered localization of Drosophila Smoothened protein activates Hedgehog signal transduction.* Genes Dev, 2003. **17**(10): p. 1240-52.
111. Zhang, C., et al., *Extensive phosphorylation of Smoothened in Hedgehog pathway activation.* Proc Natl Acad Sci U S A, 2004. **101**(52): p. 17900-7.
112. Apionishev, S., et al., *Drosophila Smoothened phosphorylation sites essential for Hedgehog signal transduction.* Nat Cell Biol, 2005. **7**(1): p. 86-92.
113. Zhou, Q., S. Apionishev, and D. Kalderon, *The contributions of protein kinase A and smoothened phosphorylation to hedgehog signal transduction in Drosophila melanogaster.* Genetics, 2006. **173**(4): p. 2049-62.
114. Jia, J., et al., *Hedgehog signalling activity of Smoothened requires phosphorylation by protein kinase A and casein kinase I.* Nature, 2004. **432**(7020): p. 1045-50.
115. Zhao, Y., C. Tong, and J. Jiang, *Hedgehog regulates smoothened activity by inducing a conformational switch.* Nature, 2007. **450**(7167): p. 252-8.
116. Robbins, D.J., et al., *Hedgehog elicits signal transduction by means of a large complex containing the kinesin-related protein costal2.* Cell, 1997. **90**(2): p. 225-34.
117. Lum, L., et al., *Hedgehog signal transduction via Smoothened association with a cytoplasmic complex scaffolded by the atypical kinesin, Costal-2.* Mol Cell, 2003. **12**(5): p. 1261-74.
118. Wilson, C.W., et al., *Fused has evolved divergent roles in vertebrate Hedgehog signalling and motile ciliogenesis.* Nature, 2009. **459**(7243): p. 98-102.
119. Milenkovic, L., M.P. Scott, and R. Rohatgi, *Lateral transport of Smoothened from the plasma membrane to the membrane of the cilium.* J Cell Biol, 2009. **187**(3): p. 365-74.
120. Wang, Y., et al., *Selective translocation of intracellular Smoothened to the primary cilium in response to Hedgehog pathway modulation.* Proc Natl Acad Sci U S A, 2009. **106**(8): p. 2623-8.
121. Rohatgi, R., et al., *Hedgehog signal transduction by Smoothened: pharmacologic evidence for a 2-step activation process.* Proc Natl Acad Sci U S A, 2009. **106**(9): p. 3196-201.
122. Pitcher, J.A., N.J. Freedman, and R.J. Lefkowitz, *G protein-coupled receptor kinases.* Annu Rev Biochem, 1998. **67**: p. 653-92.
123. Reiter, E. and R.J. Lefkowitz, *GRKs and beta-arrestins: roles in receptor silencing, trafficking and signaling.* Trends Endocrinol Metab, 2006. **17**(4): p. 159-65.
124. Chen, Y., et al., *G protein-coupled receptor kinase 2 promotes high-level Hedgehog signaling by regulating the active state of Smo through kinase-dependent and kinase-independent mechanisms in Drosophila.* Genes Dev. **24**(18): p. 2054-67.
125. Molnar, C., et al., *The G protein-coupled receptor regulatory kinase GPRK2 participates in Hedgehog signaling in Drosophila.* Proc Natl Acad Sci U S A, 2007. **104**(19): p. 7963-8.

126. Cheng, S., D. Maier, and D.R. Hipfner, *Drosophila G-protein-coupled receptor kinase 2 regulates cAMP-dependent Hedgehog signaling.* Development. **139**(1): p. 85-94.
127. Molnar, C., et al., *Role of the Drosophila non-visual ss-arrestin kurtz in hedgehog signalling.* PLoS Genet. **7**(3): p. e1001335.
128. Chen, Y., et al., *Sonic Hedgehog dependent phosphorylation by CK1alpha and GRK2 is required for ciliary accumulation and activation of smoothened.* PLoS Biol. **9**(6): p. e1001083.
129. Chen, W., et al., *Activity-dependent internalization of smoothened mediated by beta-arrestin 2 and GRK2.* Science, 2004. **306**(5705): p. 2257-60.
130. Meloni, A.R., et al., *Smoothened signal transduction is promoted by G protein-coupled receptor kinase 2.* Mol Cell Biol, 2006. **26**(20): p. 7550-60.
131. Wilbanks, A.M., et al., *Beta-arrestin 2 regulates zebrafish development through the hedgehog signaling pathway.* Science, 2004. **306**(5705): p. 2264-7.
132. Kovacs, J.J., et al., *Beta-arrestin-mediated localization of smoothened to the primary cilium.* Science, 2008. **320**(5884): p. 1777-81.
133. Molla-Herman, A., et al., *Targeting of beta-arrestin2 to the centrosome and primary cilium: role in cell proliferation control.* PLoS One, 2008. **3**(11): p. e3728.
134. Price, M.A., *CKI, there's more than one: casein kinase I family members in Wnt and Hedgehog signaling.* Genes Dev, 2006. **20**(4): p. 399-410.
135. Jia, J., et al., *Phosphorylation by double-time/CKIepsilon and CKIalpha targets cubitus interruptus for Slimb/beta-TRCP-mediated proteolytic processing.* Dev Cell, 2005. **9**(6): p. 819-30.
136. Greer, Y.E. and J.S. Rubin, *Casein kinase 1 delta functions at the centrosome to mediate Wnt-3a-dependent neurite outgrowth.* J Cell Biol. **192**(6): p. 993-1004.
137. Mashhoon, N., et al., *Crystal structure of a conformation-selective casein kinase-1 inhibitor.* J Biol Chem, 2000. **275**(26): p. 20052-60.
138. Rena, G., et al., *D4476, a cell-permeant inhibitor of CK1, suppresses the site-specific phosphorylation and nuclear exclusion of FOXO1a.* EMBO Rep, 2004. **5**(1): p. 60-5.
139. Kohout, T.A., et al., *beta-Arrestin 1 and 2 differentially regulate heptahelical receptor signaling and trafficking.* Proc Natl Acad Sci U S A, 2001. **98**(4): p. 1601-6.
140. Jaber, M., et al., *Essential role of beta-adrenergic receptor kinase 1 in cardiac development and function.* Proc Natl Acad Sci U S A, 1996. **93**(23): p. 12974-9.
141. Iino, M., et al., *Rational design and evaluation of new lead compound structures for selective betaARK1 inhibitors.* J Med Chem, 2002. **45**(11): p. 2150-9.
142. Evangelista, M., et al., *Kinome siRNA screen identifies regulators of ciliogenesis and hedgehog signal transduction.* Sci Signal, 2008. **1**(39): p. ra7.
143. Evron, T., et al., *Growth Arrest Specific 8 (Gas8) and G protein-coupled receptor kinase 2 (GRK2) cooperate in the control of Smoothened signaling.* J Biol Chem. **286**(31): p. 27676-86.
144. Kohout, T.A. and R.J. Lefkowitz, *Regulation of G protein-coupled receptor kinases and arrestins during receptor desensitization.* Mol Pharmacol, 2003. **63**(1): p. 9-18.
145. Shenoy, S.K. and R.J. Lefkowitz, *Multifaceted roles of beta-arrestins in the regulation of seven-membrane-spanning receptor trafficking and signalling.* Biochem J, 2003. **375**(Pt 3): p. 503-15.
146. Bohn, L.M., et al., *Enhanced morphine analgesia in mice lacking beta-arrestin 2.* Science, 1999. **286**(5449): p. 2495-8.

147. Conner, D.A., et al., *beta-Arrestin1 knockout mice appear normal but demonstrate altered cardiac responses to beta-adrenergic stimulation.* Circ Res, 1997. **81**(6): p. 1021-6.
148. Massotte, D. and B.L. Kieffer, *The second extracellular loop: a damper for G protein-coupled receptors?* Nat Struct Mol Biol, 2005. **12**(4): p. 287-8.
149. Minneman, K.P., *Heterodimerization and surface localization of G protein coupled receptors.* Biochem Pharmacol, 2007. **73**(8): p. 1043-50.
150. Carron, C., et al., *Frizzled receptor dimerization is sufficient to activate the Wnt/beta-catenin pathway.* J Cell Sci, 2003. **116**(Pt 12): p. 2541-50.
151. Fotiadis, D., et al., *Atomic-force microscopy: Rhodopsin dimers in native disc membranes.* Nature, 2003. **421**(6919): p. 127-8.
152. Fotiadis, D., et al., *Structure of the rhodopsin dimer: a working model for G-protein-coupled receptors.* Curr Opin Struct Biol, 2006. **16**(2): p. 252-9.
153. Banaszynski, L.A., C.W. Liu, and T.J. Wandless, *Characterization of the FKBP.rapamycin.FRB ternary complex.* J Am Chem Soc, 2005. **127**(13): p. 4715-21.
154. Xu, Y., et al., *Functional consequences of a CKIdelta mutation causing familial advanced sleep phase syndrome.* Nature, 2005. **434**(7033): p. 640-4.
155. Schwab, C., et al., *Casein kinase 1 delta is associated with pathological accumulation of tau in several neurodegenerative diseases.* Neurobiol Aging, 2000. **21**(4): p. 503-10.
156. Meng, Q.J., et al., *Setting clock speed in mammals: the CK1 epsilon tau mutation in mice accelerates circadian pacemakers by selectively destabilizing PERIOD proteins.* Neuron, 2008. **58**(1): p. 78-88.
157. Gao, Z.H., et al., *Casein kinase I phosphorylates and destabilizes the beta-catenin degradation complex.* Proc Natl Acad Sci U S A, 2002. **99**(3): p. 1182-7.
158. Preuss, F., et al., *Drosophila doubletime mutations which either shorten or lengthen the period of circadian rhythms decrease the protein kinase activity of casein kinase I.* Mol Cell Biol, 2004. **24**(2): p. 886-98.
159. Roebroek, A.J., P.L. Gordts, and S. Reekmans, *Knock-in approaches.* Methods Mol Biol. **693**: p. 257-75.
160. Singla, V., et al., *Floxin, a resource for genetically engineering mouse ESCs.* Nat Methods. **7**(1): p. 50-2.
161. Stryke, D., et al., *BayGenomics: a resource of insertional mutations in mouse embryonic stem cells.* Nucleic Acids Res, 2003. **31**(1): p. 278-81.
162. Singla, V., et al., *Ofd1, a human disease gene, regulates the length and distal structure of centrioles.* Dev Cell. **18**(3): p. 410-24.
163. Kiprilov, E.N., et al., *Human embryonic stem cells in culture possess primary cilia with hedgehog signaling machinery.* J Cell Biol, 2008. **180**(5): p. 897-904.
164. Maye, P., et al., *Hedgehog signaling is required for the differentiation of ES cells into neurectoderm.* Dev Biol, 2004. **265**(1): p. 276-90.
165. Hunkapiller, J., et al., *The ciliogenic protein Oral-Facial-Digital 1 regulates the neuronal differentiation of embryonic stem cells.* Stem Cells Dev. **20**(5): p. 831-41.
166. Hui, C.C., et al., *Expression of three mouse homologs of the Drosophila segment polarity gene cubitus interruptus, Gli, Gli-2, and Gli-3, in ectoderm- and mesoderm-derived tissues suggests multiple roles during postimplantation development.* Dev Biol, 1994. **162**(2): p. 402-13.
167. Platt, K.A., J. Michaud, and A.L. Joyner, *Expression of the mouse Gli and Ptc genes is adjacent to embryonic sources of hedgehog signals suggesting a*

conservation of pathways between flies and mice. Mech Dev, 1997. **62**(2): p. 121-35.
168. Schimmang, T., et al., *Expression of the zinc finger gene Gli3 is affected in the morphogenetic mouse mutant extra-toes (Xt).* Development, 1992. **116**(3): p. 799-804.
169. Hui, C.C. and A.L. Joyner, *A mouse model of greig cephalopolysyndactyly syndrome: the extra-toesJ mutation contains an intragenic deletion of the Gli3 gene.* Nat Genet, 1993. **3**(3): p. 241-6.
170. Vortkamp, A., et al., *Deletion of GLI3 supports the homology of the human Greig cephalopolysyndactyly syndrome (GCPS) and the mouse mutant extra toes (Xt).* Mamm Genome, 1992. **3**(8): p. 461-3.
171. Mo, R., et al., *Specific and redundant functions of Gli2 and Gli3 zinc finger genes in skeletal patterning and development.* Development, 1997. **124**(1): p. 113-23.
172. Motoyama, J., et al., *Essential function of Gli2 and Gli3 in the formation of lung, trachea and oesophagus.* Nat Genet, 1998. **20**(1): p. 54-7.
173. Matise, M.P., et al., *Gli2 is required for induction of floor plate and adjacent cells, but not most ventral neurons in the mouse central nervous system.* Development, 1998. **125**(15): p. 2759-70.
174. Ding, Q., et al., *Diminished Sonic hedgehog signaling and lack of floor plate differentiation in Gli2 mutant mice.* Development, 1998. **125**(14): p. 2533-43.
175. Kimmel, S.G., et al., *New mouse models of congenital anorectal malformations.* J Pediatr Surg, 2000. **35**(2): p. 227-30; discussion 230-1.
176. Park, H.L., et al., *Mouse Gli1 mutants are viable but have defects in SHH signaling in combination with a Gli2 mutation.* Development, 2000. **127**(8): p. 1593-605.
177. Bai, C.B., D. Stephen, and A.L. Joyner, *All mouse ventral spinal cord patterning by hedgehog is Gli dependent and involves an activator function of Gli3.* Dev Cell, 2004. **6**(1): p. 103-15.
178. Cho, A., H.W. Ko, and J.T. Eggenschwiler, *FKBP8 cell-autonomously controls neural tube patterning through a Gli2- and Kif3a-dependent mechanism.* Dev Biol, 2008. **321**(1): p. 27-39.
179. Wang, Q.T. and R.A. Holmgren, *Nuclear import of cubitus interruptus is regulated by hedgehog via a mechanism distinct from Ci stabilization and Ci activation.* Development, 2000. **127**(14): p. 3131-9.
180. Mo, R., et al., *Anorectal malformations caused by defects in sonic hedgehog signaling.* Am J Pathol, 2001. **159**(2): p. 765-74.
181. Milenkovic, L., et al., *Mouse patched1 controls body size determination and limb patterning.* Development, 1999. **126**(20): p. 4431-40.
182. Ballabeni, A., et al., *Cell cycle adaptations of embryonic stem cells.* Proc Natl Acad Sci U S A. **108**(48): p. 19252-7.
183. Garcia-Gonzalo, F.R., et al., *A transition zone complex regulates mammalian ciliogenesis and ciliary membrane composition.* Nat Genet. **43**(8): p. 776-84.
184. Marigo, V., et al., *Sonic hedgehog differentially regulates expression of GLI and GLI3 during limb development.* Dev Biol, 1996. **180**(1): p. 273-83.
185. Alexandre, C., A. Jacinto, and P.W. Ingham, *Transcriptional activation of hedgehog target genes in Drosophila is mediated directly by the cubitus interruptus protein, a member of the GLI family of zinc finger DNA-binding proteins.* Genes Dev, 1996. **10**(16): p. 2003-13.
186. Pavletich, N.P. and C.O. Pabo, *Crystal structure of a five-finger GLI-DNA complex: new perspectives on zinc fingers.* Science, 1993. **261**(5129): p. 1701-7.

187. Croker, J.A., S.L. Ziegenhorn, and R.A. Holmgren, *Regulation of the Drosophila transcription factor, Cubitus interruptus, by two conserved domains.* Dev Biol, 2006. **291**(2): p. 368-81.
188. Sasaki, H., et al., *Regulation of Gli2 and Gli3 activities by an amino-terminal repression domain: implication of Gli2 and Gli3 as primary mediators of Shh signaling.* Development, 1999. **126**(17): p. 3915-24.
189. Hughes, D.C., et al., *Cloning and sequencing of the mouse Gli2 gene: localization to the Dominant hemimelia critical region.* Genomics, 1997. **39**(2): p. 205-15.
190. Akimaru, H., et al., *Drosophila CBP is a co-activator of cubitus interruptus in hedgehog signalling.* Nature, 1997. **386**(6626): p. 735-8.
191. Yoon, J.W., et al., *GLI activates transcription through a herpes simplex viral protein 16-like activation domain.* J Biol Chem, 1998. **273**(6): p. 3496-501.
192. Hepker, J., et al., *Drosophila cubitus interruptus forms a negative feedback loop with patched and regulates expression of Hedgehog target genes.* Development, 1997. **124**(2): p. 549-58.
193. Sheng, H., et al., *Dissecting the oncogenic potential of Gli2: deletion of an NH(2)-terminal fragment alters skin tumor phenotype.* Cancer Res, 2002. **62**(18): p. 5308-16.
194. Cervantes, S., et al., *Primary cilia regulate Gli/Hedgehog activation in pancreas.* Proc Natl Acad Sci U S A. **107**(22): p. 10109-14.
195. Wong, S.Y., et al., *Primary cilia can both mediate and suppress Hedgehog pathway-dependent tumorigenesis.* Nat Med, 2009. **15**(9): p. 1055-61.
196. Huntzicker, E.G., et al., *Dual degradation signals control Gli protein stability and tumor formation.* Genes Dev, 2006. **20**(3): p. 276-81.
197. Chen, Y., et al., *Protein kinase A directly regulates the activity and proteolysis of cubitus interruptus.* Proc Natl Acad Sci U S A, 1998. **95**(5): p. 2349-54.
198. Ruppert, J.M., et al., *GLI3 encodes a 190-kilodalton protein with multiple regions of GLI similarity.* Mol Cell Biol, 1990. **10**(10): p. 5408-15.
199. Tian, L., R.A. Holmgren, and A. Matouschek, *A conserved processing mechanism regulates the activity of transcription factors Cubitus interruptus and NF-kappaB.* Nat Struct Mol Biol, 2005. **12**(12): p. 1045-53.
200. Jiang, J. and G. Struhl, *Regulation of the Hedgehog and Wingless signalling pathways by the F-box/WD40-repeat protein Slimb.* Nature, 1998. **391**(6666): p. 493-6.
201. Smelkinson, M.G. and D. Kalderon, *Processing of the Drosophila hedgehog signaling effector Ci-155 to the repressor Ci-75 is mediated by direct binding to the SCF component Slimb.* Curr Biol, 2006. **16**(1): p. 110-6.
202. Smelkinson, M.G., Q. Zhou, and D. Kalderon, *Regulation of Ci-SCFSlimb binding, Ci proteolysis, and hedgehog pathway activity by Ci phosphorylation.* Dev Cell, 2007. **13**(4): p. 481-95.
203. Wang, Y. and M.A. Price, *A unique protection signal in Cubitus interruptus prevents its complete proteasomal degradation.* Mol Cell Biol, 2008. **28**(18): p. 5555-68.
204. Kaesler, S., B. Luscher, and U. Ruther, *Transcriptional activity of GLI1 is negatively regulated by protein kinase A.* Biol Chem, 2000. **381**(7): p. 545-51.
205. Tempe, D., et al., *Multisite protein kinase A and glycogen synthase kinase 3beta phosphorylation leads to Gli3 ubiquitination by SCFbetaTrCP.* Mol Cell Biol, 2006. **26**(11): p. 4316-26.
206. Wang, B. and Y. Li, *Evidence for the direct involvement of {beta}TrCP in Gli3 protein processing.* Proc Natl Acad Sci U S A, 2006. **103**(1): p. 33-8.

207. Tyurina, O.V., et al., *Zebrafish Gli3 functions as both an activator and a repressor in Hedgehog signaling.* Dev Biol, 2005. **277**(2): p. 537-56.
208. Pan, Y., et al., *Sonic hedgehog signaling regulates Gli2 transcriptional activity by suppressing its processing and degradation.* Mol Cell Biol, 2006. **26**(9): p. 3365-77.
209. Pan, Y. and B. Wang, *A novel protein-processing domain in Gli2 and Gli3 differentially blocks complete protein degradation by the proteasome.* J Biol Chem, 2007. **282**(15): p. 10846-52.
210. Bhatia, N., et al., *Gli2 is targeted for ubiquitination and degradation by beta-TrCP ubiquitin ligase.* J Biol Chem, 2006. **281**(28): p. 19320-6.
211. Pan, Y., C. Wang, and B. Wang, *Phosphorylation of Gli2 by protein kinase A is required for Gli2 processing and degradation and the Sonic Hedgehog-regulated mouse development.* Dev Biol, 2009. **326**(1): p. 177-89.
212. Epstein, D.J., et al., *Antagonizing cAMP-dependent protein kinase A in the dorsal CNS activates a conserved Sonic hedgehog signaling pathway.* Development, 1996. **122**(9): p. 2885-94.
213. Li, J., et al., *Increased proteolytic processing of full-length Gli2 transcription factor reduces the hedgehog pathway activity in vivo.* Dev Dyn. **240**(4): p. 766-74.
214. Buttitta, L., et al., *Interplays of Gli2 and Gli3 and their requirement in mediating Shh-dependent sclerotome induction.* Development, 2003. **130**(25): p. 6233-43.
215. McDermott, A., et al., *Gli2 and Gli3 have redundant and context-dependent function in skeletal muscle formation.* Development, 2005. **132**(2): p. 345-57.
216. Zhang, Q., et al., *Multiple Ser/Thr-rich degrons mediate the degradation of Ci/Gli by the Cul3-HIB/SPOP E3 ubiquitin ligase.* Proc Natl Acad Sci U S A, 2009. **106**(50): p. 21191-6.
217. Zhang, Q., et al., *A hedgehog-induced BTB protein modulates hedgehog signaling by degrading Ci/Gli transcription factor.* Dev Cell, 2006. **10**(6): p. 719-29.
218. Di Marcotullio, L., et al., *Numb is a suppressor of Hedgehog signalling and targets Gli1 for Itch-dependent ubiquitination.* Nat Cell Biol, 2006. **8**(12): p. 1415-23.
219. Barzi, M., et al., *Sonic-hedgehog-mediated proliferation requires the localization of PKA to the cilium base.* J Cell Sci. **123**(Pt 1): p. 62-9.
220. Cortellino, S., et al., *Defective ciliogenesis, embryonic lethality and severe impairment of the Sonic Hedgehog pathway caused by inactivation of the mouse complex A intraflagellar transport gene Ift122/Wdr10, partially overlapping with the DNA repair gene Med1/Mbd4.* Dev Biol, 2009. **325**(1): p. 225-37.
221. May, S.R., et al., *Loss of the retrograde motor for IFT disrupts localization of Smo to cilia and prevents the expression of both activator and repressor functions of Gli.* Dev Biol, 2005. **287**(2): p. 378-89.
222. Liu, A., B. Wang, and L.A. Niswander, *Mouse intraflagellar transport proteins regulate both the activator and repressor functions of Gli transcription factors.* Development, 2005. **132**(13): p. 3103-11.
223. Methot, N. and K. Basler, *Suppressor of fused opposes hedgehog signal transduction by impeding nuclear accumulation of the activator form of Cubitus interruptus.* Development, 2000. **127**(18): p. 4001-10.
224. Wang, G., et al., *Interactions with Costal2 and suppressor of fused regulate nuclear translocation and activity of cubitus interruptus.* Genes Dev, 2000. **14**(22): p. 2893-905.

225. Barnfield, P.C., et al., *Negative regulation of Gli1 and Gli2 activator function by Suppressor of fused through multiple mechanisms.* Differentiation, 2005. **73**(8): p. 397-405.
226. Wang, C., Y. Pan, and B. Wang, *Suppressor of fused and Spop regulate the stability, processing and function of Gli2 and Gli3 full-length activators but not their repressors.* Development. **137**(12): p. 2001-9.
227. Cheung, H.O., et al., *The kinesin protein Kif7 is a critical regulator of Gli transcription factors in mammalian hedgehog signaling.* Sci Signal, 2009. **2**(76): p. ra29.
228. Endoh-Yamagami, S., et al., *The mammalian Cos2 homolog Kif7 plays an essential role in modulating Hh signal transduction during development.* Curr Biol, 2009. **19**(15): p. 1320-6.
229. Liem, K.F., Jr., et al., *Mouse Kif7/Costal2 is a cilia-associated protein that regulates Sonic hedgehog signaling.* Proc Natl Acad Sci U S A, 2009. **106**(32): p. 13377-82.
230. Farzan, S.F., et al., *Costal2 functions as a kinesin-like protein in the hedgehog signal transduction pathway.* Curr Biol, 2008. **18**(16): p. 1215-20.
231. Marks, S.A. and D. Kalderon, *Regulation of mammalian Gli proteins by Costal 2 and PKA in Drosophila reveals Hedgehog pathway conservation.* Development. **138**(12): p. 2533-42.
232. Hsu, S.H., et al., *Kif7 promotes hedgehog signaling in growth plate chondrocytes by restricting the inhibitory function of Sufu.* Development. **138**(17): p. 3791-801.
233. Dafinger, C., et al., *Mutations in KIF7 link Joubert syndrome with Sonic Hedgehog signaling and microtubule dynamics.* J Clin Invest. **121**(7): p. 2662-7.
234. Sorokin, A.V., E.R. Kim, and L.P. Ovchinnikov, *Nucleocytoplasmic transport of proteins.* Biochemistry (Mosc), 2007. **72**(13): p. 1439-57.
235. Wente, S.R. and M.P. Rout, *The nuclear pore complex and nuclear transport.* Cold Spring Harb Perspect Biol. **2**(10): p. a000562.
236. Dishinger, J.F., et al., *Ciliary entry of the kinesin-2 motor KIF17 is regulated by importin-beta2 and RanGTP.* Nat Cell Biol. **12**(7): p. 703-10.
237. Hurd, T.W., S. Fan, and B.L. Margolis, *Localization of retinitis pigmentosa 2 to cilia is regulated by Importin beta2.* J Cell Sci. **124**(Pt 5): p. 718-26.
238. Kee, H.L., et al., *A size-exclusion permeability barrier and nucleoporins characterize a ciliary pore complex that regulates transport into cilia.* Nat Cell Biol.
239. Paces-Fessy, M., et al., *The negative regulator of Gli, Suppressor of fused (Sufu), interacts with SAP18, Galectin3 and other nuclear proteins.* Biochem J, 2004. **378**(Pt 2): p. 353-62.
240. Riobo, N.A., et al., *Phosphoinositide 3-kinase and Akt are essential for Sonic Hedgehog signaling.* Proc Natl Acad Sci U S A, 2006. **103**(12): p. 4505-10.
241. Hahn, H., et al., *Patched target Igf2 is indispensable for the formation of medulloblastoma and rhabdomyosarcoma.* J Biol Chem, 2000. **275**(37): p. 28341-4.
242. Rao, G., et al., *c-Myc enhances sonic hedgehog-induced medulloblastoma formation from nestin-expressing neural progenitors in mice.* Neoplasia, 2003. **5**(3): p. 198-204.
243. Obata, T., et al., *Peptide and protein library screening defines optimal substrate motifs for AKT/PKB.* J Biol Chem, 2000. **275**(46): p. 36108-15.
244. Canettieri, G., et al., *Histone deacetylase and Cullin3-REN(KCTD11) ubiquitin ligase interplay regulates Hedgehog signalling through Gli acetylation.* Nat Cell Biol. **12**(2): p. 132-42.

245. Cox, B., J. Briscoe, and F. Ulloa, *SUMOylation by Pias1 regulates the activity of the Hedgehog dependent Gli transcription factors.* PLoS One. **5**(8): p. e11996.
246. Zhao, J., *Sumoylation regulates diverse biological processes.* Cell Mol Life Sci, 2007. **64**(23): p. 3017-33.
247. Liu, Q., Q. Jiang, and C. Zhang, *A fraction of Crm1 locates at centrosomes by its CRIME domain and regulates the centrosomal localization of pericentrin.* Biochem Biophys Res Commun, 2009. **384**(3): p. 383-8.
248. Wang, W., et al., *Temporal and spatial control of nucleophosmin by the Ran-Crm1 complex in centrosome duplication.* Nat Cell Biol, 2005. **7**(8): p. 823-30.
249. Chen, Y., et al., *Dual Phosphorylation of suppressor of fused (Sufu) by PKA and GSK3beta regulates its stability and localization in the primary cilium.* J Biol Chem. **286**(15): p. 13502-11.
250. Ishikawa, H., et al., *Proteomic analysis of Mammalian primary cilia.* Curr Biol. **22**(5): p. 414-9.

Appendix I

Building it up and taking it down: the regulation of vertebrate ciliogenesis

Nicole Santos and Jeremy Reiter

Developmental Dynamics, 2008 August; 237 (8): 1972-81.

Abstract

Primary cilia project from the surface of most vertebrate cells, and function in sensation and signaling during both development and adult tissue homeostasis. Mounting evidence links ciliary defects with a wide variety of diseases, underscoring the importance of understanding how these dynamic organelles are assembled and maintained. However, despite their physiological and clinical relevance, the logic and machinery that regulate ciliogenesis remain largely enigmatic. Here, we summarize emerging data that connect the assembly and disassembly of the primary cilium to cell cycle progression and examine how regulators of cell architecture, including the planar cell polarity pathway, may regulate ciliogenesis. Additionally, identification of the genes underlying diverse ciliopathies in human patients is shedding light on the genes that regulate the formation of this complex organelle.

Introduction

One fundamental problem that confronts every cell is how to collect information about its environment. Extending from the surface of most vertebrate cells is a single, sophisticated microtubule-based projection called the primary cilium. Although many biologists once considered this organelle to be “vestigial”, it is now becoming clear that primary cilia play important roles in receiving information [1]. Photoreceptors and odorant receptors function on modified cilia, and cilia are essential for sound reception. Therefore, it is not much of an exaggeration to say that we see, smell and hear through cilia. Moreover, it is now clear that cells also use primary cilia to communicate with each other [2]. For instance, cilia play roles in establishing proper left-right patterning, regulating intracellular calcium levels, and interpreting several intercellular signals, including Hedgehog (Hh), PDGF and Wnt [2-5].

Given these diverse cellular functions during both development and adult tissue homeostasis, it is not surprising that a growing variety of diseases are attributed to ciliary disfunction [6]. Whereas defects in ciliary motility lead to primary cilia dyskinesia (PCD) and defective left-right axis patterning, defects in immotile primary cilia function are frequently associated with kidney cysts, retinal degeneration, polydactyly, obesity and/or neural tube defects (here, referred to collectively as ciliopathies). The pleitropic nature of these disorders may reflect the many roles cilia play in mechanosensation and signal transduction, highlighting the clinical importance of understanding how these organelles are assembled and maintained.

The formation of the primary cilium requires dynamic and intricate cellular movements, initially involving the migration and docking of the mother centriole to the plasma membrane [7]. The nine doublet microtubules of the ciliary axoneme then extend from

the nine triplet microtubules of the basal body, a centriole-derived microtubule-organizing center. Elongation of the axoneme at the distal tip relies on intraflagellar transport (IFT), the bi-directional transit system that carries cargo within the cilium [8]. IFT particles, comprised of at least sixteen components including IFT88, IFT80, and IFT27, are transported in the anterograde direction by the Kinesin-2 motor, and in the retrograde direction by a Dynein motor [8]. Disruption of either the IFT motors themselves or the basal body proteins essential for their function leads to impaired cilia assembly [7, 8]

As the structural components of the cilium continue to be identified and characterized, an understanding of the regulatory mechanisms of ciliogenesis has begun to emerge. Clearly, this process must be regulated in some way, as many mammalian cells that have the ability to form cilia are not always ciliated. For example, endocardial cells can be ciliated, but the majority are not [9].

The regulatory influences that trigger a cell to begin the process of ciliary assembly or disassembly remain largely enigmatic. Ciliogenesis is exquisitely coordinated with the cell cycle, and recent studies have identified centrosomal proteins involved in this coordination. Moreover, the identification of the genes underlying human ciliopathies has suggested many additional candidates that may participate in the regulation of ciliogenesis. Here, we review recent data from both areas.

Coordination of ciliogenesis and the cell cycle

Centrosome dynamics are precisely synchronized with, and essential for the fidelity of, the cell cycle [10-12]. During cytokinesis, each daughter cell inherits a single centrosome associated with one spindle pole (Figure 1). This centrosome is duplicated at the G1/S

transition under the control of Cdk2 [13, 14]. During G2, centrioles lengthen and centrosomes separate before mitotic entry in order to form spindle pole bodies. Thus, much like chromosomes, centrosomes duplicate once and only once per cell cycle. Failure to obey this rule can result in disastrous consequences including multipolar mitotic spindles and chromosomal missegregation [15, 16]. Indeed, centrosome amplification is thought to be a significant cause of aneuploidy in cancer cells [17, 18]. However, like all rules, there are exceptions. For example, multi-ciliated cells such as tracheal and ependymal cells must synthesize at least as many centrioles as there are cilia. Multi-ciliated cells may avoid the difficulties of dividing with greater than two centrosomes by terminally differentiating and permanently exiting the cell cycle [19, 20].

Given the intimate connection between cilia and centrosomes, it is perhaps not surprising that ciliogenesis is also coordinated with the cell cycle. Cilia are assembled during G1, most abundant in G0, and retracted in many cells at the entry into mitosis (Figure 1) [21, 22]. However, in some cell types, disassembly of the cilium can occur at other cell cycle phases, including prior to S-phase [21-23].

Ciliary disassembly at some point prior to entry into mitosis would seem to be essential, as the centrioles that template the microtubules of the ciliary axoneme during interphase are the same centrioles that form the spindle pole bodies during mitosis. However, centrioles are not required for cell cycle progression or mitotic spindle organization in either plants or *Drosophila* [24]. In support of idea that centrosomes are more important for animal cell mitosis and cell cycle progression, reduction of centrosomal components such as Pericentrin and Centriolin leads to a p53-dependent arrest of human RPE1 cells in G1 [25]. However, other cell types, such as HeLa and RPE1 cells, progress through the cell cycle despite the loss of centrioles suggesting that the way in which the

centrosome cycle is coordinated with the cell cycle differs in some cell types or is perturbed in some tumor cell lines [26, 27].

Like the centriole, centrosomal proteins can participate both in cell cycle progression and cilium formation [28, 29] Indeed, study of the centrosomal proteins CP110 and Cep97 have begun to reveal some of the ways in which ciliogenesis is controlled. CP110 is phosphorylated by CDKs [30] and recruited to the centrosome by Cep97 [31]. Depletion of either CP110 or Cep97 in U2OS cells leads to defective cytokinesis and abnormal mitotic spindles, as well as the production of cilia-like structures that emanate from the distal ends of centrioles. These cilia-like structures contain nonciliary proteins such as Centrin and α-Tubulin, suggesting that their composition is not identical to that of normal cilia.

In cells that can normally form cilia such as RPE-1 and NIH-3T3 cells, inhibition of CP110 or Cep97 increases the proportion of cells displaying cilia. Conversely, ectopic expression of CP110 in non-proliferating cells results in the suppression of cilia formation. Together, these results suggest that one of the centrosomal functions of CP110 and Cep97 is to suppress ciliogenesis. Given that CP110 is phosphorylated by CDKs, one attractive model is that active CDK2 phosphorylation of centrosomal CP110 in G1 inhibits the repressive functions of CP110, allowing ciliogenesis to occur.

If repression of CP110 function leads to the induction of ciliogenesis in G1, what accounts for the dismantling of cilia prior to mitosis? Recent work has implicated a known regulator of mitosis, AuroraA, and an interacting protein, HEF1, in the control of cilia disassembly [32, 33]. AuroraA is a member of the Ipl family of kinases modestly related to CALK, a kinase involved in *Chlamydomonas* flagellar retraction [10, 34, 35].

Over-activation of AuroraA and HEF1 is associated with supernumerary centrosomes and multipolar spindles [33]. Both proteins localize to the centrosome during G2 and M phases, and just prior to cilia disassembly, both are activated at the basal bodies of hTERT-RPE cells [32]. Pharmacological or siRNA inhibition of AuroraA blocks ciliary disassembly, whereas injection of active AuroraA initiates loss of cilia. Furthermore, siRNA against *HEF1* leads to reduced levels of AuroraA activation. Thus, Hef1 may stabilize and activate AuroraA, which initiates ciliary disassembly.

HDAC6, an α-tubulin deacetylase that promotes microtubule destabilization may be a key player in AuroraA-mediated ciliary disassembly [32]. Activated AuroraA does not induce efficient ciliary disassembly in HDAC6 depleted cells, indicating that HDAC6 acts downstream of AuroraA [32]Moreover, AuroraA can phosphorylate HDAC6 *in vitro* [32]. Taken together, these findings suggest that growth factors may induce ciliary disassembly through the induction of *HEF1* expression, thereby activating AuroraA (Figure 2). AuroraA subsequently phosphorylates HDAC6, which destabilizes the microtubules of the primary cilium by deacetylating axonemal tubulin, leading to rapid cilium resorption. Thus, inhibition of CP110 may generate cilia in G1, whereas the activation of AuroraA may precipitate the disassembly of cilia in G2, accounting for one means of coordinating cilium formation with the cell cycle.

Another important class of regulatory proteins that may act in the coordination of ciliogenesis with the cell cycle is the NIMA-related kinase (Nek) family. Several Neks are essential for cell cycle progression and some of these localize to the centrosome [36] [37, 38]. Mutations in the gene encoding Nek8, a ciliary Nek, cause cystic kidney disease in both mice and humans, further underscoring the connection between Neks, cilia, and cell proliferation [39-42]. Although the functions of many of the Neks remain to

be clearly elucidated, phylogenetic analysis suggests that the Nek family is expanded in organisms that have cilia on cells that have not permanently exited from the cell cycle [43]suggesting that one role for Neks may be in coordinating ciliary disassembly and the commitment to mitosis.

As proteins like the Neks are associated both with cell cycle control and the regulation of ciliogenesis, the question arises as to whether the cilium itself reciprocally regulates any aspect of cell cycle progression. Depletion of some centrosomal proteins, including many required for cilium formation, does not result in G1 arrest in hTERT-RPE1 cells, indicating that cilia are not essential for cell cycle progression in all cell types [28]. Additionally, mouse embryonic carcinoma cells that cannot form primary cilia due to loss of centrosomal protein Odf2 progress normally through the cell cycle [44].

However, other proteins with essential functions in ciliogenesis, but with no known roles in centrosome duplication, also function in the cell cycle. Inhibition of *Chlamydomonas* IFT27, a small G-protein most similar to mammalian Rabl4, results in the expected loss of flagella and the unexpected inhibition of cytokinesis [45]. In vertebrates, IFT88, another essential component of the IFT machinery, also serves as a centrosomal protein that can inhibit cell cycle progression of HeLa cells [46]. IFT88 may interact with the S-phase regulator Che1 to relieve its repression of the tumor suppressor Rb, providing some insight as to how IFT88 may restrain cell cycle progression [46]. Thus, inhibiting the function of ciliogenic proteins can promote cycle progression (e.g., IFT88), disrupt the cell cycle (e.g., IFT27), or have no effect (e.g., Odf2).

These contrasting findings might reflect cilium-independent functions for these various proteins. However, it should be noted that each of these proteins has been studied in

different systems, and transformed cells such as HeLa and embryonic carcinoma cells may differ from untransformed cell lines in terms of the influence that the cilium has on the cell cycle. Similarly, the cell cycles of different organisms or cell types within an organism may be regulated differently by cilia.

Even if there is no strict ciliary control over the cell cycle, the cilium may influence the cell cycle through its signaling functions. One of the most well-established functions for mammalian cilia is in the interpretation of Hedgehog (Hh) signals [2]. Mutations that disrupt cilia also disrupt Hh signal transduction [4, 47-49] and many components of the Hh signal transduction pathway localize to cilia [50-52]. Although not as well understood as their roles in tissue patterning, Hh signals also regulate cell proliferation. Hh signaling turns on the expression of *Cyclin D* and *Cyclin E* and the proto-oncogene *N-myc*, promoting progress through the G1-S transition and inducing cell proliferation [53-55]. Hh signals also block the function of tumor suppressors such as p21 and Rb and inhibit apoptosis by downregulating *Fas* expression [55, 56]. Similarly, the cilium can transmit PDGF signals which can influence cell cycle progression through the Mek1/2-Erk1/2 pathways [5], and cilium-associated proteins can restrain canonical Wnt signaling which promotes cell cycle progression [3, 57, 58]. Thus, it is possible that the signaling functions of the cilium may modulate cell cycle progression.

Taken together, these studies strongly suggest that primary cilium formation and cell cycle progression may reciprocally influence one another. Furthermore, centriole sharing by the cilium and the centrosome, as well as the dual use of key players such as AuroraA, CP110, Neks and IFT88, may underlie the decision to commit to either ciliogenesis or cell division.

The influence of growth factors on ciliogenesis

Many cell types produce cilia upon serum starvation [12, 22]. As discussed above, one reason for this phenomenon can be attributed to the ability of serum starvation to promote exit from the cell cycle, increasing the proportion of cells in G0. However, serum starvation may promote ciliogenesis through other means, such as the removal of secreted factors that directly inhibit ciliogenesis. In support of this possibility, serum stimulation of primary mouse embryonic fibroblasts lacking *Vhlh*, the mouse homolog of the gene underlying von Hippel-Lindau (VHL) syndrome, causes loss of the cilium [59, 60]. This inhibition of ciliogenesis is dependent on intact phosphoinositide signaling, implicating PI(3)K in mediating an anti-ciliogenic cue normally counteracted by VHL activity.

von Hippel-Lindau syndrome is a rare autosomal dominant cancer syndrome. The *VHL* gene acts as a classic tumor suppressor; germline inheritance of a single loss-of-function mutant allele of *VHL* combined with somatic inactivation of the remaining wild-type allele can lead to hemangioblastomas, pheochromocytomas, and clear cell renal carcinomas (CCRCCs) [61]. Although VHL can perform diverse cellular functions, perhaps its most widely appreciated role is as a hypoxia sensor. VHL is a component of an E3 ubiquitin ligase complex that targets Hypoxia-Inducible Factor (HIF) for destruction in the presence of oxygen. Also relevant to its functions as a tumor suppressor, VHL can associate with and increase the activity of p53 [62].

One of the hallmarks of von Hippel-Lindau syndrome is the development of cysts in the kidney or pancreas, similar to those caused by defective ciliary function. Indeed, the renal cysts of von Hippel-Lindau patients lack primary cilia [63] and some, but not all, *VHL*$^{-}$ CCRCC cell lines lack cilia [59, 63]. Importantly, lentivirally-mediated re-

expression of wild-type *VHL* in unciliated *VHL*$^{-}$ CCRCC cells restores ciliogenesis [63]. Thus, VHL promotes ciliogenesis in at least some cell types.

In contrast to some CCRCC cells, however, VHL appears to be dispensable for cilia formation in primary cells. As noted above, deletion of *Vhlh* and shRNA against *VHL* in embryonic fibroblasts and human kidney epithelial cells, respectively, only inhibit ciliogenesis if the phosphoinositide pathway is active [59]. How might PI(3)K activity restrict ciliogenesis? One consequence of phosphoinositide signaling is the inactivation of GSK3β through Akt-mediated phosphorylation of serine 9 [64]. GSK3β is a ubiquitous protein kinase that regulates microtubule dynamics and is required for ciliogenesis in *Chlamydomonas* [65]. GSK3β is closely related to another kinase, GSK3β, collectively referred to as GSK3. Although inhibition of GSK3 alone does not affect ciliogenesis, when combined with loss of VHL, GSK3 inhibition abrogates ciliogenesis in both fibroblasts and kidney epithelial cells [59]. It is possible that the anti-ciliogenic factor(s) found in serum induces PI(3)K activation of Akt, and the subsequent inactivation of GSK3β. Thus, GSK3 and VHL may have parallel or overlapping functions in promoting ciliogenesis.

How VHL and GSK3 collaborate to promote ciliogenesis remains enigmatic, although several independent studies have provided some insight. It is not yet clear whether VHL inhibition of HIF function contributes to its ciliogenic functions. Esteban et al. found that siRNA-mediated knockdown of *HIF-1α* significantly restores ciliogenesis in *VHL*$^{-}$ CCRCC lines, whereas activation of HIF-1*α* in *VHL*$^{+}$ CCRCC cells abolishes cilia formation, suggesting that the constitutive activation of HIF may underlie the absence of cilia [63] (Figure 3, model 1). However, hypoxia itself does not sensitize CCRCC or kidney

epithelial cells to ciliary disassembly, implying that some of the ciliogenic activity of VHL may be HIF-independent [59, 66].

A second possible explanation for the role of VHL in regulating cilia arises from the observations that VHL regulates microtubule stability and orients microtubule growth [67-69]. VHL associates with and protects microtubules from nocodazole-induced depolymerization [69]. Interestingly, *VHL*$^{-}$ cells have uncoordinated microtubule movement, as assessed by live imaging of the plus-end microtubule-binding protein EB1. Specifically, in wild-type cells, newly formed microtubules migrate toward the outer plasma membrane, whereas migration in *VHL*$^{-}$ cells is randomized. Thus, VHL may participate in ciliogenesis through its ability to stabilize and orient microtubular growth (Figure 3, model 2).

A third explanation for how VHL may promote ciliogenesis stems from the observation that VHL interacts with the Par3-Par6-aPKC proteins, a trimeric complex involved in establishing cell polarity [69]. Perhaps unsurprisingly given its roles in apicobasal polarization of epithelial cells and centrosomal positioning in migrating cells, aPKC is essential for ciliogenesis in MDCK cells [56]. Like the Par3-Par6-aPKC complex, VHL may promote ciliogenesis by simply promoting apicobasal polarization and correct docking of the centrosome at the apical membrane (Figure 3, model 3). In support of this possibility, VHL increases CCRCC cell polarization [66].

Finally, biochemical analyses show that Kinesin-2, the anterograde IFT motor, interacts with both VHL and the Par3-Par6-aPKC protein complex [56, 70]. This association with Kinesin-2 raises the possibility that VHL may function directly in regulating ciliary axoneme growth or stability. Consistent with this hypothesis, both the Par3-Par6-aPKC

complex and VHL localize to primary cilia of kidney epithelial cells [56, 59, 69]. Moreover, like VHL, the Par3-Par6-aPKC complex can regulate microtubule dynamics. During Drosophila cellularization, aPKC has a critical role in dissociating microtubules from centrosomes [71]. VHL can ubiquitinate aPKC [72], raising the intriguing possibility that VHL controls the ability of the Par3-Par6-aPKC complex to sever microtubule-centrosome associations. Perhaps VHL-mediated ubiquitination of aPKC keeps this activity in check during ciliogenesis, and the absence of VHL allows aPKC to release axonemal microtubules from the basal body leading to ciliary resorption or shedding (Figure 3, model 4). Like VHL, GSK3 can also interact functionally with Par3 and aPKC to affect microtubule orientation and centrosome positioning [73], perhaps explaining the functional overlap between VHL and GSK3 in promoting ciliogenesis. It should be noted that none of these four models of how VHL may participate in ciliary dynamics are mutually exclusive, and more than one mechanism may be operating in cells.

PCP pathway and ciliogenesis

Studies of wing bristle formation and eye development in Drosophila have identified many genes required for the coordinate orientation of cells along an axis orthogonal to the apicobasal axis. This planar cell polarity (PCP) pathway depends on many components known to be critical for Wnt signal transduction, including Frizzled and Dishevelled (Dvl). Other components of the PCP pathway, like Inturned and Fuzzy, are not shared with the Wnt pathway and act downstream of Dvl in Drosophila bristle orientation. Morpholino knockdown of Inturned and Fuzzy in *Xenopus* embryos disrupts convergent extension, a coordinated morphogenetic cell movement known to depend on the vertebrate PCP pathway [74].

Interestingly, inhibition of many components of the PCP pathway also abrogates ciliogenesis. For example, morpholino knockdown of *Frizzled-2*, a Frizzled-2 target called *duboraya*, or interference with Dvl function abrogates cilium formation in the zebrafish Kuppfer's vesicle [75]. Similarly, inhibition of *Xenopus* Inturned and Fuzzy inhibits formation of epidermal motile cilia [74]. Inhibition of Inturned and Fuzzy also disrupts *Xenopus* Hh signaling suggesting that primary cilium formation may also be affected [74].

How might PCP pathway components participate in ciliogenesis? Knockdown of these genes disrupts the organization of the apical actin network [74, 75]. Although neither Inturned nor Fuzzy have well-defined biochemical activities, they appear to affect microtubule orientation in addition to the actin network. Disorganization of the actin and microtubule cytoskeletons might compromise ciliogenesis through the mispositioning of basal bodies. Thus, while one manifestation of this cytoskeletal coordination accomplished by the PCP pathway may be planar polarization of the cell, a perhaps functionally distinct manifestation may be the apical docking of the mother centriole and the subsequent production of a cilium.

Reciprocally, do cilia regulate any aspect of PCP signaling? Mutation of several BBS genes, which encode ciliary, centrosomal and basal body proteins, cause phenotypes similar to those caused by PCP defects[4]. Inversin, a component of primary cilia [76, 77] can act as a molecular switch between the β-catenin-dependent and PCP signaling pathways [57], and the core PCP protein Vangl2 localizes to the basal body and the cilium [57, 73].

Polarized localization of a non-ciliary pool of Vangl2 precedes asymmetric kinocilium positioning in hair cells [73]. Whereas loss of Ift88 in the cochlea does not alter Vangl2 localization, it does cause misorientation of basal bodies and disruption of cochlear convergent extension. These data suggests that Ift88, and perhaps the cilium itself, are important for basal body polarization and subsequent interpretation of cues from the core PCP pathway [73].

Human diseases may provide clues to the regulation of ciliogenesis

In addition to its role in cystic kidney diseases, defective cilia formation and function are implicated in inherited pleiotropic diseases such as Bardet-Biedl Syndrome, Alstrom Syndrome, Jeune Syndrome, and Meckel-Gruber Syndrome (MKS). These diseases share many overlapping clinical manifestations that point to malfunctioning cilia as the shared underlying cause. Whereas some of these human mutations are believed to affect basal body dynamics [78, 79], ciliary structure [4] or function [80], others may compromise the regulation of ciliogenesis itself. Indeed, studies of MKS have begun to identify novel regulators of ciliogenesis.

MKS is a perinatally lethal autosomal recessive disease, whose clinical manifestations can include occipital encephalocele, cystic kidneys, and polydactyly. MKS can be caused by mutations in multiple genes and to date four underlying genes have been identified: *MKS1, Meckelin, CEP290* and *RPGRIP1L* [81-85]. These four genes all encode cilia- and centrosome-related proteins. MKS1, CEP290 and RPGRIP1L localize to the basal body of ciliated cells, whereas Meckelin, a transmembrane protein, localizes to the cilium itself [81-84]. Loss of cilia causes MKS-like phenotypes in developing mice, suggesting that MKS-associated genes may be essential for ciliogenesis. This

hypothesis is borne out by knockdown studies in IMCD3 cells indicating that MKS1 and Meckelin are essential for correct centrosomal positioning and ciliogenesis.

MKS1 encodes a B9 domain-containing protein originally suggested to have a ciliary role by comparative genomics [86]. Consistent with its involvement in ciliary function, *MKS1* is related to an Rfx-regulated gene in worms, and its orthologue in *Chlamydomonas* is thought to encode a core centrosomal component [87, 88]. Rfx transcription factors bind to an evolutionarily conserved X-box motif found in the regulatory regions of many genes encoding components of the cilium [87]. The promoter for the gene encoding the multipass transmembrane protein Meckelin also contains an X-box motif, implicating Meckelin in ciliary biology [85]. In mice, *Mks1* and *Meckelin* are both broadly expressed, notably in tissues affected by the disease, including the brain, lung, liver, kidney and digits [81].

MKS shares substantial allelism with other less severe syndromes, including Joubert Syndrome, Leber congenital amaurosis, retinal degeneration, nephronophthisis, and anosmia [82, 83, 89-91], suggesting that varying degrees of ciliary dysfunction may underlie the pathogenesis of a wide variety of human syndromes. Perhaps anosmia or retinal degeneration result from minimal disruption of ciliary function, and Meckel syndrome results from more profound abrogation of ciliogenesis.

This hypothesis suggests that disruption of any gene encoding an essential regulatory or structural component of cilia would result in an MKS-like phenotype in humans. Several of the MKS loci encode interacting proteins. MKS1 and Meckelin co-immunoprecipitate [81], and RPGRIP1L interacts with NPHP4, the product of a gene mutated in one form of nephronophthisis [92]. NPHP4 interacts in turn with Nephrocystin, another

nephronophthisis-associated protein [93]. This biochemical evidence suggests that the MKS- and NPHP-associated proteins may form one or a few discrete biochemical complexes, and may be involved in the same biological processes, such as promoting proper apicobasal polarization or correct docking of the centrosome to the plasma membrane. Whether the other NPHP, Joubert syndrome, and Leber congenital amaurosis-associated proteins share these functions or operate in discrete processes remains to be elucidated.

Conclusions and perspectives

The primary cilium is clearly a dynamic organelle whose assembly and disassembly is just beginning to be understood. Here, we have examined emerging data regarding how ciliogenesis and the cell cycle are coordinated, and how signaling pathways and disease-associated proteins may modulate ciliogenesis. Less is known about other possible modulating influences, such as mechanical shear stress in the case of endothelial cilia, and even oxygen tension in the case of Tetrahymena [94, 95]. Additional research will shed light on the molecular mechanisms by which these influences intersect with the ciliary machinery and, undoubtedly, still other ciliogenic influences remain to be uncovered. In particular, much remains to be investigated to elucidate how cell cycle control, centrosomal components and disease-associated proteins collectively contribute to these coordinated processes. This understanding may provide novel insights into the etiology and therapy of diverse ciliopathies.

In addition to providing important as insights into pathogenesis, research into the regulation of ciliogenesis may lead to increased understanding of the mechanisms by which cells can alter their responsiveness to a range of environmental influences. Given that this sensory organelle transduces information about the extracellular space,

regulating ciliary assembly and disassembly may be one way that a cell can control its receptivity to this information. Thus, by modulating fundamental aspects of cytoarchitecture, including polarity, centriole association with the membrane, and microtubule stability, the cell might regulate ciliogenesis and, consequently, the repertoire of environmental and intercellular influences it can sense. These fascinating studies into ciliogenesis begin to link the regulation of cell architecture to the regulation of signal transduction, and suggest that the cell itself is an active and dynamic participant in shaping both.

Acknowledgments

We thank members of the Reiter lab for helpful discussions. This work was supported by funding from the NSF (N.S.), the Sandler Family Supporting Foundation, the Burroughs Wellcome Fund, and the NIH (R01AR054396).

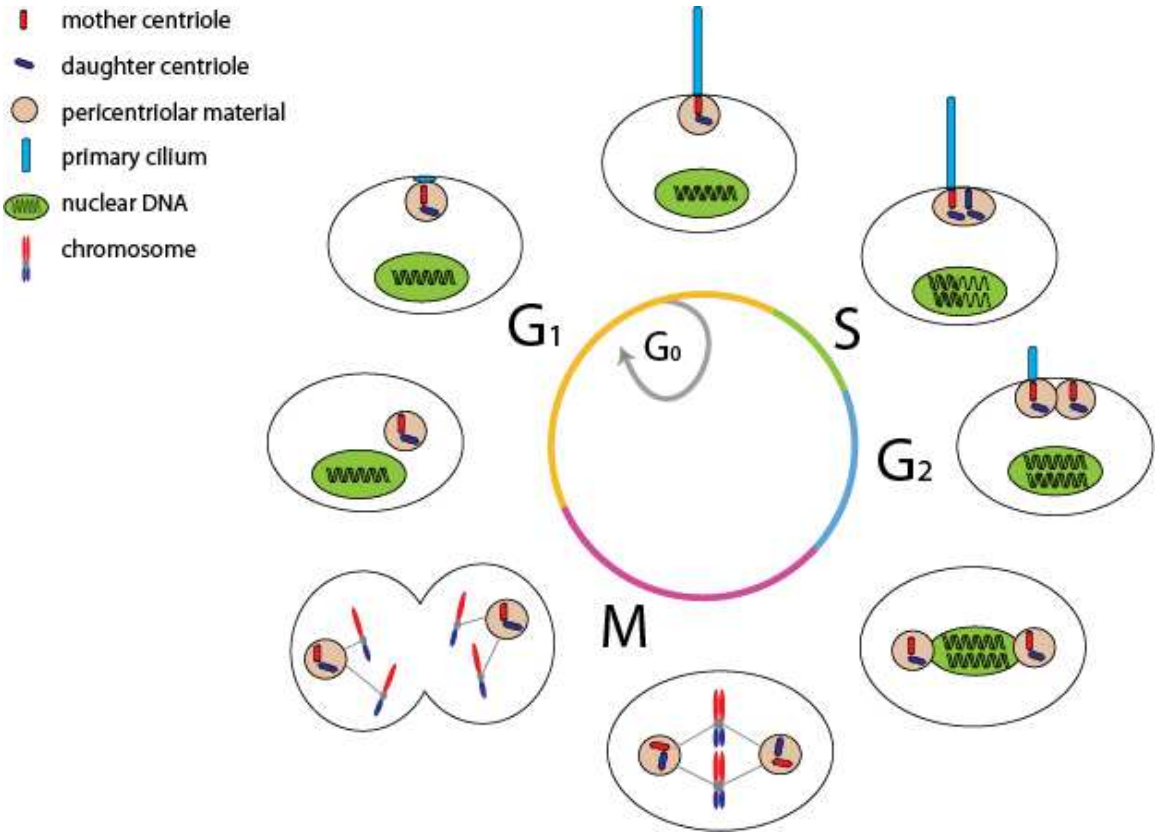

Figure 31. Dual use of the centrioles during cell cycle and primary cilium formation.

In most cells, cilia formation first occurs during G1 following centrosomal docking to the membrane. IFT and accessory proteins build the ciliary axoneme, which extends directly from the mother centriole's triplet microtubules. During this stage of the cell cycle, as well as in G0, the cilium functions as a cellular antenna, interpreting extracellular signals such as Hedgehogs. Upon entry into S phase, the cell's centrioles and the DNA begin to replicate. The centrioles reach maturity during late G2, at which point the cilium is disassembled so that the engaged centrioles can be liberated for mitotic spindle formation. Once cell division is complete, the centrioles can proceed to ciliary re-assembly in G1.

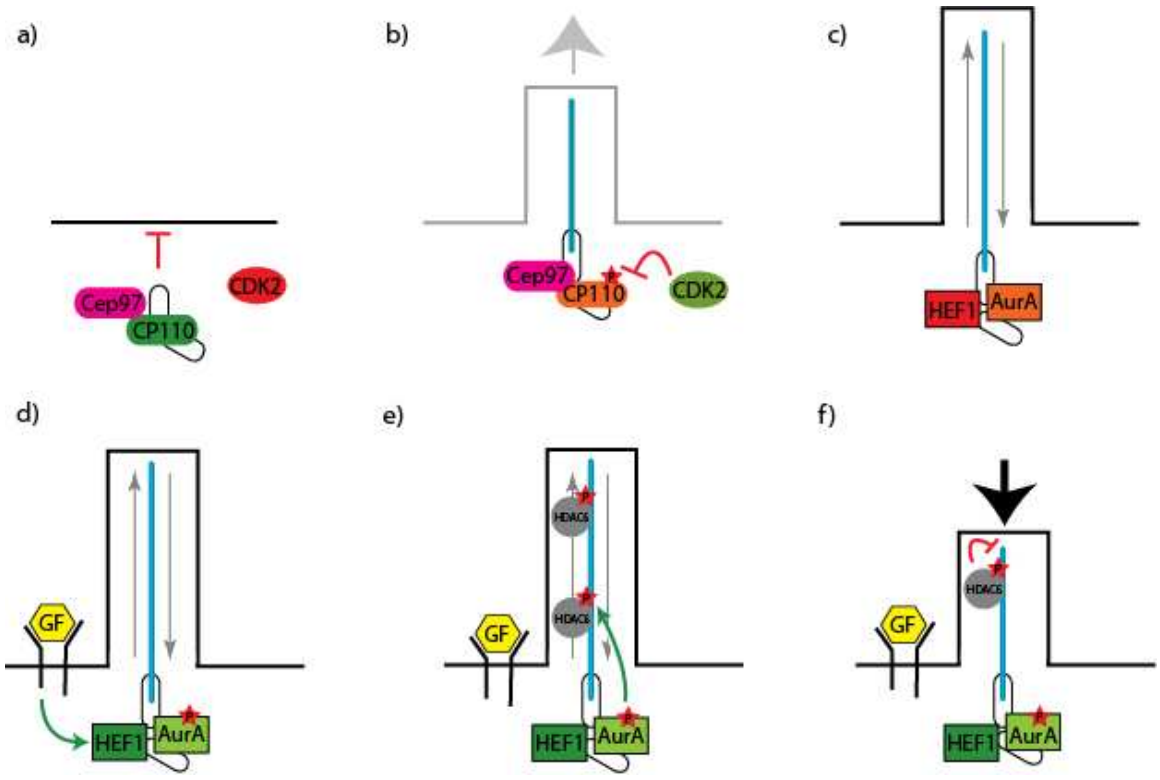

Figure 32. The HEF1/AuroraA complex induces primary cilium disassembly in response to growth factors.
In ciliated cells, HEF1 and AuroraA (AurA) localize to the basal body. Upon growth factor (GF) stimulation, HEF1 activates AurA, which subsequently phosphorylates HDAC6. HDAC6 promotes ciliary disassembly by de-acetylating axonemal tubulin.

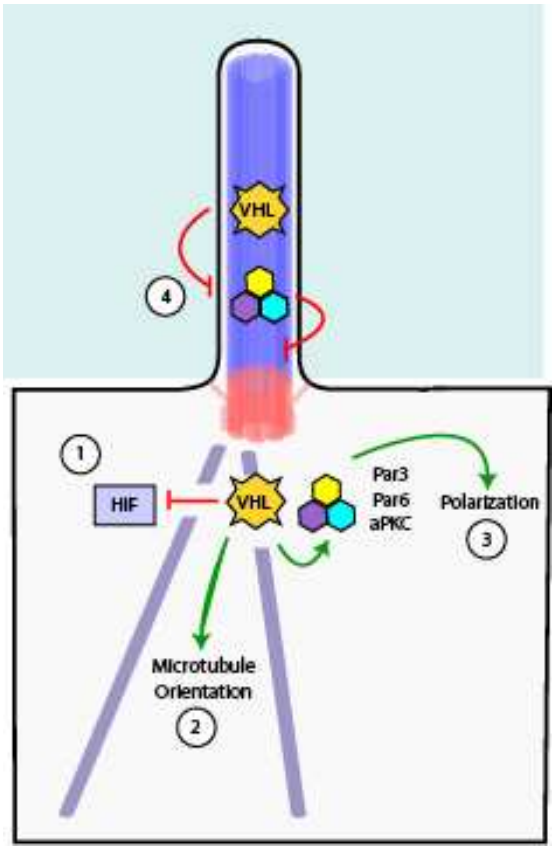

Figure 33. Possible mechanisms by which VHL promotes ciliogenesis.
1) VHL serves as an E3 ubiquitin ligase that targets HIF for destruction. HIF may inhibit ciliogenesis itself. 2) VHL binds and promotes the oriented growth of microtubules. As microtubules form the core of the ciliary axoneme, VHL-mediated stabilization of these microtubules may be necessary for ciliary maintenance. 3) VHL binds to the Par3-Par6-aPKC complex, which is necessary for apicobasal polarization. This polarization may be necessary for correct docking of the mother centriole to the apical plasma membrane, an early step in ciliogenesis. 4) VHL may ubiquitinate cilium-associated aPKC, inhibiting the ability of aPKC to dissociate microtubules from the basal body.

References

1. Singla, V. and J.F. Reiter, *The primary cilium as the cell's antenna: signaling at a sensory organelle.* Science, 2006. **313**(5787): p. 629-33.
2. Eggenschwiler, J.T. and K.V. Anderson, *Cilia and developmental signaling.* Annu Rev Cell Dev Biol, 2007. **23**: p. 345-73.
3. Corbit, K.C., et al., *Kif3a constrains beta-catenin-dependent Wnt signalling through dual ciliary and non-ciliary mechanisms.* Nat Cell Biol, 2007.
4. Ross, A.J., et al., *Disruption of Bardet-Biedl syndrome ciliary proteins perturbs planar cell polarity in vertebrates.* Nat Genet, 2005. **37**(10): p. 1135-40.
5. Schneider, L., et al., *PDGFRalphaalpha signaling is regulated through the primary cilium in fibroblasts.* Curr Biol, 2005. **15**(20): p. 1861-6.
6. Bisgrove, B.W. and H.J. Yost, *The roles of cilia in developmental disorders and disease.* Development, 2006. **133**(21): p. 4131-43.
7. Pazour, G.J. and G.B. Witman, *The vertebrate primary cilium is a sensory organelle.* Curr Opin Cell Biol, 2003. **15**(1): p. 105-10.
8. Rosenbaum, J., *Intraflagellar transport.* Curr Biol, 2002. **12**(4): p. R125.
9. Iomini, C., et al., *Primary cilia of human endothelial cells disassemble under laminar shear stress.* J Cell Biol, 2004. **164**(6): p. 811-7.
10. Khaliullina, H., et al., *Patched regulates Smoothened trafficking using lipoprotein-derived lipids.* Development, 2009. **136**(24): p. 4111-21.
11. Tsou, M.F. and T. Stearns, *Mechanism limiting centrosome duplication to once per cell cycle.* Nature, 2006. **442**(7105): p. 947-51.
12. Vorobjev, I.A. and S. Chentsov Yu, *Centrioles in the cell cycle. I. Epithelial cells.* J Cell Biol, 1982. **93**(3): p. 938-49.
13. Hinchcliffe, E.H. and G. Sluder, *Two for two: Cdk2 and its role in centrosome doubling.* Oncogene, 2002. **21**(40): p. 6154-60.
14. Lacey, K.R., P.K. Jackson, and T. Stearns, *Cyclin-dependent kinase control of centrosome duplication.* Proc Natl Acad Sci U S A, 1999. **96**(6): p. 2817-22.
15. Boveri, T., *Zur Frage der Entstehung maligner Tumoren* ed. G. Fischer. 1914, Jena. 64.
16. Boveri, B.M., *The origin of malignant tumors* 1929, Baltimore: Williams & Wilkins. 119p.
17. Lingle, W.L., et al., *Centrosome hypertrophy in human breast tumors: implications for genomic stability and cell polarity.* Proc Natl Acad Sci U S A, 1998. **95**(6): p. 2950-5.
18. Pihan, G.A., et al., *Centrosome defects and genetic instability in malignant tumors.* Cancer Res, 1998. **58**(17): p. 3974-85.
19. Vladar, E.K. and T. Stearns, *Molecular characterization of centriole assembly in ciliated epithelial cells.* J Cell Biol, 2007. **178**(1): p. 31-42.
20. Spassky, N., et al., *Adult ependymal cells are postmitotic and are derived from radial glial cells during embryogenesis.* J Neurosci, 2005. **25**(1): p. 10-8.
21. Rieder, C.L., C.G. Jensen, and L.C. Jensen, *The resorption of primary cilia during mitosis in a vertebrate (PtK1) cell line.* J Ultrastruct Res, 1979. **68**(2): p. 173-85.
22. Tucker, R.W., A.B. Pardee, and K. Fujiwara, *Centriole ciliation is related to quiescence and DNA synthesis in 3T3 cells.* Cell, 1979. **17**(3): p. 527-35.
23. Quarmby, L.M. and J.D. Parker, *Cilia and the cell cycle?* J Cell Biol, 2005. **169**(5): p. 707-10.
24. Basto, R., et al., *Flies without centrioles.* Cell, 2006. **125**(7): p. 1375-86.

25. Srsen, V., et al., *Inhibition of centrosome protein assembly leads to p53-dependent exit from the cell cycle.* J Cell Biol, 2006. **174**(5): p. 625-30.
26. Habedanck, R., et al., *The Polo kinase Plk4 functions in centriole duplication.* Nat Cell Biol, 2005. **7**(11): p. 1140-6.
27. Uetake, Y., et al., *Cell cycle progression and de novo centriole assembly after centrosomal removal in untransformed human cells.* J Cell Biol, 2007. **176**(2): p. 173-82.
28. Graser, S., et al., *Cep164, a novel centriole appendage protein required for primary cilium formation.* J Cell Biol, 2007. **179**(2): p. 321-30.
29. Mikule, K., et al., *Loss of centrosome integrity induces p38-p53-p21-dependent G1-S arrest.* Nat Cell Biol, 2007. **9**(2): p. 160-70.
30. Chen, Z., et al., *CP110, a cell cycle-dependent CDK substrate, regulates centrosome duplication in human cells.* Dev Cell, 2002. **3**(3): p. 339-50.
31. Spektor, A., et al., *Cep97 and CP110 suppress a cilia assembly program.* Cell, 2007. **130**(4): p. 678-90.
32. Pugacheva, E.N., et al., *HEF1-dependent Aurora A activation induces disassembly of the primary cilium.* Cell, 2007. **129**(7): p. 1351-63.
33. Pugacheva, E.N. and E.A. Golemis, *The focal adhesion scaffolding protein HEF1 regulates activation of the Aurora-A and Nek2 kinases at the centrosome.* Nat Cell Biol, 2005. **7**(10): p. 937-46.
34. Bischoff, J.R., et al., *A homologue of Drosophila aurora kinase is oncogenic and amplified in human colorectal cancers.* Embo J, 1998. **17**(11): p. 3052-65.
35. Marumoto, T., D. Zhang, and H. Saya, *Aurora-A - a guardian of poles.* Nat Rev Cancer, 2005. **5**(1): p. 42-50.
36. Tan, B.C. and S.C. Lee, *Nek9, a novel FACT-associated protein, modulates interphase progression.* J Biol Chem, 2004. **279**(10): p. 9321-30.
37. Yissachar, N., et al., *Nek7 kinase is enriched at the centrosome, and is required for proper spindle assembly and mitotic progression.* FEBS Lett, 2006. **580**(27): p. 6489-95.
38. Yin, M.J., et al., *The serine/threonine kinase Nek6 is required for cell cycle progression through mitosis.* J Biol Chem, 2003. **278**(52): p. 52454-60.
39. Mahjoub, M.R., M.L. Trapp, and L.M. Quarmby, *NIMA-related kinases defective in murine models of polycystic kidney diseases localize to primary cilia and centrosomes.* J Am Soc Nephrol, 2005. **16**(12): p. 3485-9.
40. Taylor, M.D., et al., *Mutations in SUFU predispose to medulloblastoma.* Nat Genet, 2002. **31**(3): p. 306-10.
41. Otto, E.A., et al., *Mutation analysis in nephronophthisis using a combined approach of homozygosity mapping, CEL I endonuclease cleavage, and direct sequencing.* Hum Mutat, 2007.
42. Otto, E.A., et al., *NEK8 Mutations Affect Ciliary and Centrosomal Localization and May Cause Nephronophthisis.* J Am Soc Nephrol, 2008.
43. Parker, J.D., et al., *Phylogenetic analysis of the neks reveals early diversification of ciliary-cell cycle kinases.* PLoS ONE, 2007. **2**(10): p. e1076.
44. Ishikawa, H., et al., *Odf2-deficient mother centrioles lack distal/subdistal appendages and the ability to generate primary cilia.* Nat Cell Biol, 2005. **7**(5): p. 517-24.
45. Qin, H., et al., *Intraflagellar transport protein 27 is a small G protein involved in cell-cycle control.* Curr Biol, 2007. **17**(3): p. 193-202.
46. Robert, A., et al., *The intraflagellar transport component IFT88/polaris is a centrosomal protein regulating G1-S transition in non-ciliated cells.* J Cell Sci, 2007. **120**(Pt 4): p. 628-37.

47. Huangfu, D. and K.V. Anderson, *Cilia and Hedgehog responsiveness in the mouse.* Proc Natl Acad Sci U S A, 2005. **102**(32): p. 11325-30.
48. Huangfu, D., et al., *Hedgehog signalling in the mouse requires intraflagellar transport proteins.* Nature, 2003. **426**(6962): p. 83-7.
49. Liu, A., B. Wang, and L.A. Niswander, *Mouse intraflagellar transport proteins regulate both the activator and repressor functions of Gli transcription factors.* Development, 2005. **132**(13): p. 3103-11.
50. Corbit, K.C., et al., *Vertebrate Smoothened functions at the primary cilium.* Nature, 2005. **437**(7061): p. 1018-21.
51. Haycraft, C.J., et al., *Gli2 and Gli3 localize to cilia and require the intraflagellar transport protein polaris for processing and function.* PLoS Genet, 2005. **1**(4): p. e53.
52. Rohatgi, R. and M.P. Scott, *Patching the gaps in Hedgehog signalling.* Nat Cell Biol, 2007. **9**(9): p. 1005-9.
53. Duman-Scheel, M., et al., *Hedgehog regulates cell growth and proliferation by inducing Cyclin D and Cyclin E.* Nature, 2002. **417**(6886): p. 299-304.
54. Kenney, A.M., M.D. Cole, and D.H. Rowitch, *Nmyc upregulation by sonic hedgehog signaling promotes proliferation in developing cerebellar granule neuron precursors.* Development, 2003. **130**(1): p. 15-28.
55. Kenney, A.M. and D.H. Rowitch, *Sonic hedgehog promotes G(1) cyclin expression and sustained cell cycle progression in mammalian neuronal precursors.* Mol Cell Biol, 2000. **20**(23): p. 9055-67.
56. Preuss, F., et al., *Drosophila doubletime mutations which either shorten or lengthen the period of circadian rhythms decrease the protein kinase activity of casein kinase I.* Mol Cell Biol, 2004. **24**(2): p. 886-98.
57. Simons, M., et al., *Inversin, the gene product mutated in nephronophthisis type II, functions as a molecular switch between Wnt signaling pathways.* Nat Genet, 2005. **37**(5): p. 537-43.
58. Gerdes, J.M., et al., *Disruption of the basal body compromises proteasomal function and perturbs intracellular Wnt response.* Nat Genet, 2007. **39**(11): p. 1350-60.
59. Nakano, Y., et al., *Functional domains and sub-cellular distribution of the Hedgehog transducing protein Smoothened in Drosophila.* Mech Dev, 2004. **121**(6): p. 507-18.
60. Lolkema, M.P., et al., *Allele-specific regulation of primary cilia function by the von Hippel-Lindau tumor suppressor.* Eur J Hum Genet, 2008. **16**(1): p. 73-8.
61. Kuehn, E.W., G. Walz, and T. Benzing, *Von hippel-lindau: a tumor suppressor links microtubules to ciliogenesis and cancer development.* Cancer Res, 2007. **67**(10): p. 4537-40.
62. Roe, J.S. and H.D. Youn, *The positive regulation of p53 by the tumor suppressor VHL.* Cell Cycle, 2006. **5**(18): p. 2054-6.
63. Esteban, M.A., et al., *Formation of primary cilia in the renal epithelium is regulated by the von Hippel-Lindau tumor suppressor protein.* J Am Soc Nephrol, 2006. **17**(7): p. 1801-6.
64. Cross, D.A., et al., *Selective small-molecule inhibitors of glycogen synthase kinase-3 activity protect primary neurones from death.* J Neurochem, 2001. **77**(1): p. 94-102.
65. Chen, M.H., et al., *Cilium-independent regulation of Gli protein function by Sufu in Hedgehog signaling is evolutionarily conserved.* Genes Dev, 2009. **23**(16): p. 1910-28.

66. Lutz, M.S. and R.D. Burk, *Primary cilium formation requires von hippel-lindau gene function in renal-derived cells.* Cancer Res, 2006. **66**(14): p. 6903-7.
67. Hergovich, A., et al., *Regulation of microtubule stability by the von Hippel-Lindau tumour suppressor protein pVHL.* Nat Cell Biol, 2003. **5**(1): p. 64-70.
68. Lolkema, M.P., et al., *The von Hippel-Lindau tumor suppressor protein influences microtubule dynamics at the cell periphery.* Exp Cell Res, 2004. **301**(2): p. 139-46.
69. Schermer, B., et al., *The von Hippel-Lindau tumor suppressor protein controls ciliogenesis by orienting microtubule growth.* J Cell Biol, 2006. **175**(4): p. 547-54.
70. Lolkema, M.P., et al., *The von Hippel-Lindau tumour suppressor interacts with microtubules through kinesin-2.* FEBS Lett, 2007. **581**(24): p. 4571-6.
71. Harris, T.J. and M. Peifer, *The positioning and segregation of apical cues during epithelial polarity establishment in Drosophila.* J Cell Biol, 2005. **170**(5): p. 813-23.
72. Okuda, H., et al., *The von Hippel-Lindau tumor suppressor protein mediates ubiquitination of activated atypical protein kinase C.* J Biol Chem, 2001. **276**(47): p. 43611-7.
73. Xu, Y., et al., *Functional consequences of a CKIdelta mutation causing familial advanced sleep phase syndrome.* Nature, 2005. **434**(7033): p. 640-4.
74. Park, T.J., S.L. Haigo, and J.B. Wallingford, *Ciliogenesis defects in embryos lacking inturned or fuzzy function are associated with failure of planar cell polarity and Hedgehog signaling.* Nat Genet, 2006. **38**(3): p. 303-11.
75. Oishi, I., et al., *Regulation of primary cilia formation and left-right patterning in zebrafish by a noncanonical Wnt signaling mediator, duboraya.* Nat Genet, 2006. **38**(11): p. 1316-22.
76. Watanabe, D., et al., *The left-right determinant Inversin is a component of node monocilia and other 9+0 cilia.* Development, 2003. **130**(9): p. 1725-34.
77. Otto, E.A., et al., *Mutations in INVS encoding inversin cause nephronophthisis type 2, linking renal cystic disease to the function of primary cilia and left-right axis determination.* Nat Genet, 2003. **34**(4): p. 413-20.
78. Kim, J.C., et al., *The Bardet-Biedl protein BBS4 targets cargo to the pericentriolar region and is required for microtubule anchoring and cell cycle progression.* Nat Genet, 2004. **36**(5): p. 462-70.
79. Kim, J.C., et al., *MKKS/BBS6, a divergent chaperonin-like protein linked to the obesity disorder Bardet-Biedl syndrome, is a novel centrosomal component required for cytokinesis.* J Cell Sci, 2005. **118**(Pt 5): p. 1007-20.
80. Li, G., et al., *A role for Alstrom syndrome protein, alms1, in kidney ciliogenesis and cellular quiescence.* PLoS Genet, 2007. **3**(1): p. e8.
81. Dawe, H.R., et al., *The Meckel-Gruber Syndrome proteins MKS1 and meckelin interact and are required for primary cilium formation.* Hum Mol Genet, 2007. **16**(2): p. 173-86.
82. Delous, M., et al., *The ciliary gene RPGRIP1L is mutated in cerebello-oculo-renal syndrome (Joubert syndrome type B) and Meckel syndrome.* Nat Genet, 2007. **39**(7): p. 875-81.
83. Frank, V., et al., *Mutations of the CEP290 gene encoding a centrosomal protein cause Meckel-Gruber syndrome.* Hum Mutat, 2007.
84. Kyttala, M., et al., *MKS1, encoding a component of the flagellar apparatus basal body proteome, is mutated in Meckel syndrome.* Nat Genet, 2006. **38**(2): p. 155-7.
85. Jaber, M., et al., *Essential role of beta-adrenergic receptor kinase 1 in cardiac development and function.* Proc Natl Acad Sci U S A, 1996. **93**(23): p. 12974-9.

86. Li, J.B., et al., *Comparative genomics identifies a flagellar and basal body proteome that includes the BBS5 human disease gene.* Cell, 2004. **117**(4): p. 541-52.
87. Efimenko, E., et al., *Analysis of xbx genes in C. elegans.* Development, 2005. **132**(8): p. 1923-34.
88. Keller, L.C., et al., *Proteomic analysis of isolated chlamydomonas centrioles reveals orthologs of ciliary-disease genes.* Curr Biol, 2005. **15**(12): p. 1090-8.
89. Baala, L., et al., *The Meckel-Gruber syndrome gene, MKS3, is mutated in Joubert syndrome.* Am J Hum Genet, 2007. **80**(1): p. 186-94.
90. Chang, B., et al., *In-frame deletion in a novel centrosomal/ciliary protein CEP290/NPHP6 perturbs its interaction with RPGR and results in early-onset retinal degeneration in the rd16 mouse.* Hum Mol Genet, 2006. **15**(11): p. 1847-57.
91. McEwen, D.P., et al., *Hypomorphic CEP290/NPHP6 mutations result in anosmia caused by the selective loss of G proteins in cilia of olfactory sensory neurons.* Proc Natl Acad Sci U S A, 2007. **104**(40): p. 15917-22.
92. Roepman, R., et al., *Interaction of nephrocystin-4 and RPGRIP1 is disrupted by nephronophthisis or Leber congenital amaurosis-associated mutations.* Proc Natl Acad Sci U S A, 2005. **102**(51): p. 18520-5.
93. Mollet, G., et al., *Characterization of the nephrocystin/nephrocystin-4 complex and subcellular localization of nephrocystin-4 to primary cilia and centrosomes.* Hum Mol Genet, 2005. **14**(5): p. 645-56.
94. Meng, Q.J., et al., *Setting clock speed in mammals: the CK1 epsilon tau mutation in mice accelerates circadian pacemakers by selectively destabilizing PERIOD proteins.* Neuron, 2008. **58**(1): p. 78-88.
95. van der Heiden, P.L., et al., *Efficacy and toxicity of gemtuzumab ozogamicin in patients with acute myeloid leukemia.* Eur J Haematol, 2006. **76**(5): p. 409-13.

Publishing Agreement

It is the policy of the University to encourage the distribution of all theses, dissertations, and manuscripts. Copies of all UCSF theses, dissertations, and manuscripts will be routed to the library via the Graduate Division. The library will make all theses, dissertations, and manuscripts accessible to the public and will preserve these to the best of their abilities, in perpetuity.

Please sign the following statement:

I hereby grant permission to the Graduate Division of the University of California, San Francisco to release copies of my thesis, dissertation, or manuscript to the Campus Library to provide access and preservation, in whole or in part, in perpetuity.

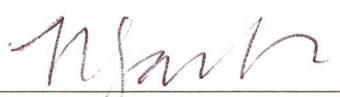

Author Signature

March 23, 2012

Date